Synthesis and Structural Characterization of Lanthanide-Containing Polyoxometalates

by

Amal Hamdy Ismail

A thesis submitted in partial fulfilment of the requirements for the degree

of

Doctor of Philosophy in Chemistry

Approved Dissertation Committee:

Prof. Ulrich Kortz (mentor, Jacobs University)

Prof. Gerd-Volker Röschenthaler (Jacobs University)

Prof. Bernold Hasenknopf (Université Pierre et Marie Curie, Paris)

Date of Defense: 21st of February, 2011

School of Engineering and Science

2011

To my parents, sisters, brothers, nieces, and nephews

Acknowledgements

I am very grateful to my supervisor Prof. Dr. Ulrich Kortz for offering me the possibility to join his group, for guidance and for introducing me to the field of polyoxometalates. I deeply appreciate the grant from the Ministry of Higher Education of the Arab Republic of Egypt, allowing me to pursue my Ph.D. studies in Bremen. My thanks go to Dr. Michael H. Dickman and Dr. Bassem S. Bassil for their help in Crystallography. I thank all the former and current members of the Kortz group. Finally, I would like to thank my parents and my whole family for all their priceless support.

Abstract

Polyoxometalates (POMs) represent a large class of nanosized metal-oxo anions. POMs are remarkable not only in terms of molecular and electronic structural versatility, but also due to their reactivity and relevance in fields such as photochemistry, analytical chemistry, clinical chemistry, magnetism, catalysis, biology, medicine and materials science. Lanthanide-containing POMs have been investigated less than those containing 3d-transition metals. The former have shown interesting properties in the areas of photoluminescence, catalysis, electrochemistry, and magnetism.

Chapter I contains an extensive introduction to the class of POMs. Chapter II describes the synthetic procedures for some POM precursors and presents the different experimental techniques used for the characterization of the products. Chapter III comprises the lanthanide-containing polyoxotungstates results, divided into two sections, the lanthanide isopolytungstates and the lanthanide heteropolytungstates. In the first section, the polyanions $[Ln_2(H_2O)_{10}W_{22}O_{71}(OH)_2]^{8-}$ (Ln = La, Ce, Tb, Dy, Ho, Er, Tm, Yb, Lu, Y) {**Ln_2W_{22}**} and the V-shaped polyanions $[Ln_2(H_2O)_{10}W_{28}O_{93}(OH)_2]^{14-}$ (Ln = Sm, and Eu) {**Ln_2W_{28}**} were discussed. The {**Ln_2W_{22}**} family consists of the $[H_2W_{22}O_{74}]^{14-}$ fragment and two $\{Ln(H_2O)_5\}^{3+}$ supporting units while the {**Ln_2W_{28}**} consists of the $[H_2W_{28}O_{95}]^{20-}$ unit and two $\{Ln(H_2O)_n\}^{3+}$ supporting groups. The $[H_2W_{22}O_{74}]^{14-}$ cluster is made up of two undecatungstate fragments while the $[H_2W_{28}O_{95}]^{20-}$ cluster consists of two undecatungstate and a hexatungstate fragment. In the second section, the mono- and di-lanthanide derivatives of the tungstoarsenates(III) $[Yb(H_2O)_2K(H_2O)_2As_2W_{19}O_{67}(H_2O)]^{10-}$ {**$YbAs_2W_{19}$**}; $[La_2(H_2O)_6As_2W_{19}O_{67}(H_2O)]^{8-}$ {**$La_2As_2W_{19}$**}, the mono- and di-lanthanide derivatives of the tungstoantimonates(III) $[Ln(H_2O)_3Sb_2W_{21}O_{72}(OH))]^{10-}$ (Ln = Yb, Lu, Y) {**$LnSb_2W_{21}$**}; $[Ln_2(H_2O)_6Sb_2W_{20}O_{70})]^{8-}$ (Yb, Lu, Y) {**$Ln_2Sb_2W_{20}$**}, and the acetate sandwich-type tungstogermanates $[(Ln(GeW_{11}O_{39})(H_2O))_2(\mu\text{-}CH_3COO)_2]^{12-}$ (Ln = Eu, Gd, Lu) have been

presented. Polyanions {**YbAs$_2$W$_{19}$**}, {**La$_2$As$_2$W$_{19}$**}, {**LnSb$_2$W$_{21}$**} and {**Ln$_2$Sb$_2$W$_{20}$**} were synthesized in simple, one-pot reactions of Ln^{3+} ions with the lone pair containing polyanion precursors ($[As_2W_{19}O_{67}(H_2O)]^{14-}$, [*B*-*α*-$AsW_9O_{33}]^{9-}$, $[Sb_2W_{22}O_{74}(OH)_2]^{12-}$, [*B*-*α*-$SbW_9O_{33}]^{9-}$).

Chapter IV describes the mixed lanthanide/d-transition metal containing POMs, the novel open-ring shaped polyanions $[Fe_{16}O_2(OH)_{23}(H_2O)_9(P_8W_{49}O_{189})Ln_4(H_2O)_{20}]^{11-}$ {**Ln$_4$Fe$_{16}$P$_8$W$_{49}$**}(Ln = Eu and Gd) which have been synthesized by reaction of the known $[H_7P_8W_{48}O_{184}]^{33-}$ {**P$_8$W$_{48}$**} cyclic precursor with Fe^{3+} and Ln^{3+} ions in acidic aqueous medium in the presence of hydrogen peroxide. The unique novel open-ring tungstophosphate(V) unit $\{P_8W_{48}O_{188}(WO_3)\}^{44-}$ exists in the structure of the {**Ln$_4$Fe$_{16}$P$_8$W$_{49}$**}compounds in addition to the $\{Fe_{16}O_2(OH)_{20}(H_2O)_{12}\}^{21+}$ nanocluster and four $\{Ln(H_2O)_5\}^{3+}$ grafted units.

Chapter V comprises non-lanthanide-containing POMs, divided into two sections, tellurium and *d*-transition metal containing POMs. The tungstotellurates(IV) $[H_2Te_4W_{20}O_{80}]^{22-}$ and $[NaTeW_{15}O_{54}]^{13-}$ and the molybotellurate(IV) $[H_2Te_{24}Mo_{44}O_{198}]^{34-}$ are described in the first section. In the second section, the sandwich-type tungstogermanates $[Cu_3(H_2O)(B\text{-}\beta\text{-}GeW_9O_{33}(OH))(B\text{-}\beta\text{-}GeW_8O_{30}(OH))]^{12-}$, $[Co(H_2O)_2\{Co_3(B\text{-}\beta\text{-}GeW_9O_{33}(OH))(B\text{-}\beta\text{-}GeW_8O_{30}(OH))\}_2]^{22-}$ and $[Mn(H_2O)_2\{Mn_3(H_2O)(B\text{-}\beta\text{-}GeW_9O_{33}(OH))(B\text{-}\beta\text{-}GeW_8O_{30}(OH))\}_2]^{22-}$ are presented.

All obtained compounds have been characterized in the solid state by FTIR, single-crystal XRD, TGA and elemental analyses. Furthermore, solution studies of the diamagnetic derivatives (La, Lu and Y analogues) by ^{183}W and ^{89}Y NMR spectroscopy were also performed, in addition to ^{13}C NMR and ^{1}H NMR spectroscopy for the acetate containing POMs.

Table of Contents

List of Figures

List of Tables

Codes of Compounds

Compound	*Code*
$Na_2La_2[La_2(H_2O)_{10}W_{22}O_{72}(OH)_2]\cdot 44H_2O$	**NaLa-1**
$Na_2Ce_2[Ce_2(H_2O)_{10}W_{22}O_{72}(OH)_2]\cdot 44H_2O$	**NaCe-2**
$Na_5Tb[Tb_2(H_2O)_{10}W_{22}O_{72}(OH)_2]\cdot 41H_2O$	**NaTb-3**
$Na_8[Dy_2(H_2O)_{10}W_{22}O_{72}(OH)_2]\cdot 49H_2O$	**Na-4**
$Na_5Ho[Ho_2(H_2O)_{10}W_{22}O_{72}(OH)_2]\cdot 45H_2O$	**NaHo-5**
$Na_8[Er_2(H_2O)_{10}W_{22}O_{72}(OH)_2]\cdot 44H_2O$	**Na-6**
$Na_8[Tm_2(H_2O)_{10}W_{22}O_{72}(OH)_2]\cdot 41H_2O$	**Na-7**
$Na_8[Yb_2(H_2O)_{10}W_{22}O_{72}(OH)_2]\cdot 46H_2O$	**Na-8**
$Na_5Lu[Lu_2(H_2O)_{10}W_{22}O_{72}(OH)_2]\cdot 44H_2O$	**NaLu-9**
$Na_8[Y_2(H_2O)_{10}W_{22}O_{72}(OH)_2]\cdot 46H_2O$	**Na-10**
$Na_{14}[Sm_2(H_2O)_{10}W_{28}O_{93}(OH)_2]\cdot 40H_2O$	**Na-11**
$Na_8Eu_2[Eu_2(H_2O)_{10}W_{28}O_{93}(OH)_2]\cdot 47H_2O$	**NaEu-12**
$K_{9.5}Na_{0.5}[Yb(H_2O)_2K(H_2O)_2As_2W_{19}O_{67}(H_2O)]\cdot 25H_2O$	**KNa-13**
$Na_8[La_2(H_2O)_6As_2W_{19}O_{67}(H_2O)]\cdot 16H_2O$	**Na-14**
$Na_{10}[Yb(H_2O)_3Sb_2W_{21}O_{72}(OH)]\cdot 41H_2O$	**Na-15**
$Na_{10}[Lu(H_2O)_3Sb_2W_{21}O_{72}(OH)]\cdot 42H_2O$	**Na-16**
$Na_{10}[Y(H_2O)_3Sb_2W_{21}O_{72}(OH)]\cdot 40H_2O$	**Na-17**
$Na_8[Yb_2(H_2O)_6(Sb_2W_{20}O_{70})]\cdot 37H_2O$	**Na-18**
$Na_8[Lu_2(H_2O)_6(Sb_2W_{20}O_{70})]\cdot 38H_2O$	**Na-19**
$Na_8[Y_2(H_2O)_6(Sb_2W_{20}O_{70})]\cdot 37\ H_2O$	**Na-20**
$K_{12}[(Eu(GeW_{11}O_{39})(H_2O))_2(\mu\text{-}CH_3COO)_2]\cdot 24H_2O$	**K-21**
$K_{12}[(Gd(GeW_{11}O_{39})(H_2O))_2(\mu\text{-}CH_3COO)_2].\ 24H_2O$	**K-22**

$K_8Cs_3Na[(Lu(GeW_{11}O_{39})(H_2O))_2(\mu\text{-}CH_3COO)_2]\cdot 18H_2O$	**KCsNa-23**
$K_{8.5}Na_{0.5}Li_{0.5}Eu_{0.5}[P_8W_{49}O_{189}Fe_{16}O_2(OH)_{23}(H_2O)_9Eu_4(H_2O)_{20}]\cdot 70H_2O$	**KLiNa-24**
$K_9LiNa[P_8W_{49}O_{189}Fe_{16}O_2(OH)_{23}(H_2O)_9Gd_4(H_2O)_{20}]\cdot 50H_2O$	**KLiNa-25**
$Na_{22}[H_2Te_4W_{20}O_{80}]\cdot 64H_2O$	**Na-26**
$Na_{13}[NaTeW_{15}O_{54}]\cdot 26H_2O$	**Na-27**
$K_{12}[Cu_3(H_2O)(B\text{-}\beta\text{-}GeW_9O_{33}(OH))(B\text{-}\beta\text{-}GeW_8O_{30}(OH))]\cdot 31H_2O$	**K-29**
$K_{22}[Co(H_2O)_2\{Co_3(B\text{-}\beta\text{-}GeW_9O_{33}(OH))(B\text{-}\beta\text{-}GeW_8O_{30}(OH))\}_2]\cdot 52H_2O$	**K-30**
$K_{22}[Mn(H_2O)_2\{Mn_3(H_2O)(B\text{-}\beta\text{-}GeW_9O_{33}(OH))(B\text{-}\beta\text{-}GeW_8O_{30}(OH))\}_2]\cdot 45H_2O$	**K-31**

Chapter I

Introduction

Polyoxometalates (POMs) represent a class of discrete structurally and chemically diverse nanosized metal-oxygen molecular anions of early transition metals (groups V and VI) in their highest oxidation states. POMs are remarkable not only in terms of molecular and electronic structural versatility, but also due to their reactivity and relevance in fields such as photochemistry, analytical chemistry, clinical chemistry, magnetism, catalysis, biology, medicine and materials science.[1]

1.1 Historical perspective

The class of POMs has been known since 1826 when Berzelius noted the formation of a yellow precipitate from the reaction of molybdate with phosphoric acid, which is now known as the 12-molybdophosphate, $(NH_4)_3[PMo_{12}O_{40}]$.[2] About 20 years later, Svenberg and Struve introduced this insoluble compound into analytical chemistry for the gravimetric determination of phosphours.[3] The systematic studies of POMs was started by Marignac in 1862 who prepared and precisely analyzed two isomers of 12-tungstosilicic acid, $H_3SiW_{12}O_{40}$ which are now known as α and β isomers and their salts.[4] After that, the field developed rapidly, so that by the early part of the twentieth century about 60 different types of heteropoly acids had been prepared and analyzed by many groups. A review of this early work was reported by Rosenheim and Jänicke.[5] Miolati and Pizzighelli suggested a structural hypothesis for these compounds based on Werner's coordination theory as first attempts to understand the composition of heteropolyanions.[6] This hypothesis was developed by Rosenheim and then according to the so-called Miolati-Rosenheim theory, the heteroatom was considered to have an octahedral coordination with MO_4^{2-} or $M_2O_7^{2-}$ anions as ligands or bridging groups (6:1 complexes). This theory was criticized by Pauling in 1929 who

proposed a structure for the 12:1 complexes based on a central XO_4 tetrahedron surrounded by twelve MO_6 octahedra, where he noted that Mo^{6+} and W^{6+} had crystal radii appropriate for octahedral coordination with oxygens. In order to minimize the electrostatic repulsions, all polyhedra were believed to be linked via only shared corners.[7]

In 1933, Keggin solved the structure of $H_3[PW_{12}O_{40}]$ by powder X-ray diffraction and reported the first polyoxoanion "the parent structure" which is now known as Keggin polyanion.[8] Keggin showed that anion was based on WO_6 octahedral units and these octahedra were linked by shared edges as well as corners. Thereafter other types of structure were reported such as the Anderson-Evans, Lindqvist and Wells-Dawson structures in 1948, 1950, and 1953, respectively.[9-11] The development of modern experimental techniques such as single-crystal X-ray diffraction and NMR spectroscopy was the turning point for the determination of structures in POM chemistry. Furthermore, these developments in combination with the use of modern analytical techniques such as electrochemistry or electrospray ionization (ESI) mass spectrometry have allowed establishing important links between solid and solution structures of polyanions.[1b] Hence, in the past fifty years, hundreds of structures have been reported and new classes of structures with unexpected reactivity and application are still being studied.

1.2 Structural principles of polyoxometalates

POMs are composed of metallic centers or addenda atoms (M) surrounded by oxygen atoms. Oxygen atoms are the common ligands in polyanions, hence the term "polyoxo", and are usually present as bridging and terminal oxo ligands. In some cases protonation of in particular bridging oxygen atoms can also be observed.

POMs are composed of MO_n units, where 'n' indicates the coordination number of M (n = 4, 5, 6 or 7). Usually the distorted octahedral coordination (n = 6) is observed. Two main types of POMs are known, based on their chemical composition: isopoly and heteropoly anions.

Isopolyanions are represented by the general formula $[M_mO_y]^{n-}$, where M is the addendum; usually molybdenum or tungsten, less frequently vanadium, niobium or tantalum in high oxidation states.[1a] However, recently it was shown that palladium(II) and gold(III) can act as addenda as well.[12] Heteropolyanions are represented with the general formula $[X_xM_mO_y]^{q-}$ ($x \leq m$) where X, the heteroatom (hence the terminology "hereropoly"), can be one of many elements of the periodic table, most commonly P^{5+}, As^{5+}, Si^{4+}, Ge^{4+} and B^{3+}. Furthermore, there is no restriction on the heteroatom, X, and can be either tetrahedrally coordinated (as in the Keggin structure) or octahedrally coordinated (as in the Anderson-Evans structure). In the latter capacity are found more than sixty-five elements from all groups of the periodic table (except the rare gases). However, the metallic elements that can function as addenda atoms are limited to those with both a favorable combination of ionic radius and charge (charge/radius ratio), and the ability of empty d-orbitals to form π M-O bonds via $d\pi$-$p\pi$ overlaping. POMs can be mixed, where the addenda positions can be occupied by two or more elements (e.g. Mo/V, W/V), or non-mixed, where M is exclusively one metal.[1a]

1.2.1 Structural units

There is an enormous molecular diversity of POMs and many reports, books and reviews have been published about this inorganic family of molecules.[1] POMs can be regarded as packed arrays of pyramidal MO_5 and octahedral MO_6 units (building blocks) and these entities can be considered as similar as the $-CH_2-$ in organic chemistry. These MO_n units can be packed to form different shapes, but there are some simple rules for them to join one another in order to build the POM frameworks. The molecules as a whole are built by edge- and/or corner-sharing MO_n polyhedra, and very rare by face-sharing (Figure 1.1). The most stable linkages are the edge- and corner-sharing models (A and B in Figure 1.1), in which the M^{n+} ions are far enough from each other in order to decrease the columbic repulsion between them (Table 1.1). In the case of the face-sharing contact (C in Figure 1.1) the metallic centers are closer than in

A or B. At such distances the repulsion is not balanced by the stabilization due to the chemical bonding. Nevertheless, Linking of MO_6 octahedra by face-sharing was first reported by Dexter and Silverton in 1968 presented the structure of $[CeMo_{12}O_{42}]^{8-}$.[13] This species consists of six pairs of face-shared octahedra (Mo_2O_9 unit) resulting in icosahedral geometry. The molybdenum atom positions with mean Mo…Mo separations of 3.18 and 3.84 Å (face- and corner-shared contacts respectively).[1a]

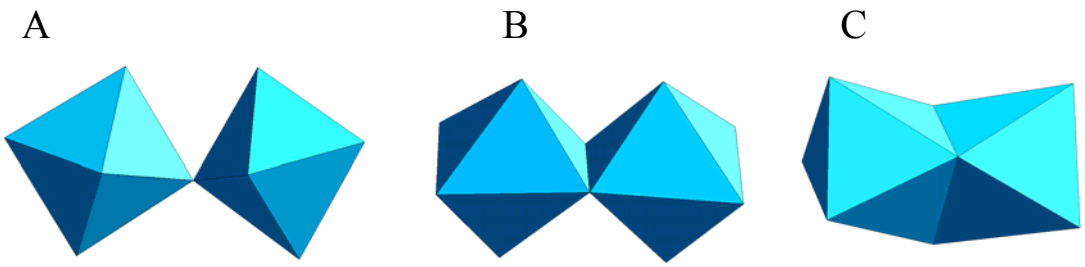

Figure 1.1 Polyhedral models that represent the possible linkages between two MO_6 octahedral units. A) corner-sharing, B) edge-sharing and C) face-sharing. Each corner represents an oxygen position.

Table 1.1. M … M distances (Å) of corner- and edge- sharing octahedra in POMs.

Metal Ion	corner- sharing	edge- sharing
W(VI)	3.70	3.41
Mo(VI)	3.70	3.41
V(V)	3.50	3.20

1.2.2 Some common structures

Some common structural types of isopoly- and heteropolyanions are depicted in Figure 1.2 and 1.3:[1]

1.2.2.1 Isopolymetalates, $[M_mO_y]^{n-}$:

a) The hexametalate $[M_6O_{19}]^{n-}$ "Lindqvist" structure, (O_h symmetry), is a compact arrangement of six edge-shared MO_6 octahedra, (M = Nb, Ta, n = 8; M = Mo, W, n = 2).

b) The paratungstate-B structure $[H_2W_{12}O_{42}]^{10-}$ (C_{2h} symmetry) is based on the arrangements of twelve edge- and corner-shared WO_6 octahedra.

c) The metatungstate α-$[(H_2)W_{12}O_{40}]^{6-}$ structure (T_d symmetry) is composed of twelve WO_6 octahedra arranged in four M_3O_{13} groups of three edge-shared WO_6 octahedra, linked via corner-sharing to each other.

d) The heptametalate $[M_7O_{24}]^{6-}$ structure, (C_{2v} symmetry), is based on the arrangements of seven edge-shared MO_6 octahedra (M = Mo, W).

a) $[M_6O_{19}]^{n-}$

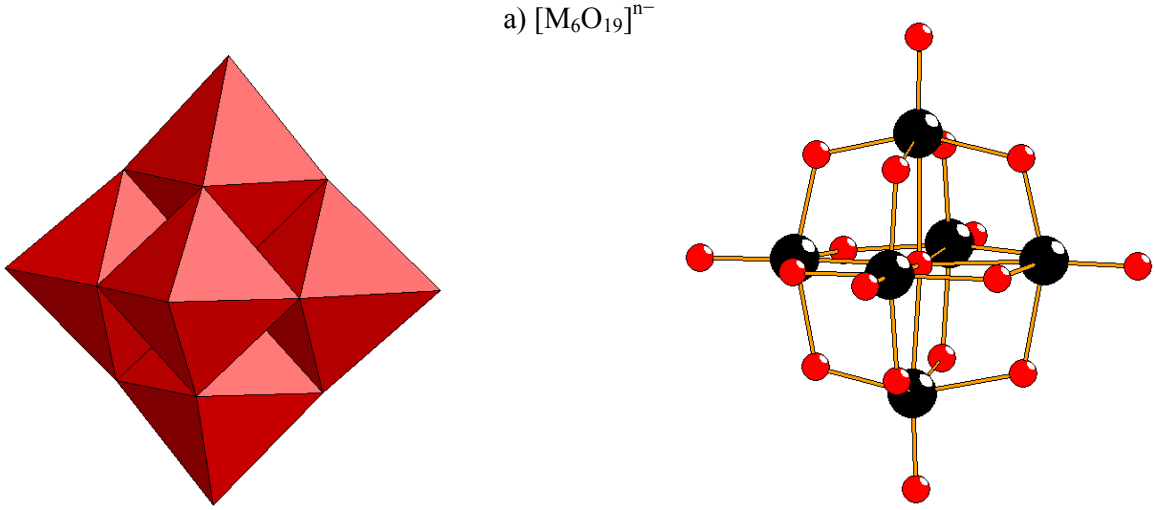

b) $[H_2W_{12}O_{42}]^{10-}$

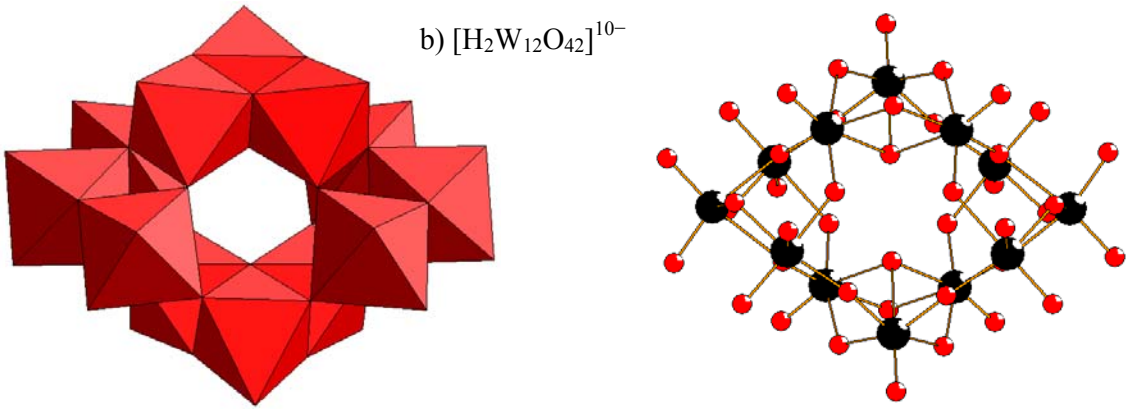

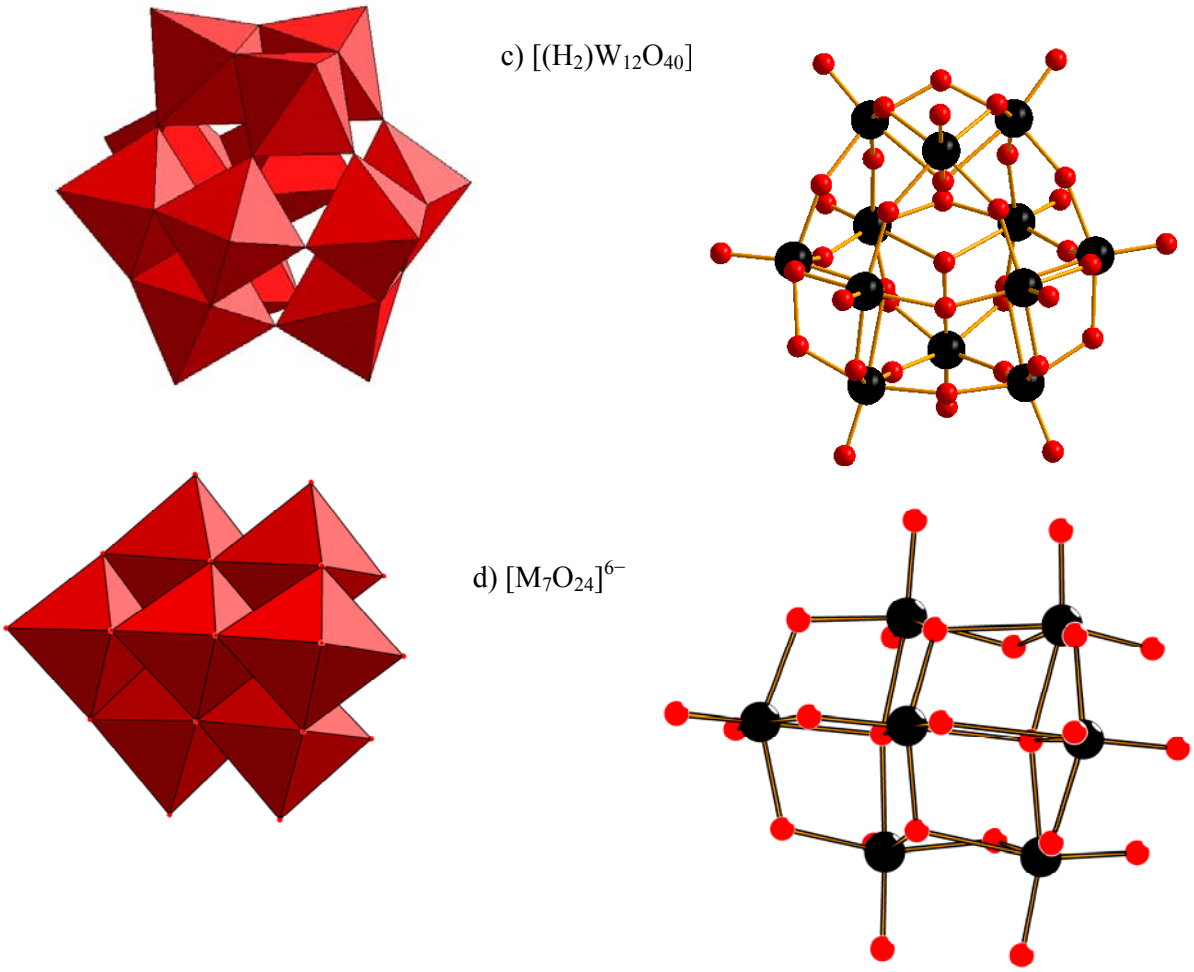

Figure 1.2 Polyhedral and ball-and-stick representations of some common isopolyanions. The colour code is as follows: MO_6 octahedra (red), black spheres are metal centers and red ones are oxygens.

1.2.2.2 Heteropolymetalates, $[X_xM_mO_y]^{q-}$:

a) The Keggin α-$[XM_{12}O_{40}]^{n-}$ structure (T_d symmetry) is composed of twelve MO_6 octahedra arranged in four M_3O_{13} groups of three edge-shared MO_6 octahedra, linked via corner-sharing to each other and to the central heteroatom XO_4 tetrahedron.

b) The Wells-Dawson structure (D_{3h} symmetry) is composed of two fused A-α-$[XM_9O_{34}]^{n-}$ via corners (M = Mo(VI), W(VI), X = P(V), As(V), and n = 6).

c) The Anderson-Evan $[XM_6O_{24}]^{n-}$ structure (D_{3h} symmetry) is based on a central heteroatom XO_6 octahedral surrounded by a planer arrangement of six MO_6 octahedra edge-sharing. The Keggin and Wells-Dawson structures will be discussed in some details below.

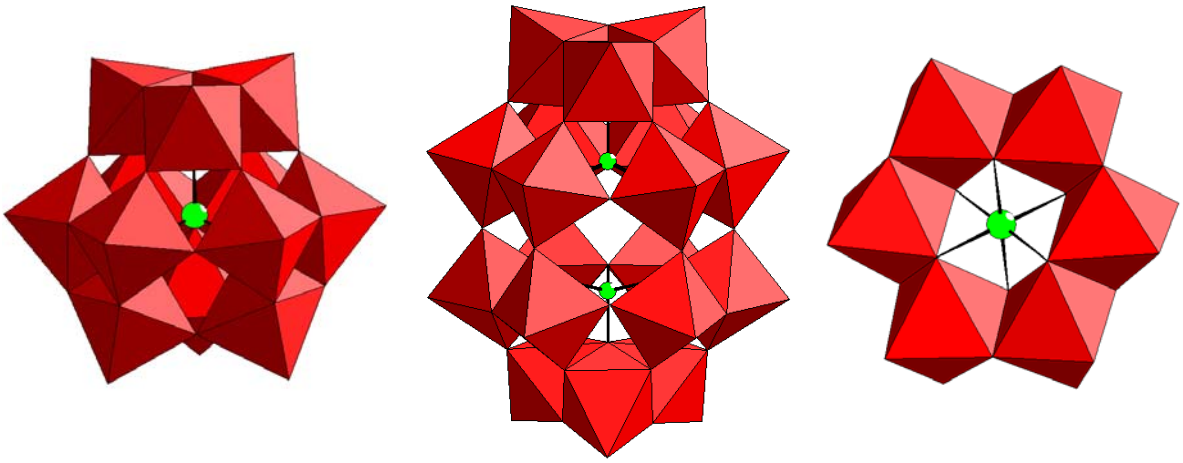

a) α-$[XM_{12}O_{40}]^{n-}$ b) α-$[X_2M_{18}O_{62}]^{n-}$ c) $[XM_6O_{24}]^{n-}$

Figure 1.3 Combined polyhedral/ball-and-stick representations of some common heteropolyanions. The colour code is as follows: MO_6 octahedra (red), green spheres are X heteroatoms.

It is noteworthy that POMs structures appear to be governed by two general principles:[1b]

1- Each metal atom occupies an MO_n coordination polyhedron in which the metal atoms are shifted as a result of metal-oxygen π bonding, towards those polyhedral vertices that form the surface of the structure. Thereby, the addenda atom M does not lie at the center of the polyhedron of the oxide ion but displaces strongly towards the exterior of the polyanion structure. Therefore, the metal atoms M are never located at inversion centers. The heptatungstate $[M_7O_{24}]^{6-}$ structure is an exception (C_{2v} symmetry with central W^{6+} ion).

2- Structures with MO_6 octahedra that contain more than two free vertices are, in general, not observed. This principle for understanding the limitation of POMs structures was suggested by Lipscomb in 1964,[14] which states that each metal atom should bear no more than two terminal oxo groups. Structures that have a metal atom with three terminal oxygens (three free vertices) and appear to contradict the Lipscomb principle are very rare and may be rationalize

by protonation of a *fac*-MO_3 group to cis-$MO_2(OH)$. However, such structures are likely uncommon, since the terminal oxygens of the MO_3 groups are more basic/nucleophilic than those of MO_2 and MO and will therefore undergo further polymerization. Furthermore, structures that have a metal atom with no terminal oxo groups (e.g. $[M_7O_{24}]^{6-}$, $[V_{10}O_{28}]^{6-}$) may be rationalize by displacements of that atom towards the edge of its MO_6 octahedral. Moreover, Pope classifies polyanions in the term of the number of terminal oxygen atoms M=O per addenda MO_6 octahedron as type I "monooxo complexes" and type II "cis-dioxo complexes". Type I complexes have one W=O bond while type II two in cis positions. Since type I MO_6 octahedra (mono-oxo MOL_5) can accommodate addenda atoms with d^0, d^1, and d^2 electronic configurations, type II octahedra (cis dioxo MO_2L_4) are restricted to only d^0 addenda atoms .[1a]

1.3 Keggin-type POMs and derivatives

The structure depicted in Figure 1.3-a "$[XM_{12}O_{40}]^{n-}$" was first reported as aforementioned by Keggin in 1933 in the form of 12- tungtophosphoric acid and has been confirmed and refined in many other structure determinations afterwards. The Keggin structure and its derivatives are the most widely studied.

The $[(XO_4)(M_{12}O_{36})]^{n-}$ Keggin structure is based on a central heteroatom XO_4 tetrahedron surrounded by four M_3O_{13} groups "triads" of three edge-shared MO_6 octahedra. These triads are linked via corner-sharing to each other and to the central XO_4 tetrahedron via μ_2- and μ_4-oxo bridges respectively, this results in a high symmetry (T_d) as shown in Figures 1.3-a and 1.4.

The Keggin is a type I complex with one terminal oxygen atoms M=O per addendum and a significantly longer trans bond. IR spectroscopy differentiates that bands of such types of bonding with the W=O vibration band lying at higher wave number side.

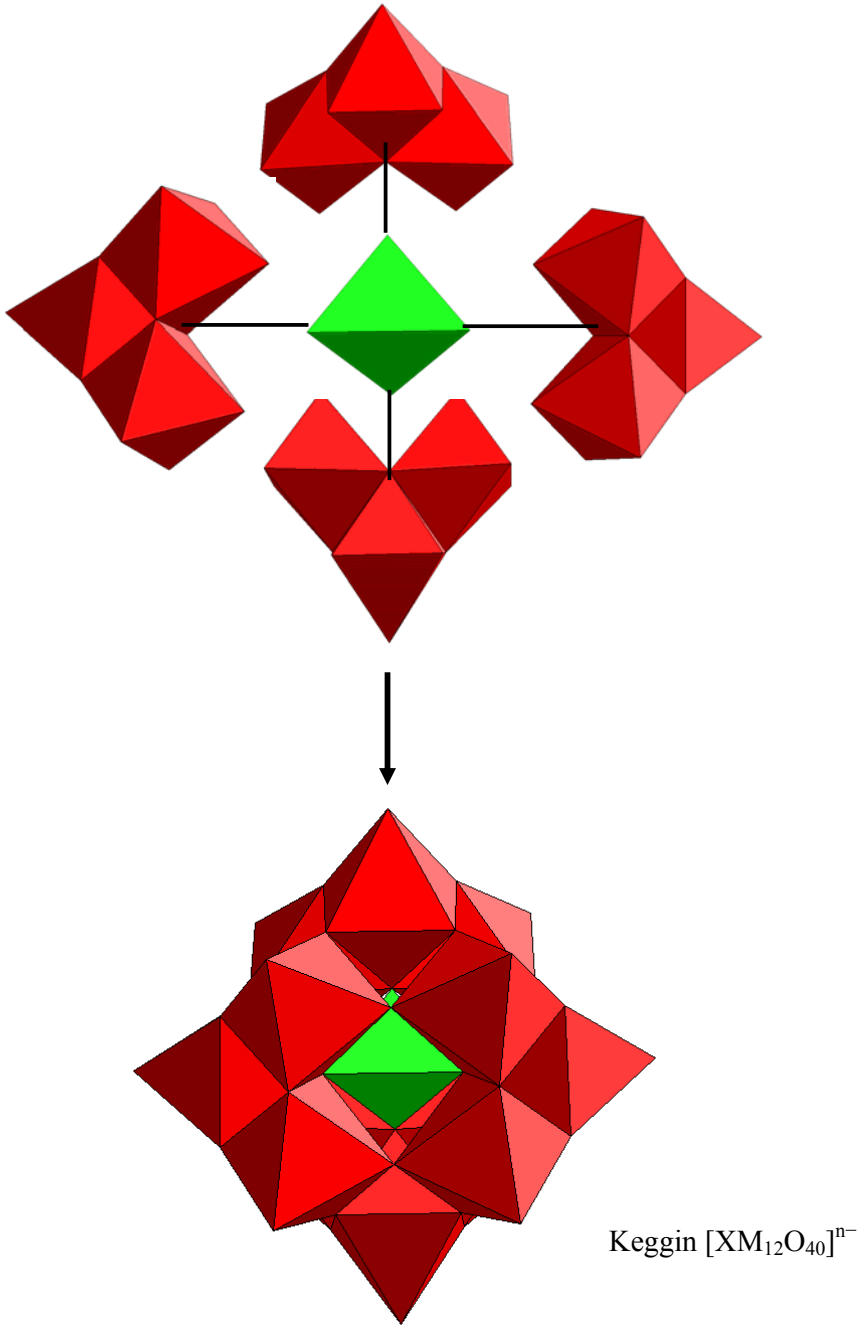

Figure 1.4 The four M_3O_{13} triads and one XO_4 tetrahedron generate the Keggin-type $[XM_{12}O_{40}]^{n-}$ heteropolyanion. The colour code is as follows: MO_6 octahedra (red) and XO_4 tetrahedal (green).

As aforementioned, the tetrahedral heteroatom at the center of the Keggin unit can be any of a wide array of elements. The most commonly investigated structures are those containing, P^V, As^V, Si^{IV}, Ge^{IV} as the heteroatom but other transition metals and non-metals have been observed playing this role. Few types of addenda atoms have been observed in Keggin

structures; typically, the addenda are molybdenum and tungsten, being the W the most common due to the stability of the polyoxotungstates in solution. Keggin-type heteropolyanions are known to be the most investigated POMs and with the most applications found, mostly due to their properties as electron/ proton givers and acceptors.[1]

1.3.1 Baker-Figgis isomers

Keggin-type heteropolyanions can have five different rotational isomers known as Baker-Figgis.[17] The structure illustrated in Figures 1.3-a and 1.4 with T_d symmetry is called α isomer. By a 60˚ rotation of one, two, three or all four triads, the isomers β, γ, δ and ε can be formed, generating structures of C_{3v}, C_{2v}, C_{3v} and T_d symmetry respectively, see Figure 1.5.[1a]

It is noteworthy that the symmetry of β structure is reduced from T_d to C_{3v} and the new corner-shared W-O-W contacts between the rotated triad and the rest of the anion have two features which may account for its lower stability than α isomer, shorter W … W separation and more acute W-O-W angles than the α isomer. This results in an increasing of the coulumbic repulsion and less favourable dπ-pπ interactions.

Isomers γ, δ and ε have some triads with edge-sharing which results in a decrease in the dπ-pπ interactions, therefore, these isomers are less stable than the α and β ones. Although, γ, δ and ε isomers are coulumbically-unfavourable and isomerize to α in aqueous solution,[18] derivatives of γ-structure have been reported.

Isomers α and β have no edge-sharing triads, therefore should have similar stability, but it is experimentally observed that β is less stable and isomerizes to α in aqueous solution as well. Nevertheless, the equilibria between α and β isomers of Keggin heteropolytungstates have been studied confirming that α and β isomers are similar in energy.[19] Recently, it has been proven by theoretical calculations that the β isomer is more polarizable than α one due to its lower symmetry. Furthermore, the stability of the β isomer is dependent on the nature of the central XO_4 group and the net charge of the cluster.[20]

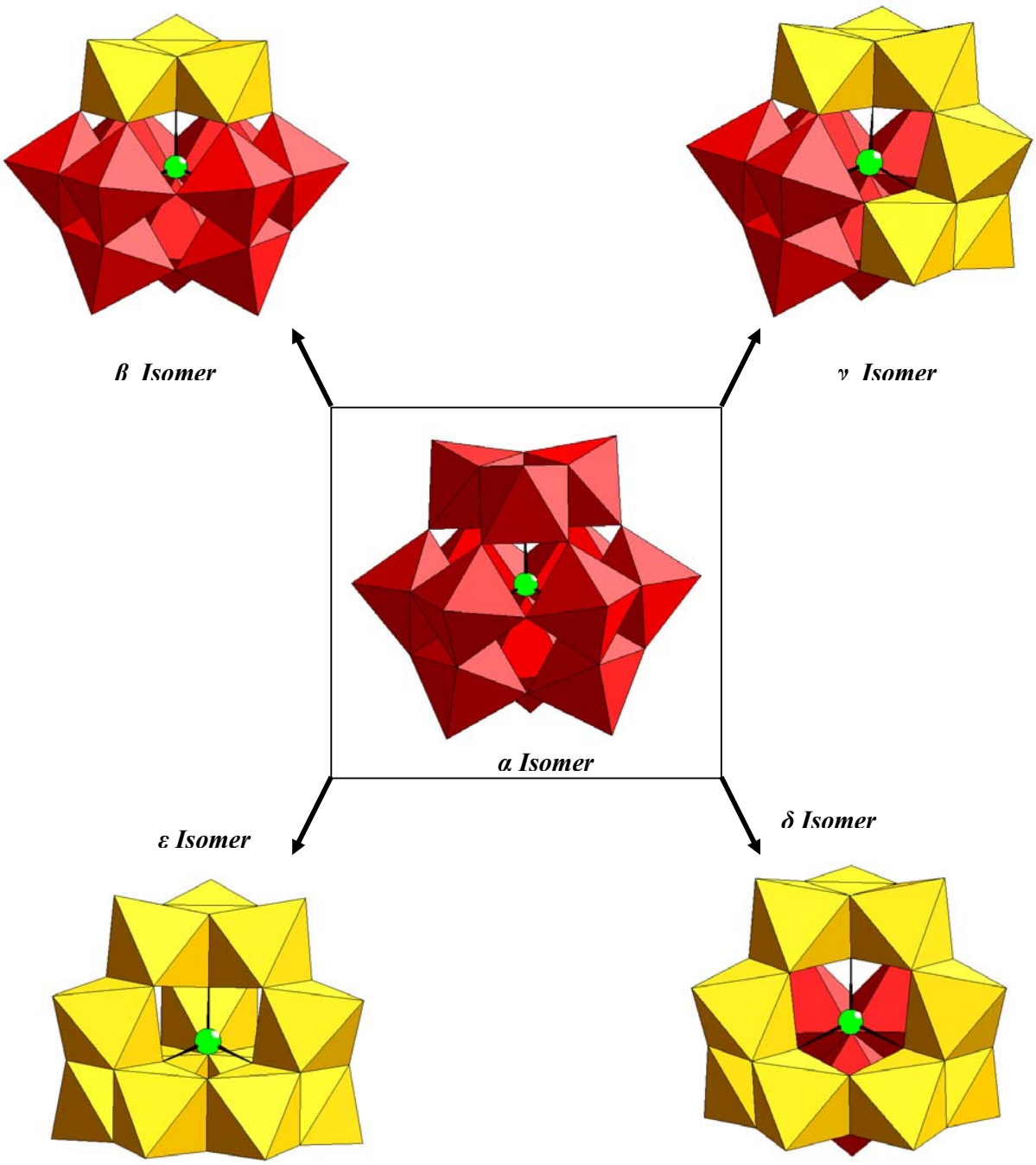

Figure 1.5 Baker-Figgis isomers of the Keggin anion. Red and yellow octahedra: MO_6, green sphere: X heteroatom. The rotated triads were colored yellow for clarification.

1.3.2 Lacunary species

Lacunary (vacant) species or defect derivatives of the Keggin structures are obtained by removal of one, two, or three MO_6 octahedra under basic conditions forming what so-called

mono-, di-, and tri-lacunary species.[1a] They can be obtained from three of the Baker-Figgis isomers, α, β and γ, by removing adjacent MO_6 octahedra. These lacunary species can act as ligands towards the transition metal ions that can bind to the POMs at the vacant sites.

The plenary α-$[XW_{12}O_{40}]^{n-}$ Keggin ion is stabilized under acidic conditions but it can lose one or three adjacent MO_6 octahedra to form mono- and tri-lacunary species by increasing the pH of the solution. The trilacunary species can be either *A*-α-, in which three corner-shared octahedra have been lost "$[XW_9O_{34}]^{n-}$" (tetrahedral), or *B*-α, in which three edge-shared octahedra have been lost "$[XW_9O_{33}]^{n-}$" (pyramidal), see Figure 1.6. Therefore, the type *A* relates to the association of one W_3O_{10} and three W_2O_6 groups around the central XO_4 tetrahedron and the type *B* to the association of three W_3O_{10} groups around the central XO_3 pyramid. It is noteworthy that only one type for the mono-lacunary α-$[XW_{11}O_{39}]^{n-}$ isomer can be obtained, due to the T_d symmetry, by which the all twelve octahedra of the parent Keggin ion are equivalent.

In contrast, the non-equivalent octahedra due to C_{3v} symmetry of the β isomer, implies the formation of different types of lacunary species depending on the position and the type of octahedra removed. Therefore, three types of the mono-lacunary species can be obtained (β_1, β_2, β_3-$[XW_{11}O_{39}]^{n-}$), that differ in the position of the vacant. The vacancy is located in the opposite triad to the rotated one for β_1 (unconnected with the rotated triad) and in the belt for β_2 (connected with the rotated triad), while β_3 is generated by the removal of one of the three octahedra that are part of the rotated triad, see Figure 1.7. Two trilacunary species, *A*-β and *B*-β can be obtained from the plenary β-$[XW_{12}O_{40}]^{n-}$ Keggin by removal a triad, the opposite triad to the rotated one (three corner-shared octahedra) for *A*-β type, and any triad (three edge-shared octahedra) except for the rotated one for *B*-β type, see Figure 1.7.

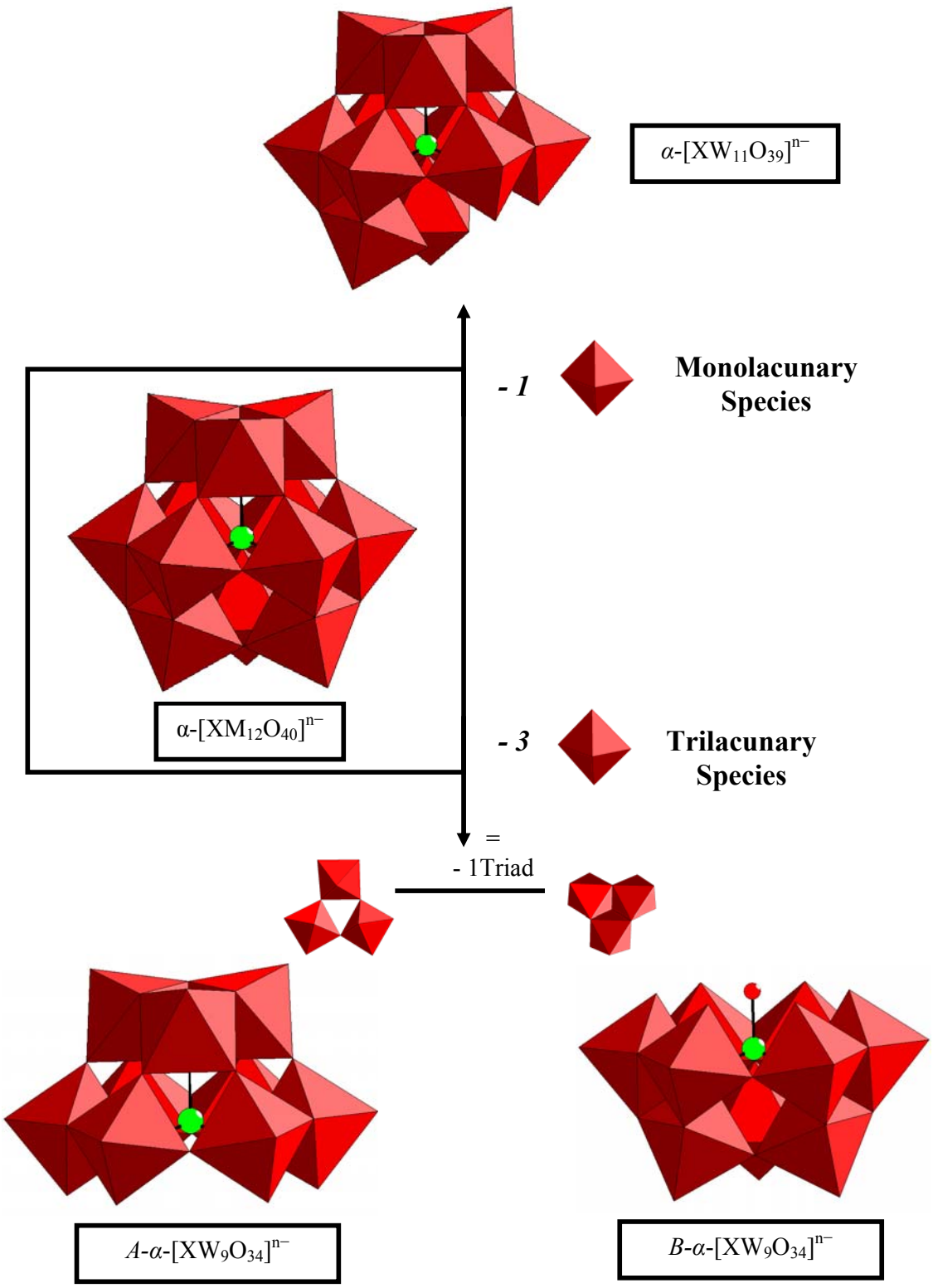

Figure 1.6 Lacunary species derived from the *α*-Keggin structure. Red octahedra: MO_6, green sphere: X heteroatom, red sphere: oxygen.

Removal of two adjacent octahedra from α- and β-$[XW_{12}O_{40}]^{n-}$ isomers has not been observed, but only for the γ isomer, the $[XM_{10}O_{36}]^{n-}$, see Figure 1.8. The plenary polyanions are stabilized under very acidic conditions (pH 0-2), monolacunary species are found at slightly acidic pH (4-6), and trilacunary ones are stable at pH (8-10).

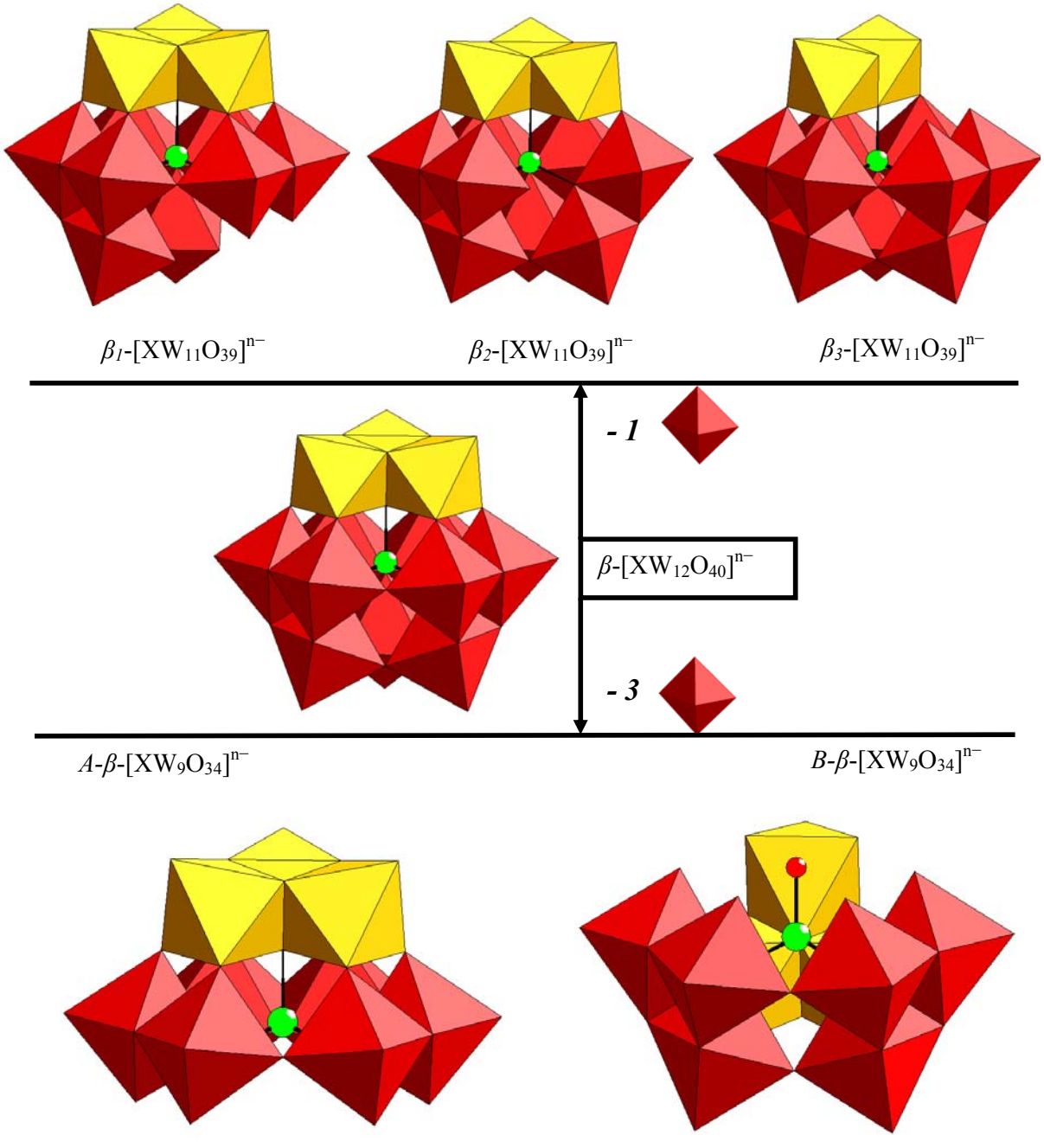

Figure 1.7 Lacunary species derived from the β-Keggin structure. Red and yellow octahedra: MO_6, green sphere: X heteroatom, red sphere: oxygen.

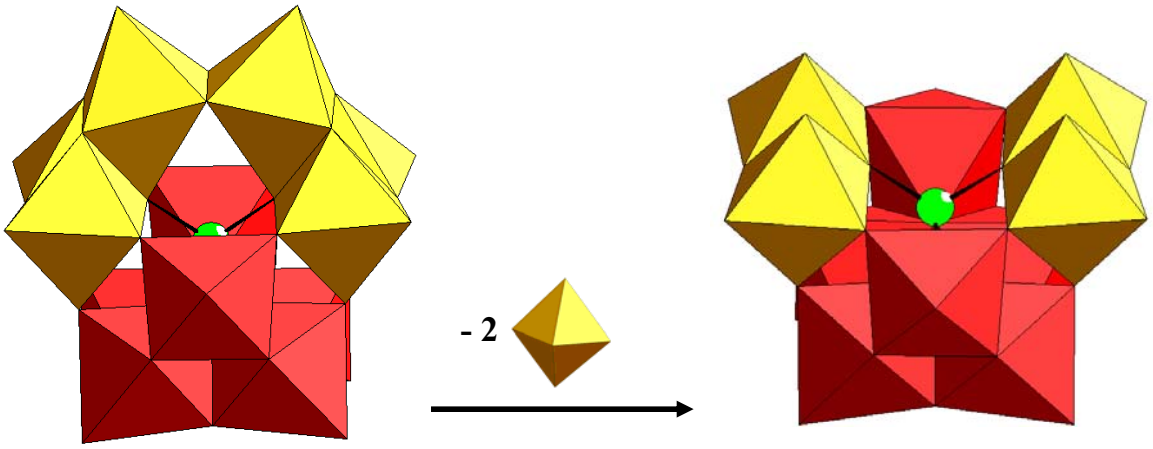

Figure 1.8 Dilacunary species derived from the γ-Keggin structure. The color code is the same as in Figure 1.5.

1.4 Wells-Dawson-type POMs and derivatives

In 1952, Wells synthesized the 18-tungstophosphate complex and proposed its structure as $[P_2W_{18}O_{62}]^{6-}$ afterwards, in 1953, the structure was determined by a single-crystal X-ray diffraction by Dawson and the structure was named after them.[1a] This is now known as α-$[P_2W_{18}O_{62}]^{6-}$ "Wells-Dawson" structure which consists of two *A*-α-$[PW_9O_{34}]^{9-}$ units (trilacunary Keggin) fused into a cluster of virtual D_{3h} symmetry. The structure involves two types of tungsten atoms, six "polar" and twelve "equatorial" forming the two caps and the two belts of the polyanion, respectively. Each cap is composed of three edge-shared octahedra (triad), whereas the two belts are formed via alternative corner- and edge-shared MO_6 units, as depicted in Figures 1.3-b and 1.9. It is noteworthy that the Wells-Dawson structure is known for the heteroatoms P(V), As(V), and S(VI) and for the addenda atoms W(VI) and Mo(VI). The β isomer can be formed by a 60˚ rotation of one cap, reducing the symmetry from D_{3h} to C_{3v}. The α and β isomers have been distinguished by ^{183}W-NMR technique.

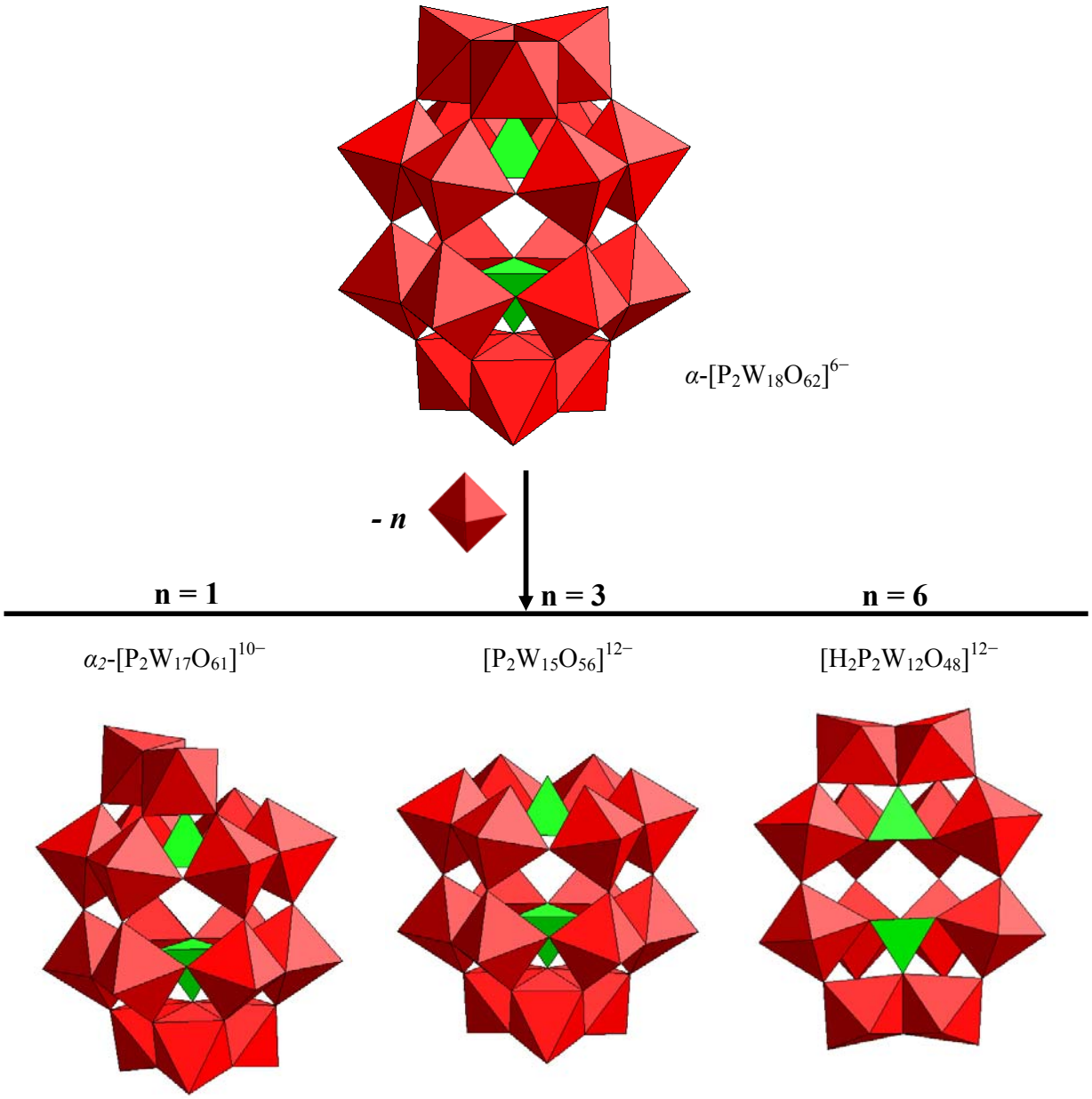

Figure 1.9 Polyhedral representation of lacunary species of the Wells-Dawson structure. WO_6 octahedra (red), PO_4 tetrahedra (green).

1.4.1 The Mono- and tri-lacunary species

Some vacant species corresponding to the complete α-$[P_2W_{18}O_{62}]^{6-}$ (**P_2W_{18}**) anion can be formed and isolated in aqueous solution depending on the pH and counter-cations present during their synthesis. The monovacant anion $[P_2W_{17}O_{61}]^{10-}$ (**P_2W_{17}**) is isolated as a

potassium salt by hydrolysis of **P_2W_{18}** at pH 6-7 using $KHCO_3$. The trivacant anion $[P_2W_{15}O_{56}]^{12-}$ (**P_2W_{15}**) (Figure 1.9) is however formed by hydrolysis of **P_2W_{18}** using Na_2CO_3 without the presence of potassium at pH 9-10, and is isolated as a sodium salt.

Two isomers of the monolacunary α_1-$[P_2W_{17}O_{61}]^{10-}$ and α_2-$[P_2W_{17}O_{61}]^{10-}$ species exist, where the vacant site in the belt or in the cap, respectively. However, the α_1-**P_2W_{17}** anion is unstable and readily undergoes isomerization to the α_2-**P_2W_{17}**, which is depicted in Figure 1.9.[1f]

1.4.2 The hexa-lacunary species

The hexavacant anion $[H_2P_2W_{12}O_{48}]^{12-}$ (**P_2W_{12}**) (Figure 1.9) is formed by interaction of **P_2W_{18}** with the base (tris-hydroxymethylaminomethane) and is isolated as a potassium salt.[1f] Although **P_2W_{12},** being hexavacant, is regarded as a multi-dentate ligand for interaction with electrophiles, it rearranges in acidic aqueous medium to the monolacunary α_1-**P_2W_{17}** which in turn is unstable and rearranges to the more stable α_2-**P_2W_{17}**, due the metastability of **P_2W_{12}** in solution.[1a,1f]

Contant and Tézé were able to condense four **P_2W_{12}** units in lithium acetate buffer, resulting in the cyclic polyanion $[H_7P_8W_{48}O_{184}]^{33-}$ (**P_8W_{48}**) which can be isolated as a mixed potassium/lithium salt.[21] The wheel-shaped phosphotungstate **P_8W_{48}** polyanion is stable at an unusually large pH range (1-8) and has D_{4h} point symmetry, as depicted in Figure 1.10. The multi-vacant **P_8W_{48}**, having 16 donor oxygens and a large central cavity (diameter of around 10 Å), can be considered as 'super-lacunary', but its stability and inertness were noteworthy.

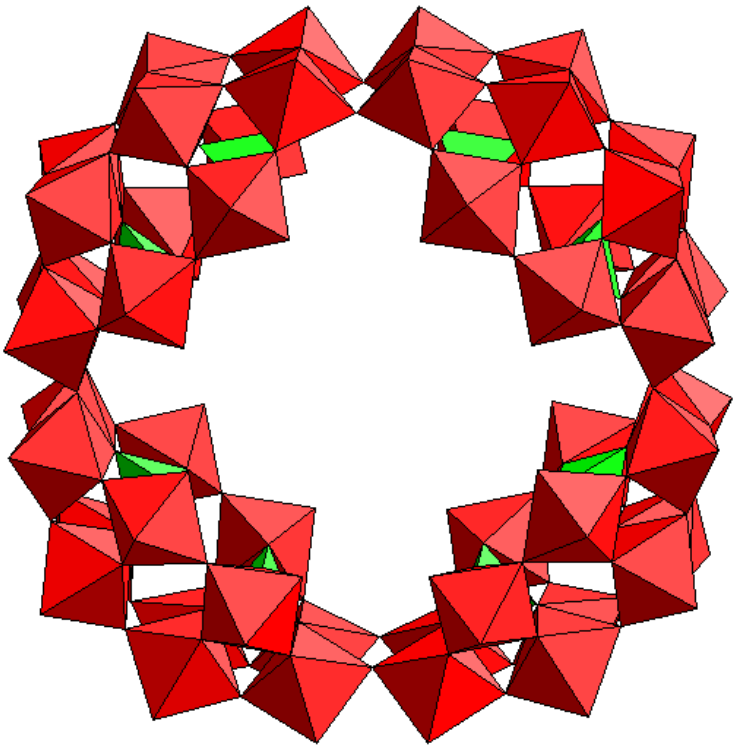

Figure 1.10 Polyhedral representation of $\mathbf{P_8W_{48}}$ polyanion. Red octahedra: WO_6, green tetrahedra: PO_4.

1.5 Typical properties of POMS

POMs are discrete and high symmetrical species with a wide versatility in terms of their size, charge, structure and molecular weight. They are thermally robust and stable against oxidants. Isopoly- and heteropolyanions can be prepared and isolated from both aqueous and non-aqueous solutions. By far, the most common preparative method involves acidification of aqueous solutions of simple oxoanions $[MO_n]^{m-}$ that will reorganize to a packed molecular array of MO_n units. In a formal sense, POMs are formed via Brønsted acid-base condensation-addition processes, e.g.[1]

$$7WO_4^{2-} + 8H^+ \longrightarrow [W_7O_{24}]^{6-} + 4H_2O$$

$$12MO_4^{2-} + H_3PO_4 + 21H^+ \longrightarrow [PM_{12}O_{40}]^{3-} + 12H_2O$$

The equilibrium constant and the rate of formation of this type of structures is determined by a series of factors[1a,15]: pH and ionic strength of the reaction media, concentration and ratio of the reagents and the sequence in which they are mixed, temperature, and even the employed counter ion. In many cases, the equilibrium constant and rate of formation are large enough that the polyanions can be crystallized as salts at room temperature.[1a]

POMs can usually be isolated from aqueous solution as solid salts with appropriate counter cations which may be alkali metal cations (e.g. Li^+, Na^+, K^+, Rb^+, Cs^+) or organic cations (e.g. guanidinium, alkylammonium). Lithium and sodium salts tend to be more water-soluble than those of the larger cations. Furthermore, salts of cations of organic nature such as tetrabutylammonium (TBA) are soluble in nonaqueous media as well as aqueous ones.

The majority of POMs studies have been achieved in aqueous solution,[16] and they have shown that for a certain pH many species can coexist in equilibrium, therefore the structure isolated as crystals doesn't have to be the predominant one in solution, but the one that yields the less soluble compound.[1b] It is noteworthy that although the first POM was made in 1826, the mechanism of POM formation is still not completely understood and is often described as a self-assembly process. Furthermore, the driving force for the formation of high-nuclearity clusters is a big challenge to understand.

The structure of the isolated polyanions can be determined in the solid state by single-crystal X-ray diffraction and a diamagnetic nature enables the use of multinuclear NMR, which is the most powerful technique for studying the structure in solution. The thermal stability of the polyanion salts can be determined in the solid state by thermogravimetric analyses (TGA) technique. Furthermore, Infrared and Raman spectroscopy are extensively used in POM chemistry either for fingerprint assignments or for structural elucidation. The most characteristic region of the POM spectra is *ca*. 1000 – 400 cm^{-1}, where the absorptions of Metal–Oxygen stretching vibrations occur.

In general, POMs exhibit a multitude of properties: stability in solution and in the solid state, solubility in organic and aqueous solvents, electrochemical activity and incorporation of main group elements, transition metals, rare earths or organic groups. Two of these properties will be discussed below.

1.5.1 Acid properties of polyoxometalates

The free acids of POMs, in which the proton H^+ acts as the only counter-cations on the anion, "heteropoly acids, HPAs" have high Brønsted acidity of the corresponding acids. The strengths of the common Keggin molybdic and tungstic acids are stronger in a Brønsted sense than the common mineral acids such as HCl, H_2SO_4 and HNO_3. Early methods of characterization of HPAs involved titration with base to determine stoichiometry. Two end-points can be detected, the first corresponding to the neutralization of the acid protons and the second to the complete dissociation of the anions.[1a,1f] As aforementioned the first X-ray investigation of POMs were made on the acids, started by Keggin in 1933. Keggin structure was redetermined on various types of heteroatoms by both X-ray and neutron diffraction, the latter showed and confirmed the number of the protons attached to the polyoxometalate anions. Furthermore, the acid centers are considered to be at the bridging oxygen atoms on the surface of the anion.[1a,1f]

1.5.2 Redox activity of polyoxometalates

The addenda metal atoms in most POMs are in their highest oxidation states (d^0), therefore many POMs are powerful oxidizing agents and undergo multiple reversible one- or two-electron reductions which lead to form intensely colored mixed-valence species "heteropoly blue". POMs are known which can accept many electrons up to 32 without major structural change. Therefore, POMs are unequaled in their "electron reservoir" properties. The reduction process depends on the acidity of the solution and the polyanion charge where the additional

negative charges have to be accompanied by protonation from the solution to keep the electro-neutrality. Therefore, the reductions involve addition of electrons and simultaneously acceptance of protons.

Cyclic voltammetry and spectroscopy measurements can be used to study the redox property of POMs. Cyclic voltammograms of molybdate and tungstate Keggin anions (type I, mon-oxo structure) display sequences of reversible of one and two-electron reductions which result in the deeply blue species. Electronic spectra of the reduced species show intensity-enhanced d-d bands in the visible and intervalence charge transfer (IVCT) in the near-IR regions. ESR spectroscopy demonstrated that the unpaired electron added to the Keggin undergoes rapid hopping (intramolecular electron transfer) amongst the 12 addenda centers at room temperature. Anions generated by two-electrons reduction are ESR silent.[1a, 1b,1f] POMs can be reduced by various means, e.g. chemical, electrochemical, photocatalytic, producing blue species.

1.6 Applications

The applications of POMs are mainly based on their unique properties, including size, mass, electron- and proton-transfer/storage abilities, thermal stability, and high Brønsted acidity of the corresponding acids. Applications of POMs as catalysts focus on their redox and acid-base properties. POMs can efficiently absorb light in the near UV-vis region and can therefore be used as photocatalysts.[22] The intrinsic chemical properties of POMs as electron acceptors or as very strong Brønsted acids (in their protonated form) make them useful as catalysts in organic transformations, and their abilities to form peroxo complexes or to serve as supports for catalytically active metal ions in high oxidation states are particularly useful in oxidation reactions. Furthermore, chemical modifications in the composition of POMs allow for fine tuning of their Lewis acidity.[23]

1.6.1 Photocatalysis

POMs, especially polyoxotungstates, are effective homogeneous photocatalysts for the mineralization of organic pollutants in the aquatic environment (i.e. degradation of organic pollutants to CO_2, H_2O and the corresponding inorganic anions).[22] POMs (in a particular $[PW_{12}O_{40}]^{3-}$ and $[SiW_{12}O_{40}]^{4-}$) are at least as effective as the well-studied TiO_2 (metal oxide particulates) in their photocatalytic activity. Furthermore, POMs as photocatalysts have advantages relative to TiO_2 in terms of their selective reduction precipitation of metal ions and their unique to form metal nanoparticles in which POMs act as both reducing reagents and stabilizers. The redox chemistry of POMs renders them to act as multielectron relays. $OH^{\cdot}$ radicals generated by the reaction of the photo-excited polyoxotungstates with H_2O seem to play a key role in the process. The photocatalytic cycle is closed by reoxidation (regeneration) of the reduced POMs by either dioxygen O_2 which is the mainly process or by metal ions, in the latter process metal ions are reduced and precipitated and removed from the solution. Hence, POMs as photocatalysts can be used for decontamination of waste waters from both organic and inorganic pollutants:

$$POM + S \xrightarrow{h\upsilon} POM_{red} + S_{ox}$$

$$POM_{red} + M^{n+} \longrightarrow POM + M_{red}$$

It is noteworthy that in the absence of O_2, the regeneration of the catalyst will not take place, at least at the first stages of the photolysis. Therefore, the blue color of the one-electron reduced POMs, $[XW_{12}O_{40}]^{(n+1)-}$, will be accumulated.

The two previous simplified equations (where POM = $[XW_{12}O_{40}]^{n-}$, S = organic substrate, and M^{n+} = metal ion) can be clarified as the followings: POM can efficiently absorb light in the near UV-vis region and subsequently excite at the O−M CT band (Ligand−Metal Charge

Transfer). This excitation of POM leads to electron (e^-) hole (h^+) separation in analogy to semiconductors (e.g. TiO_2);

$$POM \xrightleftharpoons{h\upsilon} POM\,(e^- + h^+)$$

The generated photoholes act as powerful oxidizing species towards a diversified number of organic compounds through either a direct or indirect process;

Direct Oxidation:

$$POM\,(e^- + h^+) + S \longrightarrow POM\,(e^-) + S^+$$
(*oxidation products*)

Indirect Oxidation:

$$POM\,(e^- + h^+) + H_2O \longrightarrow POM\,(e^-) + OH^{\cdot} + H^+$$

$$POM\,(e^-) + H^+ + (OH^{\cdot} + S) \longrightarrow POM\,(e^-) + H_2O\,(OH^- + H^+) + S^+$$
(*oxidation products*)

The action of $OH^{\cdot}$ radicals (indirect oxidation) relative to h^+ seems to be more pronounced with $[XW_{12}O_{40}]^{n-}$ than TiO_2, where POM($e^- + h^+$) and POM(e^-) represent the excited state of $[XW_{12}O_{40}]^{n-}$ and the reduced form $[XW_{12}O_{40}]^{(n+1)-}$, respectively.

The photocatalytic degradation mostly mineralizes the organic compounds forming CO_2, H_2O and the corresponding inorganic anions; e.g. NO_3^-, SO_4^{2-}, PO_4^{3-}. The characteristic reactions can include for examples; hydroxylation, H-abstraction, dehalogenation, decarboxylation, denitration, and desulfurization followed by C−C bond cleavage. Hence, the final degradation products for most organic substrates are CO_2, H_2O and inorganic anions as aforementioned.

In the photocatalytic treatment with POM, the reoxidation (regeneration) of the catalyst is a crucial reaction to close the photocatalytic cycle;

$$POM\,(e^-) + \text{oxidant} \longrightarrow POM$$

It is noteworthy that dioxygen, the most common and benign oxidant, undergoes reduction in the process (O_2^-) which initiates further oxidations of organic compounds. Although,

dioxygen is the most effective oxidant, other oxidants can be used for the same purpose, e.g. H^+ and M^{n+}. This reaction produces O_2^- ($O_2^{\cdot}$), H_2, or M^0 and decolorizes the solution. However, the ability of photoreduced POM to be oxidized by metal ions depends on the reducing ability of POM, the oxidizing ability of the metal ion and a lesser extent on the nature of the organic substrate;

$$POM\ (e^-) + M^{n+} \longrightarrow POM + M^{(n-1)+}$$

By using better oxidizing reagents for roxidation of the reduced POM leads to produce more catalyst in the oxidized form which is available to reabsorb light and oxidize organic compounds. Therefore, a faster photocatalytic degradation process can be achieved.

1.6.2 Acid catalysis

Acid catalysis by heteropoly acids (HPAs) can be related to the known data on their acidity. Keggin compounds of the type $H_n[XM_{12}O_{40}]$ are very strong Brønsted acids. Therefore, HPAs are often completely dissociated in aqueous solution. Upon reduction, the anions basicity increase and, consequently, the anions have a tendency to become protonated (the proton-transfer/storage ability) and may themselves be reoxidized with oxygen.

HPAs as catalysts have the advantages of being nonvolatile, odorless, and thermally stable which make them more attractive rather than mineral acids like sulfuric and hydrochloric acid. Their acid-base and redox properties can be varied by changing the chemical composition where the acid strength of the HPAs in solution decreases in the series PW > SiW ≥ PMo > SiMo. They can be used in homogeneous acid catalysis as well as in heterogeneous catalysis using supports like silica gel or activated charcoal. An additional advantage of POMs is the fact that heteropoly acids can be separated and enriched by extraction into organic solvents.[1a,b,f, 23]

1.6.3 Oxidation catalysis

Compared to the use of heteropoly acids in acid catalysis, the use of POMs in oxidation catalysis is a much more diverse area. It is noteworthy that complex anions such as $[SiW_{11}O_{39}]^{n-}$ have been used as inorganic analogues of metalloporphylins,[24] but with some differences and advantages:

1) The inorganic POM ligand is not susceptible to oxidative degradation and is thermally more robust than porphin or other macrocyclic ligands.

2) The acceptor properties of the POMs ligand are dependent on its reducibility and can be modified by metal replacement or by partial reduction.

3) The electron population on metal and ligand is considerably more variable than for the metalloporphyrins.

POMs as catalysts can be used, for instance, in the formation of carboxylic acids from the corresponding aldehydes, as well as in the dehydrogenation of alcohols, aldehydes, and carboxylic acids to form C=C and C=O bonds;

$$[POM]_{ox} + nH^+ + S \longrightarrow H_n[POM]_{red} + S_{ox}$$

$$H_n[POM]_{red} + n\backslash 4\ O_2 \longrightarrow [POM]_{ox} + n\backslash 2\ H_2O$$

Heterogeneous catalytic oxidation processes involving well-characterized POMs have been reviewed.[25] Homogeneous oxidative catalytic activity has been demonstrated for thermal dehydrogenation.[26] Polymolybdovanadates have been used as reoxidants in Wacker chemistry (e.g. oxidation of alkenes) and may themselves be reoxidized with oxygen;[27]

$$Pd^o + [POM]_{ox} + 2H^+ \longrightarrow Pd^{II} + H_2[POM]_{red}$$

$$H_2[POM]_{red} + ½\ O_2 \longrightarrow [POM]_{ox} + H_2O$$

Use of the heteropolyanion instead of the normal $CuCl_2$ oxidant avoids corrosion by HCl.

1.7 Lanthanide-containing polyoxotungstates

Lanthanide-containing POMs have been investigated less than those containing 3d-transition metals. Because of the larger size of the lanthanide ions compared to 3d metals, they are not fully incorporated into the lacunary site(s) of vacant POM precursors. Due to their higher coordination numbers, each lanthanide ion can be used as linkers to one or more other lacunary POM units. Lanthanide-containing POMs can be of interest due to photoluminescence as well as catalytic, electrochemical, and magnetic properties.[28-29] The area of lanthanide-containing POMs is dominated by tungsten based POMs, as a large number of vacant (lacunary) POM precursors is known (as opposed to vanadium or molybdenum based POMs). The two main subclasses in this field are lanthanide-containing iso- and hetero-polyoxotungstates. The number of the reported lanthanide-containing POMs in the latter class is significantly larger than the former, probably because more lacunary hetero- than iso-polytungstates are known. In 2007, Pope reported a review presenting the structural chemistry and properties, and applications of POMs that incorporate one or more lanthanide ions.[30] Furthermore, another subclass in this field is mixed lanthanide and d-transition metal containing heteropolyoxotungstates.

1.7.1 Lanthanide-containing isopolyoxotungstates

Until very recently, there has been only one family of lanthanide-containing isopolyanions reported so far. Peacock and Weakley first reported the decatungstate, sandwich-type family of the general formula $[Ln(W_5O_{18})_2]^{n-}$.[31a] This was synthesized for Ln^{3+} = La, Ce, Pr, Nd, Sm, Ho, Yb and Y, and for Ce^{4+} by reaction of the lanthanide ions with Na_2WO_4 in hot aqueous (pH 6.5−7.5) solution.[31] The structure of the $[Ln(W_5O_{18})_2]^{n-}$ polyanions (D_{4d}) consist of two monolacunary, Lindqvist based fragments $[W_5O_{18}]^{6-}$ encapsulating a central metal ion exhibiting a square antiprismatic coordination, as depicted in Figure 1.11.

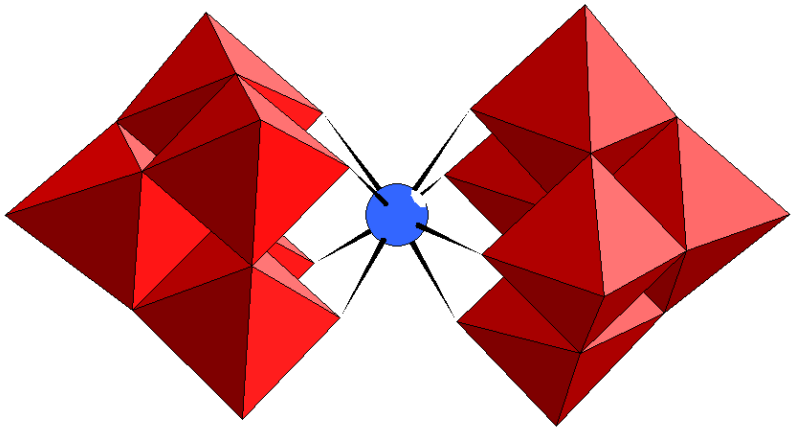

Figure 1.11 Combined polyhedral/ball-and-stick representation of $[Ln(W_5O_{18})_2]^{n-}$. Red octahedra: WO_6, blue ball: lanthanide.

Yamase et al. reported the crystal structures of the Pr, Nd, Dy, Sm, Eu, Gd and Tb derivatives with different types of alkali counter cations.[32] The lanthanum analogue, $[La(W_5O_{18})_2]^{9-}$ has also been reported in 2005.[33] Also, some actinide analogues ($[Th(W_5O_{18})_2]^{8-}$, $[U(W_5O_{18})_2]^{8-}$) have been crystallographically studied.[34,35] Our group has also reported very recently the synthesis and structure of the yttrium-containing POM $[YW_{10}O_{36}]^{9-}$ with its ^{89}Y NMR.[36] Polyanions containing lanthanides have been attracting interest mostly due to their fluorescent activity. The Lindqvist family $[Ln^{III}W_{10}O_{36}]^{9-}$, (Ln = Pr, Nd, Sm, Eu, Tb, Dy), has shown high quantum efficiency for luminescence.[32,37,38] Furthremore, Griffith and coworkers studied the lanthanoisopolytungstates $[Ln^{III}W_{10}O_{36}]^{9-}$, (Ln = Y, La, Ce, Pr, Sm, Eu, Gd, Dy, Er, Lu), as calalytic oxidants with H_2O_2 for alcohol oxiditions and alkene epoxidations.[39]

Apart from this Lindqvist family, another cerium-containing isopolyanion was recently reported by Cao et al. The isopolyanion corresponds to a pentadecatungstate ring-shaped unit capped by two Ce^{3+} cations with a terminal aqua ligand from one side and a terminal chloro ligand from the other side $[H_6Ce_2(H_2O)ClW_{15}O_{54}]^{7-}$, see Figure 1.12. This represents the second structural example of an isopolyanion bearing lanthanide ion to date.[40] The mixed sodium-potassium salt of this polyanion was prepared by reaction of tungsten(VI) with cerium(III) in aqueous acidic medium (optimal pH = 5.0). The chloride ion acts as a terminal

ligand for one of the cerium ions, and its presence during the synthesis is crucial since replacement of $HCl_{(aq.)}$ by $HNO_{3(aq.)}$ as acidification reagent and of $KCl_{(aq.)}$ by $KNO_{3(aq.)}$ as crystallization agent did not result in the desired product.

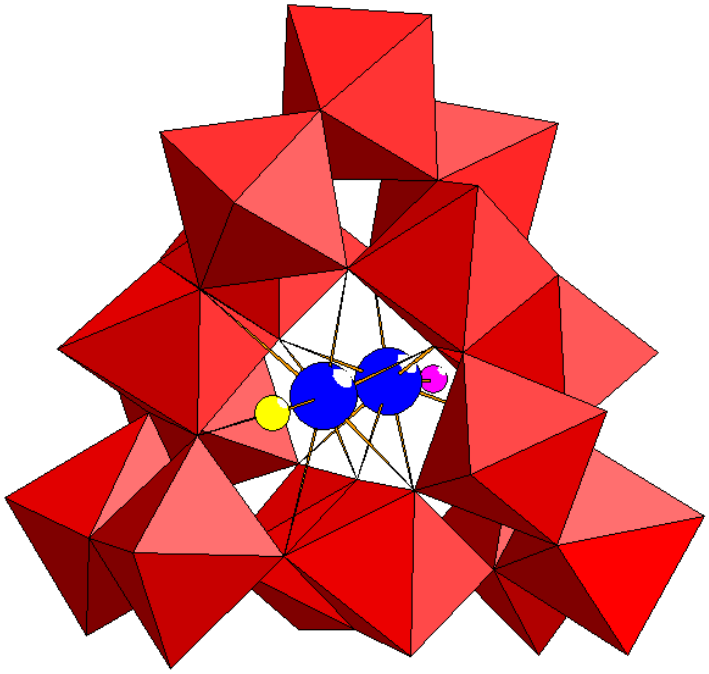

Figure 1.12 Combined polyhedral/ball-and-stick representation of $[H_6Ce_2(H_2O)ClW_{15}O_{54}]^{7-}$. Red octahedra: WO_6, blue balls: cerium, red ball: oxygen, pink ball: H_2O, yellow ball: chlorine.

The polyanion $[H_6Ce_2(H_2O)ClW_{15}O_{54}]^{7-}$ consists of an assembly of 15 WO_6 octahedra stabilized by two nonacoordinate cerium(III) ions by W–O–Ce bridges resulting in a polyanion with idealized C_3 symmetry. The isopolyanion part corresponds to three $\{W_5O_{18}\}$ units, each comprising three edge-shared and two corner-shared WO_6 octahedra. These three $\{W_5O_{18}\}$ units are joined to form a 15-membered ring which is capped on each side by a stabilizing cerium(III) ion. Six protons were also identified to be delocalized on the isopolyanion. Each cerium(III) ion exhibits a highly distorted, tri-capped trigonal-prismatic coordination, with eight oxygen donors from the isopolyanion units. One of the cerium ions has a terminal aqua ligand and the other a chloro ligand. This polyanion was investigated in solution by UV/Vis spectroscopy, photoluminescence and cyclic voltammetry studies.

1.7.2 Lanthanide-containing heteropolytungstates

To date, heteropolyanions are the most reported of the known lanthanide-containing POMs. In recent years, there has been an increase in the number of lanthanide-containing heteropolyoxotungstates. Here we review some examples of lanthanide-containing heteropolytungstates which include discrete molecular species as well as 1-, 2- and 3-D solid-state assemblies. For a detailed survey, Pope and Kortz groups have recently reported reviews presenting lanthanide-containing POMs, the former reviewed this field in a comprehensive fashion and the latter the recent example of polyoxotungstates.[30,41]

Peacock and Weakley reported sandwich type silicotungstates containing lanthanides, of general formula $[Ln(SiW_{11}O_{39})_2]^{13-}$.[31a] Pope et al. reported one-dimensional chains of lanthanide-containing monolacunary silicotungstates, the lanthanides being the linkers between the different chain elements.[42] Xu et al. also reported similar extended structures forming not only one-dimensional chain structures but also two-dimensional layers via potassium cations.[43] The Pope group reported lanthanide derivatives of the Preyssler anion $[Na(H_2O)P_5W_{30}O_{110}]^{14-}$ in which Ln^{3+} replaced the internal Na^+ atom.[44] Also, Wang et al. reported four extended phosphotungstate structures built from the Preyssler anion and lanthanide linkers to form one-dimensional chains.[45] Polymeric large molecular polyoxoanions were demonstrated by Francesconi's europium-containing phosphotungstate $[(PEu_2W_{10}O_{38})_4(W_3O_{14})]^{30-}$, and by Gouzerh's $[(SbW_9O_{33})_4\{WO_2(H_2O)\}_2Ce_3(H_2O)_8(Sb_4O_4)]^{19-}$.[46,47] Also, Fukaya and Yamase reported two crown-shaped, europium-containing tungstoarsenates(III), $[K\subset\{Eu(H_2O)_2(\alpha\text{-}AsW_9O_{33})\}_6]^{35-}$ and $[Cs\subset\{Eu(H_2O)_2(\alpha\text{-}AsW_9O_{33})\}_4]^{23-}$.[46–48] Recently, Pope et al. synthesized $[K\subset P_8W_{48}O_{184}(H_4W_4O_{12})_2Ln_2(H_2O)_{10}]^{25-}$ by the reaction of $[P_8W_{48}O_{184}]^{40-}$ with lanthanide cations resulting in 3D networks.[49] Patzke et al. has very recently reported the synthesis and structure of the octa-gadolinium(III)-containing 124-tungsto-12-arsenate(III)

$[Gd_8As_{12}W_{124}O_{432}(H_2O)_{22}]^{60-}$ ($\{Gd_8As_{12}W_{124}\}$) from the reaction of Gd^{3+} ions with the dilacunary polyanion precursor $[As_2W_{19}O_{67}(H_2O)]^{14-}$.[50] The polyanion $\{Gd_8As_{12}W_{124}\}$ exhibits C_i point group symmetry and comprises two identical $[Gd_4As_6W_{62}O_{216}(H_2O)_{11}]^{30-}$ subunits linked by two Gd–O–W bridges. Each subunit is composed of six trilacunary tungstoarsenates(III) $(\alpha\text{-}As^{III}W_9O_{33})^{9-}$ $\{AsW_9\}$ building blocks and two $\{Gd_2W_4\}$ fragments. The gadolinium ions are octacoordinate with two terminal aqua ligands. Finally, the largest molecular polytungstate to date is the cerium containing arsenotungstate $[Ce_{16}As_{12}W_{148}O_{524}(H_2O)_{36}]^{76-}$, reported in 1997 by Pope and coworkers, and containing 16 ceriums and 148 tungstens.[51]

Our group has also been working on lanthanide-containing heteropolytungstates.[52] We have reported the ytterbium-containing tungstoarsenate $[YbAs_2W_{20}O_{68}(H_2O)_3]^{7-}$ resulting from the interaction of the monolacunary $[As_2W_{20}O_{68}(H_2O)]^{10-}$ with Yb^{3+} ions in acidic aqueous medium. The polyanion consists of two $(\alpha\text{-}As^{III}W_9O_{33})^{9-}$ fragments connected by a V-shaped $(H_2O)Yb(OW(H_2O))_2$ fragment (Figure 1.13).[52a]

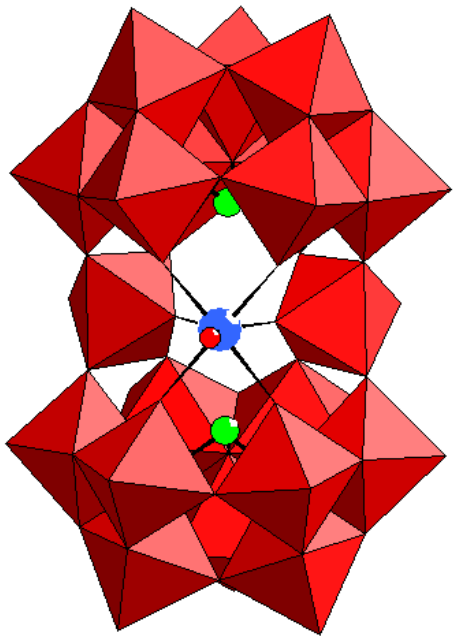

Figure 1.13 Combined polyhedral/ball-and-stick representation of $[YbAs_2W_{20}O_{68}(H_2O)_3]^{7-}$. Red octahedra: WO_6, green balls: As, red ball: O, blue ball: Yb.

The lanthanum-containing Wells–Dawson dimer $[\{La(CH_3COO)(H_2O)_2(\alpha_2\text{-}P_2W_{17}O_{61})\}_2]^{16-}$ which consists of two monolacunary Wells–Dawson α_2-$\mathbf{P_2W_{17}}$ fragments connected by a lanthanum-acetate dimer, $(La_2(CH_3COO)(H_2O)_4)^{4+}$ has been reported. Each La^{3+} ion is nine-coordinated in a monocapped, square-antiprismatic fashion (Figure 1.14).[52b]

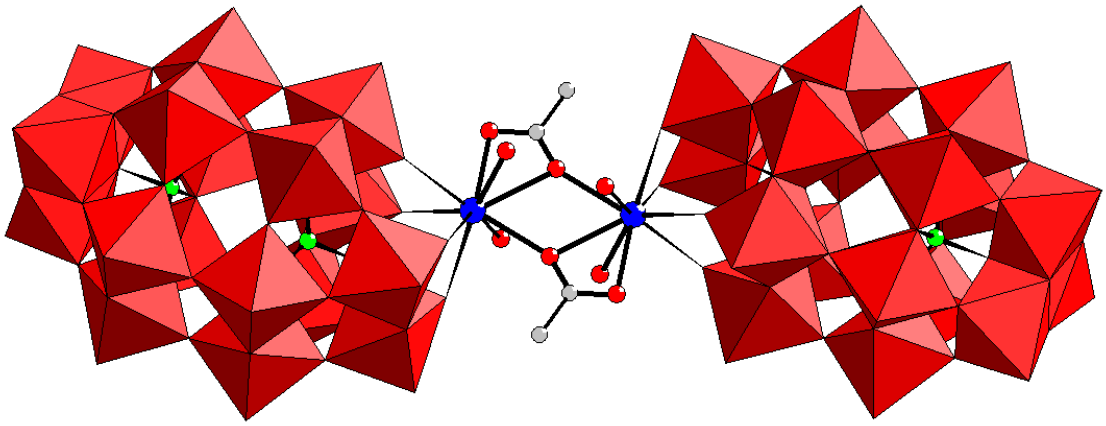

Figure 1.14 Combined polyhedral/ball-and-stick representation of $[\{La(CH_3COO)(H_2O)_2(\alpha_2\text{-}P_2W_{17}O_{61})\}_2]^{16-}$. Red octahedra: WO_6, green balls: P, blue balls: La, grey balls: C, red balls: O. No hydrogen atoms shown.

The monolanthanide-containing polyanion family $[Ln(\beta_2\text{-}SiW_{11}O_{39})_2]^{13-}$ (Ln = La, Ce, Sm, Eu, Gd, Tb, Yb, Lu) has also been synthesized and structurally characterized. These polyanions are composed of two chiral (β_2-$SiW_{11}O_{39}$) units sandwiching the Ln^{3+} ion (Figure 1.15).[52c]

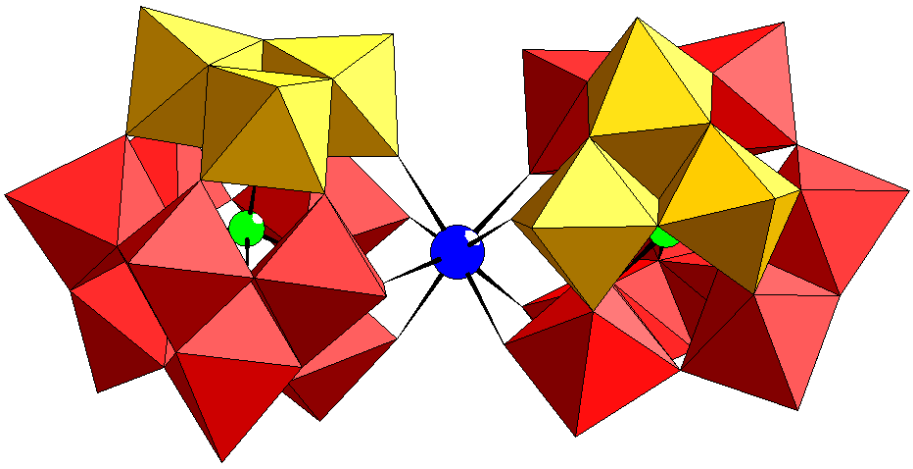

Figure 1.15 Combined polyhedral/ball-and-stick representation of $[Ln(\beta_2\text{-}SiW_{11}O_{39})_2]^{13-}$. Red and yellow octahedra: WO_6, green balls: silicon, blue balls: lanthanide, the rotated triad was colored yellow for clarification.

Recently, we reported the tungstogermanate ion $[Ce_{20}Ge_{10}W_{100}O_{376}(OH)_4(H_2O)_{30}]^{56-}$ containing 20 cerium atoms, the highest cerium-containing polytungstate to date. We synthesized this polyanion by the reaction of the trilacunary POM precursor $[\alpha\text{-}GeW_9O_{34}]^{10-}$ with Ce^{3+} ions in acidic aqueous medium (Figure 1.16).[52d]

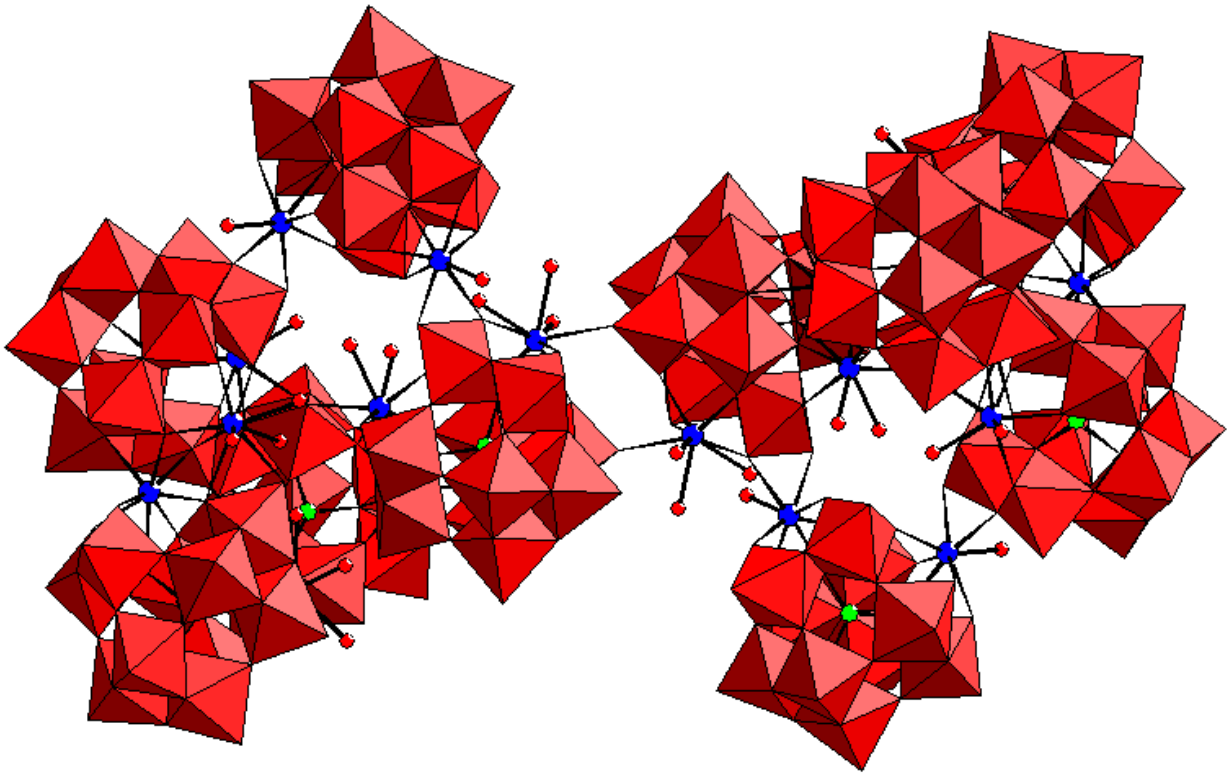

Figure 1.16 Combined polyhedral/ball-and-stick representation of $[Ce_{20}Ge_{10}W_{100}O_{376}(OH)_4(H_2O)_{30}]^{56-}$. Red octahedra: WO_6, green balls: Ge, blue balls: Ce, red ball: O.

Recently, the cyclic $\mathbf{P_8W_{48}}$ was reacted with lanthanide cations resulting in the only lanthanide derivative of $\mathbf{P_8W_{48}}$ known to date. The lanthanide series $[K\subset P_8W_{48}O_{184}(H_4W_4O_{12})_2Ln_2(H_2O)_{10}]^{25-}$ (Ln = La, Ce, Pr, Nd) was synthesized by the reaction of $\mathbf{P_8W_{48}}$ polyanion with lanthanide cations under hydrothermal and conventional conditions. The central cavity of the $\mathbf{P_8W_{48}}$ was occupied by lanthanide and potassium cations, and W_4O_{12} groups (Figure 1.17).[49]

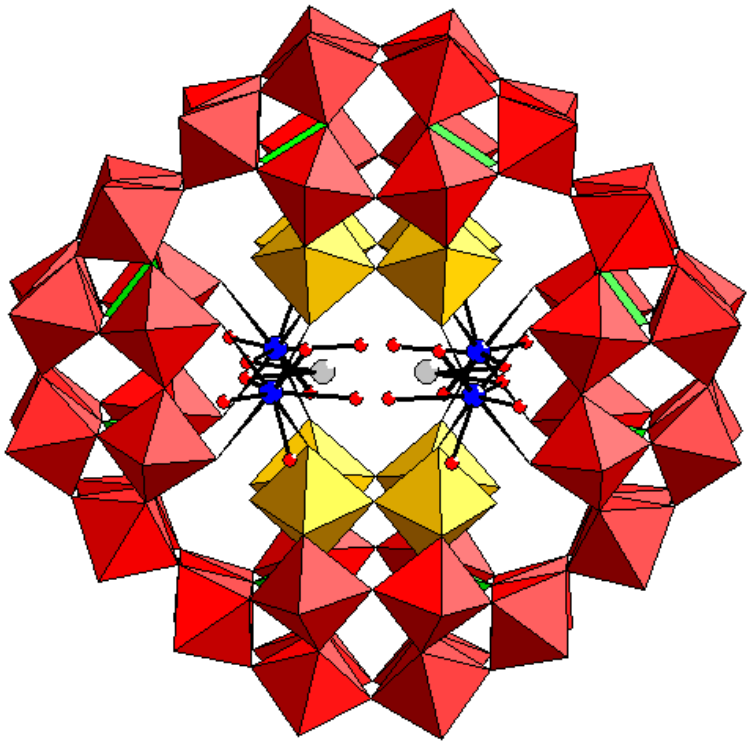

Figure 1.17 Combined polyhedral/ball-and-stick representation of $[K\subset P_8W_{48}O_{184}(H_4W_4O_{12})_2Ln_2(H_2O)_{10}]^{25-}$. Note that the K^+ ion is disordered over 2 positions, and the two Ln^{3+} ions are disordered over four positions (for details see reference 49). The color code is as follows: tungsten octahedra WO_6 (red and yellow), lanthanide (blue), potassium (grey), and oxygen (red).

1.7.3 Mixed lanthanide / d-transition metal ions containing POMs

Few examples in literature on mixed incorporation of lanthanides and d-transition metal ions into POMs (also known as 3d-4f heterometalic POMs) are known.[53–57] Krebs et al. successfully synthesized $[((VO)_2Dy(H_2O)_4K_2(H_2O)_2Na(H_2O)_2)(\alpha\text{-}B\text{-}AsW_9O_{33})_2]^{8-}$, which is constructed from two trilacunary Keggin anions, two VO^{2+} and one Dy^{3+} ion forming a sandwich-type structure with C_{2v} symmetry; the magnetic properties of this compound were also studied.[53] Kögerler et al. reported two compounds,[54] $[(CH_3)_2NH_2]_6H_2[\{\alpha\text{-}P_2W_{16}O_{56}(OH)_2\}\{Ce^{IV}Mn^{IV}{}_6O_9(O_2CCH_3)_8\}]\cdot 20H_2O$ and $K_{36}Na_{11}[\{\alpha\text{-}P_2W_{15}O_{56}\}_6\{Ce_3Mn_2(\mu_3\text{-}O)_4(\mu_2\text{-}OH)_2\}_3(\mu_2\text{-}OH)_2(H_2O)_2(PO_4)]\cdot 106H_2O$, which were synthesized by interaction of the high oxidation state heterometallic clusters $[CeMn_6O_9(O_2CCH_3)_9(NO_3)(H_2O)_2]$ and $[Ce_3^{IV}Mn_2^{IV}O_6(OH)_2]^{6+}$ respectively with the tri-vacant Wells-Dawson phosphotungstate [α-

$P_2W_{16}O_{56}]^{12-}$ which have an ability to coordinate transition metal and lanthanide ions.[54] Mialane's group synthesized polyanions containing Cu(II) and Ln(III) cations by reaction of the [*A*-*α*-$SiW_9O_{34}]^{10-}$ unit with the Cu(II) acetate and $Ln(NO_3)_3$.[55] As well, Wang et al. have been synthesizing several polyanions containing 3d-transition metal centers and having lanthanide cations as linkers between the different POM units.[56] They also reported the synthesis of a polyanion based 3d-4f heterometallic aggregate, constructed from three {*α*-AsW_9O_{38}} fragments bridged by three {Fe-(μ_3-O)$_3$-Ce} heterometalic clusters.[56c] Reinoso et al. reported [{$Ce(H_2O)_2$}$_2$$Mn_2$(*B*-*α*-$GeW_9O_{34})_2]^{8-}$ polyanion constituting the first example of a heterometallic 3d-4f cluster related to the Weakley-type dimeric structure, and it contains $Ce^{III}_2Mn^{III}_2O_{20}$ rhomblike moiety.[57]

The aforementioned three subclasses of this subfield in POM chemistry will be our interests in this work. Firstly, the area of lanthanide-containing polyanions based on isopolytungstate fragments has a lack of discovering of new units (rather than the monolacunary Lindqvist $[W_5O_{18}]^{6-}$ anion) that can be stabilized by lanthanide ions. Hence, the production of novel isopolytungstate based lanthanides represents a challenge in POM syntheses and applications, especially with the labile coordination environment of the lanthanides. This provides an impetus to prepare other, novel isopolyanion structures coordinated to lanthanide ions. Secondly, it is more likely that the bulk of novel lanthanide-containing polyoxotungstates will be based on heteropoly rather than isopoly fragments. This is due to the fact that a large number of lacunary, stable heteropolytungstates are known. Nevertheless, it becomes apparent that several lacunary heteropolytungstates have not yet been reacted systematically with lanthanide ions. Trilacunary POM precursors and in a particular lacunary POM precursors containing a hetero group with a lone pair of electrons (e.g. As^{III}, Sb^{III}) might result in unusual compounds. Thirdly, a paramagnetic 3d metal oxo-cluster interacting with paramagnetic lanthanide centers is an interesting combination for

magnetic interactions. Therefore, the mixed incorporation of lanthanides and d-transition metal ions into POMs might be an interesting example for the magnetic studies.

1.8 References

[1] a) M. T. Pope in *Heteropoly and Isopoly Oxometalates*, Springer-Verlag, Berlin, 1983; b) M. T. Pope, A. Müller, *Angew. Chem.* **1991**, *103*, 56, *Angew. Chem. Int. Ed. Engl.* **1991**, *30*, 34; c) M. T. Pope, A. Müller in *Polyoxometalates: From Platonic Solids to Anti- Retroviral Activity* (Eds.: M. T. Pope, A. Müller), Kluwer: Dordrecht, The Netherlands, 1994; d) A. Müller, H. Reuter, S. Dillinger, *Angew. Chem.* **1995**, *107*, 2505, *Angew. Chem. Int. Ed. Engl.* **1995**, *34*, 2328; e) C. Hill in *Polyoxometalates: Chemical Reviews*, 1998 (special thematic issue on polyoxometalates); f) J. J. Borrás-Almenar, E. Coronado, A. Müller, M. T. Pope, in *Polyoxometalate Molecular Science* (Eds.: J. J. Borrás-Almenar, E. Coronado, A. Müller, M. T. Pope), Kluwer: Dordrecht, The Netherlands, 2001; g) M. T. Pope, A. Müller in *Polyoxometalate Chemistry: From Topology via Self-Assembly to Applications (*Eds.: M. T. Pope, A. Müller), Kluwer: Dordrecht, The Netherlands, 2001; h) T. Yamase, M. T. Pope in *Polyoxometalate Chemistry for Nano-Composite Design (*Eds.: T. Yamase, M. T. Pope), Kluwer: Dordrecht, The Netherlands, 2002; i) D.-L. Long, H. Abass, P. Kögerler, L. Cronin, *J. Am. Chem. Soc.* **2004**, *126*, 13880; j) D.-L. Long, E. Burkholder, L. Cronin, *Chem. Soc. Rev.* **2007**, *36*, 101; k) D.-L. Long, R. Tsunashima, L. Cronin, *Angew. Chem.* **2010**, *122*, 1780, *Angew. Chem. Int. Ed.* **2010**, *49*, 1736.

[2] J. J. Berzelius, *Pogg. Ann. Phy.* **1826**, *6*, 369.

[3] L. Svanberg, H. Struve, *J. Prakt. Chem.* **1848**, *44*, 291.

[4] C. Marignac, *C. R. Acad. Sci*. **1862**, *55*, 888; *Ann. Chim.* **1862**, *25*, 362; *Ann. Chim. Phys.,* **1864**, *69*, 41.

[5] A. Rosenheim, H. Jänicke, *Z. Anorg. Chem.* **1917**, *100*, 304.

[6] A. Miolati, R. Pizzighelli, *J. Prakt. Chem.* **1908**, *77*, 417.

[7] L. C. Pauling, *J. Am. Chem. Soc.* **1929**, *51*, 2868.

[8] a) J. F. Keggin, *Nature* **1933**, *131*, 908. b) J. F. Keggin, *Proc. Roy. Soc. A* **1934**, *144*, 75.

[9] Jr., H. T. Evans, *J. Am.Chem. Soc.* **1948**, *70*, 1291.

[10] I. Lindqvist, *Arkiv. Kemi.* **1950**, *2*, 341.

[11] B. Dawson, *Acta Crystallogr.* **1953**, *6*, 113.

[12] a) E. V. Chubarova, M. H. Dickman, B. Keita, L. Nadjo, M. Mifsud, I. W. C. E. Arends, U. Kortz, *Angew. Chem.,* **2008**, *47*, 9542; b) N. V. Izarova, R. Ngo Biboum, B. Keita, M. Mifsud, I. W. C. E. Arends, G. B. Jameson, U. Kortz, *Dalton Trans.* **2009**, 9385; c) N. V. Izarova, M. H. Dickman, R. Ngo Biboum, B. Keita, L. Nadjo, V. Ramachandran, N. S. Dalal, U. Kortz, *Inorg. Chem.* **2009**, *48*, 7504; d) N. V. Izarova, N. Vankova, T. Heine, R. Ngo Biboum, B. Keita, L. Nadjo, U. Kortz, *Angew. Chem.,* **2010**, *49*, 1886.

[13] D. D. Dexter, J. V. *J.* Silverton, *Am. Chem. Soc.* **1968**, *90*, 3589.

[14] W. N. Lipscomb, *Inorg. Chem.* **1965**, *4*, 132.

[15] W. G. Klemperer, (Ed.) "Early Transition Metal Polyoxoanions" *Inorg. Synth*. **1990**, *27*, 71.

[16] a) K. H. Tytko, O. Glemser, *Adv. Inorg. Chem. Radiochem*. **1976**, *19*, 239; b) L. Pettersson, I. Andersson, L. O. Ohman, *Inorg. Chem*. **1986**, *25*, 4726 ; c) D. C. Crans, *Comments Inorg. Chem*. **1994**, *16*, 1.

[17] L. C. W. Baker, J. S. Figgis, *J. Am. Chem. Soc.* **1970**, *92*, 3794.

[18] S. H. Wang, S. A. Jansen, *Chem. Mater*. **1994**, *6*, 2130.

[19] M. T. Pope, *Inorg. Chem*. **1976**, *15*, 2068.

[20] X. López, J. M. Maestre, C. Bo, J. M. Poblet, *J. Am. Chem. Soc*. **2001**, *123*, 9571.

[21] R. Contant, A. Tézé, *Inorg. Chem.* **1985** *24,* 4610.

[22] a) A. Mylonas, E. Papaconstantinou, *J. Mol. Catalysis A: Chemical* **1994**, *92*, 3, 261; b) A. Mylonas, A. Hiskia, E. Papaconstantinou, *J. Mol. Catalysis A: Chem.* **1996**, *114*, 191; c) A. Hiskia, A. Mylonas, E. Papaconstantinou, *Chemical Society Reviews,* **2001**, *30*, 62; d) A.

Hiskia, A. Troupis, E. Papaconstantinou, *Int. J. Photoenergy* **2002**, *4*, 35; e) E. Gkika, P. Kormali, S. Antonaraki, D. Dimoticali, E. Papaconstantinou, A. Hiskia, Int. *J. Photoenergy* **2004**, *6*, 227; f) A. Hiskia, A. Troupis, S. Antonaraki, E. Gkika, P. Kormali, E. Papaconstantinou, *Int. J. Envir. Anal. Chem.* **2006**, 233; g) P. Kormali, A. Troupis, T. Triantis, A. Hiskia, E. Papaconstantinou, *Catalysis Today* **2007**, *124*, 149.

[23] a) I. V. Kozhevnikov, *Chem. Rev.* **1998**, *98*, 171- 198; b) N. Mizuno, M. Misono, *Chem. Rev.* **1998**, *98*, 199.

[24] a) D. E. Katsoulis, M. T. Pope, *J. Chem. Soc. Chem. Commun.* **1986**, 1186; b) C. L. Hill, Jr. R. B. Brown, *J. Am. Chem. Soc.* **1986**,*108*, 536.

[25] a) M. Misono, *Catal. Rev. Sci. Eng.* **1987**, *29*, 269; b) J. B. Moffat, *Chem. Eng. Commun.* **1989**, *83*, 9.

[26] R. Neumann. M. Lissel, *J. Org. Chem.* **1989**, *54*, 4607.

[27] I.V. Kozhevnikov, K. I. Matveev, *Appl. Card.* **1983**, *5*, 135.

[28] a) M. M. Gresely, W. P. Griffith, A. C. Lämmel, H. I. S. Nogueira, B. C. Parkin, *J. Mol. Catal. A: Chemical* **1997**, *117*, 185; b) W. P. Griffith, N. Morley-Smith, H. I. S. Nogueira, A. G. F. Shoair, M. Suriaatmaja, A. J. P. White, D. J. Williams, *J. Organomet. Chem.* **2000**, *607*, 146; c) J. A. Fernández, X. López, C. Bo, C. de Graaf, E. J. Baerend, J. M. Poblet, *J. Am. Chem. Soc.* **2005**, *129*, 12244; d) F. Li, L. Xu, Y. Wei, G. Gao, L. Fan, Z. Li, *Inorg. Chim. Acta* **2006**, *359*, 3795; e) W. Chen, Y. Li, Y. Wang, E. Wang, Z. Su, *J. Chem. Soc., Dalton Trans.* **2007**, 4293; f) W. Huang, L. C. Francesconi, T. Plenova, *Inorg. Chem.* **2007**, *43*, 7861; g) A. Merca, A. Müller, J. van Slageren, M. Läge, B. Krebs, *J. Clust. Sci.* **2007**, *168*, 711.

[29] a) S. Bareyt, S. Piligkos, B. Hasenknopf, P. Gouzerh, E. Lacôte, S. Thorimbert, M. Malacria, *J. Am. Chem. Soc.* **2005**, *127*, 6788; b) C. Boglio, G. Lemiére, B. Hasenknopf, S. Thorimbert, E. Lacôte, M. Malacria, *Angew. Chem.,* **2006**, *118*, 3402, *Angew. Chem., Int. Ed. Engl.* **2006**, *45*, 3324; c) C. Boglio, G. Lenoble, C. Duhayon, B. Hasenknopf, R. Thouvenot, C. Zhang, R. C. Howell, B. P. Burton-Pye, L. C. Francesconi, E. Lacôte, S. Thorimbert, M.

Malacria, C. Afonso, J.-C. Tabet, *Inorg. Chem.* **2006**, *45*, 1389; d) C. Boglio, K. Micoine, R. Rémy, B. Hasenknopf, S. Thorimbert, E. Lacôte, M. Malacria, C. Afonso, J.-C. Tabet, *Chem. Eur. J.* **2007**, *13*, 5426; e) K. Micoine, B. Hasenknopf, S. Thorimbert, E. Lacôte, M. Malacria, *Org. Lett.* **2007**, *9*, 3981; f) E. Derat, E. Lacôte, B. Hasenknopf, S. Thorimbert, M. Malacria, *J. Phys. Chem. A* **2008,** *112,* 13002; g) C. Boglio, K. Micoine, E. Derat, R. Thouvenot, B. Hasenknopf, S. Thorimbert, E. Lacôte, M. Malacria, *J. Am. Chem. Soc.* **2008**, *130*, 4553.

[30] M. T. Pope, *Handbook on the Physics and Chemistry of Rare Earths*, 38, **2007**, 337.

[31] a) R. D. Peacock, T. J. R. Weakley, *J. Chem. Soc. A* **1971**, 1836; b) J. Iball, J. N. Low, T. J. R. Weakley, *J. Chem. Soc. Dalton Trans*. **1974**, 2021.

[32] a) T. Ozeki, M. Takahashi, T. Zeki, M. Takahashi, T. Yamase, *Acta Crystallogr*. **1992**, *C48*, 1370; b) T. Ozeki, T. Yamase, *Acta Crystallogr. B*. **1994**, *50*, 128; c) T. Ozeki, T. Yamase, *Acta Crystallogr. C*. **1993**, *49*, 1574; d) T. Ozeki, T. Yamase, *Acta Crystallogr. C*. **1994**, *50*, 327; e) T. Yamase, T. Ozeki, K. Ueda, *Acta Crystallogr. C*. **1993**, *49*, 1572; f) T. Yamase, T. Ozeki, *Acta Crystallogr.* **1993**, *49*, 1577; g) T. Yamase, T. Ozeki, M. Tosaka, *Acta Crystallogr. C.* **1994**, *50*, 1849; h) T. Ozeki, M. Takaahashi, T. Yamase, *Acta Crystallogr. C.* **1992**, *48*, 1370; i) T. Yamase, H. Naruke, Y. Sasaki, *J. Chem. Soc. Dalton Trans.* **1990**, 1687.

[33] F.A. Almeida Paz, M. S. S. Balula, A. M. V. Cavaleiro, J. Klinowski, H. I. S. Nogueira, *Acta Cryst.* **2005**, *E61*, 1370.

[34] W. P. Griffith, N. M-Smith, H. I. S. Nogueira, A. G. F. Shoair, M. Suriaatmaja, A. J. P. White, D. J. Williams, *J. Organomet. Chem.* **2000**, *606*, 146.

[35] A. M. Golubev, L. P. Kazanskii, E. A. Torchenkova, V. I. Simonov, V. I. Spitsyn, *Dokl. Acad. Nauk.* **1975**, *221*, 351.

[36] M. Barsukova, M. H. Dickman, E. Visser, S. S. Mal, U. Kortz, *Z. Anorg. Allg. Chem.* **2008**, *634*, 2423.

[37] M. J. Stillman, A. J. Thomson, *J. Chem.Soc. Dalton Trans.* **1976**, 1138.

[38] G. Blasse, G. Dirksen, F. Zonnevulle, *Chem. Phys. Lett.* **1981**, *83*, 449.

[39] W. P. Griffith, N. Morley-Smith, H. I. S. Nogueira, A. G. F. Shoair, M. Suriaatmaja, A. J. P. White, D. J. Williams, *J. Organomet. Chem.* **2000**, *607*, 146.

[40] T. Li, F. Li, J. Lü, Z. Guo, S. Gao, R. Cao, *Inorg. Chem.* **2008**, *47*, 5612.

[41] B. S. Bassil, U. Kortz, *Z. Anorg. Allg. Chem.* **2010**, *636*, 2222.

[42] M. Sadakane, M. H. Dickman, M. T. Pope, *Angew. Chem., Int. Ed. Engl.* **2000**, *39*, 2914.

[43] F. Li, L. Xu, Y. Wei, G. Gao, L. Fan, Z. Li, *Inorg. Chim. Acta* **2006**, *359*, 3799.

[44] M. H. Dickman, G. J. Gama, K-C. Kim, M. T. Pope, *J. Clust. Sc.* **1996**, *7*, 567.

[45] Y. Lu, Y. Li, E. Wang, X. Xe, Y. Ma, *Inorg. Chim. Acta* **2006**, *360*, 2063.

[46] R. C. Howell, F. G. Perez, S. Jain, W. DeW. Jr. Horrocks, A. L. Rheingold, L. C. Francesconi, *Angew. Chem., Int. Ed. Engl.* **2001**, *40*, 4031.

[47] G. L. Xue, J. Vaissermann, P. Gouzerh, *J. Cluster Sci.* **2002**, *13*, 409.

[48] K. Fukaya, T. Yamase, *Angew. Chem., Int. Ed. Engl.* **2003**, *42*, 654.

[49] M. Zimmermann, N. Belai, R. J. Butcher, M. T. Pope, E. V. Chubarova, M. H. Dickman, U. Kortz, *Inorg. Chem.* **2007**, *46*, 1737.

[50] F. Hussain, F. Conrad, G. R. Patzke, *Angew. Chem.,* **2009**, *121*, 9252, *Angew. Chem., Int. Ed. Engl.* **2009**, *48*, 9088.

[51] K. Wassermann, M. H. Dickman, M. T. Pope, *Angew. Chem., Int. Ed. Engl.* **1997**, *36*, 1445.

[52] a) U. Kortz, C. Holzapfel, M. Reicke, *J. Mol. Struct.* **2003**, *656*, 93; b) U. Kortz, *J. Clust. Sci.* **2003**, *14*, 205; c) B. S. Bassil, M. H. Dickman, B. Kammer, U. Kortz, *Inorg. Chem.* **2007**, *46*, 2452; d) B. S. Bassil, M. H. Dickman, I. Römer, B. Kammer, U. Kortz, *Angew. Chem., Int. Ed. Engl.* **2007**, *46*, 6192.

[53] A. Merca, A. Müller, J. van Slageren, M. Läge, B. Krebs, *J. Clust. Sci.* **2007**, *16*, 711.

[54] a) X. Fang and P. Kögerler, *Chem. Commun.* **2008**, 3396; b) X. Fang and P. Kögerler, *Angew. Chem.* **2008**, *120*, 8243, *Angew. Chem. Int. Ed.* **2008**, *47*, 8123.

[55] B. Nohra, P. Mialane, A. Dolbecq, E. Riviére, J. Marrot, F. Séecheresse, *Chem. Commun.* **2009**, 2703.

[56] a) W.-L. Chen, Y.-G. Li, Y.-H. Wang, E.-B. Wang, *Eur. J. Inorg. Chem.* **2007**, 2216; b) Z.-M. Zhang, Y.-G. Li, W.-L. Chen, E.-B. Wang, X.-L. Wang, *Inorg. Chem. Commun.* **2008**, 11, 879; c) W.-L. Chen, Y.-G. Li, Y.-H. Wang, E.-B. Wang, Z.-M. Zhang, *Dalton Trans.* **2008**, 865; d) Y-W. Li, Y-G. Li, Y-H. Wang, X-J. Feng, Y Lu, E.-B. Wang, *Inorg. Chem.* **2009,** *48*, 6452; e) S. Yao, Z. Zhang, Y. Li, Y. Lu, E.-B. Wang, Z. Su, *Cryst. Growth Des.* **2010**, *10*, 135.

[57] S. Reinoso, J. R. Galán-Mascarós, *Inorg. Chem.* **2010**, *49*, 377.

Chapter II

Experimental

2.1 Reagents

All chemicals were purchased from well-known chemical companies, and used as received without further purification: $Na_2WO_4 \cdot 2H_2O$, $Na_2MoO_4 \cdot 2H_2O$, $YCl_3 \cdot 6H_2O$, and $MnCl_2 \cdot 4H_2O$ were purchased from Riedel-deHaën; $FeCl_3 \cdot 6H_2O$, HCl and D_2O were purchased from AppliChem; $CuCl_2 \cdot 2H_2O$, $CoCl_2 \cdot 6H_2O$, H_2O_2 (30%), TeO_2, GeO_2, As_2O_3 and Sb_2O_3 were purchased from Fluka Chemie.

Table 2.1 Information about the lanthanide salts products used.

Name	Formula	Purity (%)	Supplier
Lanthanum(III) chloride heptahydrate	$LaCl_3 \cdot 7H_2O$	99.0	Merick
Cerium(III) chloride heptahydrate	$CeCl_3 \cdot 7H_2O$	98.5	Fluka Chemika
Praseodymium(III) chloride hexahydrate	$PrCl_3 \cdot 6H_2O$	99.9	Sigma-Aldrich
Neodymium(III) chloride hexahydrate	$NdCl_3 \cdot 6H_2O$	99.9	Fluka Chemika
Samarium(III) chloride hexahydrate	$SmCl_3 \cdot 6H_2O$	99.9	Sigma-Aldrich
Europium(III) chloride hexahydrate	$EuCl_3 \cdot 6H_2O$	99.9	Sigma-Aldrich
Gadolinium(III) chloride hexahydrate	$GdCl_3 \cdot 6H_2O$	99.9	Sigma-Aldrich
Terbium(III) acetate hydrate	$Tb(CH_3COO)_3 \cdot H_2O$	99.9	Sigma-Aldrich
Dysprosium(III) chloride hexahydrate	$DyCl_3 \cdot 6H_2O$	99.9	Sigma-Aldrich
Holmium(III) chloride hexahydrate	$HoCl_3 \cdot 6H_2O$	99.9	Sigma-Aldrich
Erbium(III) acetate hydrate	$Er(CH_3COO)_3 \cdot H_2O$	99.9	Sigma-Aldrich
Thulium(III) chloride hexahydrate	$TmCl_3 \cdot 6H_2O$	99.9	Sigma-Aldrich
Ytterbium(III) nitrate pentahydrate	$Yb(NO_3)_3 \cdot 5H_2O$	99.9	Sigma-Aldrich
Lutetium(III) chloride hexahydrate	$LuCl_3 \cdot 6H_2O$	99.9	Sigma-Aldrich

2.2 Instrumentation

2.2.1 Fourier transform infrared spectroscopy

Infrared spectra with 4 cm^{-1} resolution were recorded on a Nicolet Avatar 370 FT-IR spectrophotometer as KBr pellet samples. The following abbreviations were used to assign the peak intensities: w = weak; m = medium; s = strong; vs = very strong; b = broad; sh = shoulder.

2.2.2 Single crystal X-ray diffraction

The crystals were mounted in Hampton cryoloops using light oil for data collection at 173 K. Indexing and data collection were performed using a Bruker X8 APEX II CCD diffractometer with kappa geometry and MoK_α radiation (λ = 0.71073 Å). Data integration and routine processing were performed using the SAINT software suite. Direct Methods (SHELXS97) solutions successfully located the W atoms, and successive Fourier syntheses (SHELXL97) revealed the remaining atoms.[1-2] Refinements were done with full-matrix least-squares methods against F^2 using all data. Further data processing, including multi-scan absorption corrections, was performed using SADABS.[3] Some water molecules of hydration were modeled with varying degrees of occupancy, a common situation for polytungstate structures. In the final refinements, all non-disordered heavy atoms were refined anisotropically, while the O and disordered countercations were refined with fractional occupancies. No H or Li atoms were included in the models. The degree of refinement is commonly expressed by the R factor, which is a measure of the degree of deviation of the predicted model (calculated) from the scattering amplitudes (observed):

$$R = \Sigma \| F(obs) | - | F(calc) \| / \Sigma | F(obs) |$$

2.2.3 Thermogravimetry

Thermogravimetric (TGA) analyses were performed using a TA Instruments SDT Q600 thermobalance from room temperature to 900 ºC with a heating rate of 5°/min for 10-30 mg of sample in alumina pans under 100 mL/min flow of nitrogen.

2.2.4 Multinuclear magnetic resonance spectroscopy

NMR spectra were recorded on a JEOL 400 ECX spectrometer operating at 9.39 T (400 MHz for proton) magnetic field. Chemical shifts were given relative to external standards, 2 M solution of Na_2WO_4 for ^{183}W in D_2O, $Si(CH_3)_4$ in $CDCl_3$ for ^{1}H- and ^{13}C-NMR and YCl_3 in D_2O for ^{89}Y-NMR. The resonance frequency employed was 16.656 MHz for ^{183}W. All aqueous ^{183}W-NMR spectra were collected on highly concentrated solution.

2.3 Preparation of starting materials

Synthetic procedures of starting materials (lacunary POM precursors) that served as building blocks for all the heteropolyoxotungstates presented in this work are detailed in the following sections.

2.3.1 Synthesis of $K_{14}[As_2W_{19}O_{67}(H_2O)]$

0.89 g (4.5 mmol) of As_2O_3, 18.8 g (57.0 mmol) of $Na_2WO_4{\cdot}2H_2O$, and 0.67 g (9.0 mmol) of KCl were added to 50 mL H_2O at 80˚ C with stirring. After dissolution, the pH was adjusted to 6.3 by adding 12 M HCl dropwise. The solution was kept at 80˚ C for 10 min and then filtered. Finally 15 g KCl was added and the solution stirred for 15 minutes. The white precipitate formed was isolated by filtration and dried at 80˚ C.[4]

2.3.2 Synthesis of $Na_9[B\text{-}\alpha\text{-}AsW_9O_{33}]\cdot 27H_2O$

11 g (0.056 mol) of As_2O_3 were added to a hot solution of 330 g (1.0 mol) $Na_2WO_4\cdot 2H_2O$ in 350 ml water. After the addition of 83 ml 11M HCl with vigorous stirring over 2 min, the solution was heated at 95° C for 10 min. The product was kept in a beaker to crystallize overnight. The crystals obtained were filtered off and air dried.[5]

2.3.3 Synthesis of $Na_9[B\text{-}\alpha\text{-}SbW_9O_{33}]\cdot 27H_2O$

A solution of 1.96 g (6.72 mmol) of Sb_2O_3 in 10 mL concentrated HCl was added dropwise to a hot solution of 40 g (121 mmol) of $Na_2WO_4\cdot 2H_2O$ in 80 ml water. The mixture was refluxed for 1 h and then kept to crystalize. After evaporation of one-third of the solution volume, the crystals were formed and then filtered off and air dried.[6]

2.3.4 Synthesis of $Na_{12}[Sb_2W_{22}O_{74}(OH)_2]$

10 g (3.49 mmol) of $Na_9[B\text{-}\alpha\text{-}SbW_9O_{33}]\cdot 27H_2O$ and 2.3 g (6.99 mmol) of $Na_2WO_4\cdot 2H_2O$ were dissolved in 10 mL water with gently heated. After the addition of ~ 23.5 mL of 1M HC1 dropwise to adjust the pH to 4 – 5, the mixture was evaporated to one-third of its volume. After cooling, the crystals were formed which were filtered off and air dried.[6]

2.3.5 Synthesis of $K_8[\beta_2\text{-}GeW_{11}O_{39}]\cdot 14H_2O$

5.4 g (0.052 mol) of GeO_2 were dissolved in 100 mL water (solution A). Then, 182 g (0.552 mol) of $Na_2WO_4\cdot 2H_2O$ were dissolved in 300 mL of water in a separate beaker (solution B). After addition of 165 mL of 4M HCl to the solution B with vigorous stirring in small portions over 15 min, solution A was poured into the tungstate solution (solution B) and the pH adjusted to 5.2 – 5.8 by addition of 4 M HCl solution (~ 40 mL). This pH was kept at this value for 100 min. by addition of the HCl solution. Then, 90 g of solid KCl were added with

gentle stirring. After 15 min., the product was collected by filtration on a sintered glass filter and air dried.[7]

2.3.6 Synthesis of $K_8[\gamma\text{-}GeW_{10}O_{36}]\cdot 6H_2O$

15.2 g (4.63 mmol) of $K_8[\beta_2\text{-}GeW_{11}O_{39}]\cdot 14H_2O$ were dissolved in 150 mL of water. A small amount of insoluble material was removed by rapid filtration on a fine frit or through Celite. The pH of the solution was quickly adjusted to 8.7 – 8.9 by addition of 2 M K_2CO_3 solution. The pH was kept at this value by addition of the K_2CO_3 solution for 16 min. The product was then precipitated by addition of 40 g solid KCl. During the precipitation, the pH was maintained at 8.8 by addition of small amounts of the K_2CO_3 solution or diluted HCl as needed for 10 min. Then, the solid was filtered off and air-dried.[7]

2.3.7 Synthesis of $K_8Na_2[A\text{-}\alpha\text{-}GeW_9O_{34}]\cdot 25H_2O$

To prepare $K_8Na_2[A\text{-}\alpha\text{-}GeW_9O_{34}]\cdot 25H_2O$, at first **$K_6Na_2[\alpha\text{-}GeW_{11}O_{39}]\cdot 13H_2O$** precusor should be prepared: A solution of 72.6 g of $Na_2WO_4\cdot 2H_2O$ in 120 mL of water was added to a solution of 2.05 g of GeO_2 in 40 mL of 1 M NaOH solution. The mixture was stirred and heated. After dropwise addition of 80-mL of 4 M HCl to the hot solution under vigorous stirring, the solution was boiled for about 1 h and cooled to room temperature. A white salt was precipitated upon addition of 30 g of solid potassium chloride. The salt was recrystallized from hot water, then filtered off and air-dried.[8a]

In order to obtain $K_8Na_2[A\text{-}\alpha\text{-}GeW_9O_{34}]\cdot 25H_2O$, 43.5 g (13.5 mmol) sample of $K_6Na_2[\alpha\text{-}GeW_{11}O_{39}]\cdot 13H_2O$ was dissolved in 400 mL of water with stirring. Then 22.5 g (162.8 mmol) of K_2CO_3 was added in small portions to this solution. After stirring for about 30 min. (pH~9.5), a white precipitate appeared slowly. After an additional 20 min. of stirring, the white solid product was collected on a sintered glass frit, washed with saturated KCl solution (20 mL), and air dried. [8b]

2.3.8 Synthesis of $Na_{10}[A\text{-}\alpha\text{-}GeW_9O_{34}]\cdot 4H_2O$

18 g (0.55 mol) of $Na_2WO_4\cdot 2H_2O$ and 5.23 g (50 mmol) of GeO_2 were dissolved in 200 ml of hot water (80-100° C) in an 1L beaker. After addition of 130 ml of 6M HCl to this solution with vigorous stirring over~30 min, the solution was boiled until the volume was ~300 ml and cooled down to room temperature and then filtered over a fine frit to remove the unreacted species. A solution of 50 g of anhydrous Na_2CO_3 in 150 ml of water was slowly added to the first solution with gentle stirring. A precipitate was slowly formed (overnight). This precipitate was collected by filtering using a sintered glass filter. For purification the precipitate was stirred in 1L of 4M NaCl solution and filtered again, and washed successively with two 100-ml portions of ethanol and 100 ml of diethyl ether and then dried at room temperature.[9]

2.3.9 Synthesis of $K_8[BW_{11}O_{39}H]\cdot 13H_2O$

A 300 g sample of $Na_2WO_4\cdot 2H_2O$ and a 20 g sample of H_3BO_3 were dissolved in 500 mL of boiling water. After addition of ~ 190 mL of 6 M HCl over 20 minutes with vigorous stirring in order to dissolve the local precipitate of tungstic acid until the pH was 6, the solution was kept boiling for 1 h and after cooling to room temperature it was kept 24 h at 4 °C. The precipitate was removed by filtration, and then the potassium salt was precipitated from the solution by addition of KCl (~100 g). The crude potassium salt was dissolved in 1 L of water, the insoluble part eliminated, and the potassium salt precipitated again by addition of KCl (~100 g).[10]

2.3.10 Synthesis of $K_6[\alpha\text{-}P_2W_{18}O_{62}]\cdot 20H_2O$

A sample of $Na_2WO_4\cdot 2H_2O$ (300 g; 0.91 mol) dissolved in 350 mL water was acidified by fractional addition of 4M HCl (250 mL) under vigorous stirring. After slowly addition of 250 mL 4M H_3PO_4 to the limpid solution, the formed pale yellow solution was refluxed for at

least 24 h. After this reaction time, the yellow color of the solution had become more intense. This solution was allowed to cool to room temperature and was then treated with 150 g KCl. The precipitate which appeared was filtered off and air-dried. This crude material was dissolved in 650 mL water, and the solution was, eventually, filtered to remove insoluble impurities. The clear solution was then heated to ~80°C for at least 72 h. The solution was then allowed to cool to room temperature before being placed finally in a refrigerator at 4°C. After a few days, the yellow crystals were collected.[11]

2.3.11 Synthesis of $K_{12}[H_2P_2W_{12}O_{48}]\cdot 24H_2O$

83 g of $K_6[\alpha\text{-}P_2W_{18}O_{62}]\cdot 20H_2O$ were dissolved in 300 mL of water. A solution of 48.4 g tris(hydroxymethyl)aminomethane in 200 mL water was then added. The mixture was stirred at room temperature for 30 minutes and then 80 g of KCl were added. After complete dissolution, a solution of 55.3 g of K_2CO_3 in 200 mL water was added. The resulting mixture was vigorously stirred for 15 minutes and the white precipitate that appeared after a few minutes was filtered on a sintered glass frit, and air dried overnight, washed 2-3 times with 50 mL ethanol, dried under suction. The product was then air-dried for 3 days.[12]

2.3.12 Synthesis of $K_{28}Li_5[H_7P_8W_{48}O_{184}]\cdot 92H_2O$

In 950 mL of water were dissolved, successively, 60 g (1 mol) glacial acetic acid, 21g (0.5 mol) of lithium hydroxide, 21g (0.5 mol) of lithium chloride, and 28 g (0.07 mol) of $K_{12}[H_2P_2W_{12}O_{48}]\cdot 24H_2O$. The solution was left in an open beaker. After 9 days the volume of the solution had evaporated to ca. 650 mL and the crystals were collected by suction filtration on a coarse frite and washed with 40 mL ethanol (50%), 40 mL of ethanol and 40 mL of ether and finally air-dried for 1 day.[13]

2.4 References

[1] G. M. Sheldrick, SHELXS-97, *Program for Solution of Crystal Structures*; University of Göttingen: Germany, **1997**.

[2] G. M. Sheldrick, *Acta. Crystallogr.* **2008**, *A64*, 112.

[3] G. M. Sheldrick, SADABS; University of Göttingen: Germany, **1996**.

[4] U. Kortz, M. G. Savelieff, B. S. Bassil, M. H. Dickman, *Angew. Chem., Int. Ed. Engl.* **2001**, *40*, 3384.

[5] K.-C. Kim, A. Gaunt, M. T. Pope, *J. Cluster Sci.* **2002***, 13*, 432.

[6] M. Boesing, I. Loose, H. Pohlmann, B. Krebs, *Chem. Eur. J.* **1997**, *3*, 1232.

[7] N. H. Nsouli, B. S. Bassil, M. H. Dickman, U. Kortz, B. Keita, L. Nadjo, *Inorg. Chem.*, **2006**, *45*, 3858.

[8] a) N. Haraguchi, Y. Okaue, T. Isobe, Y. Matsuda, *Inorg. Chem.* **1994,** *33*, 1015; b) L.-H. Bi, U. Kortz, S. Nellutla, A. C. Stowe, J. van Tol, N. S. Dalal, B. Keita, L. Nadjo, *Inorg. Chem.* **2005**, *44*, 1015.

[9] a) A. Tézé, G. Hervé, *J. Inorg. Nucl. Chem.* **1977**, *39*, 999; b) A. Tézé, G. Hervé, *J. Inorg. Nucl. Chem.* **1977**, *39*, 2151; c) G. Hervé, A. Tézé, *Inorg. Chem.* **1977**, *16*, 2115.

[10] A. Tézé, M. Michelon, G. Hervé, *Inorg. Chem*. **1997**, *36*, 505.

[11] I. M. Mbomekalle, Y. W. Lu, B. Keita, L. Nadjo, *Inorg. Chem. Commun.* **2004**, *7***,** 86.

[12] R. Contant, *Inorg. Synth.* **1990**, 27, 108.

[13] a) R. Contant, A. Tézé, *Inorg. Chem.* **1985**, *24*, 4610; b) M. Zimmermann, N. Belai, R. J. Butcher, M. T. Pope, E. V. Chubarova, M. H. Dickman, U. Kortz, *Inorg. Chem.* **2007**, *46*, 1737.

Chapter III

Lanthanide-Containing POMs

3.A. Lanthanide-Containing Isopolytungstates:

3.A.1. The 22-Isopolytungstate Fragment $[H_2W_{22}O_{74}]^{14-}$ Coordinated to Lanthanide Ions

A. H. Ismail, M. H. Dickman, U. Kortz, *Inorg. Chem.* **2009** *48,* 1559

3.A.1.1. Introduction

Polyoxometalates (POMs) represent a large class of nanosized metal-oxo anions. POMs are remarkable not only in terms of molecular and electronic structural versatility but also because of their reactivity and relevance in fields such as photochemistry, analytical chemistry, clinical chemistry, magnetism, catalysis, biology, medicine, and materials science.[1] Polyoxoanions which result from the condensation of metalate anions in acidified solutions (usually aqueous) can efficiently absorb light in the near UV-vis region and can therefore be used as photocatalysts.[2] The intrinsic chemical properties of POMs as electron acceptors or as very strong Brønsted acids (in their protonated form) make them useful as catalysts in organic transformations, and their abilities to form peroxo complexes or to serve as supports for catalytically active metal ions in high oxidation states are particularly useful in oxidation reactions.[1b,3]

Although the first POM was synthesized already in 1826 by Berzelius,[1a] the mechanism of POM formation is still not completely understood and is often described as a self-assembly. POMs can usually be isolated from aqueous solution as solid salts with appropriate counter cations which may be alkali metal cations (e.g., Li^+, Na^+, K^+, Rb^+, Cs^+) or organic cations (e.g., guanidinium, alkylamines). Two main types of POMs are known, based on their chemical composition: isopoly and heteropoly anions. Isopolyanions are represented by the

general formula $[M_mO_y]^{n-}$, where M is the addendum atom, usually molybdenum or tungsten and less frequently vanadium, niobium, or tantalum in their higher oxidation states. Heteropolyanions are represented with the general formula $[X_xM_mO_y]^{q-}$ ($x \leq m$) where X, the heteroatom, can be one of many elements of the periodic table, most commonly P^{5+}, As^{5+}, Si^{4+}, Ge^{4+} and B^{3+}.[1]

Lanthanide-containing POMs have been investigated less than their 3d-transition-metal-substituted analogues. Because of the larger size of the lanthanide ions compared to 3d metals, they are not fully incorporated into the lacunary site(s) of vacant POM precursors. Because of their higher coordination numbers, each lanthanide ion can be used as a linker to one or more other lacunary POM units. This approach has resulted in polymeric or unusually large molecular POM assemblies.[4] Also, lanthanide-containing POMs can be of interest because of photoluminescence, as well as catalytic, electrochemical, and magnetic properties.[5]

Our group has also been working on lanthanide-containing heteropolytungstates. We have reported the ytterbium-containing tungstoarsenate $[YbAs_2W_{20}O_{68}(H_2O)_3]^{7-}$ resulting from the interaction of the monolacunary $[As_2W_{20}O_{68}(H_2O)]^{10-}$ with Yb^{3+} ions in acidic aqueous medium. The polyanion consists of two $(\alpha\text{-}As^{III}W_9O_{33})^{9-}$ fragments connected by a V-shaped $(H_2O)Yb(OW(H_2O))_2$ fragment.[4j] The monolanthanide-containing polyanion family $[Ln(\beta_2\text{-}SiW_{11}O_{39})_2]^{13-}$ (Ln = La, Ce, Sm, Eu, Gd, Tb, Yb, Lu) has also been synthesized and structurally characterized. These polyanions are composed of two chiral (β_2-$SiW_{11}O_{39}$) units sandwiching the Ln^{3+} ion.[4s] Recently, we reported the 20 cerium containing 100-tungsto-10-germanate $[Ce_{20}Ge_{10}W_{100}O_{376}(OH)_4(H_2O)_{30}]^{56-}$ which is the third largest molecular polytungstate known to date.[4t] We synthesized this polyanion by reaction of the trilacunary POM precursor $[\alpha\text{-}GeW_9O_{34}]^{10-}$ with Ce^{3+} ions in acidic aqueous medium.

Until very recently, only one family of lanthanide-containing isopolyanions had been reported. Peacock and Weakley were the first to describe the sandwich-type decatungstate family of the general formula $[Ln(W_5O_{18})_2]^{n-}$.[4a,6] This polyanion is now known for Ln^{3+} = La,

Ce, Pr, Nd, Sm, Ho, Yb and Y, and also for Ce^{4+}, all synthesized by reaction of the lanthanide ions with Na_2WO_4 in hot aqueous (pH 6.5−7.5) solution. The structure of the *D_{4d}* $[Ln(W_5O_{18})_2]^{n-}$ polyanions consist of two monolacunary Lindqvist based fragments $[W_5O_{18}]^{6-}$ encapsulating a central metal ion exhibiting a square-antiprismatic coordination. Yamase et al. reported the crystal structures of the Pr, Nd, Dy, Sm, Eu, Gd and Tb derivatives with different types of alkali counter cations.[7] The lanthanum analogue $[La(W_5O_{18})_2]^{9-}$ was reported in 2005,[8] and also the actinide analogues $[Th(W_5O_{18})_2]^{8-}$ and $[U(W_5O_{18})_2]^{8-}$ have been studied crystallographically.[5b,9] Very recently our group reported on the synthesis and solid state structure of the yttrium-derivative $[YW_{10}O_{36}]^{9-}$ as well as its solution properties by ^{183}W and ^{89}Y NMR.[10] Very recently, Cao and coworkers reported on a pentadecatungstate ring capped by two Ce^{3+} ions.[11]

The isopolyanion family $[Ln^{III}W_{10}O_{36}]^{9-}$, (Ln = Pr, Nd, Sm, Eu, Tb, Dy), has shown high luminescence quantum efficiency.[12] The decatungstoterbate $[Tb(W_5O_{18})_2]^{9-}$ showed green-emissive luminescence.[7h] Furthremore, Griffith and co-workers studied the lanthanoisopolytungstates $[Ln^{III}W_{10}O_{36}]^{9-}$, (Ln = Y, La, Ce, Pr, Sm, Eu, Gd, Dy, Er, Lu), as calalytic oxidants with H_2O_2 for alcohol oxiditions and alkene epoxidations.[5b] This provides an impetus to prepare other, novel isopolyanion structures coordinated to lanthanide ions.

Herein we report on the synthesis of a novel class of 22-isopolytungstates $\{W_{22}\}$ coordinated to two external lanthanide ions, $[Ln_2(H_2O)_{10}W_{22}O_{71}(OH)_2]^{8-}$ (Ln^{3+} = La (**1**), Ce (**2**), Tb (**3**), Dy (**4**), Ho (**5**), Er (**6**), Tm (**7**), Yb (**8**), Lu (**9**)) and yttrium, $[Y_2(H_2O)_{10}W_{22}O_{71}(OH)_2]^{8-}$ (**10**).

3.A.1.2. Synthesis

$Na_2La_2[La_2(H_2O)_{10}W_{22}O_{72}(OH)_2]\cdot 44H_2O$ (NaLa-1)

A sample of 10.00 g of $Na_2WO_4\cdot 2H_2O$ (30.3 mmol) was dissolved in 20 mL H_2O, followed by dropwise addition of a solution of 1.02 g of $LaCl_3\cdot 7H_2O$ (2.8 mmol) in 5 mL H_2O. Then

2.5 mL of 12M HCl was added dropwise to the resulting solution (local formation and redissolution of hydrated tungsten oxide and lanthanum hydroxide was observed) and then the pH was adjusted to 2.2 using 4M aqueous HCl. The mixture was heated to 90 ºC for 1 h with vigorous stirring. A white precipitate, which had formed, was filtered off and discarded. After cooling to room temperature, the filtrate was kept in an open vial for crystallization. Colorless crystals were obtained after several days, which were filtered off and air-dried. Although additional product continued to form subsequently, it contained NaCl impurities. Yield: 0.87 g (9.2 %). The compound **NaLa-1** could also be synthesized in higher yield under analogous reaction conditions by heating to 45 ºC instead of 90 ºC. Yield: 1.51 g (16 %). IR for **NaLa-1** in cm^{-1} (only between 400-1000 cm^{-1}): 943(m), 868(sh), 820(s), 711(s), 513(w), 419(w), see Figure 3.1. Anal. Calcd (%) for **NaLa-1**: Na, 0.7; W, 59.1; La, 8.1. Found (%): Na, 1.1; W, 59.7; La, 7.7.

$Na_2Ce_2[Ce_2(H_2O)_{10}W_{22}O_{72}(OH)_2]\cdot 44H_2O$ (NaCe-2)

A sample of 10.00 g of $Na_2WO_4\cdot 2H_2O$ (30.3 mmol) was dissolved in 20 mL H_2O followed by dropwise addition of 2.5 mL of 12M HCl (local formation and redissolution of hydrated tungsten oxide was observed). Then a solution of 1.03 g $CeCl_3\cdot 7H_2O$ (2.8 mmol) in 5 mL H_2O was added immediately and dropwise. Finally, the pH was adjusted to 2.2 using 4M aqueous HCl. The mixture was vigorously stirred at room temperature for 1 h. A yellow precipitate, which had formed, was filtered off and discarded. The filtrate was kept in an open vial for crystallization at room temperature. After a few hours, a yet unidentified polycrystalline material started to form and was filtered off successively until yellow crystals of **NaCe-2** started to appear. These crystals were in turn filtered off and air-dried. Yield: 0.63 g (3.8 %). Although additional product continued to form subsequently, it contained NaCl impurities. IR for **NaCe-2**: 944(m), 870(sh), 820(s), 721(s), 514(w), 419(w) cm^{-1}, see Figure 3.1. Anal. Calcd (%) for **NaCe-2**: Na, 0.7; W, 59.1; Ce, 8.2. Found (%): Na, 0.9; W, 58.6; Ce, 8.0.

$Na_5Tb[Tb_2(H_2O)_{10}W_{22}O_{72}(OH)_2]\cdot 41H_2O$ (NaTb-3)

A sample of 10.00 g of $Na_2WO_4\cdot 2H_2O$ (30.3 mmol) was dissolved in 20 mL H_2O and then 2.5 mL of 12M HCl was added dropwise. A sample of 0.93 g $Tb(CH_3COO)_3\cdot H_2O$ (2.8 mmol) in 5 mL H_2O was added dropwise to the acidified tungstate solution and then the pH was adjusted to 2.2 using 4M aqueous HCl. The mixture was vigorously stirred at room temperature for 1 h, and then filtered and allowed to crystallize at room temperature. Colorless crystals were obtained after several days, which were filtered off and air-dried. Yield: 0.65 g (7.0 %). Although additional product continued to form subsequently, it contained NaCl impurities. IR for **NaTb-3**: 944(m), 870(sh), 820(s), 721(s), 514(w), 419(w) cm^{-1}, see Figure 3.1. Anal. Calcd (%) for **NaTb-2**: Na, 1.7; W, 60.0; Tb, 7.1. Found (%): Na, 1.8; W, 58.9; Tb, 6.6.

$Na_8[Dy_2(H_2O)_{10}W_{22}O_{72}(OH)_2]\cdot 49H_2O$ (Na-4)

The same procedure as for **NaTb-3** was followed, but using 1.04 g $DyCl_3\cdot 6H_2O$ instead of $Tb(CH_3COO)_3\cdot H_2O$. Yield: 1.72 g (18.3 %). IR for **Na-4**: 944(m), 870(sh), 820(s), 721(s), 514(w), 419(w) cm^{-1}, see Figure 3.1. Anal. Calcd (%) for **Na-4**: Na, 2.7; W, 59.5; Dy, 4.8. Found (%): Na, 3.1; W, 61.0; Dy, 5.2.

$Na_5Ho[Ho_2(H_2O)_{10}W_{22}O_{72}(OH)_2]\cdot 45H_2O$ (NaHo-5)

The same procedure as for **NaTb-3** was followed, but using 1.05 g of $HoCl_3\cdot 6H_2O$ instead of $Tb(CH_3COO)_3\cdot H_2O$. Yield: 0.86 g (9.1 %). IR for **NaHo-5** in cm^{-1}: 943(m), 868(sh), 820(s), 711(s), 513(w), 419(w), see Figure 3.1. Anal. Calcd (%) for **NaHo-5**: Na, 1.7; W, 59.2; Ho, 7.2. Found (%): Na, 2.4; W, 59.0; Ho, 8.1.

$Na_8[Er_2(H_2O)_{10}W_{22}O_{72}(OH)_2]\cdot 44H_2O$ (Na-6)

The same procedure as for **NaTb-3** was followed, but using 0.95 g of $Er(CH_3COO)_3\cdot H_2O$ instead of $Tb(CH_3COO)_3\cdot H_2O$. Yield: 1.04 g (11.1 %). IR for **Na-6** in cm^{-1}: 943(m), 868(sh), 820(s), 711(s), 513(w), 419(w), see Figure 3.1. Anal. Calcd (%) for **Na-6**: Na, 2.7; W, 60.2; Er, 5.0. Found (%): Na, 2.5; W, 60.0; Er, 6.1.

$Na_8[Tm_2(H_2O)_{10}W_{22}O_{72}(OH)_2]\cdot 41H_2O$ (Na-7)

The same procedure as for **NaTb-3** was followed, but using 0.80 g of $TmCl_3\cdot H_2O$ instead of $Tb(CH_3COO)_3\cdot H_2O$. Yield: 1.81 g (19.8 %). IR for **Na-7** in cm^{-1}: 943(m), 868(sh), 820(s), 711(s), 513(w), 419(w), see Figure 3.1. Anal. Calcd (%) for **Na-7**: Na, 2.8; W, 60.6; Tm, 5.1. Found (%): Na, 2.9; W, 60.0; Tm, 4.8.

$Na_8[Yb_2(H_2O)_{10}W_{22}O_{72}(OH)_2]\cdot 46H_2O$ (Na-8)

The same procedure as for **NaTb-3** was followed, but using 1.24 g $Yb(NO_3)_3\cdot 5H_2O$ instead of $Tb(CH_3COO)_3\cdot H_2O$. Yield: 1.50 g (16.2 %). IR for **Na-8** in cm^{-1}: 943(m), 868(sh), 820(s), 711(s), 513(w), 419(w), see Figure 3.1. Anal. Calcd (%) for **Na-8**: Na, 2.7; W, 59.7; Yb, 5.1. Found (%): Na, 3.1; W, 59.0; Yb, 6.0.

$Na_5Lu[Lu_2(H_2O)_{10}W_{22}O_{72}(OH)_2]\cdot 44H_2O$ (NaLu-9)

The same procedure as for **NaTb-3** was followed, but using 1.07 g $LuCl_3\cdot 5\ H_2O$ instead of $Tb(CH_3COO)_3\cdot H_2O$. Yield: 1.20 g (12.5 %). IR for **NaLu-9**: 943(m), 868(sh), 820(s), 711(s), 513(w), 419(w) cm^{-1}, see Figure 3.1. Anal. Calcd (%) for **NaLu-9**: Na, 2.0; W, 59.0; Lu, 8.0. Found (%): Na, 2.4; W, 60.0; Lu, 6.8.

$Na_8[Y_2(H_2O)_{10}W_{22}O_{72}(OH)_2]\cdot 46H_2O$ (Na-10)

The same procedure as **NaTb-3** was followed using 0.69 g $YCl_3\cdot 6H_2O$. Yield: 1.10 g (12.2 %). IR for **Na-10** in cm^{-1}: 943(m), 868(sh), 820(s), 711(s), 513(w), 419(w), see also Figure 3.1. Anal. Calcd (%) for **Na-10**: Na, 2.8; W, 61.3; Y, 2.7. Found (%): Na, 2.2; W, 62.0; Y, 3.7.

Elemental analyses were carried out by Eurofins Umwelt West GmbH, Wesseling, Germany.

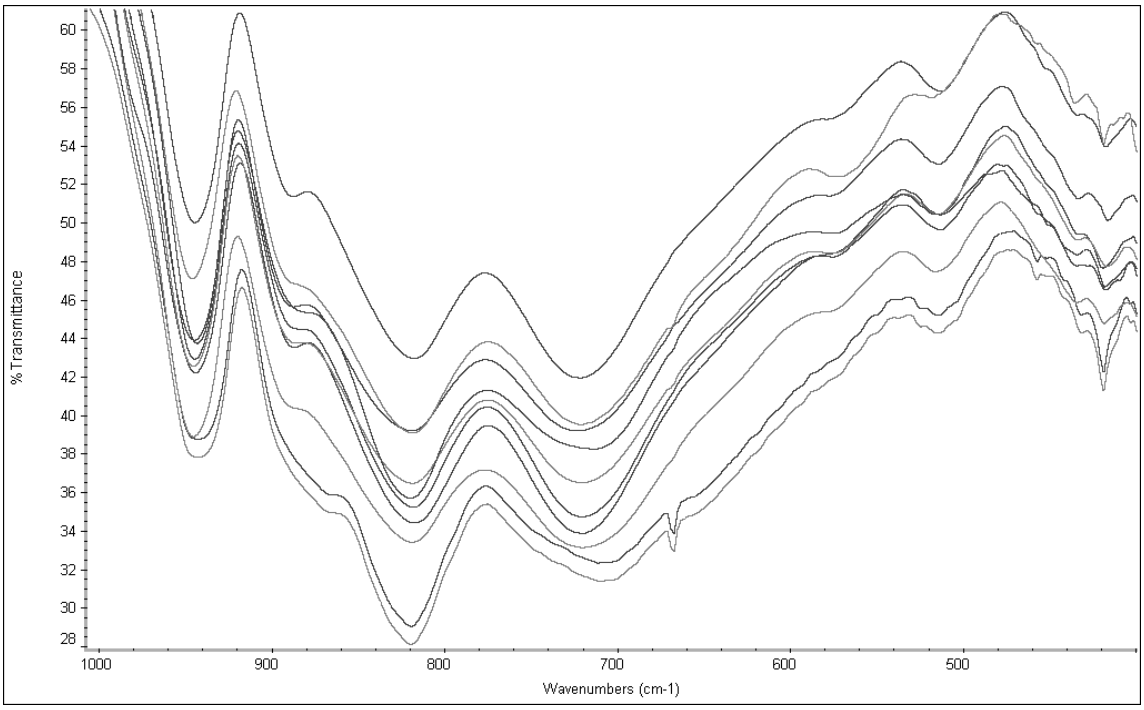

Figure 3.1. IR spectra of the ten compounds **NaLa-1**, **NaCe-2**, **NaTb-3**, **Na-4**, **NaHo-5**, **Na-6**, **Na-7**, **Na-8**, **NaLu-9**, and **Na-10** (from bottom to top).

In this paper, "Ln" will be used as an abbreviation for the lanthanide ions La^{3+}, Ce^{3+}, Tb^{3+}, Dy^{3+}, Ho^{3+}, Er^{3+}, Tm^{3+}, Yb^{3+}, Lu^{3+} as well as for the yttrium ion Y^{3+}, since the ionic radius of the latter falls in the range of lanthanides.

3.A.1.3. X-ray Crystallography

All crystals were mounted in Hampton cryoloops using light oil, for data collection at low temperature. Indexing and data collection were performed using a Bruker X8 APEX II CCD diffractometer with kappa geometry and Mo K_α radiation (λ = 0.71073 Å). Data integration and routine processing were performed using the SAINT software suite. Further data processing, including multi-scans absorption corrections, was performed using SADABS.[13] Direct methods (SHELXS97) solutions successfully located the W atoms, and successive Fourier syntheses (SHELXL97) revealed the remaining atoms.[14] Refinements were full-

matrix least squares against F^2 using all data. Some lanthanides, cations, and waters of hydration were modeled with varying degrees of occupancy, a common situation for polyoxotungstate structures. For **NaTb-3**, **NaHo-5**, and **NaLu-9**, disordered lanthanide counter cations were found in addition to the non-disordered Ln^{3+} ions bridging the $\{W_{22}\}$ polyanion. In the final refinements, all nondisordered heavy atoms (W, Ln) were refined anisotropically, while the O and Na atoms and some disordered lanthanides were refined isotropically. No H atoms were included in the models. The crystallographic data are provided in Table 3.1.

Table 3.1. Crystal Data and Structure Refinement for **NaLa-1 – Na-10.**

Code	**NaLa-1**	**NaCe-2**	**NaTb-3**	**Na-4**	**NaHo-5**
Empirical formula	$H_{114}La_4Na_2O_{130}W_{22}$	$H_{114}Ce_4Na_2O_{130}W_{22}$	$H_{104}Tb_3Na_5O_{125}W_{22}$	$H_{120}Dy_2Na_8O_{133}W_{22}$	$H_{112}Ho_3Na_5O_{129}W_{22}$
MW	6840.91	6845.75	6741.96	6802.27	6831.03
Crystal system	Triclinic	Triclinic	Triclinic	Triclinic	Triclinic
Space group (no.)	$P\bar{1}$ (2)	$P\bar{1}$ (2)	$P\bar{1}$ (2)	$P\bar{1}$ (2)	$P\bar{1}$ (2)
a/Å	13.539(2)	13.4837(12)	12.4701(7)	12.570(3)	12.516(4)
b/Å	13.882(3)	13.9216(13)	12.7195(9)	14.176(3)	12.704(4)
c/Å	17.407(5)	17.393(3)	19.4938(14)	17.714(5)	19.430(7)
α/°	104.742(17)	104.809(7)	74.144(3)	71.874(11)	74.282(18)
β/°	92.426(16)	92.404(6)	76.728(3)	75.026(11)	76.757(16)
γ/°	117.945(10)	118.043(4)	88.131(3)	83.379(10)	88.112(14)
V/Å^3	2744.6(11)	2735.2(6)	2893.4(3)	2895.9(12)	2893.4(17)
Z	1	1	1	1	1
T/ ºC	-40(2)	-100(2)	-100(2)	-100(2)	-100(2)
λ/Å	0.71073	0.71073	0.71073	0.71073	0.71073
D/ Mg m^{-3}	4.07	4.09	3.83	3.87	4.06
μ/ mm^{-1}	24.60	24.78	23.70	23.18	23.95
R[I >2sigma(I)][a]	0.057	0.049	0.055	0.052	0.074
R_w (all data)[b]	0.153	0.121	0.176	0.147	0.233

[a] $R = \sum|F_o| - |F_c| \,|\sum|\, |F_o|$. [b] $R = \sum w(F_o^2| - |F_c^2)^2| \,/\sum w(F_o^2)^2\,]^{1/2}$.

Table 3.1. (continued): Crystal Data and Structure Refinement for **NaLa-1 – Na-10.**

Code	**Na-6**	**Na-7**	**Na-8**	**NaLu-9**	**Na-10**
Empirical formula	$H_{112}Er_2Na_8O_{128}W_{22}$	$H_{104}Tm_2Na_8O_{125}W_{22}$	$H_{114}Yb_2Na_8O_{130}W_{22}$	$H_{110}Lu_3Na_5O_{128}W_{22}$	$H_{114}Y_2Na_8O_{130}W_{22}$
MW	6723.73	6671.02	6769.30	6843.13	6601.35
Crystal system	Triclinic	Triclinic	Triclinic	Triclinic	Triclinic
Space group (no.)	$P\bar{1}$ (2)	$P\bar{1}$ (2)	$P\bar{1}$ (2)	$P\bar{1}$ (2)	$P\bar{1}$ (2)
a/Å	12.546(4)	12.5155(11)	12.5045(6)	12.172(3)	12.5441(17)
b/Å	14.124(5)	12.6622(14)	12.6590(7)	12.465(3)	14.107(2)
c/Å	17.720(6)	18.3682(17)	18.3630(11)	19.469(5)	17.689(3)
α/°	72.166(18)	98.285(6)	98.284(4)	78.041(13)	71.931(9)
β/°	75.056(17)	95.498(5)	95.477(3)	77.672(15)	75.018(8)
γ/°	83.375(16)	93.339(6)	93.339(3)	86.625(11)	83.382(7)
V/Å^3	2885.7(16)	2859.6(5)	2855.6(3)	2823.0(12)	2872.5(8)
Z	1	1	1	1	1
T/ ºC	-100(2)	-100(2)	-100(2)	-100(2)	-100(2)
λ/Å	0.71073	0.71073	0.71073	0.71073	0.71073
D/ Mg m^{-3}	3.88	3.93	3.85	3.88	3.82
μ/ mm^{-1}	23.42	23.71	23.82	24.18	23.08
R[I >2sigma(I)][a]	0.106	0.049	0.043	0.048	0.034
R_w (all data)[b]	0.280	0.127	0.123	0.122	0.088

[a] $R = \sum||F_o| - |F_c|| \sum|F_o|$. [b] $R = \sum w(F_o^2| - |F_c^2)^2| / \sum w(F_o^2)^2]^{1/2}$.

3.A.1.4. Results and Discussion

The ten novel lanthanide containing isopolytungstates $[Ln_2(H_2O)_{10}W_{22}O_{71}(OH)_2]^{8-}$ (Ln = La (**1**), Ce (**2**), Tb (**3**), Dy (**4**), Ho (**5**), Er (**6**), Tm (**7**), Yb (**8**), Lu (**9**), Y (**10**)) have been prepared by reaction of WO_4^{2-} and lanthanide ions in a ratio of 11:1 in aqueous medium at pH 2.2. We discovered that three parameters are crucial for the successful formation of pure salts of **1**-**10**: reaction temperature, concentration of reagents, and pH of the solution. For example, the lanthanum analogue **1** forms only if the solution is heated. If the synthesis is performed at room temperature, a different product is formed as based on IR which has not been fully characterized yet but appears to be $\{W_{56}\}$ based on preliminary crystal structures (*vide infra*). On the other hand, the cerium analogue **2** forms only at room temperature and is isolated as a second batch using fractional crystallization. The first crop of crystals appears to be identical with the room temperature product of the La synthesis described above, as based on IR. If the synthesis solution of **2** is heated, the well-known metatungstate ion $[H_2W_{12}O_{40}]^{6-}$ is formed. Polyanions **3**–**10** also form upon heating, but the yield is much higher at room temperature. The yield is also affected by the concentration of the starting material. A tungstate concentration as high as 1.5 M is needed to obtain a pure crystalline product. Lower concentrations result in lower yields and non-crystalline powder as the main product. It is interesting that formation of a considerable amount of unidentified precipitate was also detected during the optimal synthetic procedure, which partially accounts for the low yields observed. This precipitate had an IR signature different from **1**–**10**. Finally, we discovered that the pH of the reaction solution affects the formation and yields of compounds **1**–**10**. A pH window of 2.0-3.5 can be considered for a successful synthetic procedure, with a pH of 2.2 being optimal. A pH lower than 2.0 did not result in any product, and a pH higher than 3.5 produced paradodecatungstate ($[H_2W_{12}O_{42}]^{10-}$) as the main product.

The synthetic procedures of **2–10** are very similar to Peacock and Weakley's $[Ln(W_5O_{18})_2]^{n-}$ and only differ in the pH of the reaction.[4a] These authors worked at pH ~7, whereas we used pH ~2. It is well-known that pH is a crucial parameter in POM synthesis in general. For tungstates, it is also known that paratungstate, $[H_2W_{12}O_{42}]^{10-}$, dominates in weakly acid solution and metatungstate, $[H_2W_{12}O_{40}]^{6-}$, in strongly acidic solution.[1a] Continuous acidification leads eventually to the tungsten oxide hydrate, $WO_3 \cdot 2H_2O$.[15]

Figure 3.2 shows the formation of different polytungstate structures in the absence and presence of lanthanide ions. Peacock and Weakley were able to isolate the sandwich-type, lanthanide-containing decatungstate $[Ln(W_5O_{18})_2]^{n-}$ $\{LnW_{10}\}$ in a pH range where paratungstate is the major product if no lanthanide ions are present. The pH range of formation for **1–10** falls in the same range of formation for metatungstate, if no lanthanide ions are present. Therefore, the presence of lanthanide ions in solution is essential for the isolation of $\{LnW_{10}\}$ at pH 5-7 and **1–10** at pH ~2.

We discovered experimentally that the presence of the lanthanide ions is needed at a very early stage in the synthesis of **2–10**. If the pre-acidified tungstate solution is left alone for too long before addition of the lanthanide solution, no lanthanide containing polyanion is formed but rather the metatungstate ion $[H_2W_{12}O_{40}]^{6-}$. For the synthesis of **1** the situation is even more critical, as the presence of La^{3+} ions was essential even before the first acidification step. An additional practical complication of this situation is that because of the formation of hydroxides the solution turns rather cloudy making it difficult to detect the redissolution of tungsten oxide which is formed while adding HCl_{aq}. The synthesis procedure was more straightforward for the late lanthanides Tb-Lu (**3-9**), and for the early 4d metal Y (**10**).

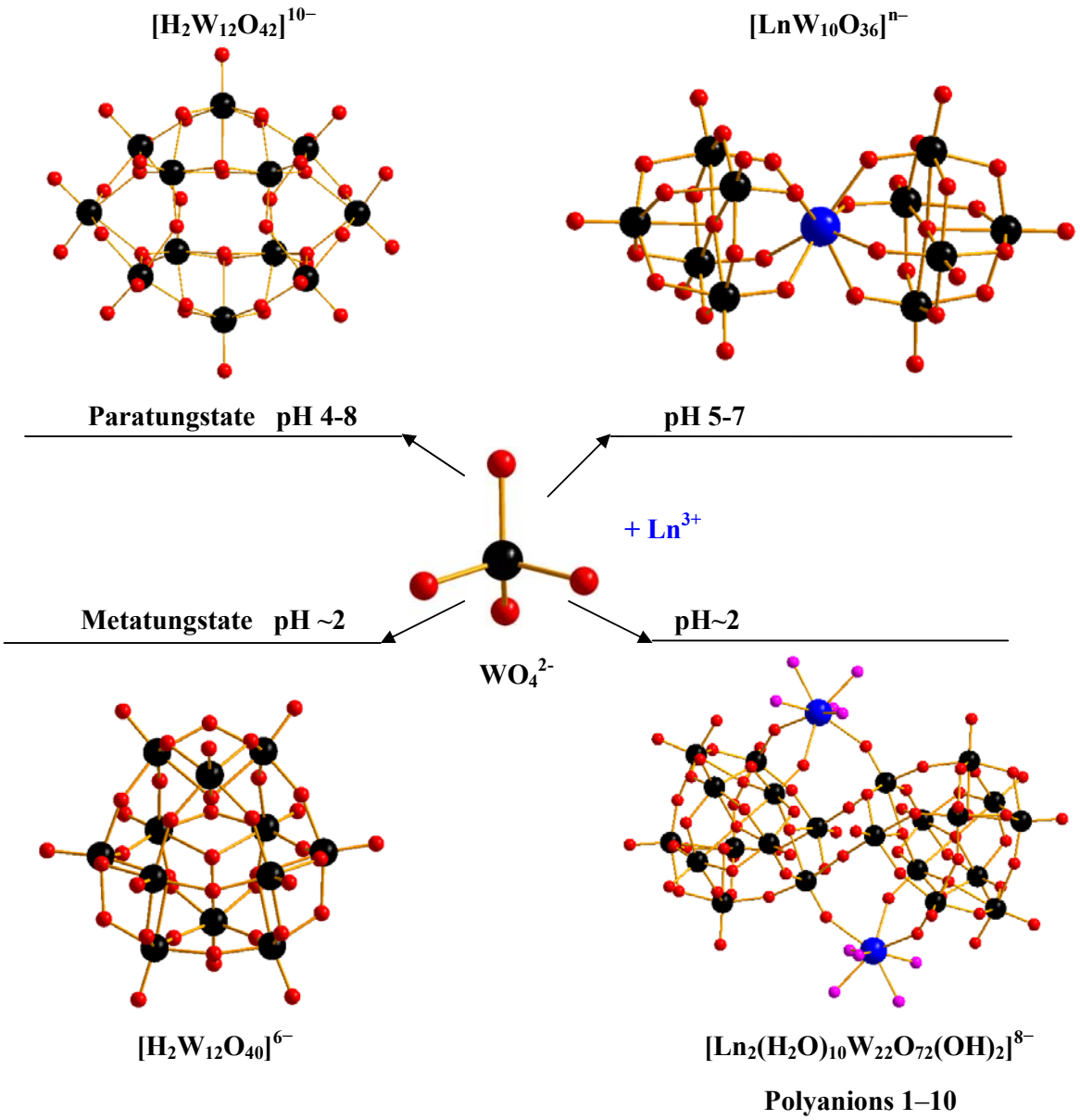

Figure 3.2. Formation scheme of two different isopolydodecatungstates (left), and two lanthanide containing isopolytungstates (right) as a function of pH. The color code is as follows: W (black); O (red); Ln (blue); H_2O (pink).

When applying such synthesis procedure to the early lanthanides, then different products are obtained. Preliminary X-ray diffraction (XRD) analysis revealed the novel, lanthanide-containing 56-tungsten isopolyanion {**W$_{56}$**} family $\{[Ln_2(H_2O)_{11}W_{28}O_{93}(OH)_2]^{14-}\}_2$, Ln = La–Gd. So far, we have obtained single-crystal XRD analyses for the lanthanum and cerium derivatives.[16] After successive filtrations, another crystalline product is formed which turned out to be $\{Ln_2W_{22}\}$ based on IR and single crystal XRD. Polyanions **1–10** are isostructural

and crystallize as hydrated sodium salts in the common triclinic space group $P\bar{1}$. This is reflected in their virtually identical IR spectra (see Figure 3.1).

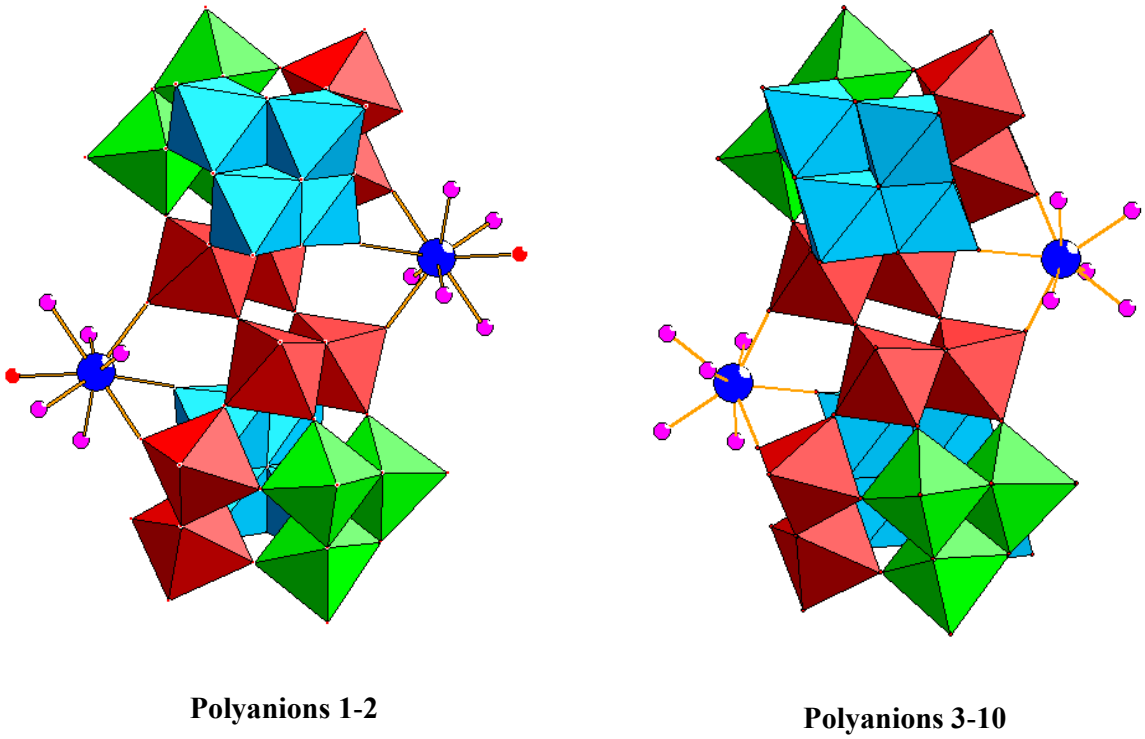

Figure 3.3. Polyhedral representation of $[Ln_2(\mathbf{H_2O})_{10}W_{22}O_{72}(OH)_2]^{8-}$ (**1–2**) (left) and $[Ln_2(\mathbf{H_2O})_{10}W_{22}O_{72}(OH)_2]^{8-}$ (**3–10**) (right). The structures of both polyanions are virtually identical, except the coordination number (8 vs 9) of the lanthanide ions (see text for details). The color code is as follows: WO_6 octahedra (light blue, green, red); Ln (blue); H_2O (pink), O (red). The WO_6 octahedra were colored differently for clarity. See also text and Figure 3.5.

Single-crystal XRD on the salts of polyanions La (**1**), Ce (**2**), Tb (**3**), Ho (**5**) and Lu (**9**) showed extra lanthanides as counter cations. These results were also confirmed by elemental analysis. The structure of polyanions **1–10** comprises the $[H_2W_{22}O_{74}]^{14-}$ isopolyanion coordinated to two $\{Ln(H_2O)_5\}^{3+}$ supporting ions. This 22-isopolytungstate consists of two undecatungstate units $\{W_{11}\}$ fused by two corner sharing W–O–W bridges (see Figure 3.3). Hence this structure can be described as a dimeric molecular entity composed of two $\{LnW_{11}\}$ half-units related by an inversion center, with point group symmetry C_i. Each Ln^{3+} is linked to the $\{W_{22}\}$ unit through three μ_2-oxo bridges, two bridges to one $\{W_{11}\}$ half-unit

and one bridge to the other half-unit. For the smaller lanthanides and yttrium (**3**–**10**), the remaining coordination sphere is filled by five aqua ligands, giving a total coordination number of eight for each metal ion resulting in idealized square-antiprismatic geometry (see Figure 3.3). For the lanthanum and cerium derivatives, **1** and **2**, an extra coordination site was found due to the larger size of the early lanthanides, hence leading to a coordination number of nine and idealized monocapped antiprismatic geometry (see Figure 3.3). This extra coordination site has important consequences with respect to the solid state structures of **1** and **2**. We observed an extra μ_2-oxo bridge between the lanthanum/cerium ions of one polyanion to a tungsten center of an adjacent polyanion, resulting in two intermolecular bridges and an overall 1D chain arrangement of the polyanions in the solid state (Figure 3.4). Average Ln-O bond lengths were calculated for **1**–**10** and are shown in Table 3.2. As expected, a difference of ca. 0.2 Å was observed between the Ln-O bonds of the early (La and Ce) and late (Tb-Lu) lanthanides. For yttrium, the average Y–O bond lengths fall in the range of the late lanthanides.

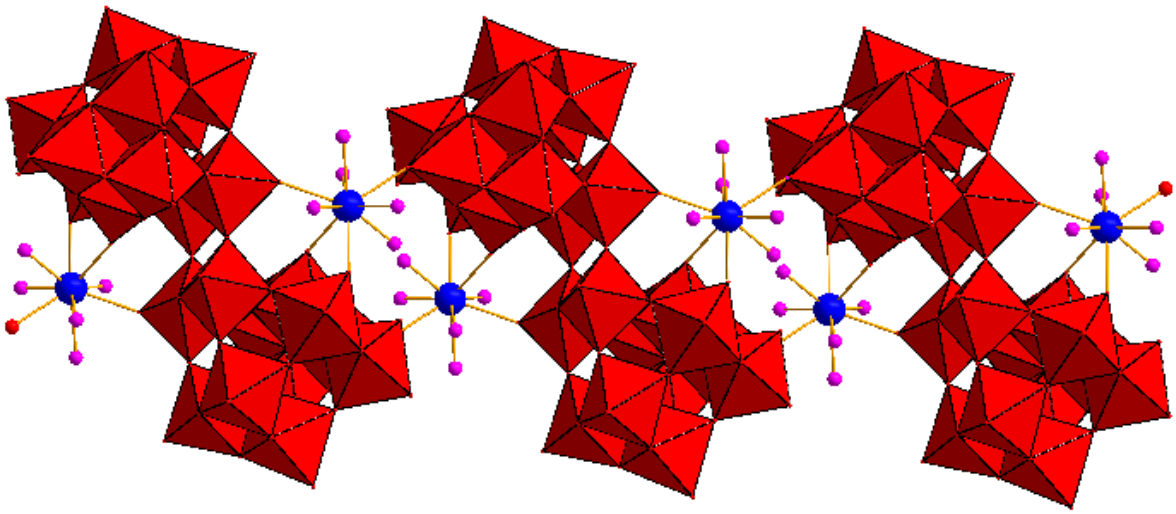

Figure 3.4. Polyhedral representation of polyanions **1** and **2** forming 1D chains in the solid state. The color code is as follows: WO_6 octahedra (red); La or Ce (blue); H_2O (pink), O (red).

Table 3.2. Average Ln–O Bond Lengths in Å $[Ln_2(H_2O)_{10}W_{22}O_{72}(OH)_2]^{8-}$ (La (**1**), Ce (**2**), Tb (**3**) Dy (**4**), Ho (**5**), Er (**6**), Tm (**7**) ,Yb (**8**), Lu (**9**), Y (**10**))

Ln	Average Ln–O(W)	Average Ln–OH_2
La (**1**)	2.551(15)	2.562(18)
Ce (**2**)	2.523(11)	2.533(12)
Tb (**3**)	2.324(13)	2.337(15)
Dy (**4**)	2.382(10)	2.388(12)
Ho (**5**)	2.339(11)	2.388(12)
Er (**6**)	2.36(3)	2.33(4)
Tm (**7**)	2.310(11)	2.350(11)
Yb (**8**)	2.302(8)	2.344(8)
Lu (**9**)	2.301(11)	2.328(12)
Y (**10**)	2.339(7)	2.361(7)

The undecatungstate subunit $\{W_{11}\}$, two of which comprise the $\{W_{22}\}$ fragment in **1**–**10**, can be considered an assembly of four distinct "building blocks", see Figure 3.5:

- One tetratungstate $\{W_4\}$ fragment (light blue in Figure 3.5) formed from four edge-shared WO_6 octahedra connected via a μ_4-oxo bridge. This tetratungstate fragment can be viewed as a dilacunary form of the Lindqvist structure.[1]
- One tritungstate $\{W_3\}$ fragment (green in Figure 3.5) formed from three edge-shared WO_6 octahedra connected via a μ_3-hydroxo bridge (*vide infra*). This fragment can be viewed as a single "triad" of the well-known Keggin or Wells-Dawson ions.[1]
- Two ditungstate $\{W_2\}$ fragments (red in Figure 3.5), each formed from two edge-shared WO_6 octahedra which are corner-sharing on one side.

This undecatungstate fragment $\{W_{11}\}$ was first reported by Fuchs in 1988.[17] Here we report on the lanthanide capped 22-isopolytungstate $\{W_{22}\}$, which represents two $\{W_{11}\}$ fragments fused via two W–O–W' bridges (see Figure 3.5).

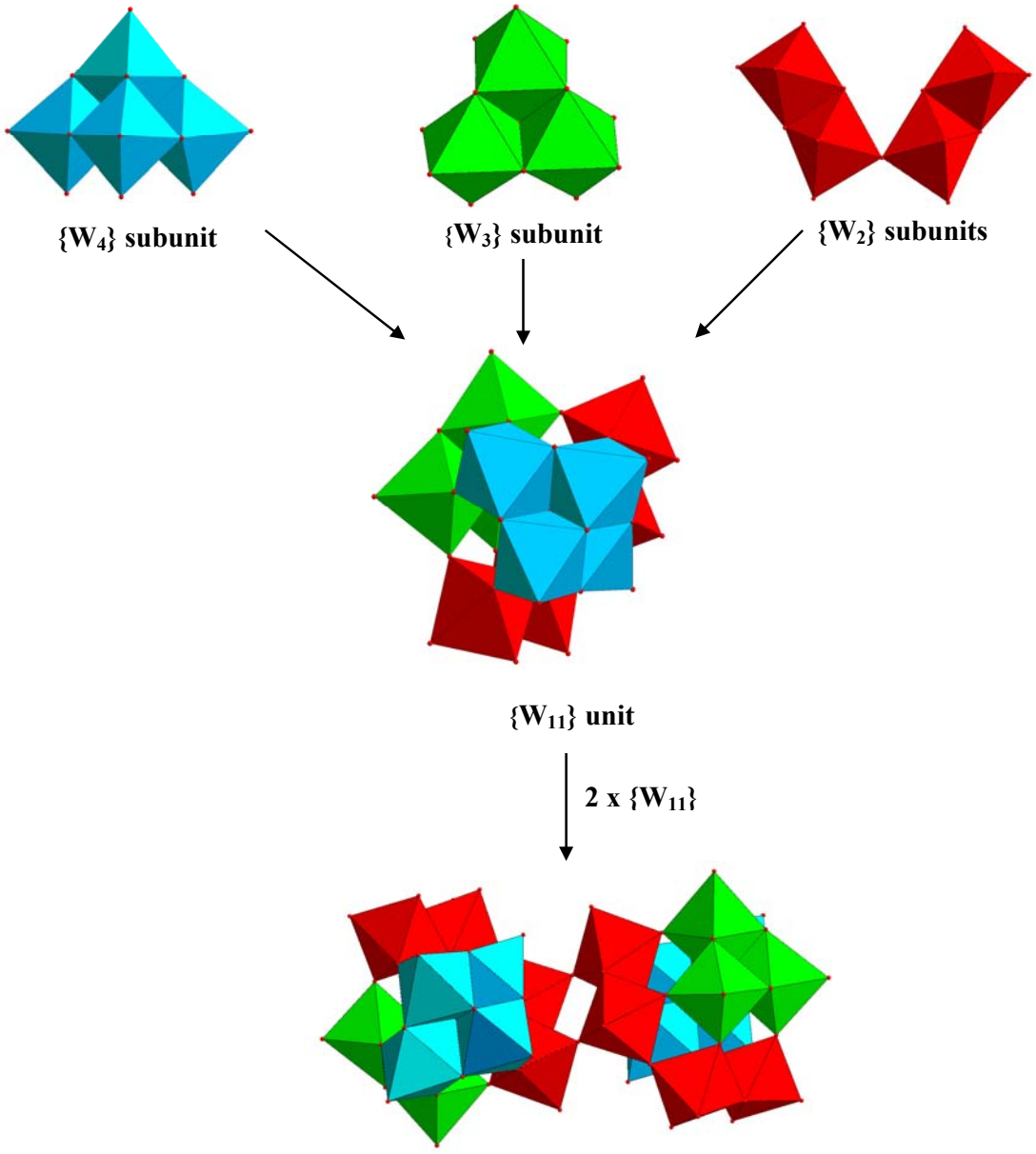

Figure 3.5. Polyhedral representation of the {**W22**} unit of **1–10** which is composed of two {W_{11}} half-units. The latter are composed of di-, tri- and tetrameric tungsten-oxo building blocks shown in different color: {W_4} (light blue), {W_3} (green), {W_2} (red).

Recently Cronin et al. reported on {W_{36}} which is a cyclic trimer of {W_{11}} linked via three extra WO_6 bridges and stabilized by a central potassium ion.[18] Figure 3.6 summarizes the three isopolytungstate structures {W_{11}}, {W_{36}} and {W_{22}} and the respective formation conditions. The {W_{22}} isopolytungstate as such offers two tridentate ligand sites, which are

coordinated to two Ln^{3+} centers in **1–10**. To the best of our knowledge, polyanions **1–10** represent the largest lanthanide-containing isopolytungstates known to date.

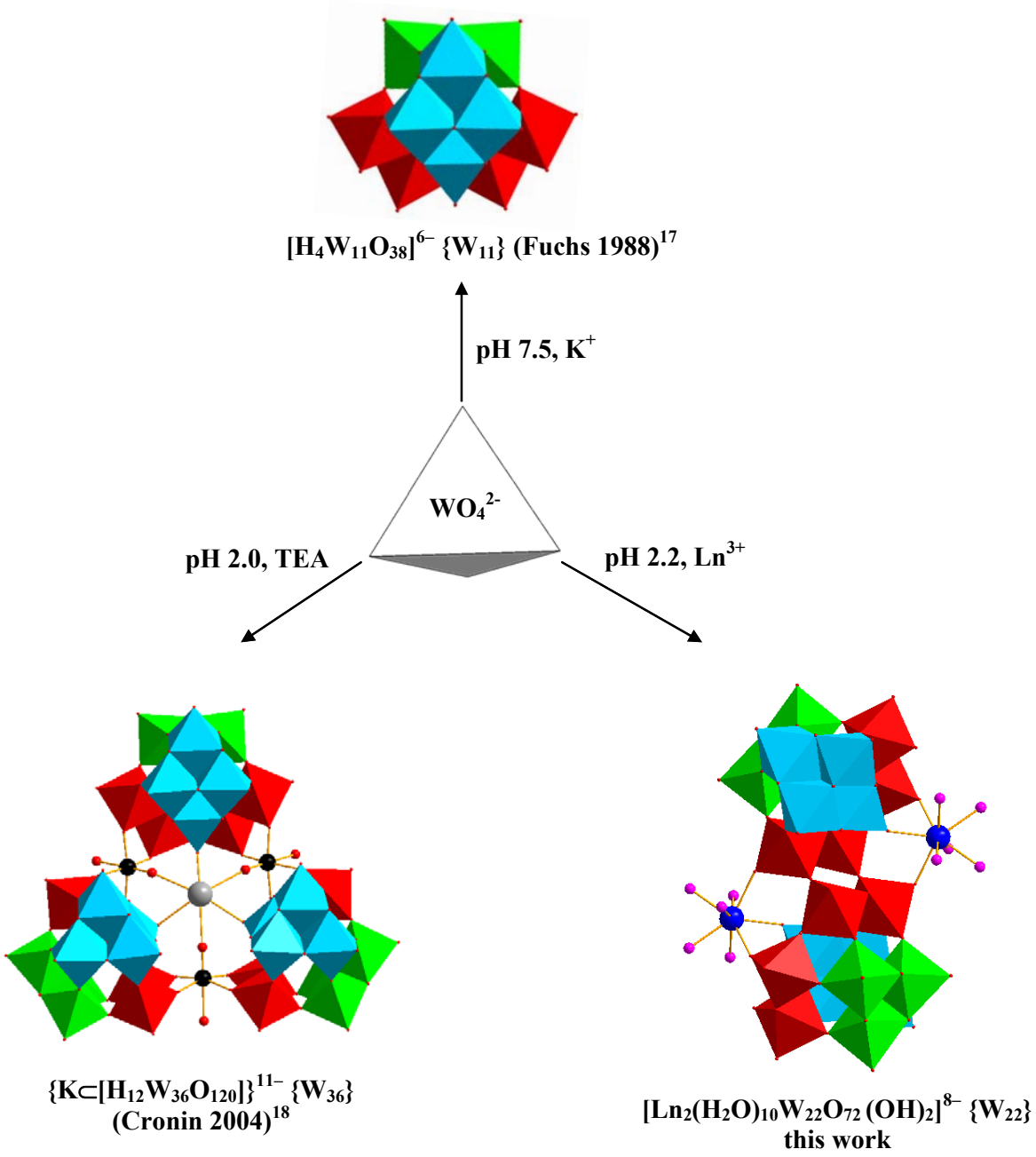

Figure 3.6. Polyhedral/ball-and-stick representation of isopolytungstates containing the {W_{11}} unit. The color code is the same as in Figure 3.5: tungsten (black); potassium (gray), oxygen (red). The abbreviation **TEA** represents triethanolamine.

We also tried to synthesize the lanthanide-free isopolyanion $[H_2W_{22}O_{74}]^{14-}$ by following the same synthetic procedure as **1–10**, but in the absence of lanthanides. We were able to isolate a solid compound with an IR spectrum very similar to that of **1–10** (Figure 3.7) and different from paratungstate and metatungstate (Figure 3.8).

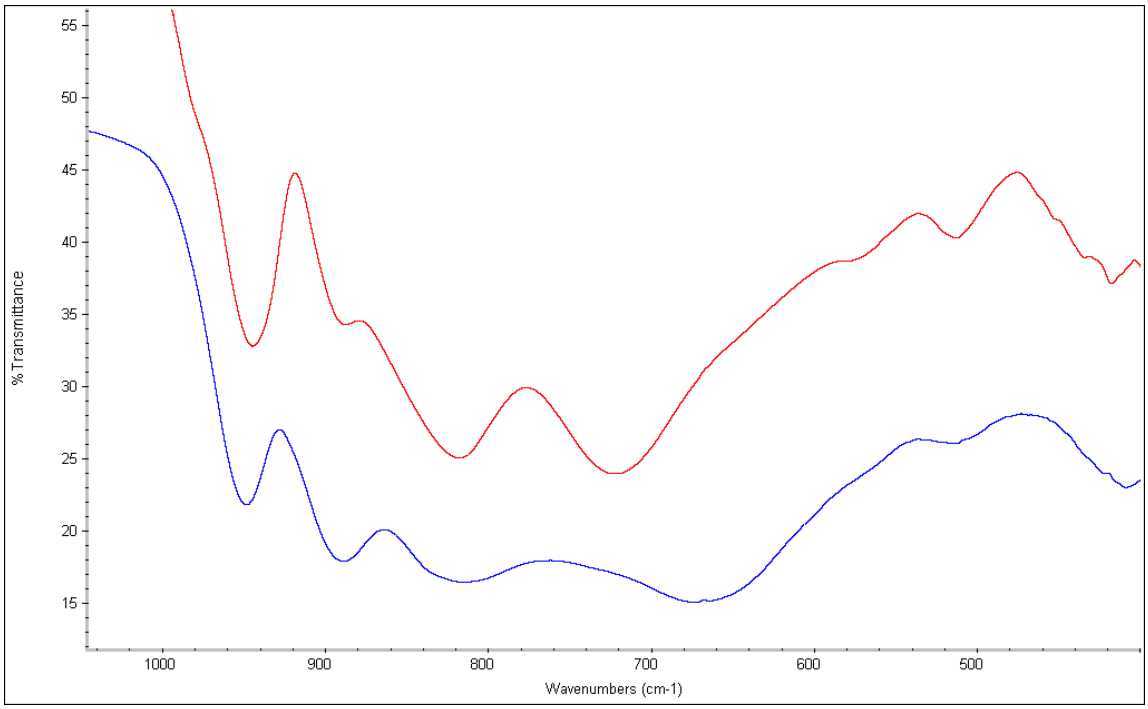

Figure 3.7. IR spectra of lanthanide-free $\{W_{22}\}$ (blue curve) and $\{Ln_2W_{22}\}$ (red curve).

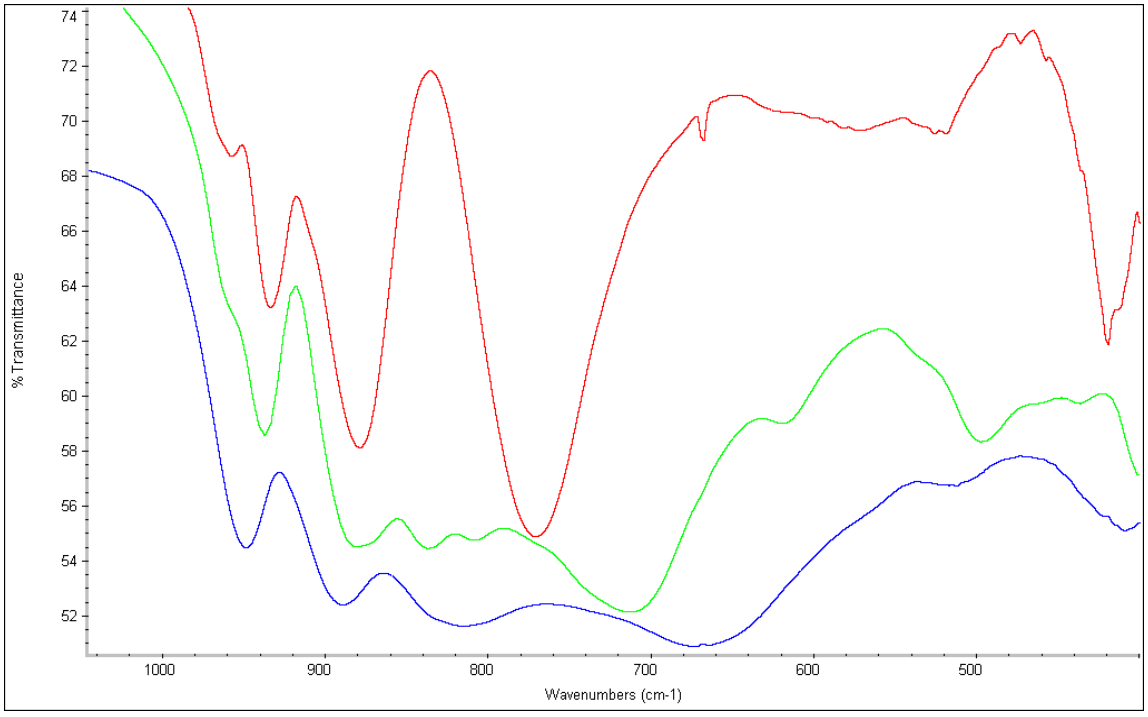

Figure 3.8. IR spectra of the lanthanide-free $[W_{22}O_{72}(OH)_2]^{14-}$ $\{W_{22}\}$ (blue curve), paratungstate $[H_2W_{12}O_{42}]^{10-}$ (green curve) and metatungstate $[H_2W_{12}O_{40}]^{6-}$ (red curve).

Bond valence sum (BVS) calculations for **1**–**10** confirmed that all tungsten atoms are in the +6 oxidation state, and that all lanthanide ions and yttrium are in the +3 oxidation state.[19] The main purpose of our BVS studies on **1**–**10** was indeed to check all polyanion oxygens for possible protonation. As stated above, one monoprotonated oxygen was identified in the asymmetric half-unit, namely the μ_3-oxo bridge of the $\{W_3\}$ fragment connecting the three tungsten atoms W5, W6 and W7 (see Figure 3.9). This results in two OH groups for the dimeric form and a total charge of -8 for all polyanions **1**–**10**. As usual, terminal W=O oxygen BVS values are low (~ 1.5) but this is typical for the distorted W=O geometry and does not indicate additional protonation.

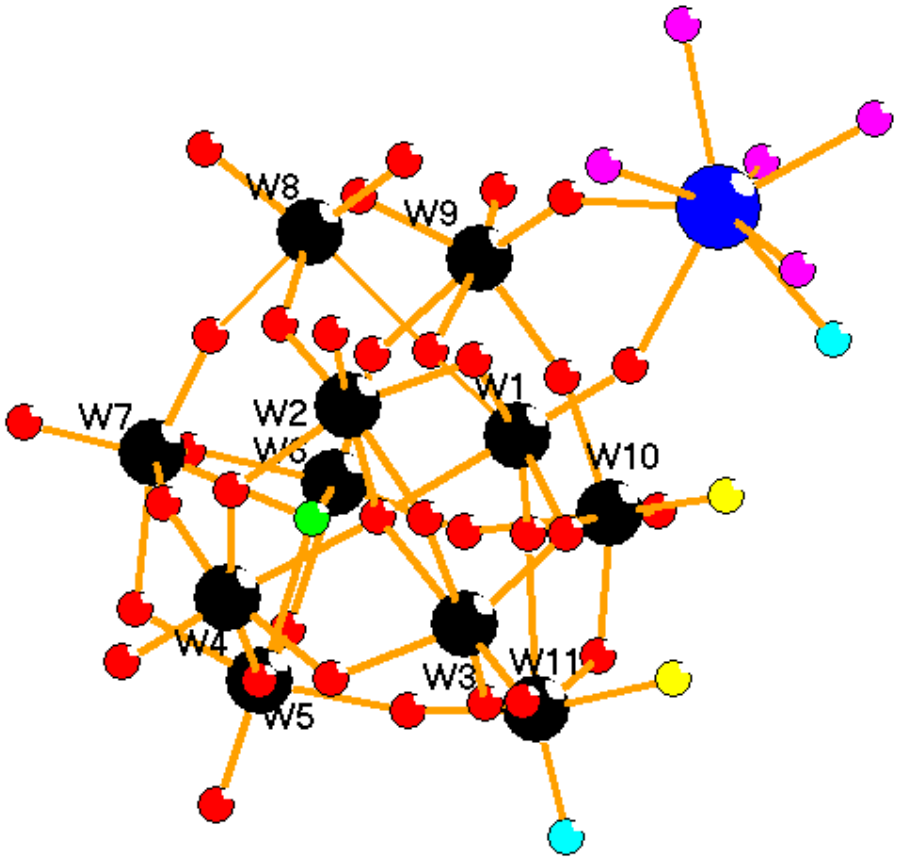

Figure 3.9. Ball-and-stick representation of the $\{Ln(H_2O)_5W_{11}O_{38}\}$ half-unit. The color code is as follows: W (black); O (red); Ln (blue); H_2O (pink); mono-protonated μ_3-oxygen (green), bridging Ln–O–W' oxygen (turquoise); bridging W–O–W' oxygen (yellow).

Polyanions **1**–**10** represent the first examples of lanthanide-containing isopolyanions with "exposed" lanthanide centers, bearing aqua ligands, which are expected to be labile. These water molecules represent good candidates for ligand substitution by other mono- or polydentate ligands, including chiral ones. The resulting chiral polyanions could be interesting for catalytic applications. Also, lipophilic alkyl ammonium salts of **1**–**10** could be useful for homogeneous catalysis applications in organic media. We plan to perform such studies in the near future.

Thermogravimetric analyses (TGA) were performed on the salts of **1**–**10** to determine the respective degree of hydration and the thermal stability. The TGA graphs of all ten compounds showed a region of weight loss due to dehydration (see Figure 3.10). This region

corresponds to a two-step weight loss in the range of ~25 – 200 ˚C and ~200 – 400 ˚C for salts of derivatives **3**–**10**. The first step is attributed to the release of all lattice water molecules and the second step to the release of the coordinated water molecules, corresponding approximately to the calculated 10 waters per molecular formula. For the La and Ce derivatives **1** and **2**, this region exhibits a one-step only weight loss in the range ~25 – 400 ˚C making the steps for the loss of crystal and coordinated water molecules indistinguishable. This reflects nicely the different solid state packing of **1** and **2**, compared to **3**–**10** (vide supra). The degree of hydration was calculated for all compounds and gave a range of 41 – 49 water molecules per formula unit. These results were also supported by elemental analysis. Furthermore, the absence of any additional weight loss indicated that all ten compounds, after loss of the water molecules, were thermally stable up to 800 – 900 °C (see Figure 3.10).

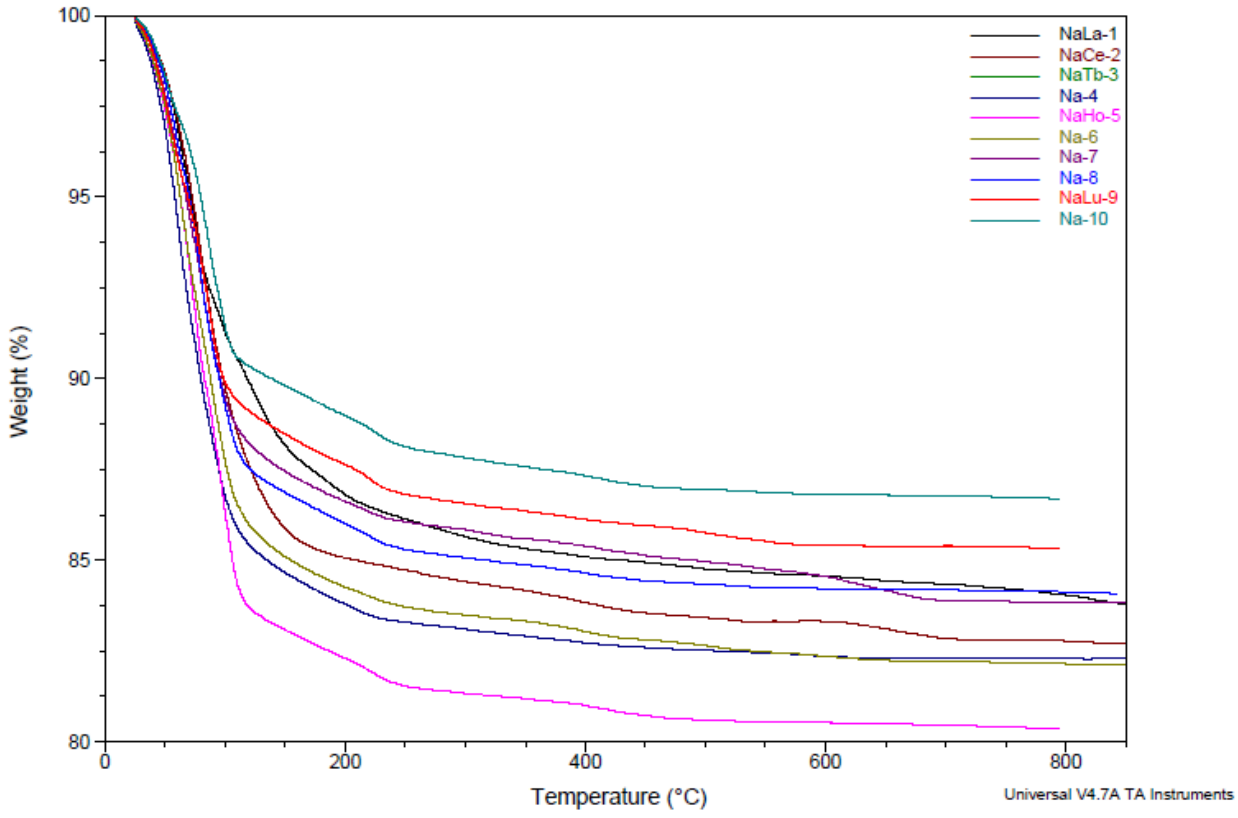

Figure 3.10. Thermograms of **NaLa-1** – **Na-10**.

We tried very hard to obtain solution ^{183}W NMR spectra of the diamagnetic derivatives **9** and **10** (Lu and Y analogues), but without success. The same also applies for ^{89}Y NMR. Both compounds were not very soluble. Although heating to ~80 ºC eventually led to partial dissolution, ^{183}W NMR of these solutions resulted in a single peak for metatungstate ($[H_2W_{12}O_{40}]^{6-}$) indicating decomposition of **9** and **10** at this temperature. The ^{89}Y spectrum of polyanion **10**, when dissolved upon heating, showed a signal typical for free Y^{3+} ions. We also tried cation exchange using a Li^+ loaded resin, which led eventually to complete dissolution of the polyanion salts. However, the ^{183}W NMR spectra for both **9** and **10** were not conclusive and showed a large number (>11) of peaks probably arising from a mixture of species in solution. We speculate that Li^+ ion exchange may have stripped the Lu^{3+} and Y^{3+} from the polyanion framework, thus initiating a decomposition pathway resulting in various products. We also performed ^{183}W NMR studies on Fuchs' original $\{W_{11}\}$, but we observed too many signals which we attributed to a mixture of $[H_2W_{12}O_{42}]^{10-}$ and $\{W_{11}\}$.

3.A.1.5. Conclusions

We have successfully synthesized and structurally characterized by IR spectroscopy, TGA and single crystal X-ray diffraction 10 novel isopolyoxotungstate anions containing lanthanides: $[Ln_2(H_2O)_{10}W_{22}O_{72}(OH)_2]^{8-}$ (Ln^{3+} = La (**1**), Ce (**2**), Tb (**3**), Dy (**4**), Ho (**5**), Er (**6**), Tm (**7**), Yb (**8**), Lu (**9**), Y (**10**)). These polyanions were synthesized in aqueous acidic medium starting from sodium tungstate and Ln^{3+} salts. Polyanions **1**–**10** were isolated as sodium or mixed sodium/lanthanide salts and they all crystallized in the triclinic space group $P\bar{1}$. Single crystal X-ray structural analysis showed that all polyanions are isostructural and are composed of a 22-tungsten isopolyanion unit $\{W_{22}\}$ coordinated to two lanthanide ions bearing terminal aqua ligands. The 22-tungstate unit $\{W_{22}\}$ is assembled from two $\{W_{11}\}$ subunits fused via two corner-sharing W-O-W bridges. The undecatungstate subunit has been reported before in a monomeric and trimeric form. Possible applications of polyanions **1**–**10**

in the field of homogeneous catalysis may prove possible if pure lipophilic organic salts can be prepared. Chiral derivatives of **1–10** can be envisioned by replacing the terminal water ligands on the lanthanide centers by chiral organic ligands. This will be the scope of further studies.

3.A.1.6. References

[1] a) *Heteropoly and Isopoly Oxometalates*; M. T. Pope, Springer-Verlag: Berlin, 1983; b) M. T. Pope, A. Müller, *Angew. Chem., Int. Ed. Engl.* **1991**, *30*, 34; c) *Polyoxometalates: From Platonic Solids to Anti- Retroviral Activity*; M. T. Pope, A. Müller, Eds.; Kluwer: Dordrecht, The Netherlands, 1994; d) A. Müller, Reuter, H.; Dillinger, S. *Angew. Chem., Int. Ed. Engl.* **1995**, *34*, 2328; e) *Polyoxometalates: Chemical Reviews*, Hill, C., 1998 (special thematic issue on polyoxometalates); f) *Polyoxometalate Chemistry: From Topology via Self-Assembly to Applications;* M. T. Pope, A. Müller, Eds.; Kluwer: Dordrecht, The Netherlands, 2001; g) *Polyoxometalate Chemistry for Nano-Composite Design;* T. Yamase, M. T. Pope, Eds.; Kluwer: Dordrecht, The Netherlands, 2002; h) Choppin, G. R. J. *Nucl. Radiochem. Sci.* **2005**, *6*, 1.

[2] a) A. Mylonas, E. Papaconstantinou, *J. Mol. Catal. A: Chemical* **1994**, *92*, 3, 261; b) A. Mylonas, A. Hiskia, E. Papaconstantinou, *J. Mol. Catal. A: Chemical* **1996**, *114*, 191; c) A. Hiskia, A. Mylonas, E. Papaconstantinou, Chem. Soc. Rev., **2001**, *30*, 62; d) A. Hiskia, A. Troupis, E. Papaconstantinou, *Int. J. Photoenergy* **2002**, *4*, 35; e) E. Gkika, P. Kormali, S. Antonaraki, D. Dimoticali, E. Papaconstantinou, A. Hiskia, *Int. J. Photoenergy* **2004**, *6*, 227; f) A. Hiskia, A. Troupis, S. Antonaraki, E. Gkika, P. Kormali, E. Papaconstantinou, *Int. J. Envir. Anal. Chem.* **2006**, 233.

[3] N. Mizuno, M. Misono, *Chem. Rev.* **1998**, *98*, 199.

[4] a) R. D. Peacock, T. J. R. Weakley, *J. Chem. Soc. A* **1971**, 1836; b) M. H. Dickman, G. J. Gama, K-C. Kim, M. T. Pope, *J. Clust. Sc.* **1996**, *7*, 567; c) K. Wassermann, M. H. Dickman,

M. T. Pope, *Angew. Chem., Int. Ed. Engl.* **1997**, *36*, 1445; d) M. Sadakane, M. H. Dickman, M. T. Pope, *Angew. Chem., Int. Ed. Engl.* **2000**, *39*, 2914; e) M. Sadakane, M. H. Dickman, M. T. Pope, *Inorg. Chem.* **2001**, *40*, 2715; f) Q. H. Luo, R. C. Howell, M. Dankova, J. Bartis, C. W. Williams, W. D. Horrocks, V. G. Young, A. L. Rheingold, L. C. Francesconi, *Inorg. Chem.* **2001**, *40*, 1894 ; g) G. L. Xue, J. Vaissermann, P. Gouzerh, *J. Clust. Sci.* **2002**, *13*, 409 ; h) Q. H. Luo, R. C. Howell, J. Bartis, M. Dankova, W. D. Horrocks, A. L. Rheingold, L. C. Francesconi, *Inorg. Chem.* **2002**, *41*, 6112; i) U. Kortz, *J. Clust. Sci.* **2003**, *14*, 205; j) U. Kortz, C. Holzapfel, M. Reicke, *J. Mol. Struct.* **2003**, *656*, 93; k) P. Mialane, L. Lisnard, A. Mallard, J. Marrot, E. Antic-Fidancev, P. Aschehoug, D. Vivien, F. Sécheresse, *Inorg. Chem.* **2003**, *42*, 2102; l) F. Li, L. Xu, Y. Wei, G. Gao, L. Fan, Z. Li, *Inorg. Chim. Acta* **2006**, *359*, 3799; m) Y. Lu, Y. Li, E. Wang, X. Xe, Y. Ma, *Inorg. Chim. Acta* **2006**, *360*, 2063; n) R. C. Howell, F. G. Perez, S. Jain, W. DeW. Jr. Horrocks, A. L. Rheingold, L. C. Francesconi, *Angew. Chem., Int. Ed. Engl.* **2001**, *40*, 4031; o) G. L. Xue, J. Vaissermann, P. Gouzerh, *J. Cluster Sci.* **2002**, *13*, 409; p) K. Fukaya, T. Yamase, *Angew. Chem., Int. Ed. Engl.* **2003**, *42*, 654; q) M. Zimmermann, N. Belai, R. J. Butcher, M. T. Pope, E. V. Chubarova, M. H. Dickman, U. Kortz, *Inorg. Chem.* **2007**, *46*, 1737; r) A. Merca, A. Müller, J. van Slageren, M. Läge, B. Krebs, *J. Clust. Sci.* **2007**, *16*, 711; s) B. S. Bassil, M. H. Dickman, B. Kammer, U. Kortz, *Inorg. Chem.* **2007**, *46*, 2452; t) B. S. Bassil, M. H. Dickman, I. Römer, B. Kammer, U. Kortz, *Angew. Chem., Int. Ed. Engl.* **2007**, *46*, 6192; u) X. Fang, P. Kögerler, *Chem. Commun.* **2008**, 3396.

[5] a) M. M. Gresely, W. P. Griffith, A. C. Lämmel, H. I. S. Nogueira, B. C. Parkin, *J. Mol. Catal. A: Chemical* **1997**, *117*, 185; b) W. P. Griffith, N. Morley-Smith, H. I. S. Nogueira, A. G. F. Shoair, M. Suriaatmaja, A. J. P. White, D. J. Williams, *J. Organomet. Chem.* **2000**, *607*, 146; c) J. A. Fernández, X. López, C. Bo, C. de Graaf, E. J. Baerend, J. M. Poblet, *J. Am. Chem. Soc.* **2005**, *129*, 12244; d) W. Chen, Y. Li, Y. Wang, E. Wang, Z. Su, *J. Chem. Soc. Dalton Trans.* **2007**, 4293; 41) F. Li, L. Xu, Y. Wei, G. Gao, L. Fan, Z. Li, *Inorg. Chim. Acta*

2006, *359*, 3799; e) W. Huang, L. C. Francesconi, T. Plenova, *Inorg. Chem.* **2007**, *43*, 7861; f) A. Merca, A. Müller, J. van Slageren, M. Läge, B. Krebs, *J. Clust. Sci.* **2007**, *16*, 711.

[6] J. Iball, J. N. Low, T. J. R. Weakley, *J. Chem. Soc. Dalton Trans*. **1974**, 2021.

[7] a) T. Ozeki, M. Takahashi, T. Zeki, M. Takahashi, T. Yamase, *Acta Crystallogr*. **1992**, *C48*, 1370; b) T. Ozeki, T. Yamase, *Acta Crystallogr.* **1994**, *B50*, 128; c) T. Ozeki, T. Yamase, *Acta Crystallogr.* **1993**, *C49*, 1574; d) T. Ozeki, T. Yamase, *Acta Crystallogr.* **1994**, *C50*, 327; e) T. Yamase, T. Ozeki, K. Ueda, *Acta Crystallogr.* **1993**, *C49*, 1572; f) T. Yamase, T. Ozeki, *Acta Crystallogr.* **1993**, *C49*, 1577; g) T. Yamase, T. Ozeki, M. Tosaka, *Acta Crystallogr.* **1994**, *C50*, 1849; h) T. Ozeki, M. Takahashi, T. Yamase, *Acta Crystallogr.* **1992**, *C*48, 1370; i) T. Yamase, H. Naruke, Y. Sasaki, *J. Chem. Soc. Dalton Trans.* **1990**, 1687.

[8] F. A. Almeida Paz, M. S. S. Balula, A. M. V. Cavaleiro, J. Klinowski, H. I. S. Nogueira, *Acta Cryst.* **2005**, *E61*, 1370.

[9] A. M. Golubev, L. P. Kazanskii, E. A. Torchenkova, V. I. Simonov, V. I. Spitsyn, *Dokl. Acad. Nauk.* **1975**, *221*, 351.

[10] M. Barsukova, M. H. Dickman, E. Visser, S. S. Mal, U. Kortz, *Z. Anorg. Allg. Chem.* **2008**, *634*, 2423.

[11] T. Li, F. Li, J. Lü, Z. Guo, S. Gao, R. Cao, *Inorg. Chem.* **2008**, *47*, 5612.

[12] a) M. J. Stillman, A. J. Thomson, *J. Chem. Soc. Dalton Trans.* **1976**, 1138; b) G. Blasse, G. Dirksen, F. Zonnevulle, *Chem. Phys. Lett.* **1981**, *83*, 449.

[13] G. M. Sheldrick, SADABS; University of Göttingen: Germany, **1996**.

[14] G. M. Sheldrick, SHELXS-97, *Program for Solution of Crystal Structures*; University of Göttingen: Germany, **1997**.

[15] J. Fuchs, H. Hartl, W. Schiller, *Angew. Chem., Int. Ed. Engl.* **1973**, *12*, 420.

[16] The cerium derivative $\{[Ce_2(H_2O)_{11}W_{28}O_{93}(OH)_2]^{14-}\}_2$ crystallizes in the triclinic system, space group P-1, with a = 21.629(2) Å, b = 26.869(3) Å, c = 31.611(3) Å, α = 80.463(3)°, β =

72.936(4)°, γ = 75.999(4)°, V = 16951.2 Å^3 and Z = 2. The full characterization will be published soon.

[17] T. Lehmann, J. Fuchs, *Z. Naturforsch. B* **1988**, *43*, 89.

[18] D-L. Long, H. Abbas, P. Kögerler, L. Cronin, *J. Am. Chem. Soc.* **2004**, *126*, 13880.

[19] D. Altermatt, I. D. Brown, *Acta. Cryst.* **1985**, *B41*, 244.

3.A.2. The 28-Isopolytungstate Fragment $[H_2W_{28}O_{95}]^{20-}$ Stabilized by two External Lanthanide Ions

A. H. Ismail, B. S. Bassil, A. Suchopar, U. Kortz, *Eur. J. Inorg. Chem.* **2009**, 5247

3.A.2.1. Introduction

Polyoxometalates (POMs) are a well-known class of anionic metal-oxo clusters of the early (group V and VI) transition metals with molecular and electronic structural versatility. POMs are remarkable due to their reactivity and relevance in fields such as photochemistry, analytical chemistry, clinical chemistry, magnetism, catalysis, biology, medicine and materials science.[1] POMs, especially polyoxotungstates, are effective homogeneous photocatalysts for the mineralization of organic pollutants (i.e. degradation of organic pollutants to CO_2, H_2O and the corresponding inorganic anions).[2] The ability of POMs to form peroxo derivatives renders them useful in oxidation reactions. Furthermore, chemical modifications in the composition of POMs allow for fine tuning of their Lewis acidity.[3]

Two main types of POMs are known: isopoly- and heteropoly-anions. Isopolyanions are represented with the general formula $[M_mO_y]^{n-}$, where M is the addenda atom in a high oxidation state (e.g. W^{VI}, Mo^{VI}). Heteropolyanions are represented with the general formula $[X_xM_mO_y]^{q-}$ ($x \leq m$) where X is the heteroatom (e.g. P^V, As^V, Si^{IV}, Ge^{IV}).[1a]

So far, lanthanide-containing POMs have been investigated less than their 3d-transition-metal analogues. The former have also shown interesting properties in the areas of photoluminescence, catalysis, electrochemistry, and magnetism.[4] Most of the lanthanide-containing POMs reported to date are actually heteropolyanions.[5] Our group has also been working on lanthanide-containing heteropolytungstates.[6] We have reported the ytterbium-containing tungstoarsenate $[YbAs_2W_{20}O_{68}(H_2O)_3]^{7-}$ resulting from the interaction of the monolacunary $[As_2W_{20}O_{68}(H_2O)]^{10-}$ with Yb^{3+} ions in acidic aqueous medium. The polyanion consists of two (α-$As^{III}W_9O_{33}$) fragments connected by a V-shaped $(H_2O)Yb(OW(H_2O))_2$ fragment.[6a] The monolanthanide-containing polyanion family $[Ln(\beta_2\text{-}SiW_{11}O_{39})_2]^{13-}$ (Ln =

La, Ce, Sm, Eu, Gd, Tb, Yb, Lu) has also been synthesized and structurally characterized.[6c] These polyanions are composed of two chiral (β_2-$SiW_{11}O_{39}$) units sandwiching the Ln^{3+} ion. Recently, we reported the tungstogermanate $[Ce_{20}Ge_{10}W_{100}O_{376}(OH)_4(H_2O)_{30}]^{56-}$ containing 20 cerium atoms and 100 tungsten centers.[6d] We synthesized this polyanion by the reaction of the trilacunary POM precursor [α-GeW_9O_{34}]$^{10-}$ with Ce^{3+} ions in acidic aqueous medium.

However, to date only two types of lanthanide-containing isopolyanions have been reported. The decatungstate $[Ln(W_5O_{18})_2]^{n-}$ ({LnW_{10}}) sandwich species (Ln^{3+} = La, Ce, Pr, Nd, Sm, Ho, Yb and Y, and Ce^{4+}), first reported by Peacock and Weakley, was synthesized by reaction of the lanthanide ions with WO_4^{2-} in a solution of pH 6.5−7.5.[5a,7a] The structure of the {LnW_{10}} family is based on two monolacunary $[W_5O_{18}]^{6-}$ Lindqvist fragments encapsulating a central metal ion in a square-antiprismatic fashion. In particular Yamase's group reported some {LnW_{10}} structures with different types of alkali counter cations.[8] Recently our group has reported the synthesis and structure of the yttrium derivative of {LnW_{10}} including the use of solution ^{89}Y NMR spectroscopy.[9] The isopolyanion family $[Ln^{III}W_{10}O_{36}]^{9-}$, (Ln = Pr, Nd, Sm, Eu, Tb, Dy), has shown high luminescence quantum efficiency.[7b-d]

On the other hand, the 22-isopolytungstate $[Ln_2(H_2O)_{10}W_{22}O_{71}(OH)_2]^{8-}$ ({Ln_2W_{22}}) (Ln^{3+} = La, Ce, Tb, Dy, Ho, Er, Tm, Yb, Lu and Y), has been reported very recently by our group.[10] These {Ln_2W_{22}} polyanions were synthesized by the reaction of Na_2WO_4 and the appropriate lanthanide salts in acidic aqueous medium (pH ~2) in an 11:1 ratio. All the {Ln_2W_{22}} polyanions are isostructural and crystallize as hydrated sodium salts in the triclinic space group $P\bar{1}$. The structures of the {Ln_2W_{22}} family comprise the isopolyanion {W_{22}} coordinated to two {$Ln(H_2O)_n$}$^{3+}$ supporting ions. The {W_{22}} structure in turn consists of two undecatungstate units {W_{11}} fused by two corner-sharing W-O-W bridges. The {Ln_2W_{22}} family can also be described as a dimeric entity composed of two {LnW_{11}} half units related by an inversion center, resulting in the point group C_i. These species are the first

isopolyanions containing lanthanide ions bearing terminal, labile aqua ligands. This may allow for ligand substitution which could lead to interesting derivatives including chiral ones interesting for catalysis.[10]

Apart from these two classes of compounds, a cerium-containing isopolyanion $[H_6Ce_2(H_2O)ClW_{15}O_{54}]^{7-}$ ($\{Ce_2W_{15}\}$) was reported by Cao's group.[11] The isopolyanion comprises a triangular pentadecatungstate ring capped by two Ce^{3+} ions, with a terminal aqua ligand on one side and a terminal chloro ligand on the other side.

The coordination sphere of the lanthanide ions in the $\{LnW_{10}\}$ family is saturated due to coordination to the monolacunary pentatungstate units. The ability to synthesize isopolyanions containing coordinatively unsaturated lanthanide centers with terminal, labile aqua ligands, such as our $\{Ln_2W_{22}\}$ family, could allow for ligand exchange and resulting applications in (chiral) catalysis. Hence, the synthesis of novel isopolytungstate-supported lanthanides represents a challenge in POM chemistry. Herein, we report the synthesis of a novel class of lanthanide-containing isopolytungstates.

3.A.2.2. Synthesis

$Na_{14}[Sm_2(H_2O)_{10}W_{28}O_{93}(OH)_2]\cdot 40H_2O$ (Na-11)

10.00 g of $Na_2WO_4\cdot 2H_2O$ (30.30 mmol) were dissolved in 20 mL H_2O followed by dropwise addition of 3 mL of concentrated HCl (local formation and redissolution of hydrated tungsten oxide was detected). This was immediately followed by the dropwise addition of 0.80 g $SmCl_3\cdot 6H_2O$ (2.20 mmol) dissolved in 5 mL H_2O and the pH was adjusted to 3.2 with 6M HCl. The mixture was vigorously stirred at room temperature for 1 hour. The white precipitate formed was filtered off and the filtrate was kept in an open vial for crystallization. Colorless crystals were obtained after several days, which were filtered off and air dried (yield 3.0 g, 38 %). IR data for **Na-11**: 946(m), 881(sh), 833(s), 801(s), 756(sh), 632(m), 595(m), 473(w), 458(w), 419(w) cm^{-1} (see Figure 3.11).

$Na_8Eu_2[Eu_2(H_2O)_{10}W_{28}O_{93}(OH)_2]\cdot 47H_2O$ (NaEu-12)

10.00 g of $Na_2WO_4\cdot 2H_2O$ (30.30 mmol) were dissolved in 20 mL H_2O followed by dropwise addition of 3 mL of concentrated HCl (local formation and redissolution of hydrated tungsten oxide was detected). This was immediately followed by the dropwise addition of 0.81 g $EuCl_3\cdot 6H_2O$ (2.20 mmol) dissolved in 5 mL H_2O and the pH was adjusted to 3.2 with 6M HCl. The mixture was vigorously stirred at room temperature for 1 hour. The white precipitate formed was filtered off and the filtrate was kept in an open vial for crystallization. Colorless crystals were obtained after several days, which were filtered off and air dried (yield 3.4 g, 41 %). IR data for **NaEu-12**: 946(m), 881(sh), 833(s), 801(s), 756(sh), 632(m), 595(m), 473(w), 458(w), 419(w) cm^{-1}(see Figure 3.11). Anal. Calcd (%) for **NaEu-2**: Na, 2.2; W, 60.6; Eu, 7.2. Found (%): Na, 1.3; W, 58.4; Eu, 7.4.

$Na_{14}[Ln_2(H_2O)_{10}W_{28}O_{93}(OH)_2]\cdot xH_2O$ (Ln = La, Ce, Pr, Nd and Gd)

The same procedure as for **Na-11** was followed, but using the respective lanthanide chloride salt instead of $SmCl_3\cdot 6H_2O$.

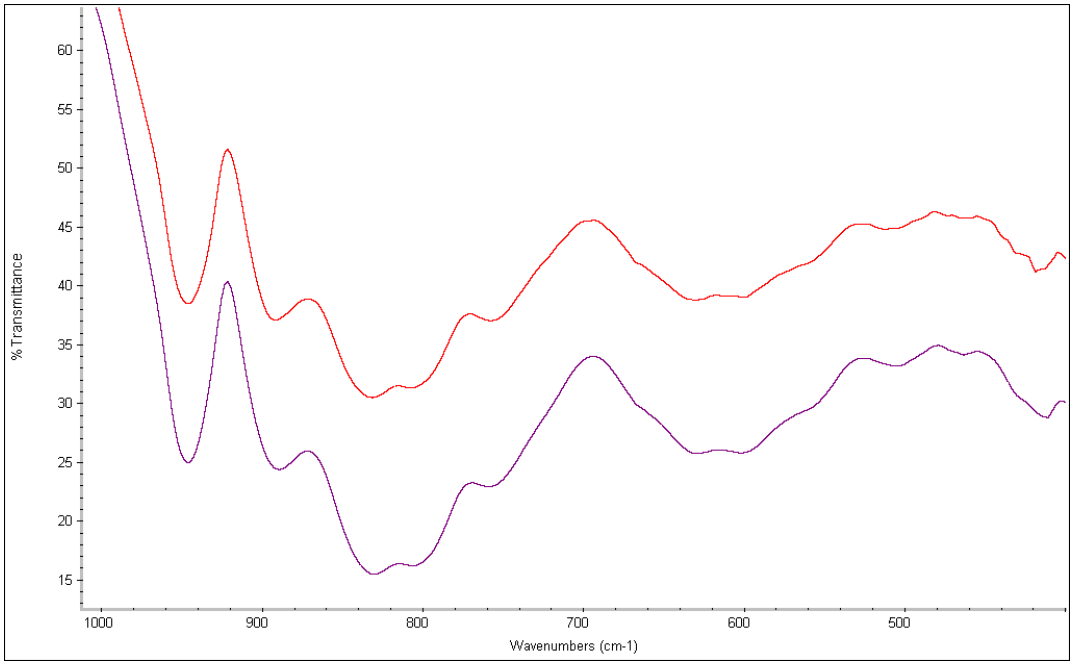

Figure 3.11. IR spectra of **Na-11** (blue curve) and **NaEu-12** (red curve) measured on KBr pellets.

3.A.2.3. X-ray Crystallography

The crystals were mounted in Hampton cryoloops using light oil, for data collection at low temperature. Indexing and data collection were performed using a Bruker X8 APEX II CCD diffractometer with kappa geometry and Mo K_α radiation (λ = 0.71073 Å). Data integration and routine processing were performed using the SAINT software suite. Further data processing, including multi-scan absorption corrections, was performed using SADABS.[12] Direct methods (SHELXS97) solutions successfully located the W atoms, and successive Fourier syntheses (SHELXL97) revealed the remaining atoms.[12] Refinements were full-matrix least squares against F^2 using all data. Some lanthanides, cations, and waters of hydration were modeled with varying degrees of occupancy, a common situation for polyoxotungstate structures. One disordered europium counter caion was found in addition to the non-disordered Eu^{3+} ions grafted to the $\{W_{28}\}$ polyanion. In the final refinements, all non-disordered heavy atoms (W, Ln) were refined anisotropically, while the O and Na atoms and the disordered europium were refined isotropically. No H atoms were included in the models. The crystallographic data are provided in Table 3.3.

Table 3.3. Crystal Data and Structure Refinement for **Na-11** and **NaEu-12.**

Code	**Na-11**	**NaEu-12**
Empirical formula	$H_{102}Sm_2Na_{14}O_{145}W_{28}$	$H_{116}Eu_{3.5}Na_{9.5}O_{152}W_{28}$
MW	8193.18	6729.17
Crystal system	Triclinic	Monoclinic
Space group (no.)	$P\bar{1}$ (2)	$P2_1/n$
a/Å	14.8727(6)	25.3862(11)
b/Å	21.7762(11)	14.6364(5)
c/Å	23.5751(10)	40.3264(16)
α/°	89.175(2)	90
β/°	86.430(2)	96.107(3)
γ/°	75.364(2)	90
V/Å^3	7373.2(6)	14898.7(10)
Z	2	4
T/ ºC	-100	-100
λ/Å	0.71073	0.71073
D/ Mg m^{-3}	3.690	3.766
μ/ mm^{-1}	22.68	23.11
R[I >2sigma(I)][a]	0.056	0.072
R_w (all data)[b]	0.158	0.203

[a] $R = \sum|F_o| - |F_c| \,|\sum| \,|F_o|$. [b] $R_w = \{\sum[w(F_o^2 - F_c^2)^2] / \sum[w(F_o^2)^2]\}^{1/2}$.

3.A.2.4. Results and Discussion

We have synthesized and structurally characterized the V-shaped polyanions $[Ln_2(H_2O)_{10}W_{28}O_{93}(OH)_2]^{14-}$ (Ln = Sm (**11**), and Eu (**12**)) by one-pot reactions of Ln^{3+} and WO_4^{2-} in aqueous acidic medium. The sodium salt $Na_{14}[Sm_2(H_2O)_{10}W_{28}O_{93}(OH)_2]\cdot 40H_2O$ (**Na-11**) and the mixed sodium-europium salt $Na_8Eu_2[Eu_2(H_2O)_{10}W_{28}O_{93}(OH)_2]\cdot 47H_2O$ (**NaEu-12**) have been characterized in the solid state by FTIR, single-crystal XRD, thermogravimetric analysis (TGA), and elemental analysis. The polyanions **11** and **12** comprise a novel isopolyanion $[H_2W_{28}O_{95}]^{20-}$ unit and two $\{Ln(H_2O)_n\}^{3+}$ supporting groups (see Figure 3.12). The $\{W_{28}\}$ cluster, which consists of two undecatungstate $\{W_{11}\}$ fragments and a hexatungstate fragment $\{W_6\}$, coordinates to the two Ln^{3+} ions acting as a tri- and tetradentate ligand, respectively.

The Ln^{3+} ions of **11** and **12** are nine-coordinated with a distorted monocapped square antiprismatic geometry. One of the Ln^{3+} ions is coordinated to the two $\{W_{11}\}$ subunits by four μ-oxo bridges with average Ln-O distances of 2.50(2) Å for **11** and 2.46(2) Å for **2**. The other Ln^{3+} ion is coordinated to the two $\{W_{11}\}$ subunits and the $\{W_6\}$ subunit by three μ-oxo bridges (one O atom from each subunit) with average Ln-O distances of 2.48(1) Å for **11** and 2.46(2) Å for **12**. A fourth oxo-bridge acts as a linker to another $\{W_{28}\}$, forming a $\{Ln_4W_{56}\}$ assembly $([Ln_2(H_2O)_{10}W_{28}O_{93}(OH)_2]^{14-})_2$, see Figure 3.13. The remaining coordination sphere is filled by aqua ligands. Hence the $\{Ln_4W_{56}\}$ structure can be described as a dimeric entity composed of two half units of $[Ln_2(H_2O)_{10}W_{28}O_{93}(OH)_2]^{14-}$ related by an inversion center, resulting in point symmetry C_i.

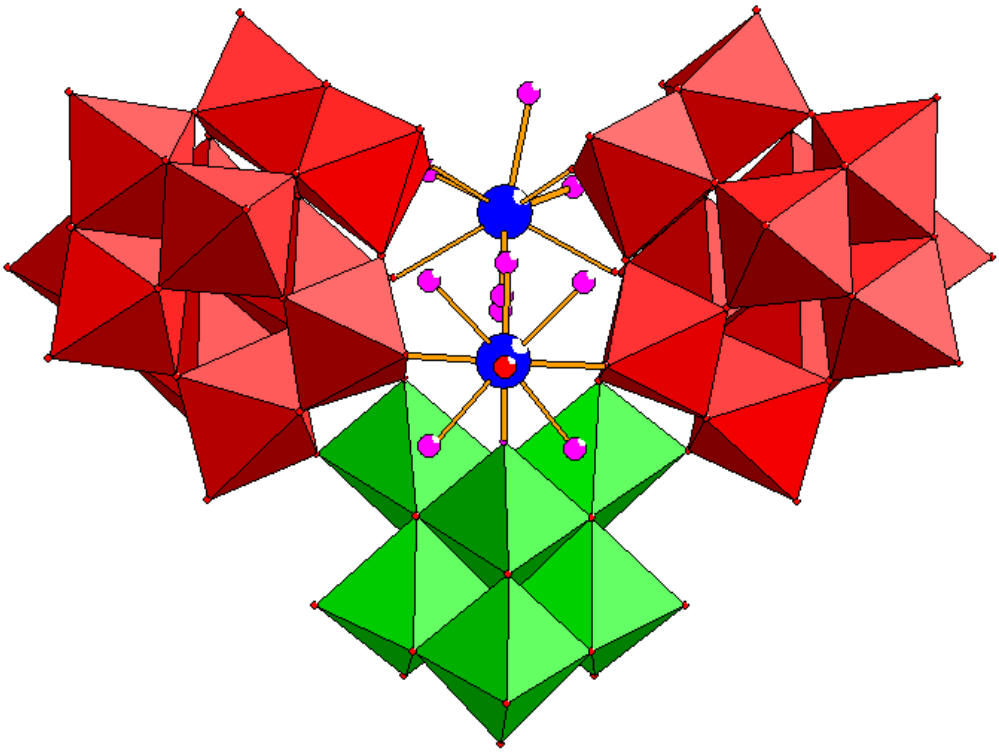

Figure 3.12. Representation of the V-shaped polyanions $[Ln_2(H_2O)_{11}W_{28}O_{93}(OH)_2]^{14-}$ (Ln = Sm, **11**; Eu, **12**). The color code is as follows: WO_6 octahedra (red and geen); Ln (blue); H_2O (pink); O (red). In the solid state the "red" oxo ligand links two $\{W_{28}\}$ units via an Ln–O–W' bridge (see also Figure 3.13). The two types of subunits were colored differently for clarity.

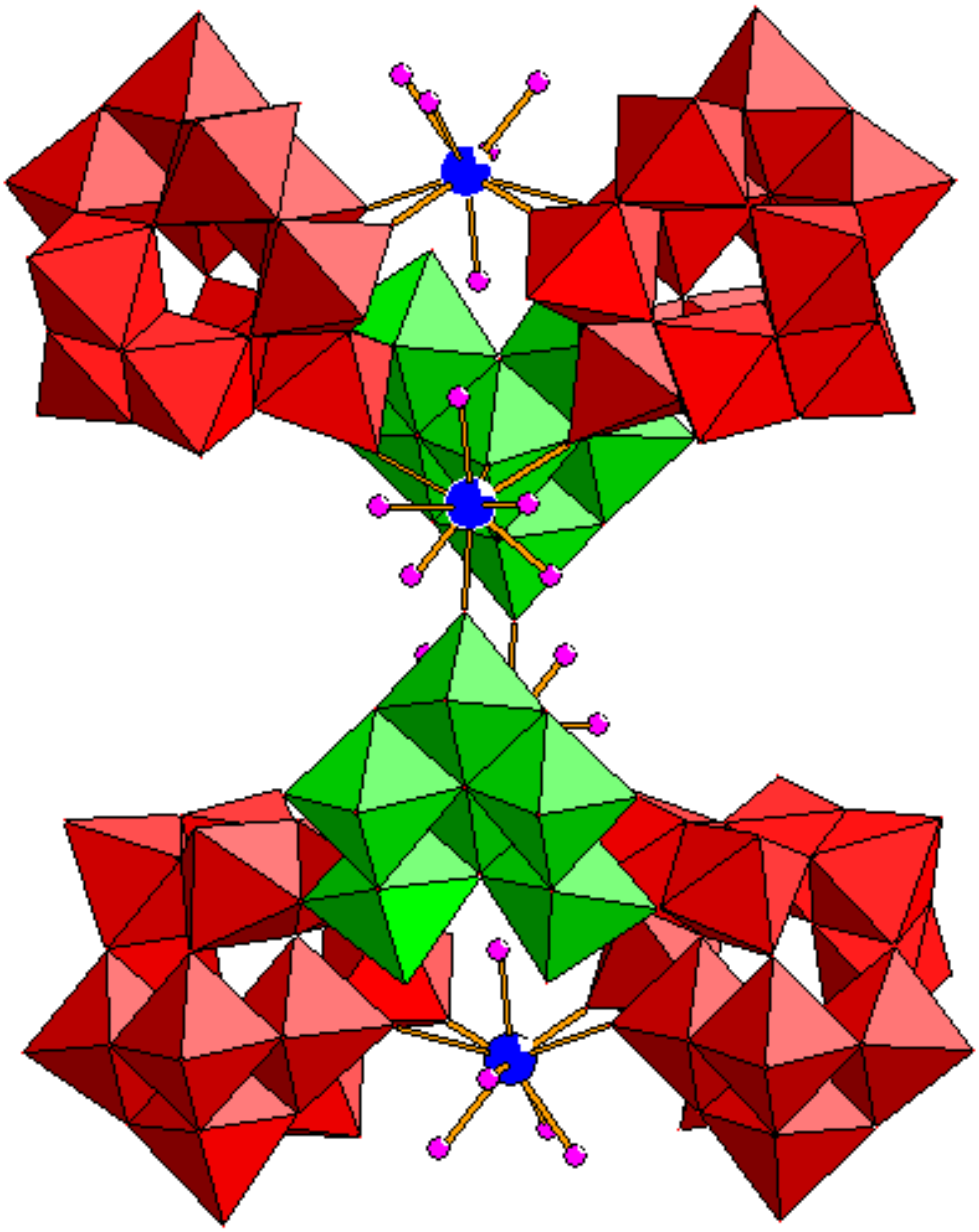

Figure 3.13. Representation of polyanions **11** and **12** forming dimers in the solid state. The color code is as follows: WO_6 octahedra (red and geen); Ln (blue); H_2O (pink).

Polyanions **11** and **12** were formed by following the same synthetic procedure of the $\{Ln_2W_{22}\}$ family reported by us recently.[10] The formation mechanism appears to be a classical tungstate condensation in aqueous acidic medium mediated by lanthanide ions (molar ratio 14:1). Besides **11** and **12** we were also able to synthesize other members of the novel $\{W_{28}\}$ family, namely for Ln = La, Ce, Pr, Nd and Gd as determined by FTIR and preliminary single-crystal X-ray diffraction analysis, see Figure 3.14.

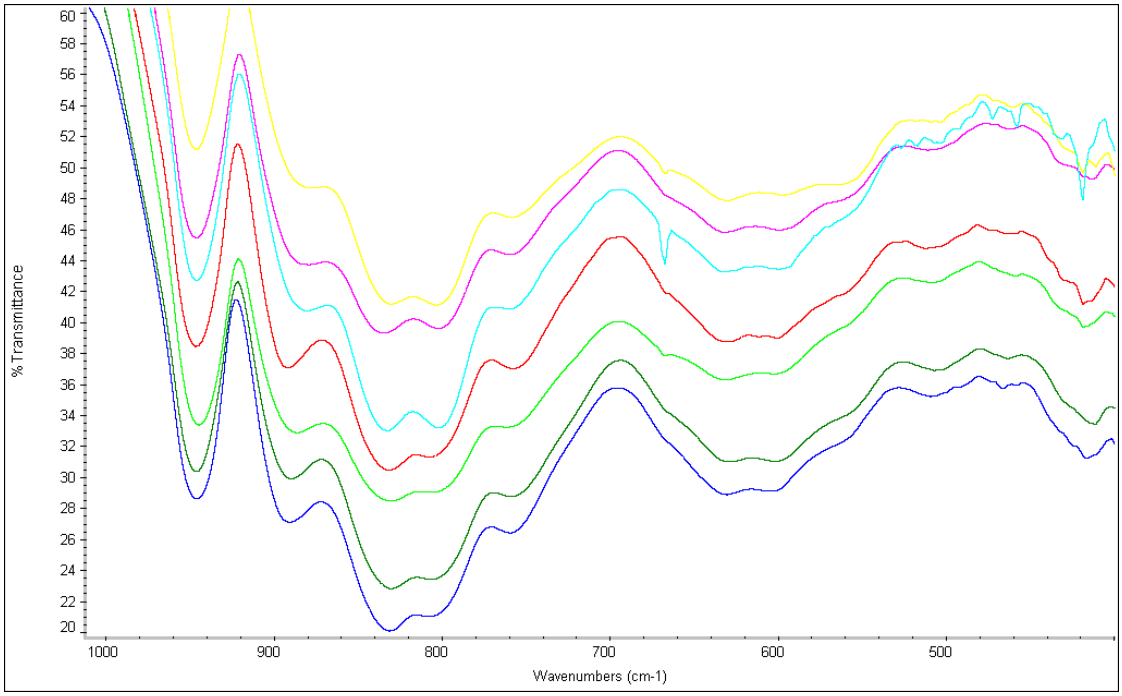

Figure 3.14. IR spectra of the seven isotructural derivatives of the $\{Ln_2W_{28}\}$ family with Ln = La, Ce, Pr, Nd, Sm, Eu and Gd (from top to bottom).

Three reaction parameters are crucial for the successful formation of **11** and **12** and to obtain pure compounds in good yields: reaction temperature, concentration of reagents, and pH of the solution.

- The polyanions **11** and **12** as well as the La, Pr, Nd and Gd analogues were formed at room temperature as well as at 80-90 ˚C, but resulted in a higher yield at room temperature. On the other hand, the cerium analogue could only be prepared at room temperature.

- The yield of **Na-11** and **NaEu-12** is also affected by the concentration of the starting materials. A tungstate concentration as high as 1.5 M is needed to obtain a pure crystalline product with the reported yields (see Synthesis Sec.). Lower reagent concentrations result in lower yields of the products.

- Also the pH of the reaction solution affects the formation and yield of polyanions **11** and **12** and their analogues. A pH window of 2.0-3.7 resulted in a successful synthetic procedure, with pH 3.2 being optimal. A pH lower than 2.0 did not provide any product, and a pH higher than 3.7 gave the well-known paradodecatungstate ($[H_2W_{12}O_{42}]^{10-}$) as the main product.

The synthetic procedures for **11** and **12** are very similar to those of our $\{Ln_2W_{22}\}$ and Weakley's $\{LnW_{10}\}$,[5a,10] except that the synthesis pH of the latter is different (see Figure 3.15). It is well known that the pH is a crucial parameter in POM synthesis in general. The synthetic procedure for our previously reported $\{Ln_2W_{22}\}$ family was successful for the middle to late lanthanides (Tb–Lu), and also for the early 4d metal ion yttrium. In contrast, the reaction procedure of the $\{Ln_2W_{28}\}$ family reported here was successful for the early lanthanide ions (La–Gd), (see Figure 3.16). Figure 3.15 summarizes the lanthanide-containing isopolytungstates reported so far and their respective formation conditions.

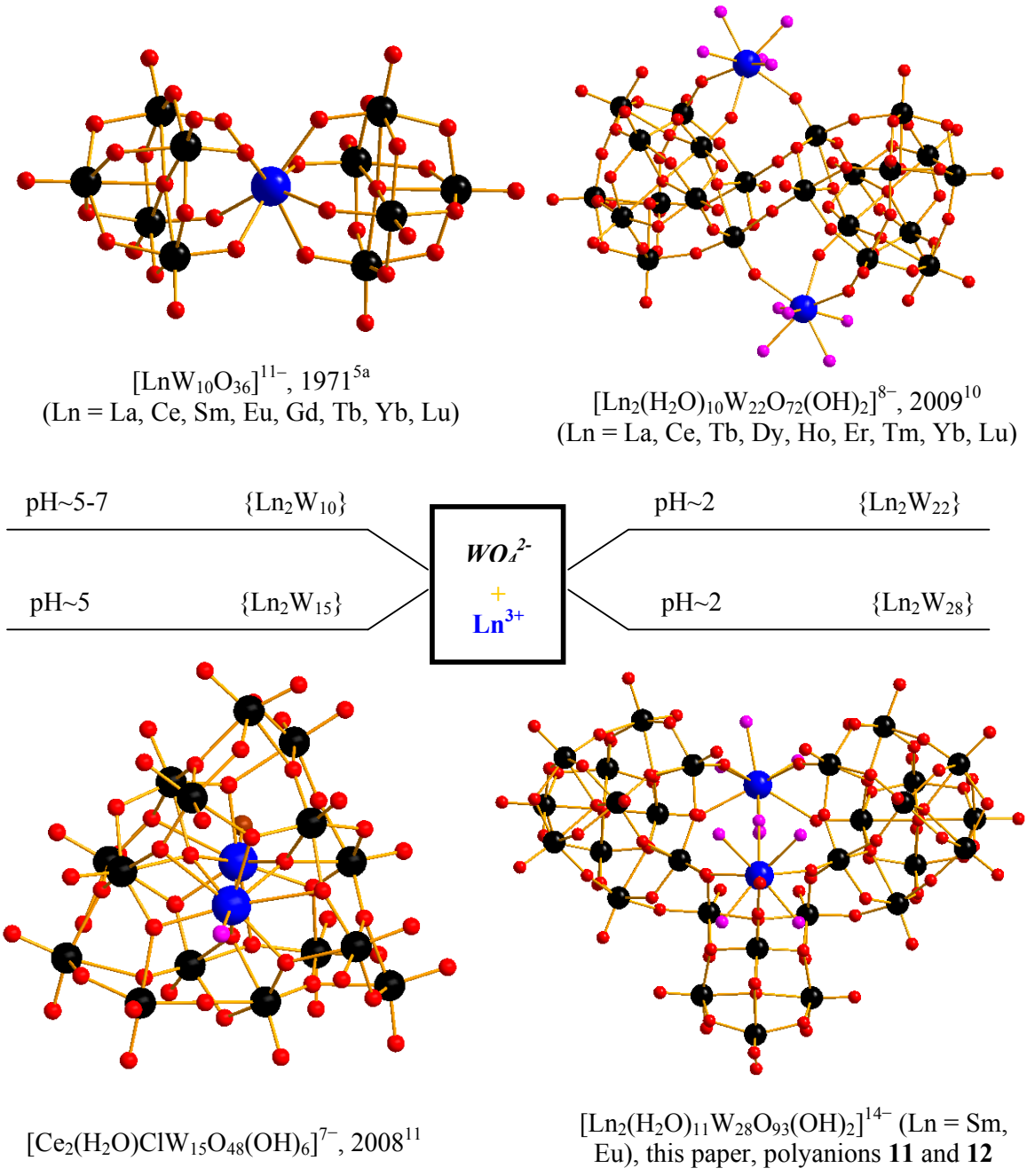

$[LnW_{10}O_{36}]^{11-}$, 1971[5a]
(Ln = La, Ce, Sm, Eu, Gd, Tb, Yb, Lu)

$[Ln_2(H_2O)_{10}W_{22}O_{72}(OH)_2]^{8-}$, 2009[10]
(Ln = La, Ce, Tb, Dy, Ho, Er, Tm, Yb, Lu)

$[Ce_2(H_2O)ClW_{15}O_{48}(OH)_6]^{7-}$, 2008[11]

$[Ln_2(H_2O)_{11}W_{28}O_{93}(OH)_2]^{14-}$ (Ln = Sm, Eu), this paper, polyanions **11** and **12**

Figure 3.15. Scheme of different types of lanthanide-containing isopolytungstates and the pH of formation. The color code is as follows: W (black); O (red); Ln (blue); H_2O (pink); Cl (brown).

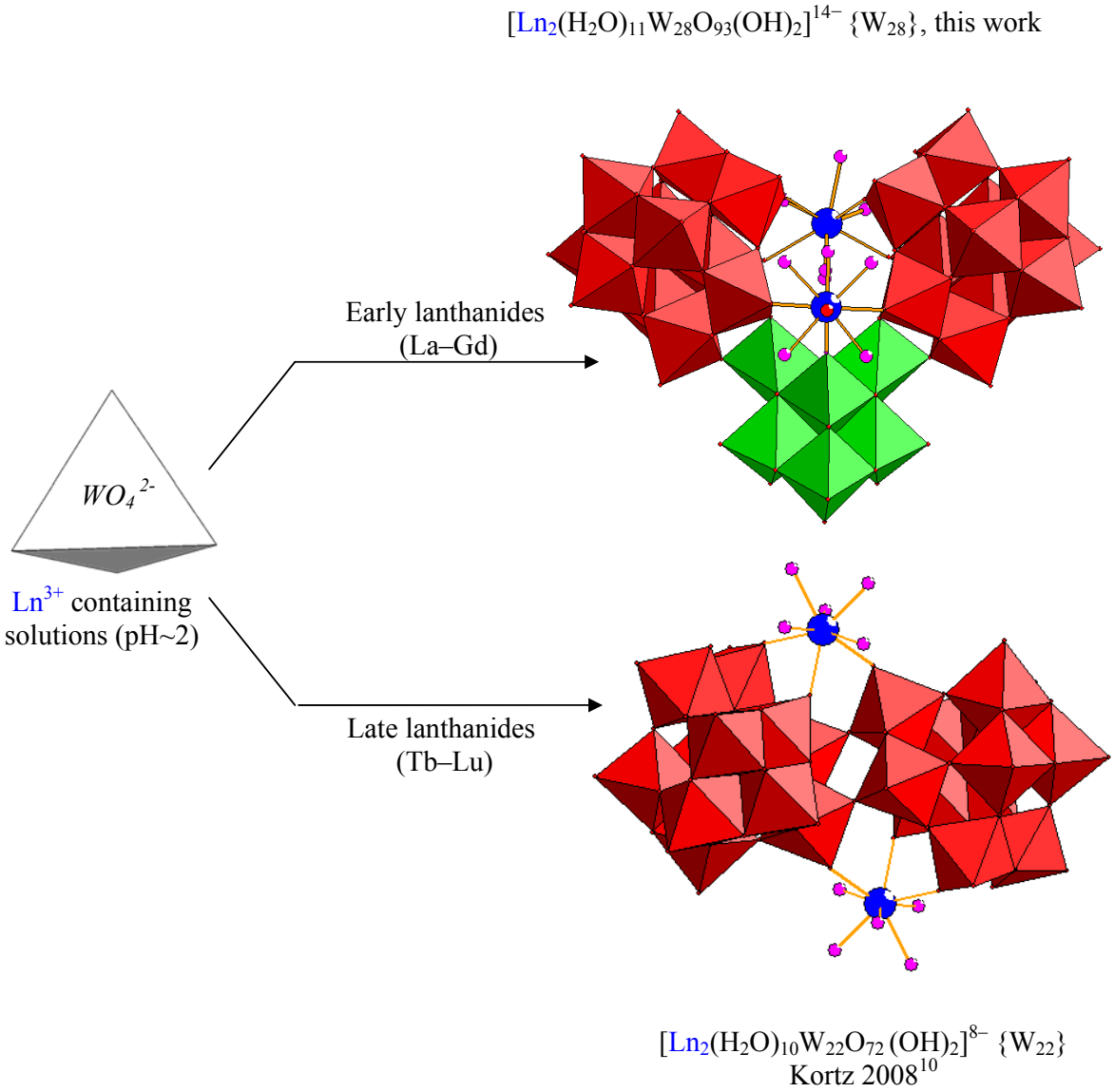

Figure 3.16. Representation of the two structures of the $\{W_{11}\}$ units containing lanthanides. The color code is as follows: WO_6 octahedra (red and green); Ln (blue); H_2O (pink), O (red).

The single crystals of the La, Ce, Pr, Nd and Gd analogues of **11** and **12** were not of sufficient quality to finalize the refinements, but the data allowed to identify the heavy atoms (W and Ln) and enough oxygens to conclude that these polyanions are isostructural with **11** and **12**.[13] On the other hand, the samarium (**11**) and europium (**12**) analogues were fully characterized by single-crystal XRD (see Table 3.3). The neodymium and gadolinium

analogues of the $\{Ln_2W_{28}\}$ family have almost the same unit cell parameters as **Na-11**, and the lanthanum, cerium and praseodymium analogues have also similar unit cell parameters. All compounds of the $\{Ln_2W_{28}\}$ family (Ln = La, Ce, Pr, Nd, Sm, Eu and Gd) have similar IR spectra (see Figure 3.14).

As mentioned above, the $\{W_{28}\}$ unit is an assembly comprising three distinct building blocks (see Figure 3.17): two undecatungstate subunits $\{W_{11}\}$ (red color) and a hexatungstate $\{W_6\}$ subunit (green color). The former consists of four distinct 'elementary blocks': one tetratungstate $\{W_4\}$ fragment formed from four edge-shared WO_6 octahedra connected through a μ_4-oxo bridge, one tritungstate $\{W_3\}$ fragment formed from three edge-shared WO_6 octahedra connected through a μ_3-hydroxo bridge, and two ditungstate $\{W_2\}$ fragments, each formed from two edge-shared WO_6 which share corners on one side. The hexatungstate $\{W_6\}$ subunit comprises six edge-shared WO_6 octahedra two of which have three *fac* terminal oxygens. These building blocks have been reported previously. The undecatungstate $[H_4W_{11}O_{38}]^{6-}$ and hexatungstate $[H_3W_6O_{22}]^{5-}$ subunits were first reported by Fuchs et al. in 1988 and 1993, respectively.[14] Recently Cronin's group reported isopolyanions composed of two or three $\{W_{11}\}$ units.[15] However, to the best of our knowledge the 28-isopolyoxotungstate $\{W_{28}\}$, which comprises two $\{W_{11}\}$ and one $\{W_6\}$ fragment linked via four oxo bridges, has not been reported yet. Notably, the two $\{W_{11}\}$ subunits in $\{W_{28}\}$ are analogous to the framework geometry of $\{W_{22}\}$ in our $\{Ln_2W_{22}\}$ family (see Figure 3.12).[10] However, they are arranged in C_s symmetry with the extra $\{W_6\}$ acting as a bridge in between them as opposed to C_i symmetry in $\{W_{22}\}$. The $\{W_{28}\}$ isopoly unit as such offers seven sites coordinating to the two Ln^{3+} centers. Polyanions **11** and **12** represent the largest lanthanide-containing isopolytungstates to date.

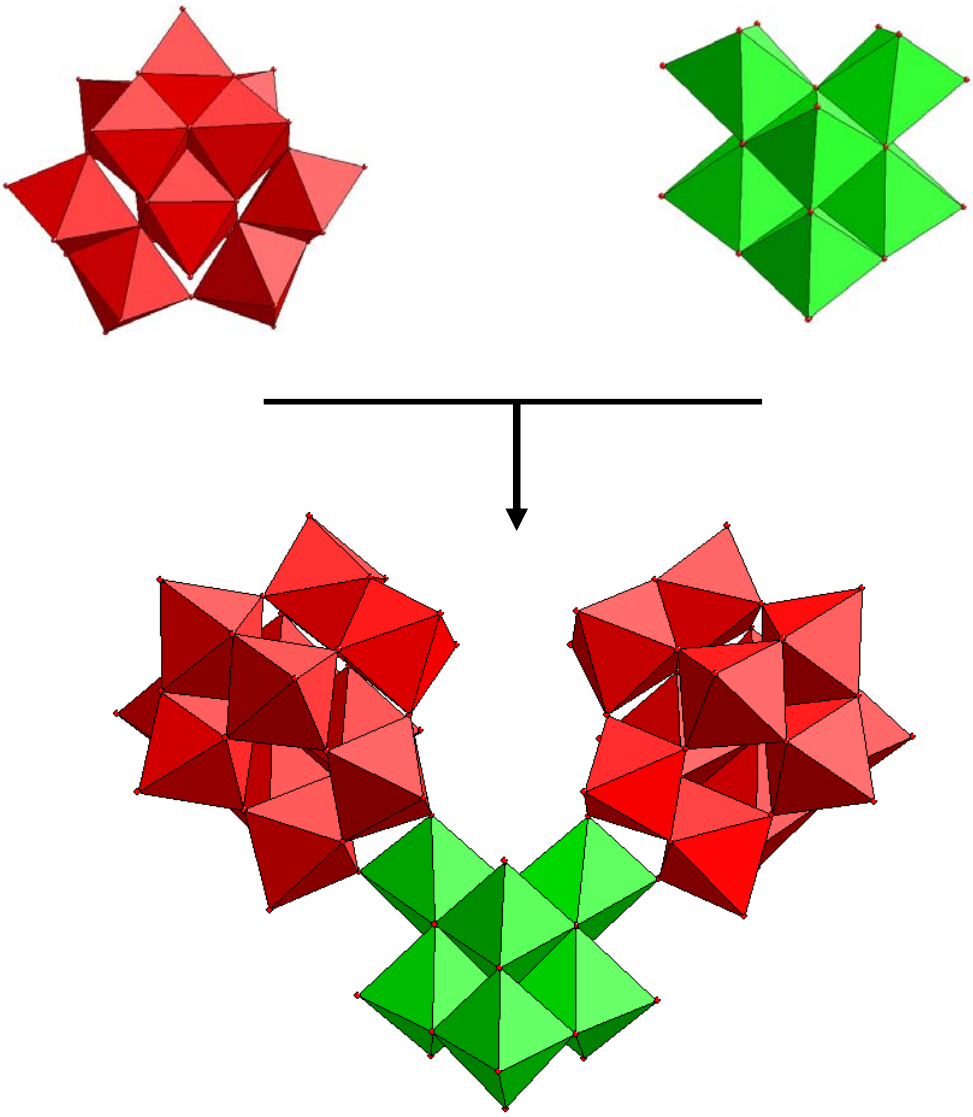

Figure 3.17. Representation of the $\{W_{28}\}$ unit in **11** and **12** which is composed of two $\{W_{11}\}$ (red) and one $\{W_6\}$ (green) fragment. The two subunit types were colored differently for clarity.

We also tried to synthesize the lanthanide-free isopolyanion $[H_2W_{28}O_{93}]^{20-}$ by following the same synthetic procedure as for **11** and **12** and without adding any lanthanide, but so far our attempts have not been successful. On the other hand, we obtained the isopolyanion $[H_{10}W_{34}O_{116}]^{18-}$ $\{W_{34}\}$ which has been reported recently by the Cronin group.[14b] In fact, we identified the crystalline product to be a mixture of Cronin's $\{W_{34}\}$ and our $\{W_{22}\}$ as based on XRD and IR.[10, 14b] Our results suggest that lanthanide ions are crucial for the stabilization of the title isopolyanion $\{W_{28}\}$.

Bond valence sum (BVS) calculations for **11** and **12** are consistent with all tungsten atoms being in the +6 oxidation state, and with all Ln ions being +3 as expected.[16] We also checked all polyanion oxygens by BVS for possible protonation. As shown in the respective formulae for **11** and **12**, two monoprotonated oxygens (BVS ~ 1.2) were localized in the two $\{W_{11}\}$ subunits, namely the μ_3-oxo bridges of the $\{W_3\}$ fragments. This results in a total of two OH groups per $\{W_{28}\}$ unit leading to a total isopolyanion charge of –20. The two grafted Ln^{3+} ions reduce this charge to –14 in **11** and **12**. The BVS values for nonprotonated oxygens range from 2.2 – 1.5. The BVS values for terminal W=O oxygens are low (ca. 1.5), which is typical and presumably does not indicate additional protonation.

We also performed TGA on the salts **Na-11** and **NaEu-12** to determine the degree of hydration and thermal stability. The thermograms show the expected weight loss domain between 25 and 400 ºC corresponding to dehydration. We calculated 40 and 47 water molecules per formula unit of **Na-11** and **NaEu-12**, respectively. These results are also supported by elemental analysis. The absence of any additional weight loss after dehydration indicated that the salts are thermally stable up to 800-900 °C (see Figure 3.18).

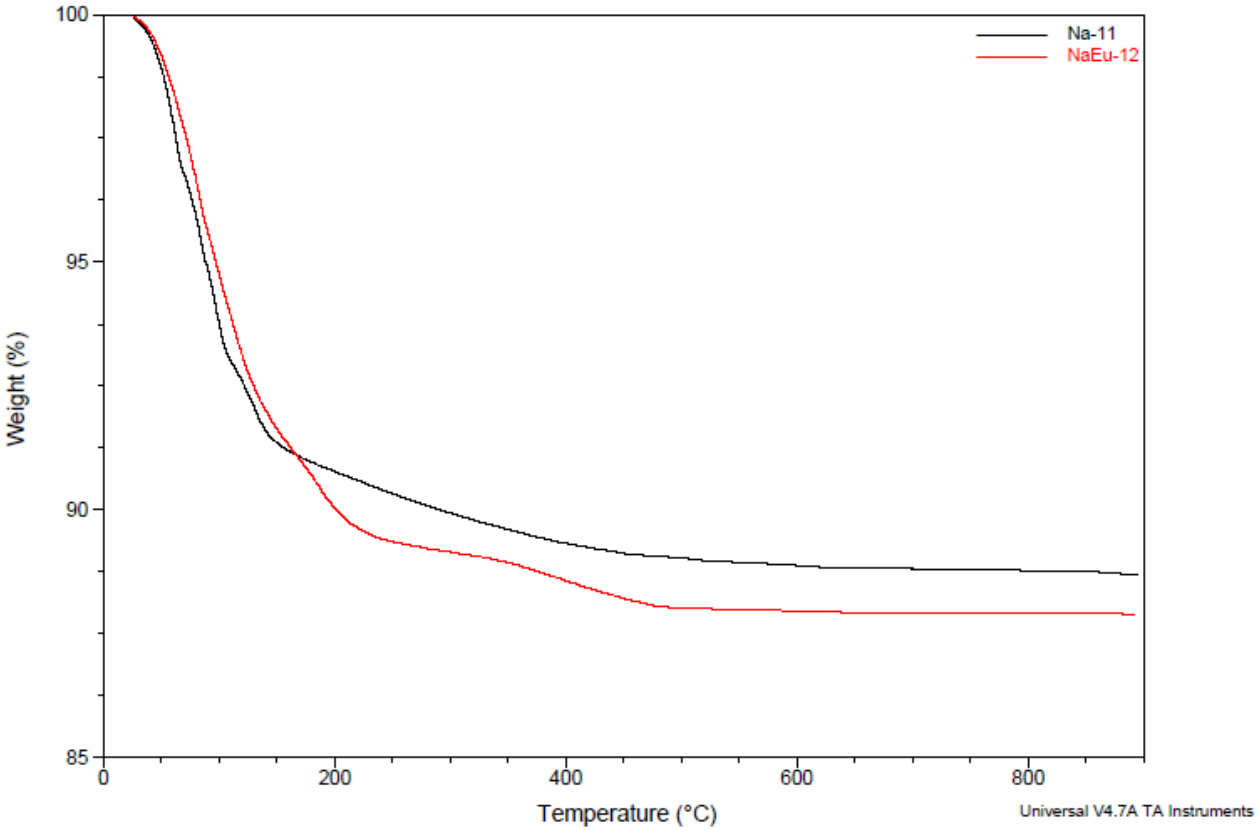

Figure 3.18. Thermograms of **Na-11** and **NaEu-12**.

3.A.2.5. Conclusions

We have successfully synthesized the V-shaped, lanthanide-containing isopolyanions $[Sm_2(H_2O)_{10}W_{28}O_{93}(OH)_2]^{14-}$ (**11**) and $[Eu_2(H_2O)_{10}W_{28}O_{93}(OH)_2]^{14-}$ (**12**) which were structurally characterized by IR spectroscopy, single-crystal X-ray diffraction, TGA and elemental analysis. The polyanions **11** and **12** were synthesized in aqueous acidic medium by simple one-pot reaction of sodium tungstate with a lanthanide(III) salt and then isolated as the hydrated sodium and mixed sodium-europium salts **Na-11** and **NaEu-12**, respectively. Polyanions **11** and **12** are composed of a 28-tungsten isopolyanion unit $\{W_{28}\}$ which consists of two undeca $\{W_{11}\}$ and one hexa $\{W_6\}$ fragments coordinated to two external lanthanide ions bearing five terminal aqua ligands. Polyanions **11** and **12** represent only the second

example of lanthanide-containing isopolyanions and they contain exposed lanthanide centers with labile terminal aqua ligands. The latter represent good candidates for ligand substitution with other mono- or polydentate ligands (e.g. carboxylic acids, amino acids), including chiral ones, providing a potential for catalysis. We also try to isolate **11** and **12** as lipophilic alkyl ammonium salts which would open the door for organic catalysis reactions.

3.A.2.6. References

[1] a) M. T. Pope in *Heteropoly and Isopoly Oxometalates*, Springer-Verlag, Berlin, 1983; b) M. T. Pope, A. Müller, *Angew. Chem., Int. Ed. Engl.* **1991**, *30*, 34; c) M. T. Pope, A. Müller in *Polyoxometalates: From Platonic Solids to Anti- Retroviral Activity* (Eds.: M. T. Pope, A. Müller), Kluwer: Dordrecht, The Netherlands, 1994; d) A. Müller, H. Reuter, S. Dillinger, *Angew. Chem., Int. Ed. Engl.* **1995**, *34*, 2328; e) C. Hill in *Polyoxometalates: Chemical Reviews*, 1998 (special thematic issue on polyoxometalates); f) M. T. Pope, A. Müller in *Polyoxometalate Chemistry: From Topology via Self-Assembly to Applications (*Eds.: M. T. Pope, A. Müller), Kluwer: Dordrecht, The Netherlands, 2001; g) T. Yamase, M. T. Pope in *Polyoxometalate Chemistry for Nano-Composite Design (*Eds.: T. Yamase, M. T. Pope), Kluwer: Dordrecht, The Netherlands, 2002; h) G. R. J. Choppin, *Nucl. Radiochem. Sci.* **2005**, *6*, 1.

[2] a) A. Mylonas, A. Hiskia, E. Papaconstantinou, *J. Mol. Catalysis A: Chem.* **1996**, *114*, 191; b) A. Hiskia, A. Troupis, E. Papaconstantinou, *Int. J. Photoenergy* **2002**, *4*, 35; c) E. Gkika, P. Kormali, S. Antonaraki, D. Dimoticali, E. Papaconstantinou, A. Hiskia*, Int. J. Photoenergy* **2004**, *6*, 227; d) A. Hiskia, A. Troupis, S. Antonaraki, E. Gkika, P. Kormali, E. Papaconstantinou, *Int. J. Envir. Anal. Chem.* **2006**, 233; e) P. Kormali, A. Troupis, T. Triantis, A. Hiskia, E. Papaconstantinou, *Catalysis Today* **2007**, *124*, 149.

[3] N. Mizuno, M. Misono, *Chem. Rev.* **1998**, *98*, 199.

[4] a) M. M. Gresely, W. P. Griffith, A. C. Lämmel, H. I. S. Nogueira, B. C. Parkin, *J. Mol. Catal. A: Chemical* **1997**, *117*, 185; b) W. P. Griffith, N. M-Smith, H. I. S. Nogueira, A. G. F. Shoair, M. Suriaatmaja, A. J. P. White, D. J. Williams, *J. Organomet. Chem.* **2000**, *607*, 146; c) J. A. Fernández, X. López, C. Bo, C. de Graaf, E. J. Baerend, J. M. Poblet, *J. Am. Chem. Soc.* **2005**, *129*, 12244; d) W. Chen, Y. Li, Y. Wang, E. Wang, Z. Su, *J. Chem. Soc. Dalton Trans.* **2007**, 4293; e) F. Li, L. Xu, Y. Wei, G. Gao, L. Fan, Z. Li, *Inorg. Chim. Acta* **2006**, *359*, 3795; f) W. Huang, L. C. Francesconi, T. Plenova, *Inorg. Chem.* **2007**, *43*, 7861; g) A. Merca, A. Müller, J. van Slageren, M. Läge, B. Krebs, *J. Clust. Sci.* **2007**, *168*, 711.

[5] a) R. D. Peacock, T. J. R. Weakley, *J. Chem. Soc. A* **1971**, 1836; b) M. H. Dickman, G. J. Gama, K-C. Kim, M. T. Pope, *J. Clust. Sc.* **1996**, *7*, 567; c) K. Wassermann, M. H. Dickman, M. T. Pope, *Angew. Chem., Int. Ed. Engl.* **1997**, *36*, 1445; d) M. Sadakane, M. H. Dickman, M. T. Pope, *Angew. Chem., Int. Ed. Engl.* **2000**, *39*, 2914; e) M. Sadakane, M. H. Dickman, M. T. Pope, *Inorg. Chem.* **2001**, *40*, 2715; f) Q. H. Luo, R. C. Howell, M. Dankova, J. Bartis, C. W. Williams, W. D. Horrocks, V. G. Young, A. L. Rheingold, L. C. Francesconi, *Inorg. Chem.* **2001**, *40*, 1894; g) G. L. Xue, J. Vaissermann, P. *J.* Gouzerh, *Clust. Sci.* **2002**, *13*, 409; h) Q. H. Luo, R. C. Howell, J. Bartis, M. Dankova, W. D. Horrocks, A. L. Rheingold, L. C. Francesconi, *Inorg. Chem.* **2002**, *41*, 6112; i) P. Mialane, L. Lisnard, A. Mallard, J. Marrot, E. Antic-Fidancev, P. Aschehoug, D. Vivien, F. Sécheresse, *Inorg. Chem.* **2003**, *42*, 2102; j) F. Li, L. Xu, Y. Wei, G. Gao, L. Fan, Z. Li, *Inorg. Chim. Acta* **2006**, *359*, 3795; k) Y. Lu, Y. Li, E. Wang, X. Xeu, Y. Ma, *Inorg. Chim. Acta* **2007**, *360*, 2063; l) R. C. Howell, F. G. Perez, S. Jain, W. DeW. Jr. Horrocks, A. L. Rheingold, L. C. Francesconi *Angew. Chem., Int. Ed. Engl.* **2001**, *40113*, 4155; m) G. L. Xue, J. Vaissermann, P. Gouzerh, *J. Cluster Sci.* **2002**, *13*, 409; n) K. Fukaya, T. Yamase, *Angew. Chem., Int. Ed. Engl.* **2003**, *42*, 654; o) Y. Lu, Y. Li, E. Wang, X. Xe, Y. Ma,, *Inorg. Chim. Acta* **2006**, *360*, 2063; p) M. Zimmermann, N. Belai, R. J. Butcher, M. T. Pope, E. V. Chubarova, M. H. Dickman, U. Kortz, *Inorg. Chem.* **2007**, *46*,

1737; q) A. Merca, A. Müller, J. van Slageren, M. Läge, B. Krebs, *J. Clust. Sci.* **2007**, *16*, 711; r) X. Fang, P. Kögerler, *Chem. Commun.* **2008**, 3396.

[6] a) U. Kortz, C. Holzapfel, M. Reicke, *J. Mol. Struct.* **2003**, *656*, 93; b) U. Kortz, *J. Clust. Sci.* **2003**, *14*, 205; c) B. S. Bassil, M. H. Dickman, B. Kammer, U. Kortz, *Inorg. Chem.* **2007**, *46*, 2452; d) B. S. Bassil, M. H. Dickman, I. Römer, B. Kammer, U. Kortz, *Angew. Chem., Int. Ed. Engl.* **2007**, *46*, 6192.

[7] a) J. Iball, J. N. Low, T. J. R. Weakley, *J. Chem. Soc. Dalton Trans*. **1974**, 2021; b) T. Yamase, H. Naruke, Y. Sasaki, *J. Chem. Soc. Dalton Trans.* **1990**, 1687; c) F.A. Almeida Paz, M. S. S. Balula, A. M. V. Cavaleiro, J. Klinowski, H. I. S. Nogueira, *Acta Cryst.* **2005**, *E61*, i28. d) M. J. Stillman, A. J. *J.* Thomson, *Chem.Soc. Dalton Trans.* **1976**, 1138.

[8] a) T. Ozeki, M. Takahashi, T. Zeki, M. Takahashi, T. Yamase, *Acta Crystallogr*. **1992**, *C48*, 1370; b) T. Ozeki, T. Yamase, *Acta Crystallogr.* **1994**, *B50*, 128; c) T. Ozeki, T. Yamase, *Acta Crystallogr.* **1993**, *C49*, 1574; d) T. Ozeki, T. Yamase, *Acta Crystallogr.* **1994**, *C50*, 327; e) T. Yamase, T. Ozeki, K. Ueda, *Acta Crystallogr.* **1993**, *C49*, 1572; f) T. Yamase, T. Ozeki, *Acta Crystallogr.* **1993**, *C49*, 1577; g) T. Yamase, T. Ozeki, M. Tosaka, *Acta Crystallogr.* **1994**, *C50*, 1849; h) T. Ozeki, M. Takahashi, T. Yamase, *Acta Crystallogr.* **1992**, *C*48, 1370.

[9] M. Barsukova, M. H. Dickman, E. Visser, S. S. Mal, U. Kortz, *Z. Anorg. Allg. Chem.* **2008**, *634*, 2423.

[10] A. H. Ismail, M. H. Dickman, U. Kortz, *Inorg. Chem.* **2009** *48,* 1559.

[11] T. Li, F. Li, J. Lü, Z. Guo, S. Gao, R. Cao, *Inorg. Chem.* **2008**, *47*, 5612.

[12] G. M. Sheldrick, *Acta. Cryst.* **2008**, *A64*, 112.

[13] a) The lanthanum derivative of the $\{Ln_2W_{28}\}$ family crystallizes in the triclinic system, space group P-1, with a = 20.577(14) Å, b = 27.020(15) Å, c = 31.090 (19) Å, α = 81.511(19)°, β = 75.062(3)°, γ = 77.11(2)°, V = 16205.7 $Å^3$ and Z = 2. b) The cerium derivative of the $\{Ln_2W_{28}\}$ family crystallizes in the triclinic system, space group P-1, with a

= 21.629(2) Å, b = 26.869(3) Å, c = 31.611(3) Å, α = 80.463(3)°, β = 72.936(4)°, γ = 75.999(4)°, V = 16951.2 Å^3 and Z = 2. c) The praseodymium derivative of the {Ln_2W_{28}} family crystallizes in the triclinic system, space group P-1, with a = 21.110(8) Å, b = 26.903(8) Å, c = 31.154(10) Å, α = 81.125(11)°, β = 73.771(13)°, γ = 76.903(12)°, V = 16467.77 Å^3 and Z = 2. d) The neodymium derivative of the {Ln_2W_{28}} family crystallizes in the triclinic system, space group P-1, with a = 14.837(3) Å, b = 21.803(4) Å, c = 23.596(4) Å, α = 88.899(7)°, β = 86.092(6)°, γ = 75.540(7)°, V = 7374.23 Å^3 and Z = 2. e) The gadolinium derivative of the {Ln_2W_{28}} family crystallizes in the triclinic system, space group P-1, with a = 14.8426(19) Å, b = 21.779(3) Å, c = 23.581(3) Å, α = 89.059(4)°, β = 86.325(4)°, γ = 75.426(4)°, V = 7362.12 Å^3 and Z = 2.

[14] a) T. Lehmann, J. Fuchs, *Z. Naturforsch. B* **1988**, *43*, 89; b) H. Hartl, R. Palm, J. Fuchs, *Angew. Chem.* **1993**, *105*, 1545; *Angew. Chem. Int. Ed. Engl.* **1993**, *32*, 1492.

[15] a) D-L. Long, H. Abbas, P. Kögerler, L. Cronin, *J. Am. Chem. Soc.* **2004**, *126*, 13880; b) H. N. Miras, J. Yan, D.-L. Long, L. Cronin, *Angew. Chem. Int. Ed.* **2008**, *47*, 8420.

[16] D. Altermatt, I. D. Brown, *Acta. Cryst.* **1985**, *B41*, 244.

3.B. Lanthanide-Containing Heteropolytungstates:

3.B.1. Mono- and Di-Lanthanide Derivatives of Tungstoarsenates(III)

A. H. Ismail, B. S. Bassil, I. Römer, N. C. Redeker, U. Kortz, *Z. Naturforsch. B*, **2010**, *65b*, 383

3.B.1.1. Introduction

Polyoxometalates (POMs) are a diverse class of anionic metal-oxygen cage complexes formed predominantly of early transition metals (groups V and VI) in high oxidation states. The large compositional and structural versatility of POMs gives rise to various applications in fields such as catalysis, medicine, analytical chemistry, and material science.[1] Although the first polyanion has been made already in 1826, the mechanism of POM formation is still not well understood and usually described as self-assembly.[1] POMs are usually formed *via* condensation of mononuclear metalate ions in acidified aqueous solutions. In particular, polyoxotungstates are effective homogeneous photocatalysts useful for the degradation of organic pollutants.[2]

Lanthanide-containing POMs are in general less investigated than their *3d*-transition-metal analogues, but recently there have been more reports on the former class.[3] POMs-containing lanthanides show interesting properties in areas such as photoluminescence, catalysis, electrochemistry, and magnetism.[4,5] Due to their larger sizes and subsequently larger coordination numbers compared to 3d transition metal ions, lanthanide ions exhibit a different coordination mode to lacunary POM precursors resulting in novel and sometimes unexpected structures.[6]

Lacunary POM precursors containing a hetero group with a lone pair of electrons (*e. g.* As^{III}, Sb^{III}) are of particular interest, because the lone pair does not allow the closed Keggin unit to form, resulting in a very different reactivity as compared to lacunary POMs with a

tetrahedral hetero group. The claw-shaped $[As_2W_{19}O_{67}(H_2O)]^{14-}$ (**As_2W_{19}**) precursor is a member of this subclass, and its structure can be rationalized as two [*B*-α-$AsW_9O_{33}]^{9-}$ (**AsW_9**) units linked through a WO_6 group *via* four equatorial W-O-W bonds and two *trans*-related terminal oxo and aqua ligands (see Figure 3.19). The dilacunary **As_2W_{19}** was first reported by Tourné *et al.* in 1973,[7] and its structure was confirmed later by our group using single-crystal X-ray diffraction.[8]

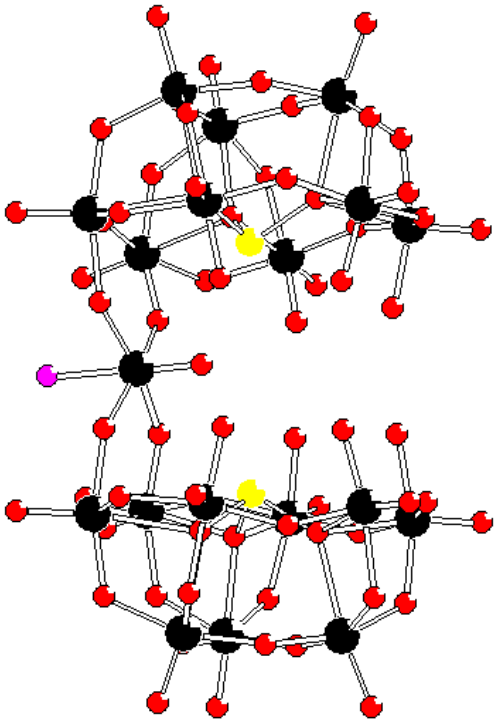

Figure 3.19. Ball-and-stick representation of the dilacunary polyanion precursor $[As_2W_{19}O_{67}(H_2O)]^{14-}$ (**As_2W_{19}**). The color code is as follows: W (black), As (yellow), H_2O (pink), O (red).

Incorporation of an additional W-bridge in the dilacunary **As_2W_{19}** unit results in the monolacunary $[As_2W_{20}O_{68}(H_2O)]^{10-}$ (**As_2W_{20}**), which was first reported by Hervé and coworkers (see Figure 3.20).[9] Interaction of **As_2W_{19}** with di- and trivalent transition metal and main group elements has been investigated by different groups and has resulted in the

expected disubstituted products $[M_2As_2W_{19}O_{67}(H_2O)_3]^{n-}$ (n = 10; M = Mn^{2+}, Co^{2+}, Ni^{2+}, Cu^{2+}, Zn^{2+}, VO^{2+}; n = 8; M = Mn^{3+}, Fe^{3+}, Ga^{3+}) .[10]

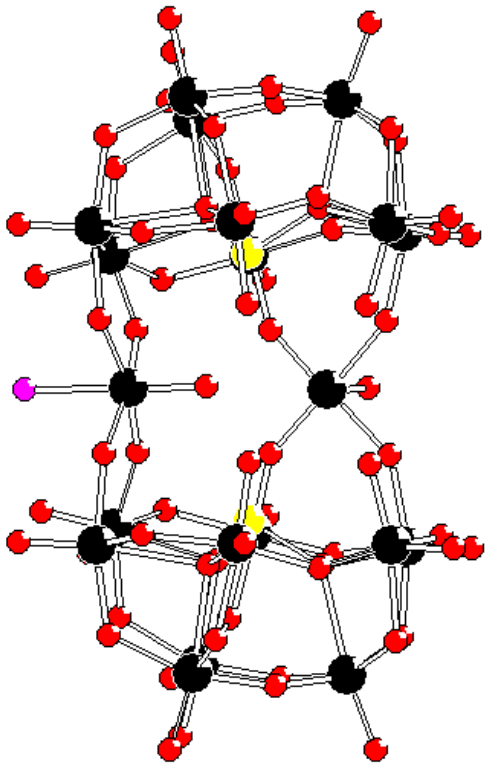

Figure 3.20. Ball-and-stick representation of the monolacunary polyanion precursor $[As_2W_{20}O_{68}(H_2O)]^{10-}$ (**As_2W_{20}**). The color code is the same as in Figure 3.19.

Our group has also been working in the area of lanthanide-containing polyoxotungstates and we have isolated species incorporating between one and twenty lanthanide centers.[11] We have also investigated the interaction of both **As_2W_{19}** and **As_2W_{20}** with ytterbium(III) in aqueous acidic (pH = 2) medium, resulting in both cases in $[YbAs_2W_{20}O_{68}(H_2O)_3]^{7-}$.[11a] This polyanion consists of two **AsW_9** units connected by a triangular $[YbW_2O_2(H_2O)_3]^{11+}$ unit which is composed of two 6-coordinated tungsten centers and a 7-coordinated Yb^{III} ion, all carrying one terminal water ligand.[11a]

Now, we have focused on the reactivity of lanthanide ions with lone pair-containing lacunary POM precursors such as **As_2W_{19}** and **AsW_9**. This work has resulted in the synthesis and structural characterization of two lanthanide-containing 19-tungsto-2-arsenates(III) reported herein.

3.B.1.2. Synthesis

The precursors $K_{14}[As_2W_{19}O_{67}(H_2O)]$ and $Na_9[B\text{-}\alpha\text{-}AsW_9O_{33}]$ used for the synthesis of the reported species were synthesized according to the procedures published by Kortz[8] and Pope,[12] respectively.

$K_{9.5}Na_{0.5}[Yb(H_2O)_2K(H_2O)_2As_2W_{19}O_{67}(H_2O)]\cdot 25H_2O$ (KNa-13)

0.10 g (0.21 mmol) of $Yb(NO_3)_3\cdot 5H_2O$ was added to 20 mL H_2O with stirring followed by addition of 1.0 g (0.19 mmol) of $K_{14}[As_2W_{19}O_{67}(H_2O)]$, and then the pH was adjusted to 5.5 - 6.5 with 1M $NaOH_{(aq)}$. The solution was stirred at 60 ˚C for 20 min, allowed to cool to r. t. and then filtered. 0.5 mL of 1M $KCl_{(aq)}$was added to the filtrate, which was kept in an open vial for crystallization. After about three weeks colorless crystals were obtained, which were filtered off and air-dried (yield 1.1 g, 95 %). The IR spectrum for **KNa-13** showed metal-oxygen bands at 948(m), 891(m), 792(sh), 720(s), 615(s), 479(w), 471(w) cm^{-1}. – $H_{60}A_{s2}K_{10\cdot 5}Na_{0.5}W_{19}Yb$ (5850.6): calcd. K 7.02, Na 0.20,Yb 2.96, As 2.60, W 59.71; found K 6.99, Na 0.18, Yb 2.76, As 2.60, W 58.84.

$Na_8[La_2(H_2O)_6As_2W_{19}O_{67}(H_2O)]\cdot 16H_2O$ (Na-14)

0.07 g (0.19 mmol) of $LaCl_3\cdot 6H_2O$ was added to 20 mL of 1M $NaCl_{(aq)}$ with stirring, followed by addition of 0.50 g (0.20 mmol) of $Na_9[B\text{-}\alpha\text{-}AsW_9O_{33}]$, and then the pH was adjusted to 5.0 with 1M HCl. The solution was stirred at 50 ˚C for 30 min, allowed to cool to r. t. and then filtered. The filtrate was kept in an open vial for crystallization. After *ca*. three weeks colorless crystals were obtained, which were filtered off and air-dried (yield 0.51 g, 89 %). The IR spectrum for **Na-14** showed metal-oxygen bands at 953(m), 878(w), 859(s), 796(m), 728(s), 615(w), 500(w), 484(w), 458(w) cm^{-1}.

3.B.1.3. X-ray Crystallography

The crystals were mounted in Hampton cryoloops using light oil for data collection at 173 K. Indexing and data collection were performed using a Bruker X8 APEX II CCD diffractometer with kappa geometry and MoK_α radiation (λ = 0.71073 Å). Data integration and routine processing were performed using the SAINT software suite. Direct Methods (SHELXS97) solutions successfully located the W atoms, and successive Fourier syntheses (SHELXL97) revealed the remaining atoms.[13,14] Refinements were done with full-matrix least-squares methods against F^2 using all data. Further data processing, including multi-scan absorption corrections, was performed using SADABS.[15] Some water molecules of hydration were modeled with varying degrees of occupancy, a common situation for polytungstate structures. In the final refinements, all non-disordered heavy atoms (W, *Ln*) were refined anisotropically, while the O, K and Na atoms were refined isotropically. No H atoms were included in the models. The crystallographic data are shown in Table 3.4.

Table 3.4. Crystal Data and Structure Refinement for **KNa-13** and **Na-14.**

Code	**KNa-13**	**Na-14**
Emp. formula	$K_{9.5}Na_{0.5}[Yb(H_2O)_2K(H_2O)_2As_2W_{19}O_{67}(H_2O)]\cdot 25H_2O$	$Na_8[La_2(H_2O)_6As_2W_{19}O_{67}(H_2O)]\cdot 16H_2O$
M_r	5811.4	5591.1
Crystal system	Triclinic	Triclinic
Space group (no.)	$P\bar{1}$ (2)	$P\bar{1}$ (2)
a / Å	12.4730(5)	14.929(2)
b / Å	17.4630(9)	17.769(3)
c/Å	21.1990(10)	20.754(4)
α / deg	72.568(3)	77.203(10)
β/ deg	85.442(2)	80.273(9)
γ/ deg	89.147(3)	72.670(9)
V / Å^3	4391.3(4)	5093.6(15)
Z	2	2
T / ºC	-100	-100
λ / Å	0.71073	0.71073
D / g cm^{-3}	4.39	3.65
μ / mm^{-1}	27.2	23.0
R $[I \geq 2\sigma(I)]$[a]	0.085	0.065
R_w (all data)[b]	0.197	0.237

[a] $R = \sum||F_o| - |F_c|| / \sum|F_o|$; [b] $R_w = \{\sum[w(F_o^2 - F_c^2)^2] / \sum[w(F_o^2)^2]\}^{1/2}$.

3.B.1.4. Results and Discussion

We have synthesized and structurally characterized the mono- and di-lanthanide-containing polyanions $[Yb(H_2O)_2K(H_2O)_2As_2W_{19}O_{67}(H_2O)]^{10-}$ (**13**) and $[La_2(H_2O)_6As_2W_{19}O_{67}(H_2O)]^{8-}$ (**14**). The mixed potassium-sodium salt of **13** $K_{9.5}Na_{0.5}[Yb(H_2O)_2K(H_2O)_2As_2W_{19}O_{67}(H_2O)]\cdot 25H_2O$ (**KNa-13**) and the sodium salt of **14** $Na_8[La_2(H_2O)_6As_2W_{19}O_{67}(H_2O)]\cdot 17H_2O$ (**Na-14**) have been characterized in the solid state by FTIR spectroscopy, single-crystal X- ray diffraction and TGA analyses. Both polyanions are based on the **As_2W_{19}** skeleton with one (**11**) or two (**14**) incorporated lanthanide ions.

The ytterbium(III)-containing polyanion $[Yb(H_2O)_2K(H_2O)_2As_2W_{19}O_{67}(H_2O)]^{10-}$ (**13**) consists of two **AsW_9** subunits sandwiching an ytterbium and a tungsten ion and a weakly bound, stabilizing potassium ion, leading to a structure with idealized C_s symmetry (see Figure 3.21). The tungsten and potassium ions in the central 'belt' of the structure are six-coordinated, whereas the ytterbium ion is seven-coordinated. The ytterbium and potassium ions have two terminal aqua ligands each while the unique tungsten atom has just one, and all aqua ligands point away from the polyanion. We checked for possible protonation of polyanion **13** by bond valence sum (BVS) calculations,[16] but no additional protonation sites besides the terminal aqua ligands described above were identified. The three metal ions in the central 'belt' are all coordinated to both **AsW_9** fragments *via* four μ_2-oxo bridges involving corner-sharing WO_6 octahedra of each **AsW_9** subunit. The average Yb−O and K−O distances in **13** are 2.266(14) and 2.836(16) Å, respectively.

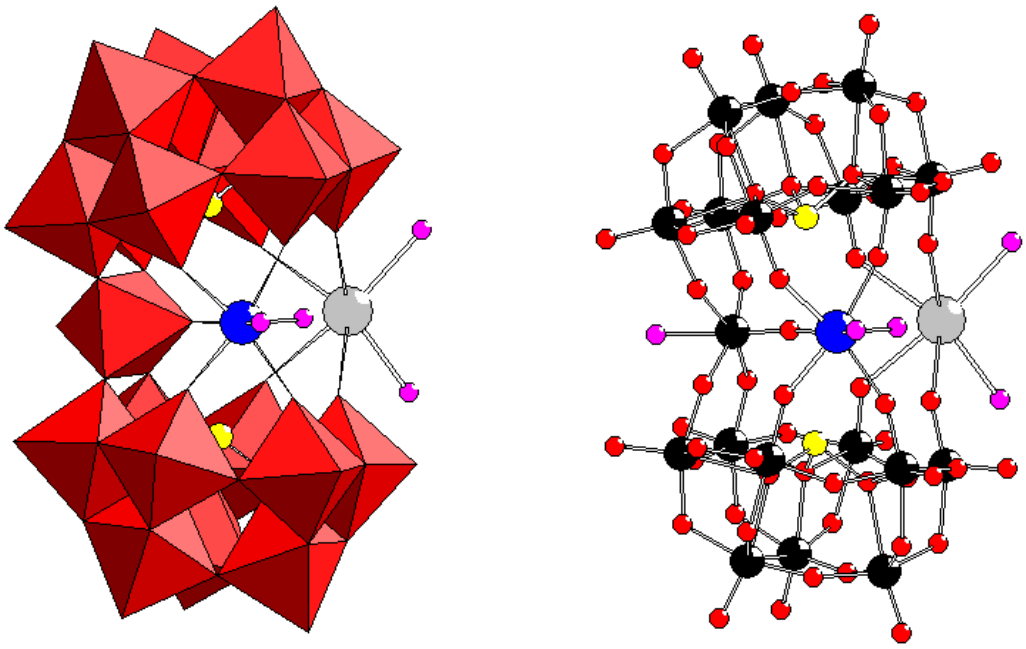

Figure 3.21. Polyhedral (left) and ball-and-stick (right) representation of $[Yb(H_2O)_2K(H_2O)_2As_2W_{19}O_{67}(H_2O)]^{10-}$ (**13**). The color code is as follows: WO_6 octahedra (red), W (black), As (yellow), Yb (blue), K (grey), H_2O (pink), O (red).

Polyanion **13** was synthesized using simple and conventional open beaker conditions by interaction of the dilacunary precursor $\mathbf{As_2W_{19}}$ with Yb^{3+} ions in aqueous acidic (pH = 6) medium. It is known that interaction of $\mathbf{As_2W_{19}}$ or $\mathbf{AsW_9}$ with transition metal ions or organometallic species at a proper pH usually results in mono- or disubstituted products based on the $\mathbf{As_2W_{19}}$ framework.[10] For example, our group has already reported di-manganese(II)/cobalt(II)/zinc(II),[10c] di-phenyltin,[10e] mono-palladium(II),[10f] and di-titanium(IV).[10g,h] At pH = 2.0, reaction of $\mathbf{As_2W_{19}}$ with ytterbium(III) led to the formation of $[YbAs_2W_{20}O_{68}(H_2O)_3]^{7-}$,[11a] whereas the same reaction at pH = 6.5 resulted in polyanion **13**. This is fully consistent with the known fact that pH ~ 2 induces condensation of an extra tungsten center at the lacunary site of $\mathbf{As_2W_{19}}$ resulting in $\mathbf{As_2W_{20}}$,[9] whereas at mildly acidic pH the $\mathbf{As_2W_{19}}$ framework is maintained, and the vacant site in the central 'belt' is occupied by a potassium ion as seen in **13**. We also tried to obtain the di-ytterbium analog of **13** using

different synthetic pathways involving **As_2W_{19}**, but without success. We believe that the potassium ion in the **As_2W_{19}** framework inhibits incorporation of an additional Yb^{3+}ion. It is interesting to note that when the same reaction was performed at pH = 2.0 in a 1M KCl solution (instead of water), anion **13** is obtained rather than the expected $[YbAs_2W_{20}O_{68}(H_2O)_3]^{7-}$, which confirms the role of potassium in mediating the reaction pathway. We were also able to synthesize other lanthanide analogues of **13**, namely $[Ln(H_2O)_2K(H_2O)_2As_2W_{19}O_{67}(H_2O)]^{10-}$ (Ln = La, Ce, Eu, Gd). The IR spectra of these analogues are all very similar and virtually identical of **13** (see Figure 3.22).

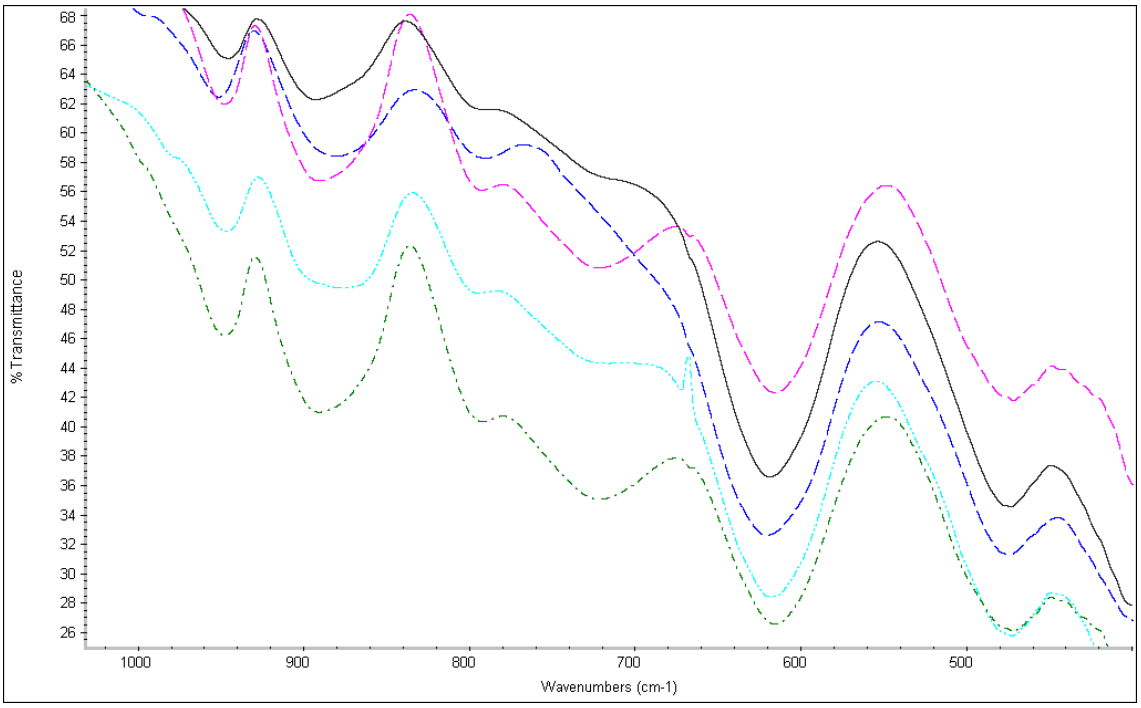

Figure 3.22. IR spectra of **KNa-13** (black line) and its four compositional analogues $[Ln(H_2O)_2K(H_2O)_2As_2W_{19}O_{67}(H_2O)]^{10-}$ (from top to bottom Ln = La, Ce, Sm, Eu, Gd).

The di-lanthanum(III) polyanion $[La_2(H_2O)_6As_2W_{19}O_{67}(H_2O)]^{8-}$ (**14**) consists of two **AsW_9** subunits sandwiching one tungsten and two lanthanum(III) ions leading to a structure with C_{2v} symmetry (see Figure 3.23). The unique tungsten atom in the central 'belt' is six-coordinated, whereas the two lanthanum ions are nine-coordinated with an average La–O

distance of 2.555(17) Å. Both lanthanum ions are linked by a bridging water molecule, and they also have three terminal aqua ligands each, whereas the tungsten ion has an inner oxo and an outer aqua terminal ligand. BVS calculations indicate that no other oxygen atoms of **14** are protonated. In analogy with polyanion **13**, all three metal atoms in the 'belt' of **14** connect both **AsW_9** fragments *via* four μ_2-oxo bridges involving corner-sharing WO_6 octahedra.

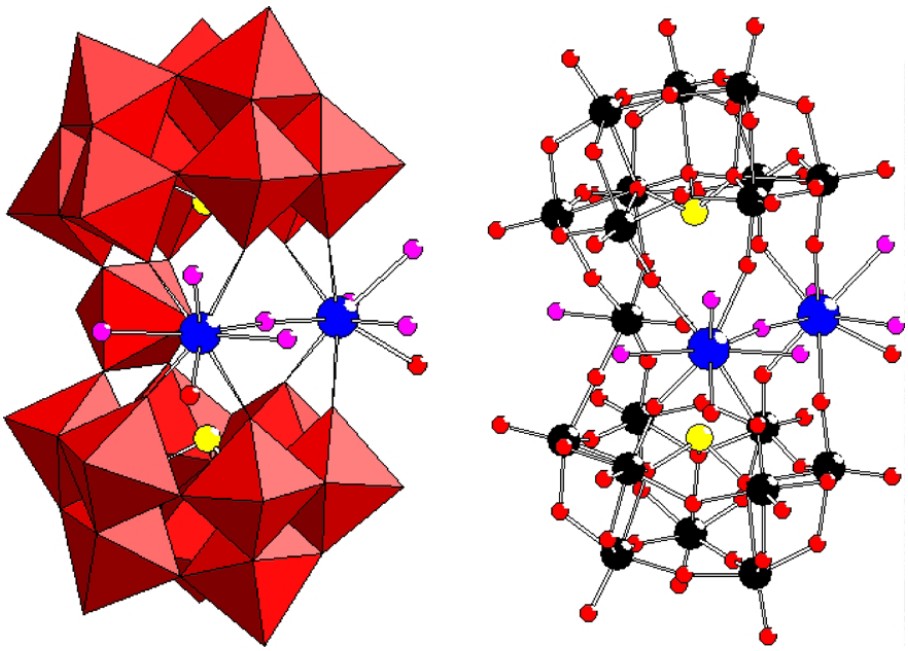

Figure 3.23. Polyhedral (left) and ball-and-stick (right) representation of $[La_2(H_2O)_8As_2W_{19}O_{67}(H_2O)]^{8-}$ (**14**). The color code is the same as in Figure 3.21, and La (blue).

The coordination sphere of each lanthanum ion is completed through a La−O−W' bridge, where W' belongs to a neighboring polyanion, leading to a zigzag 1D chain formation in the solid state (see Figure 3.24). The structures of polyanions **13** and **14** are very similar as both are based on the trilacunary **As_2W_{19}** unit. However, the potassium ion in **13** is replaced by a lanthanum(III) ion in **2**. No potassium ions were present during the synthesis of **14**, and a different precursor was used (**AsW_9** vs. **As_2W_{19}**). As expected, the coordination number of La^{3+} in **14** is larger than that of Yb^{3+} in **13** (9 vs. 7), reflecting the larger size of the former.

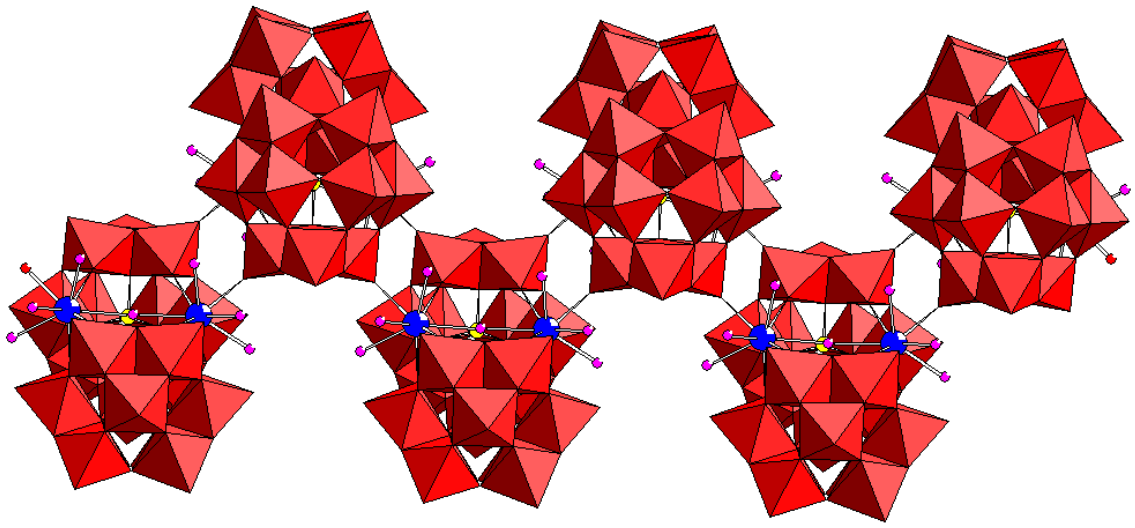

Figure 3.24. Polyhedral representation of **14** forming a 1D chain in the solid state. The color code is the same as in Figure 3.23.

Polyanion **14** was synthesized under mild, conventional conditions by interaction of the sodium salt of the trilacunary precursor **AsW_9** with La^{3+} ions in aqueous acidic (pH = 5) medium. A high concentration of NaCl (1.0 M) was needed in order to obtain the desired crystalline product. The same reaction performed in water did not result in any crystalline product. Also, polyanion **14** cannot be prepared when using the **As_2W_{19}** as precursor instead of **AsW_9**. Several variations of the synthetic procedure with **As_2W_{19}** (pH, solvent, temperature, ratio) always led to the mono-lanthanum polyanion. This observation indicates the importance of the POM precursor and the type of counterion during the synthesis of polyanions **13** and **14**. As stated above, a potassium ion preferentially coordinates to the lacunary site of the **As_2W_{19}** precursor, thereby blocking insertion of a second lanthanide ion. On the other hand, using the sodium sodium salt of **AsW_9** allowed us to prepare the di-lanthanide derivative **14**. The different role of potassium vs. sodium ions in the stabilization of lacunary polyanion fragments in aqueous solution is well known.[17] Following the same synthetic procedure as for **14**, we were able to prepare the cerium(III) analogue $[Ce_2(H_2O)_8As_2W_{19}O_{67}(H_2O)]^{8-}$, as confirmed by FTIR studies (see Figure 3.25).

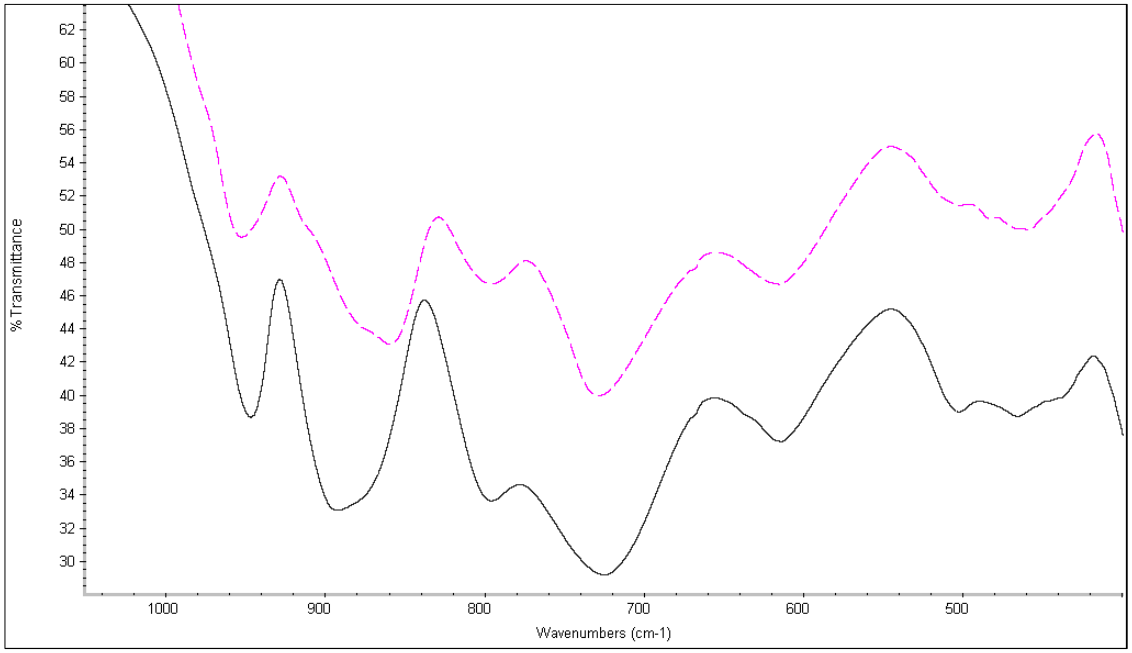

Figure 3.25. IR spectra of **Na-14** (top) and its cerium analogue (bottom).

The bonding modes of the lanthanide centers in **13** (Yb^{3+}) and **14** (La^{3+}) are different. The ytterbium ion in **1** is connected to the unique 'belt' tungsten *via* a μ_2-oxo bridge, whereas both lanthanum ions in **14** are bound to each other *via* a μ_2-aqua bridge, but not to the unique 'belt' tungsten. The W···Yb distance in **13** is *ca.* 4.0 Å whereas the average W···La distance in **14** is *ca.* 5.2 Å, which can be correlated with the size difference of Yb^{3+} *vs.* La^{3+}. The smaller ytterbium(III) ion is incorporated more deeply into the $\mathbf{As_2W_{19}}$ framework than the lanthanum(III) ion.

We also performed thermogravimetric analyses (TGA) on the salts **KNa-13** and **Na-14** to determine the degree of hydration and thermal stability. The thermograms showed the expected weight loss domain between 25 and 400 ºC corresponding to dehydration. We calculated 25 and 16 water molecules per formula unit of **KNa-13** and **Na-14**, respectively.

3.B.1.5. Conclusions

The mono-ytterbium(III) and di-lanthanum(III) 19-tungsto-2-arsenates(III) $[Yb(H_2O)_2K(H_2O)_2As_2W_{19}O_{67}(H_2O)]^{10-}$ (**13**) and $[La_2(H_2O)_6As_2W_{19}O_{67}(H_2O)]^{8-}$ (**14**), have been structurally characterized in the solid state by IR spectroscopy, single-crystal X-ray diffraction and TGA. Polyanions **13** and **14** were synthesized in simple, one-pot reactions of Yb^{3+} and La^{3+} with the dilacunary and trilacunary polyanion precursors $\mathbf{As_2W_{19}}$ and $\mathbf{AsW_9}$, respectively. The structure of **13** comprises an $\mathbf{As_2W_{19}}$ fragment with one incorporated Yb^{3+} ion, whereas **14** contains two La^{3+} ions in the vacant site of $\mathbf{As_2W_{19}}$. Different synthetic strategies were needed to deliberately and selectively prepare mono- and di-lanthanide derivatives of $\mathbf{As_2W_{19}}$. In this context it was discovered that counterions (K^+ *vs*. Na^+) play an important role. The terminal, labile water ligands in **13** and **14** are of interest for structural modifications and applications. We plan to explore aqua ligand substitution for other mono- and polydentate ligands, including chiral ones, and we envision potential applications in Lewis acid catalysis. Efforts to isolate lipophilic salts of **13** and **14** in order to study their catalytic properties in organic media are also underway.

3.B.1.6. References

[1] a) M. T. Pope in *Heteropoly and Isopoly Oxometalates*, Springer-Verlag, Berlin, 1983; b) M. T. Pope, A. Müller, *Angew. Chem.,* **1991**, *103*, 56, *Angew. Chem., Int. Ed. Engl.* **1991**, *30*, 34; c) M. T. Pope, A. Müller in *Polyoxometalates: From Platonic Solids to Anti- Retroviral Activity* (Eds.: M. T. Pope, A. Müller), Kluwer: Dordrecht, The Netherlands, 1994; d) A. Müller, H. Reuter, S. Dillinger, *Angew. Chem.,* **1995**, *107*, 2505, *Angew. Chem., Int. Ed. Engl.* **1995**, *34*, 2328; e) C. Hill in *Polyoxometalates: Chemical Reviews*, 1998 (special thematic issue on polyoxometalates); f) M. T. Pope, A. Müller in *Polyoxometalate Chemistry: From Topology via Self-Assembly to Applications (*Eds.: M. T. Pope, A. Müller), Kluwer: Dordrecht, The Netherlands, 2001; g) T. Yamase, M. T. Pope in *Polyoxometalate Chemistry for Nano-Composite Design (*Eds.: T. Yamase, M. T. Pope), Kluwer: Dordrecht, The Netherlands, 2002.

[2] a) A. Mylonas, A. Hiskia, E. Papaconstantinou, *J. Mol. Catalysis A: Chem.* **1996**, *114*, 191; b) A. Hiskia, A. Troupis, E. Papaconstantinou, *Int. J. Photoenergy* **2002**, *4*, 35; c) E. Gkika, P. Kormali, S. Antonaraki, D. Dimoticali, E. Papaconstantinou, A. Hiskia, Int. *J. Photoenergy* **2004**, *6*, 227; d) A. Hiskia, A. Troupis, S. Antonaraki, E. Gkika, P. Kormali, E. Papaconstantinou, *Int. J. Envir. Anal. Chem.* **2006**, 233; e) P. Kormali, A. Troupis, T. Triantis, A. Hiskia, E. Papaconstantinou, *Catalysis Today* **2007**, *124*, 149.

[3] a) R. D. Peacock, T. J. R. Weakley, *J. Chem. Soc. A* **1971**, 1836; b) M. H. Dickman, G. J. Gama, K-C. Kim, M. T. Pope, *J. Clust. Sc.* **1996**, *7*, 567; c) M. Sadakane, M. H. Dickman, M. T. Pope, *Angew. Chem.,* **2000**, *112*, 3036, *Angew. Chem., Int. Ed. Engl.* **2000**, *39*, 2914; d) M. Sadakane, M. H. Dickman, M. T. Pope, *Inorg. Chem.* **2001**, *40*, 2715; e) P. Mialane, L. Lisnard, A. Mallard, J. Marrot, E. Antic-Fidancev, P. Aschehoug, D. Vivien, F. Sécheresse, *Inorg. Chem.* **2003**, *42*, 2102; f) K. Fukaya, T. Yamase, *Angew. Chem.,* **2003**, *115*, 678, *Angew. Chem., Int. Ed. Engl.* **2003**, *42*, 654; g) F. Li, L. Xu, Y. Wei, G. Gao, L. Fan, Z. Li, *Inorg. Chim. Acta* **2006**, *359*, 3795; h) Y. Lu, Y. Li, E. Wang, X. Xe, Y. Ma, *Inorg. Chim.*

Acta **2006**, *360*, 2063; i) Y. Lu, Y. Li, E. Wang, X. Xeu, Y. Ma, *Inorg. Chim. Acta* **2007**, *360*, 2063; j) F. Hussain, R. W. Gable, M. Speldrich, P. Kögerler, C. Boskovic, *Chem. Commun*. **2009**, 328; k) F. Hussain, B. Spingler, F. Conrad, M. Speldrich, P. Kögerler, C. Boskovic, G. R. Patzke, *Dalton Trans*. **2009**, 4223; l) F. Hussain, F. Conrad, G. R. Patzke, *Angew. Chem.,* **2009**, *121*, 9252, *Angew. Chem., Int. Ed. Engl.* **2009**, *48*, 9088.

[4] a) M. M. Gresely, W. P. Griffith, A. C. Lämmel, H. I. S. Nogueira, B. C. Parkin, *J. Mol. Catal. A: Chemical* **1997**, *117*, 185; b) W. P. Griffith, N. Morley-Smith, H. I. S. Nogueira, A. G. F. Shoair, M. Suriaatmaja, A. J. P. White, D. J. Williams, *J. Organomet. Chem.* **2000**, *607*, 146; c) J. A. Fernández, X. López, C. Bo, C. de Graaf, E. J. Baerend, J. M. Poblet, *J. Am. Chem. Soc.* **2005**, *129*, 12244; d) F. Li, L. Xu, Y. Wei, G. Gao, L. Fan, Z. Li, *Inorg. Chim. Acta* **2006**, *359*, 3795; e) W. Chen, Y. Li, Y. Wang, E. Wang, Z. Su, *J. Chem. Soc., Dalton Trans.* **2007**, 4293; f) W. Huang, L. C. Francesconi, T. Plenova, *Inorg. Chem.* **2007**, *43*, 7861; g) A. Merca, A. Müller, J. van Slageren, M. Läge, B. Krebs, *J. Clust. Sci.* **2007**, *168*, 711.

[5] a) S. Bareyt, S. Piligkos, B. Hasenknopf, P. Gouzerh, E. Lacôte, S. Thorimbert, M. Malacria, *J. Am. Chem. Soc.* **2005**, *127*, 6788; b) C. Boglio, G. Lemiére, B. Hasenknopf, S. Thorimbert, E. Lacôte, M. Malacria, *Angew. Chem.,* **2006**, *118*, 3402, *Angew. Chem., Int. Ed. Engl.* **2006**, *45*, 3324; c) C. Boglio, G. Lenoble, C. Duhayon, B. Hasenknopf, R. Thouvenot, C. Zhang, R. C. Howell, B. P. Burton-Pye, L. C. Francesconi, E. Lacôte, S. Thorimbert, M. Malacria, C. Afonso, J.-C. Tabet, *Inorg. Chem.* **2006**, *45*, 1389; d) C. Boglio, K. Micoine, R. Rémy, B. Hasenknopf, S. Thorimbert, E. Lacôte, M. Malacria, C. Afonso, J.-C. Tabet, *Chem. Eur. J.* **2007**, *13*, 5426; e) K. Micoine, B. Hasenknopf, S. Thorimbert, E. Lacôte, M. Malacria, *Org. Lett.* **2007**, *9*, 3981; f) E. Derat, E. Lacôte, B. Hasenknopf, S. Thorimbert, M. Malacria, *J. Phys. Chem. A* **2008,** *112,* 13002; g) C. Boglio, K. Micoine, E. Derat, R. Thouvenot, B. Hasenknopf, S. Thorimbert, E. Lacôte, M. Malacria, *J. Am. Chem. Soc.* **2008**, *130*, 4553.

[6] a) K. Wassermann, M. H. Dickman, M. T. Pope, *Angew. Chem.,* **1997***, 109,*1513, *Angew. Chem., Int. Ed. Engl.* **1997**, *36*, 1445; b) R. C. Howell, F. G. Perez, S. Jain, W. DeW. Jr. Horrocks, A. L. Rheingold, L. C. Francesconi, *Angew. Chem.,* **2001**, *113,* 4155, *Angew. Chem., Int. Ed. Engl.* **2001**, *40,* 4031; c) Q. H. Luo, R. C. Howell, M. Dankova, J. Bartis, C. W. Williams, W. DeW. Jr. Horrocks, V. G. Young, A. L. Rheingold, L. C. Francesconi, *Inorg. Chem.* **2001**, *40*, 1894; d) Q. H. Luo, R. C. Howell, J. Bartis, M. Dankova, W. DeW. Jr. Horrocks, A. L. Rheingold, L. C. Francesconi, *Inorg. Chem.* **2002**, *41*, 6112; e) G. L. Xue, J. Vaissermann, P. Gouzerh, *J. Cluster Sci.* **2002**, *13*, 409; f) C. Zhang, R. C. Howell, K. B. Scotland, F. G. Perez, L. Todaro, L. C. Francesconi, *Inorg. Chem.* **2004**, *43*, 7691.

[7] C. Tourné, A. Revel, G. Tourné, M. Vendrell, *C. R. Acad. Sci. Ser. III* **1973**, *277*, 643.

[8] U. Kortz, M. G. Savelieff, B. S. Bassil, M. H. Dickman, *Angew. Chem.,* **2001**, *113*, 3488; *Angew. Chem., Int. Ed. Engl.* **2001**, *40*, 3384.

[9] F. Lefebvre, M. Leyrie, G. Hervé, C. Sanchez, J. Livage, *Inorg. Chim. Acta* **1983**, *73*, 173.

[10] a) C. Tourné, G. Tourné, *C. R. Acad. Sci. Ser. III* **1975**, *C281*, 933; b) L. G. Detusheva, L. I. Kuznetsova, V. A. Likholobov, A. A. Vlasov, N. N. Boldyreva, S. G. Poryvaev, V. V. Malakhov, *Russ. J. Coord. Chem.* **1999**, *25*, 569; c) U. Kortz, N. K. Al-Kassem, M. G. Savelieff, N. A. Al Kadi, M. Sadakane, *Inorg. Chem.* **2001**, *40*, 4742; d) P. Mialane, J. Marrot, A. Mallard, G. Hervé, *Inorg. Chim. Acta* **2002**, *328*, 81; e) F. Hussain, U. Kortz, R. J. Clark, *Inorg. Chem.* **2004**, *43*, 3237; f) L.-H. Bi, U. Kortz, B. Keita, L. Nadjo, L. Daniels, *Eur. J. Inorg. Chem.* **2005**, 3034; g) F. Hussain, B. S. Bassil, U. Kortz, O. A. Kholdeeva, M. N. Timofeeva, P. de Oliveira, B. Keita, L. Nadjo, *Chem. Eur. J.* **2007**, *13*, 4733; h) O. A. Kholdeeva, B. G. Donoeva, T. A. Trubitsina, G. Al-Kadamany, U. Kortz, *Eur. J. Inorg. Chem.*, **2009**, 5134.

[11] a) U. Kortz, C. Holzapfel, M. Reicke, *J. Mol. Struct.* **2003**, *656*, 93; b) U. Kortz, *J. Clust. Sci.* **2003**, *14*, 205; c) B. S. Bassil, M. H. Dickman, B. Kammer, U. Kortz, *Inorg. Chem.* **2007**, *46*, 2452; d) B. S. Bassil, M. H. Dickman, I. Römer, B. Kammer, U. Kortz, *Angew.*

Chem., **2007**, *119*, 6305, *Angew. Chem., Int. Ed. Engl.* **2007**, *46*, 6192; e) A. H. Ismail, M. H. Dickman, U. Kortz, *Inorg. Chem.* **2009**, *48,* 1559; f) A. H. Ismail, B. S. Bassil, A. Suchopar, U. Kortz, *Eur. J. Inorg. Chem.* **2009**, DOI: 10.1002/ejic.200900630.

[12] K.-C. Kim, A. Gaunt, M. T. Pope, *J. Cluster Sci.* **2002***, 13*, 432.

[13] Sheldrick, G. M. SHELXS-97, *Program for Solution of Crystal Structures*; University of Göttingen: Germany, **1997**.

[14] G. M. Sheldrick, *Acta. Crystallogr.* **2008**, *A64*, 112.

[15] Sheldrick, G. M. SADABS; University of Göttingen: Germany, **1996**.

[16] D. Altermatt, I. D. Brown, *Acta. Crystallogr.* **1985**, *B41*, 244.

[17] N. Laronze, J. Marrot, G. Hervé, *Inorg. Chem.* 2003, *42*, 5857.

3.B.2. Mono- and Di-Lanthanide Derivatives of Tungstoantimonate(III)

3.B.2.1. Introduction

Polyoxometalates (POMs) represent a class of discrete structurally and chemically diverse nanosized metal-oxygen molecular anions of early transition metals (groups V and VI) in their high oxidation states.[1] However, recently, polyoxopalladates and –aurates have been synthesized and structurally characterized by our group.[2] Due to the large versatility of POMs gives rise to various applications in fields such as catalysis, medicine, analytical chemistry, and material science.[1] Although the first synthetic POM is known since 1826, the mechanism of POM formation is still not completely understood and is often described as a self-assembly process. POMs are usually formed *via* condensation of mono nuclear metalate ions in acidified solutions (usually aqueous).[1]

Lacunary POM precursors containing a hetero group with a lone pair of electrons (*e. g.* As^{III}, Sb^{III}) are of particular interest, because the lone pair does not allow the closed Keggin unit to form, resulting in a very different reactivity compared to lacunary POMs with a tetrahedral hetero group. The trilacunary precursor $[B\text{-}\alpha\text{-}SbW_9O_{33}]^{9-}$ (**SbW_9**) is a member of this subclass. This **SbW_9** anion was first reported by Tourné *et al.* in 1973.[3] It is stable at pH 7.7 – 9 in *B*-**SbW_9** type and does not react with tungstate to give $Sb^{III}W_{11}$. However solution of **SbW_9** anions react with divalent metal ions to give $[M_3(B\text{-}\alpha\text{-}SbW_9O_{33})_2]^{12-}$ (M = Cu, Ni, Zn, etc.).[3] Since then, more metal ions derivatives of the **SbW_9** polyanion have been synthesized and reported.[4]

In 1997, Krebs et al. reported the $[Sb_2W_{22}O_{74}(OH)_2]^{12-}$ (**Sb_2W_{22}**) polyanion which composed of two $[B\text{-}ß\text{-}SbW_9O_{33}]^{9-}$ units linked through four WO_6 fragments (see Figure 3.26). Since, one triad (W_3O_{13}), (yellow in Figure 3.26) in the $[B\text{-}\alpha\text{-}SbW_9O_{33}]^{9-}$ unit has been rotated by 60˚ along the Sb–O bond vector. Furthermore, it has an inversion center and the

bond lengths within the **SbW_9** units are similar to those of $[B\text{-}\alpha\text{-}SbW_9O_{33}]^{9-}$ anion. This **Sb_2W_{22}** polyanion has a special feature, WO_6 octahedra with none or with three terminal oxygen ligand atoms, in addition to the usual WO_6 octahedra with one or two terminal oxygen ligand atoms. Another unusual feature in **Sb_2W_{22}** anion is the presence of terminal hydroxyl groups.[5]

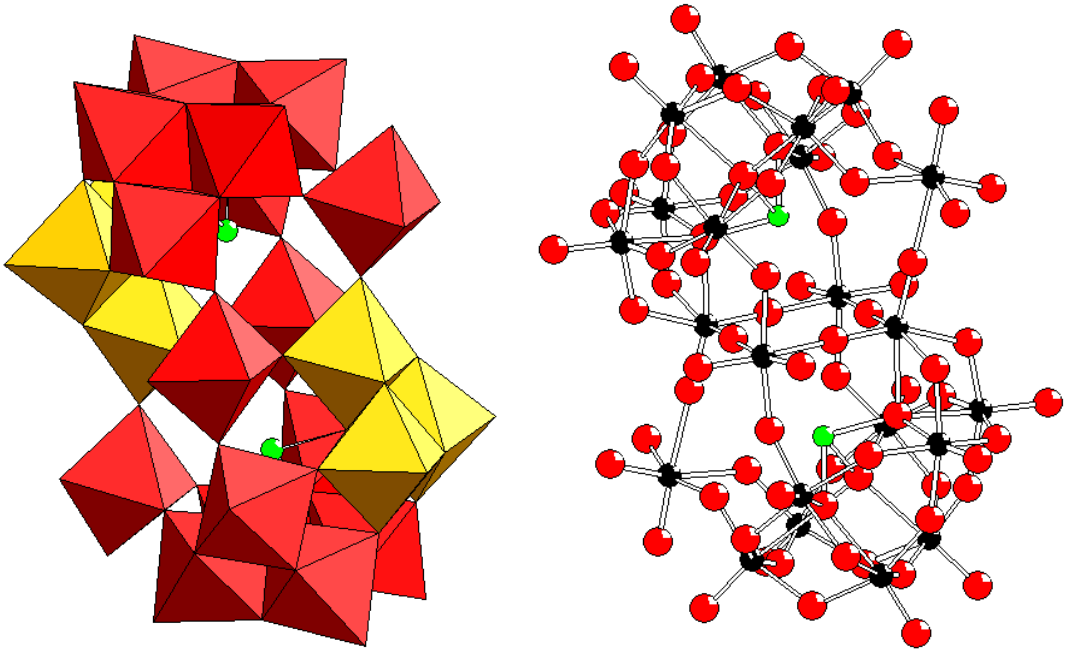

Figure 3.26. Polyhedral (left) and ball-and-stick (right) representations of $[Sb_2W_{22}O_{74}(OH)_2]^{12-}$ polyanion precursor (**Sb_2W_{22}**). The color code is as follows: WO_6 octahedra (red) and rotated WO_6 octahedra (yellow), W (black), Sb (green), O (red).

It is noteworthy that **Sb_2W_{22}** polyanion was synthesized by reaction of the sodium salt of $[B\text{-}\alpha\text{-}SbW_9O_{33}]^{9-}$ and WO_4^{2-} anions in water (pH 4 – 5). Addition of d-transition metal salts to the aqueous solution of **Sb_2W_{22}** at pH 6 – 7 forms $[M_2(H_2O)_6Sb_2W_{20}O_{70}]^{(14-2n)}$ (**$M_2Sb_2W_{20}$**) anions, M^{n+} = Fe^{3+}, Co^{2+}, Mn^{2+}, Ni^{2+}). Exchange reactions lead these anions, the two relatively weakly binding *fac*-WO_2OH groups are substituted by two $M^{n+}(H_2O)_3$ groups.[5] Since then, more metal ions derivatives of the **Sb_2W_{20}** unit have been synthesized and reported.[6]

However, in 1990, Yamase et al. have reported the first potassium salt of mixed-polyoxotungstate anion containing lanthanide $[Eu_3(H_2O)_3(SbW_9O_{33})(W_5O_{18})_3]^{16-}$, in which a central $Eu_3(H_2O)_3$ core is co-ordinated by one $[B\text{-}\alpha\text{-}SbW_9O_{33}]^{9-}$ unit and three $[W_5O_{18}]^{6-}$ units.[7a] Also, Yamase et al. have reported two structures of lanthanide-containing tungstoantimonates in 2002, $[Ln_2(H_2O)_2(SbW_9O_{33})(W_5O_{18})_2]^{15-}$ (Ln = Er, Dy, Eu, Sm, Y) and $[Lu_3(H_2O)_4(SbW_9O_{33})_2(W_5O_{18})_2]^{21-}$.[7b] Polyanions $[Ln_2(H_2O)_2(SbW_9O_{33})(W_5O_{18})_2]^{15-}$ consist of one **SbW_9** unit and two $[W_5O_{18}]^{6-}$ units. These three units are linked to each other via two lanthanide ions alternatively. Polyanion $[Lu_3(H_2O)_4(SbW_9O_{33})_2(W_5O_{18})_2]^{21-}$ consists of two $[Lu(SbW_9O_{33})(W_5O_{18})]^{12-}$ groups linked by $[Lu(H_2O)_4]^{3+}$ with C_2 configuration. Gouzerh and coworkers reported the cerium(III) complex with the same lacunary polyoxotungstate $[B\text{-}\alpha\text{-}SbW_9O_{33}]^{9-}$, $[(SbW_9O_{33})_4\{(WO_2)(H_2O)\}_2Ce_3(H_2O)_8(Sb_4O_4)]^{19-}$ which consists of a tetrahedral assembly of four **SbW_9** units connected by two additional six-coordinate tungsten atoms, three nine-coordinate monocapped square-antiprismatic cerium atoms and a Sb_4O_4 cluster.[7c] Since then, as the best of our knowledge, no lanthanide derivatives of the **SbW_9** have been synthesized nor reported so far. Furthermore, there is no lanthanide derivatives of the **Sb_2W_{20}** unit have reported previously.

POMs containing lanthanides show interesting properties in areas such as photoluminescence, catalysis, electrochemistry, and magnetism.[8]

Our group has been working in the area of lanthanide-containing polyoxotungstates.[9,10] We have also investigated the interaction of both $[As_2W_{19}O_{67}(H_2O)]^{14-}$ **As_2W_{19}** and $[As_2W_{20}O_{68}(H_2O)]^{10-}$ **As_2W_{20}** (lone-pair containing lacunary precursors) with ytterbium(III) in aqueous acidic (pH = 2) medium, resulting in both cases in $[YbAs_2W_{20}O_{68}(H_2O)_3]^{7-}$.[9a] This polyanion consists of two **AsW_9** units connected by a triangular $[YbW_2O_2(H_2O)_3]^{11+}$ unit which is composed of two 6-coordinated tungsten centers and a 7-coordinated Yb^{III} center, all carrying one terminal water ligand.[9a] Very recently, our group reported two types of

lanthanide-containing derivatives of the **As_2W_{19}** which have been synthesized in mildly acidic aqueous media and structurally characterized by single-crystal X-ray. The mono-ytterbium(III)-containing $[Yb(H_2O)_2K(H_2O)_2As_2W_{19}O_{67}(H_2O)]^{10-}$ which was formed by reaction of Yb^{3+} with the potassium salt of **As_2W_{19}**, while the di-lanthanum(III) derivative $[La_2(H_2O)_6As_2W_{19}O_{67}(H_2O)]^{8-}$ was formed by reaction of La^{3+} with the sodium salt of the trilacunary precursor $[B\text{-}\alpha\text{-}AsW_9O_{33}]^{9-}$ (**AsW_9**).[10]

It can be noticed that extended studies of **Sb_2W_{22}** or **$Sb_2W_{20}M_2$** are still limited. We have decided to continue our investigation of the reactivity of lanthanide ions containing atoms with lone pairs of electrons lacunary POM precursors, especially the **SbW_9** and **Sb_2W_{22}**. This work has resulted in the synthesis and structural characterization of six lanthanide-containing tungstoantimonates(III) reported herein. In this work, 'Ln' will be used to designate lanthanides and yttrium since the ionic radius of Y^{3+} falls within the range of lanthanides.

3.B.2.2. Synthesis

The precursors $Na_9[B\text{-}\alpha\text{-}SbW_9O_{33}]\cdot 19.5H_2O$ and $Na_{12}[Sb_2W_{22}O_{74}(OH)_2]$ used for the synthesis of the reported species were synthesized according to the published procedures by Krebs.[5]

$Na_{10}[Yb(H_2O)_3Sb_2W_{21}O_{72}(OH)]\cdot 41H_2O$ (Na-15)

0.068 g (0.175 mmol) of $YbCl_3\cdot 6H_2O$ was added to 20 mL 1M $NaCl_{(aq)}$ with stirring followed by addition of 0.50 g (0.175 mmol) of $Na_9[B\text{-}\alpha\text{-}SbW_9O_{33}]\cdot 19.5H_2O$, and then the pH was adjusted to 3 with 4M HCl. The solution was stirred at 50 ˚C for 30 min, allowed to cool to room temperature. The filtrate was kept in an open vial for crystallization. After about three weeks colorless crystals were obtained, which were filtered off and air dried (yield 0.15 g, 27 %). IR for **Na-15** showed metal-oxygen stretches at 953(s), 874(sh), 840(m), 806(s), 758(m), 660(m), 525(w), 517(w), 472(w), 459(w), 431(w), 417(w) cm^{-1} (see Figure 3.27).

Anal. Calcd for **Na-15**: Na, 3.5; Sb, 3.7; W, 59.7; Yb, 2.7. Found: Na, 3.2; Sb, 3.7; W, 59.0; Yb, 2.8.

$Na_{10}[Lu(H_2O)_3Sb_2W_{21}O_{72}(OH)]\cdot 42H_2O$ (Na-16)

The same procedure as **Na-15** was followed, except for using 0.068 g $LuCl_3\cdot 6H_2O$. Yield: 0.022 g (4 %). IR data for **Na-16**: 953(s), 874(sh), 840(m), 806(s), 758(m), 660(m), 525(w), 517(w), 472(w), 459(w), 431(w), 417(w) cm^{-1} (see Figure 3.27). Anal. Calcd for **Na-16**: Na, 3.5; Sb, 3.8; W, 59.5; Lu, 2.7. Found: Na, 3.2; Sb, 3.8; W, 58.7; Lu, 3.2.

$Na_{10}[Y(H_2O)_3Sb_2W_{21}O_{72}(OH)]\cdot 40H_2O$ (Na-17)

The same procedure as **Na-15** was followed, except for using 0.044 g $YCl_3\cdot 6H_2O$. Yield: 0.033 g (6 %). IR data for **Na-17**: 953(s), 874(sh), 840(m), 806(s), 758(m), 660(m), 525(w), 517(w), 472(w), 459(w), 431(w), 417(w) cm^{-1} (see also Figure 3.27). Anal. Calcd for **Na-17**: Na, 3.6; Sb, 3.8; W, 60.6; Y, 1.4. Found: Na, 3.2; Sb, 3.8; W, 59.1; Y, 1.4.

Using Sb_2W_{22} precursor:

$Na_{10}[Yb(H_2O)_3Sb_2W_{21}O_{72}(OH)]\cdot 41H_2O$ (Na-15)

0.031 g (0.079 mmol) of $YbCl_3\cdot 6H_2O$ was added to 20 mL 1M $NaCl_{(aq)}$ with stirring followed by addition of 0.50 g (0.079 mmol) of $Na_{12}[Sb_2W_{22}O_{74}(OH)_2]$, and then the pH was adjusted to 5 with 1M NaOH. The solution was stirred at 50 ˚C for 30 min, allowed to cool to room temperature. The filtrate was kept in an open vial for crystallization. After about one week colorless crystals were obtained, which were filtered off and air dried (yield 0.40 g, 79 %). IR for **Na-15** showed metal-oxygen stretches at 953(s), 874(sh), 840(m), 806(s), 758(m), 660(m), 525(w), 517(w), 472(w), 459(w), 431(w), 417(w) cm^{-1} (see Figure 3.27). Anal. Calcd for **Na-15**: Na, 3.5; Sb, 3.7; W, 59.7; Yb, 2.7. Found: Na, 3.2; Sb, 3.7; W, 59.0; Yb, 2.8.

$Na_{10}[Lu(H_2O)_3Sb_2W_{21}O_{72}(OH)]\cdot 42H_2O$ (Na-16)

The same procedure as **Na-15** was followed, except for using 0.031 g $LuCl_3\cdot 6H_2O$. Yield: 0.38 g, 75 %. IR data for **Na-16**: 953(s), 874(sh), 840(m), 806(s), 758(m), 660(m), 525(w), 517(w), 472(w), 459(w), 431(w), 417(w) cm^{-1} (see Figure 3.27). Anal. Calcd for **Na-16**: Na, 3.5; Sb, 3.8; W, 59.5; Lu, 2.7. Found: Na, 3.2; Sb, 3.8; W, 58.7; Lu, 3.2.

$Na_{10}[Y(H_2O)_3Sb_2W_{21}O_{72}(OH)]\cdot 40H_2O$ (Na-17)

The same procedure as **Na-15** was followed, except for using 0.020 g $YCl_3\cdot 6H_2O$. Yield: 0.35 g (70 %). IR data for **Na-17**: 953(s), 874(sh), 840(m), 806(s), 758(m), 660(m), 525(w), 517(w), 472(w), 459(w), 431(w), 417(w) cm^{-1} (see also Figure 3.27). Anal. Calcd for **Na-17**: Na, 3.6; Sb, 3.8; W, 60.6; Y, 1.4. Found: Na, 3.2; Sb, 3.8; W, 59.1; Y, 1.4.

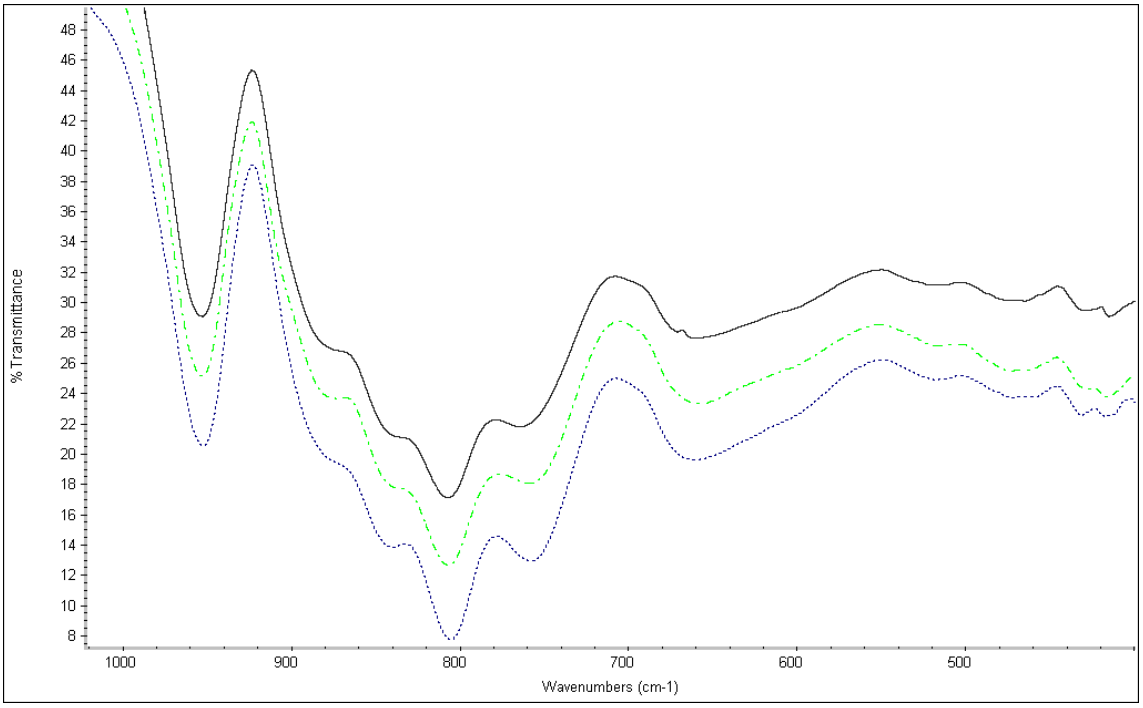

Figure 3.27. IR spectra of the three compounds **Na-15** (blue curve), **Na-16** (green curve), and **Na-17** (balck curve) (from bottom to top).

$Na_8[Yb_2(H_2O)_6(Sb_2W_{20}O_{70})]\cdot 37H_2O$ (Na-18)

0.068 g (0.175 mmol) of $YbCl_3\cdot 6H_2O$ was added to 20 mL 1M $NaCl_{(aq)}$ with stirring followed by addition of 0.50 g (0.175 mmol) of $Na_9[B\text{-}\alpha\text{-}SbW_9O_{33}]\cdot 19.5H_2O$, and then the pH was adjusted to 4.8 with 2M HCl. The solution was stirred at 50 ˚C for 30 min, allowed to cool to room temperature. The filtrate was kept in an open vial for crystallization. After about a week colorless crystals were obtained, which were filtered off and air dried (yield 0.24 g, 43 %). IR for **Na-18** showed metal-oxygen stretches at 951(s), 862(sh), 821(s), 771(m), 646(m), 527(w), 513(w), 494(w), 468(m), 421(m), 418(m) cm^{-1} (see Figure 3.28). Anal. Calcd for **Na-18**: Na, 2.9; Sb, 3.8; W, 57.9; Yb, 5.5. Found: Na, 2.4; Sb, 3.8; W, 56.0; Yb, 7.9. Therefore, the elemental analysis suggests the following formula: *$Na_{6.5}Yb_{0.5}[Yb_2(H_2O)_6(Sb_2W_{20}O_{70})]\cdot 37H_2O$.*

$Na_8[Lu_2(H_2O)_6(Sb_2W_{20}O_{70})]\cdot 38H_2O$ (Na-19)

The same procedure as **Na-18** was followed, except for using 0.068 g $LuCl_3\cdot 6H_2O$. Yield: 0.20 g (35 %). IR data for **Na-19**: 951(s), 862(sh), 821(s), 771(m), 646(m), 527(w), 513(w), 494(w), 468(m), 421(m), 418(m) cm^{-1} (see Figure 3.28). Anal. Calcd for **Na-19**: Na, 3.5; Sb, 3.8; W, 59.5; Lu, 2.7. Found: Na, 2.4; Sb, 3.8; W, 58.6; Lu, 3.2.

$Na_8[Y_2(H_2O)_6(Sb_2W_{20}O_{70})]\cdot 37\ H_2O$ (Na-20)

The same procedure as **Na-18** was followed, except for using 0.044 g $YCl_3\cdot 6H_2O$. Yield: 0.21 g (39 %). IR data for **Na-20**: 951(s), 862(sh), 821(s), 771(m), 646(m), 527(w), 513(w), 494(w), 468(m), 421(m), 418(m) cm^{-1} (see also Figure 3.28). Anal. Calcd for **Na-20**: Na, 2.98; Sb, 4.0; W, 59.5; Y, 2.9. Found: Na, 2.6; Sb, 4.1; W, 60.1; Y, 4.1. Therefore, the elemental analysis suggests the following formula: *$Na_{6.5}Y_{0.5}\ [Y_2(H_2O)_6(Sb_2W_{20}O_{70})]\cdot 37\ H_2O$.*
Elemental analyses were carried out by Zentralabteilung für chemische Analysen, Forschungszentrum Jülich GmbH, Jülich, Germany.

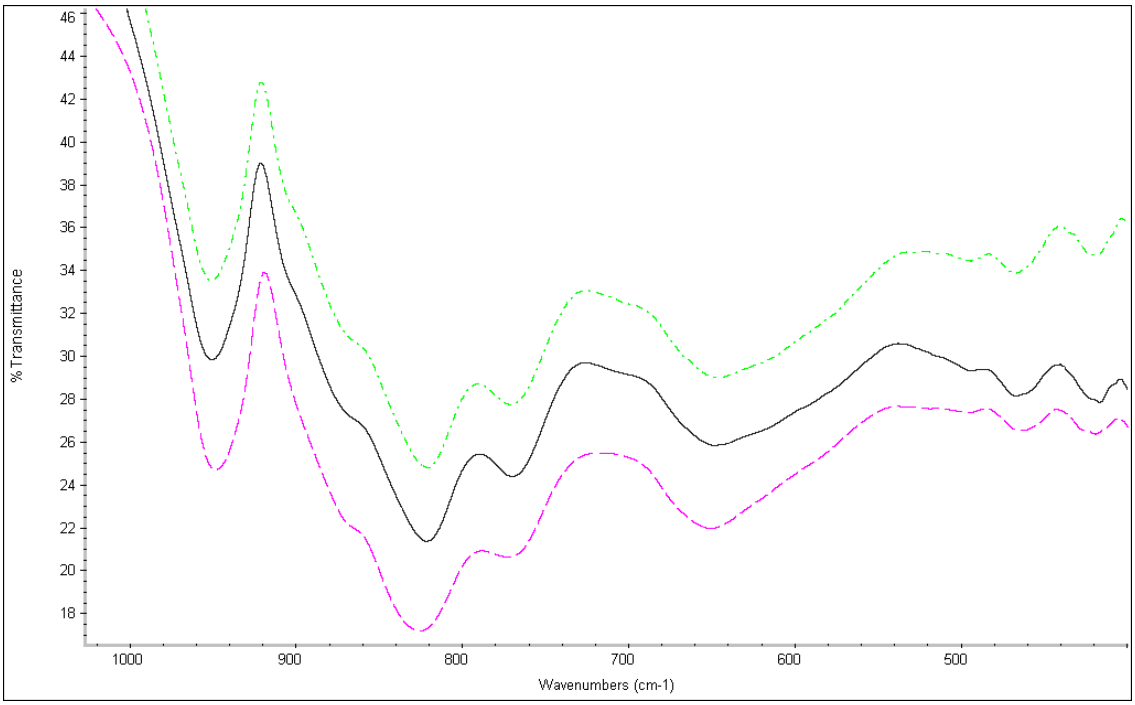

Figure 3.28. IR spectra of the three compounds **Na-18** (pink line), **Na-19** (balck line), and **Na-20** (green line) (from bottom to top).

3.B.2.3. X-ray Crystallography

The crystallographic data are summarized in Table 3.5 and 3.6.

Table 3.5. Crystal Data and Structure Refinement for Na-15 and **Na-16.**

Code	**Na-15**	**Na-16**
Emp. formula	$Na_{10}[Yb(H_2O)_3Sb_2W_{21}O_{72}(OH)]\cdot 41H_2O$	$Na_{10}[Lu(H_2O)_3Sb_2W_{21}O_{72}(OH)]\cdot 42H_2O$
M_r	6469.0	6489.0
Crystal system	triclinic	triclinic
Space group (no.)	$P\bar{1}$(2)	$P\bar{1}$(2)
a / Å	13.3196(8)	13.3368(18)
b / Å	18.1807(13)	18.198(2)
c/Å	23.8781(17)	23.895(3)
α / deg	107.974(3)	108.071(5)
ß/ deg	90.071(3)	90.048(5)
γ/ deg	108.460(3)	108.357(4)
V / Å^3	5185.6(6)	5201.5(12)
Z	2	2
T / ºC	-100	-100
λ / Å	0.71073	0.71073
D / g cm^{-3}	4.14	4.14
μ / mm^{-1}	24.8	24.7
$R\ [I \geq 2\sigma(I)]$[a]	0.0436	0.0510
R_w (all data)[b]	0.1545	0.1518

[a] $R = \sum||F_o| - |F_c|| / \sum|F_o|$; [b] $R_w = \{\sum[w(F_o^2 - F_c^2)^2] / \sum[w(F_o^2)^2]\}^{1/2}$.

Table 3.6. Crystal Data and Structure Refinement for **Na-18 – Na-20.**

Code	**Na-18**	**Na-19**	**Na-20**
Emp. formula	$Na_8[Yb_2(H_2O)_6Sb_2W_{20}O_{70}]\cdot 37H_2O$	$Na_8[Lu_2(H_2O)_6Sb_2W_{20}O_{70}]\cdot 37H_2O$	$Na_8[Yb_2(H_2O)_6Sb_2W_{20}O_{70}]\cdot 37H_2O$
M_r	6344.9	6367.1	6176.9
Crystal system	triclinic	triclinic	triclinic
Space group (no.)	$P\bar{1}$(2)	$P\bar{1}$(2)	$P\bar{1}$(2)
a / Å	13.510(3)	13.5753(7)	13.6116(7)
b / Å	13.516(3)	13.6389(8)	13.6742(8)
c/Å	14.290(2)	14.2889(7)	14.3433(7)
α / deg	106.174(11)	93.268(3)	93.180(3)
ß/ deg	93.469(12)	106.357(2)	106.647(3)
γ/ deg	106.313(13)	106.282(3)	106.078(4)
V / Å^3	2377.6(7)	2410.0(2)	2431.3(2)
Z	1	1	1
T / ºC	-100	-100	-100
λ / Å	0.71073	0.71073	0.71073
D / g cm^{-3}	4.16	4.39	4.22
μ / mm^{-1}	26.7	26.5	25.4
$R\ [I \geq 2\sigma(I)]$[a]	0.066	0.056	0.059
R_w (all data)[b]	0.1874	0.1782	0.1781

[a] $R = \sum||F_o| - |F_c|| / \sum|F_o|$; [b] $R_w = \{\sum[w(F_o^2 - F_c^2)^2] / \sum[w(F_o^2)^2]\}^{1/2}$.

3.B.2.4. Results and Discussion

We have synthesized and structurally characterized the mono- and di-lanthanide containing polyanions $[Ln(H_2O)_3Sb_2W_{21}O_{72}(OH))]^{10-}$ (**15–17**) and $[Ln_2(H_2O)_6Sb_2W_{20}O_{70})]^{8-}$ (**18 – 20**). The sodium salts of polyanions **15–20** $Na_{10}[Yb(H_2O)_3Sb_2W_{21}O_{72}(OH)]\cdot 41H_2O$ (**Na-15**), $Na_{10}[Lu(H_2O)_3Sb_2W_{21}O_{72}(OH)]\cdot 42H_2O$ (**Na-16**), $Na_{10}[Y(H_2O)_3Sb_2W_{21}O_{72}(OH)]\cdot 40H_2O$ (**Na-17**), $Na_8[Yb_2(H_2O)_6Sb_2W_{20}O_{70})]\cdot 37H_2O$ (**Na-18**), $Na_8[Lu_2(H_2O)_6Sb_2W_{20}O_{70})]\cdot 38H_2O$ (**Na-19**), and $Na_8[Y_2(H_2O)_6Sb_2W_{20}O_{70})]\cdot 37H_2O$ (**Na-20**) have been characterized in the solid state by FTIR spectroscopy, single-crystal XRD, TGA and elemental analyses. All polyanions **15–20** are based on the **Sb_2W_{20}** skeleton with one (**15–17**) or two (**18–20**) incorporated lanthanide ions.

The mono-lanthanide(III)-containing polyanions $[Ln(H_2O)_3Sb_2W_{21}O_{72}(OH))]^{10-}$ (Ln = Yb (**15**), Lu(**16**), Y(**17**)) were synthesized using simple and conventional open beaker conditions by interaction of the sodium salt of the trilacunary precursor **SbW_9** with Ln^{3+} ions in aqueous acidic (pH = 3) medium. A high concentration of NaCl (1.0 M) was needed in order to obtain the desired crystalline products. The same reaction performed in water did not result in any crystalline product. The presence of sodium ions in the synthesis medium is therefore crucial for the successful synthesis and isolation of polyanions **15–17**.

Interaction of the **SbW_9** precursor with transition metal ions at an appropriate pH is known to result in products based on two **SbW_9** subunits sandwiching either 3 ({M_3(α-SbW9)2}, "Hervé dimer") or 4 ({M_4(β-SbW9)2}, "Krebs dimer") transition metal ions.[3,4] For example, our group has reported the "Hervé dimer" for M = copper(II), zinc(II), manganese(II) and cobalt(II),[4c] palladium(II),[4g] and the "Krebs dimer" for M = iron(III),[4d] and indium(III).[4h] We have also isolated a dimethyltin-containing tungstoantimonate(III).[4m]

Polyanions **15**–**17** consist of two **SbW_9** subunits linked by two tungsten ions forming the **Sb_2W_{20}** unit, which is coordinated to an external lanthanide and tungsten ion, leading to a structure with idealized C_s symmetry (see Figure 3.29). This unique, external tungsten ion is six-coordinated, whereas the lanthanide ion is seven-coordinated in a pentagonal-bipyramidal fashion.

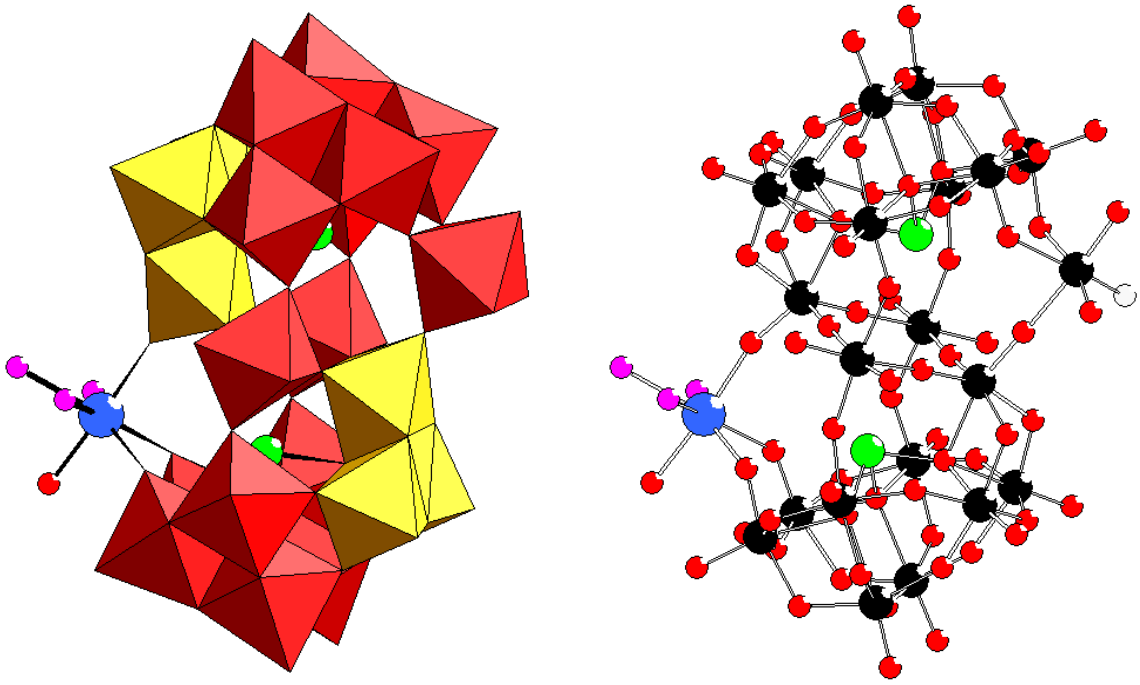

Figure 3.29. Polyhedral (left) and ball-and-stick (right) representations of $[Ln(H_2O)_3Sb_2W_{21}O_{72}(OH))]^{10-}$ (Ln = Yb (**15**), Lu(**16**), Y(**17**)). The color code is as follows: WO_6 octahedra (red), rotated WO_6 octahedra (yellow), W (black), Sb (green), Ln (blue), H_2O (pink), O (red), and OH (gray).

It is noteworthy that because of the high charge of the intermediate $[Sb_2W_{20}O_{70}]^{14-}$ **Sb_2W_{20}**, it tends to be stabilized by cations to form **$M_2Sb_2W_{20}$** or to undergo further condensation reactions to from **Sb_2W_{22}** polyanion, depending on the pH of the solution.[5] Interestingly, this intermediate **Sb_2W_{20}** unit in the presence of lanthanide ions and a lower pH value (~ 3) tends to undergo further condensation reaction forming a novel unit **Sb_2W_{21}** which coordinates to one lanthanide ion forming polyanions **15**–**17**. Furthermore, this structurally unique *fac*-WO_6 octahedron has one monoprotonated and two nonprotonated terminal oxo ligands, and hence does not violate the Lipscomb rule.[11]

In polyanions **15–17** the Ln^{3+} ion is bound to the two **SbW_9** subunits via three μ_2-oxo bridges, two bridges to one **SbW_9** unit and one bridge to the other unit through one WO_6 octahedral of the rotated triad (yellow in Figure 3.29). The lanthanide ion has three terminal aqua ligands. The coordination sphere of the lanthanide ion is completed through a Ln–O–W' bridge, where W' belongs to a neighbouring polyanion, leading to a dimer formation in the solid state (see Figure 3.30).

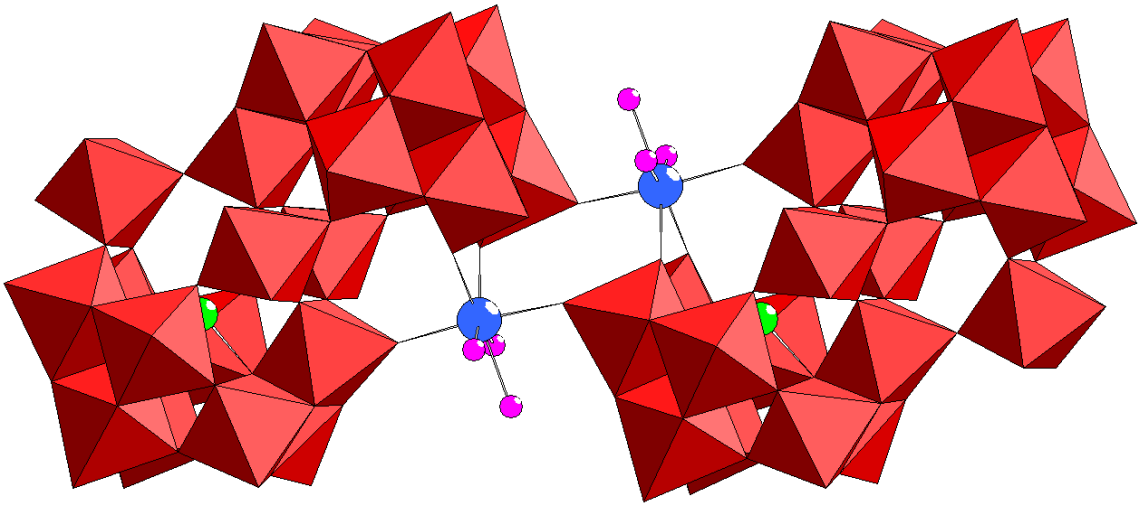

Figure 3.30. Polyhedral representation of **15–17** forming a dimer in the solid state. The color code is as follows: WO_6 octahedra (red), Sb (green), Ln (blue), H_2O (pink).

We checked for possible protonation of polyanions **15–17** by bond valence sum (BVS) calculations,[12] one monoprotonated oxygen was identified in the *fac*-WO_6 octahedral, (BVS ~ 0.99) (grey ball in Figure 3.19) and no additional protonation sites besides the terminal aqua ligands described above were identified. This results in an OH group for **15–17** and a total charge of –10 for the polyanions. It is noteworthy that the resulting protonation of one of the three terminal oxy ligand groups is most preferable to obey the Lipscomb rule.

The di-lanthanide(III) polyanions $[Ln_2(H_2O)_6Sb_2W_{20}O_{70})]^{8-}$ (Ln = Yb (**18**), Lu(**19**), Y(**20**)) were synthesized under mild, conventional conditions by interaction of the sodium salt of the trilacunary **SbW_9** with Ln^{3+} ions in aqueous acidic (pH = 5) medium. Interaction of

Sb_2W_{22} precursor with transition metal ions or organometallic species at a proper pH is known to result in disubstituted products based on the **Sb_2W_{20}** framework.[5,6] For example, our group has already reported species with the organo-Ru-supported tungstoantimonates $[Sb_2W_{20}O_{70}(RuL)_2]^{10-}$ (L = benzene, p-cymene)[6g] and organic–inorganic hybrid compounds based on dmso-coordinated heteropolytungstates.[6h]

A high concentration of NaCl (1.0 M) was also needed in order to obtain the desired crystalline products. The same reactions performed in water did not result in any crystalline product. The presence of sodium ions in the synthesis medium is therefore crucial for the successful synthesis and isolation of polyanions **15**–**20**.

Hence, the reaction procedures reported here were successful for the late lanthanide ions (Yb and Lu), and also for the early 4d metal ion yttrium. In contrast, the same synthetic procedures as **15**–**17** and **18**–**20** were tried for the early (La and Ce) and middle (Eu and Gd) lanthanide ions, but so far our attempts have not been successful.

Polyanions **18**–**20** consist of two **SbW_9** subunits sandwiching two tungsten ions forming **Sb_2W_{20}** unit which is coordinated to two lanthanide(III) ions leading to a structure with C_{2h} symmetry (see Figure 3.31). Hence this structure can be described as a dimeric molecular entity composed of two $\{LnSbW_{10}\}$ half units related by an inversion center. Each Ln^{3+} is linked to the **SbW_9** units through three μ_2-oxo bridges, two bridges to one **SbW_9** half-unit and one bridge to the other half-unit through one WO_6 octahedral of the rotated triad (yellow in Figure 3.31). The two lanthanide ions are seven-coordinated with an average Ln−O distance of 2.274(12) Å, resulting in a pentagonal-bipyramidal coordination geometry. Both lanthanide ions have three terminal aqua ligands each. The coordination sphere of each lanthanide ion is completed through a Ln–O–W' bridge, where W' belongs to a neighbouring polyanion, leading to an 1-D chain formation in the solid state (see Figure 3.32). BVS calculations indicate that no oxygen atoms of **18**–**20** are protonated.

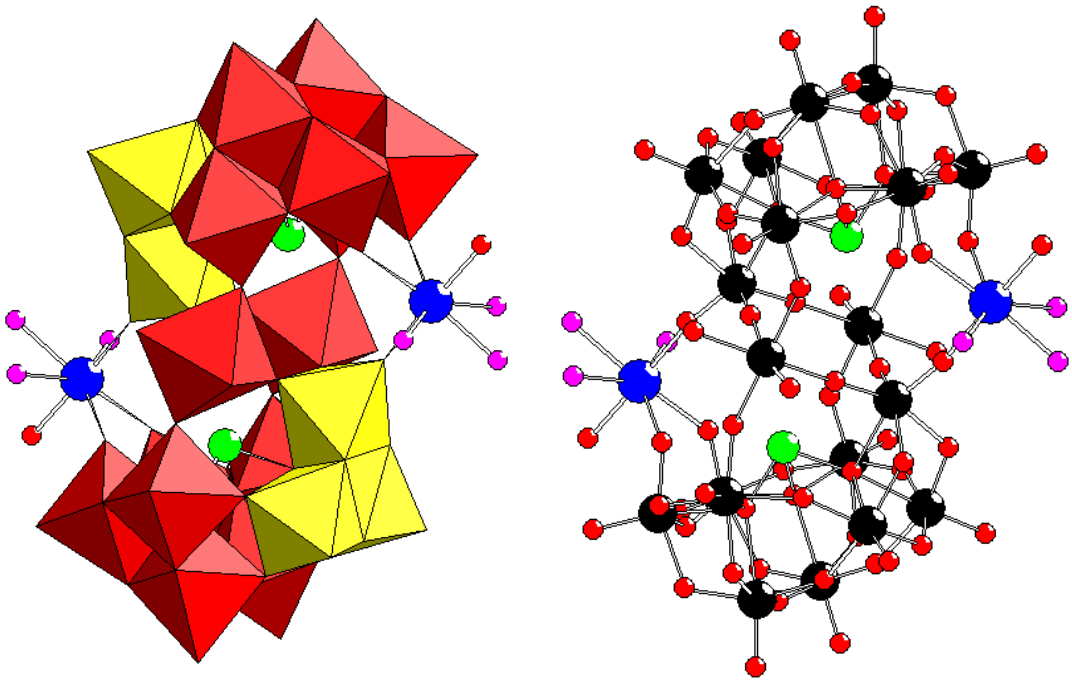

Figure 3.31. Polyhedral (left) and ball-and-stick (right) representation of $[Ln_2(H_2O)_6Sb_2W_{20}O_{70})]^{8-}$ (Ln = Yb (**18**), Lu(**19**), Y(**20**)). The color code is the same as in Figure 3.29.

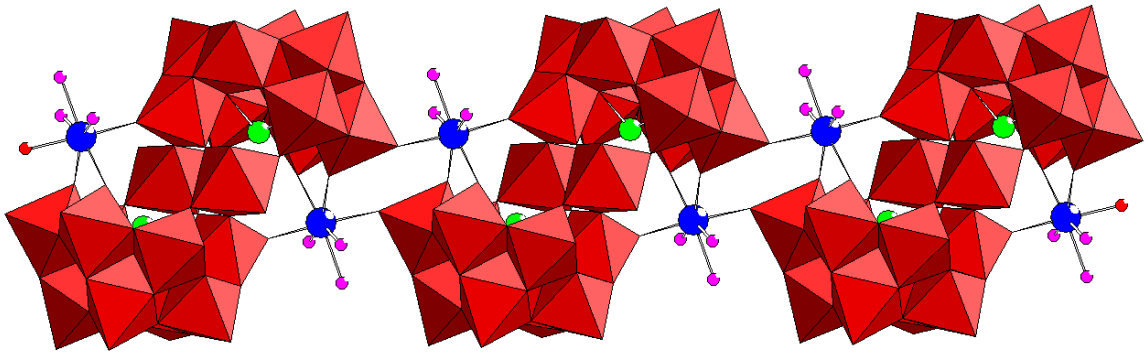

Figure 3.32. Polyhedral representation of polyanions **16-20** forming a 1D chain in the solid state. The color code is as follows: WO_6 octahedra (red), Sb (green), Ln (blue), H_2O (pink), O (red).

The two structures of polyanions **15**–**20** are very similar as both are based on the $\mathbf{Sb_2W_{20}}$ unit. The main difference lies in the composition and coordination to this $\mathbf{Sb_2W_{20}}$ unit in **15**–**17** is condensed by a WO_6 octahedral and coordinated to one lanthanide(III) ion while in **18**–**20** is coordinated to two lanthanide(III) ions. This can be rationalized by the fact that pH is the main parameter affects the syntheses of **15**–**17** and **18**–**20**. It is well known that the pH is a crucial parameter in POM synthesis in general.

Interestingly, when we followed the Krebs procedure,[5] to synthesize $\mathbf{Ln_2Sb_2W_{20}}$ instead of $\mathbf{M_2Sb_2W_{20}}$ using the $\mathbf{Sb_2W_{22}}$ precursor and the respective lanthanide salt instead of the d-transition salt, we did not get any crystalline product. Nevertheless, we have developed a synthetic approach which has led to obtain the desired crystalline products of **Na-15** – **Na-17** using the $\mathbf{Sb_2W_{22}}$ precursor with higher yields than using the $\mathbf{SbW_9}$ precursor. Several variations of the synthetic procedure with $\mathbf{Sb_2W_{22}}$ (pH, solvent, temperature, ratio) till polyanions **18**–**20** were obtained as well. However a high concentration of NaCl (1.0 M) and a pH value ~5 were needed in order to obtain the desired crystalline products of **Na-15** – **Na-20** using the $\mathbf{Sb_2W_{22}}$ precursor with ratios (1:1 and 1:2) to the lanthanide salts, respectively, based on FTIR and single-crystal XRD. This can be rationalized by the fact that ratio of the reagents is the main parameter affects the syntheses of **15**–**20** using the $\mathbf{Sb_2W_{22}}$ precursor.

Thermogravimetric analyses (TGA) were performed on the salts of **15**–**20** to determine the respective degree of hydration and the thermal stability. The thermograms of all six compounds showed the expected weight loss domain between 25 and 400 ºC corresponding to dehydration (lattice water molecules), see Figures 3.33 and 3.34. The degree of hydration was calculated for all compounds and gave a range of 40 – 42 water molecules per formula unit for **Na-15** – **Na-17** while 37– 38 for **Na-18** – **Na-20**.

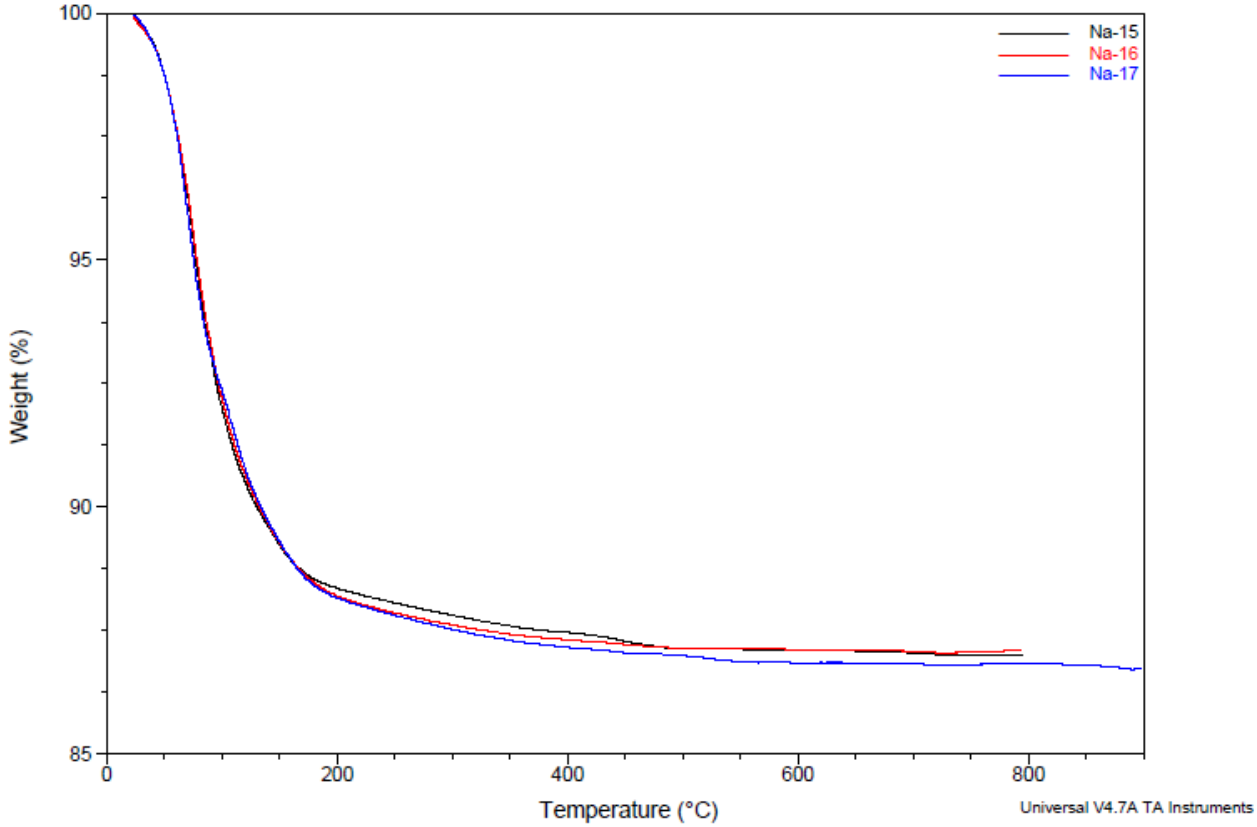

Figure 3.33. Thermograms of **Na-15** – **Na-17**.

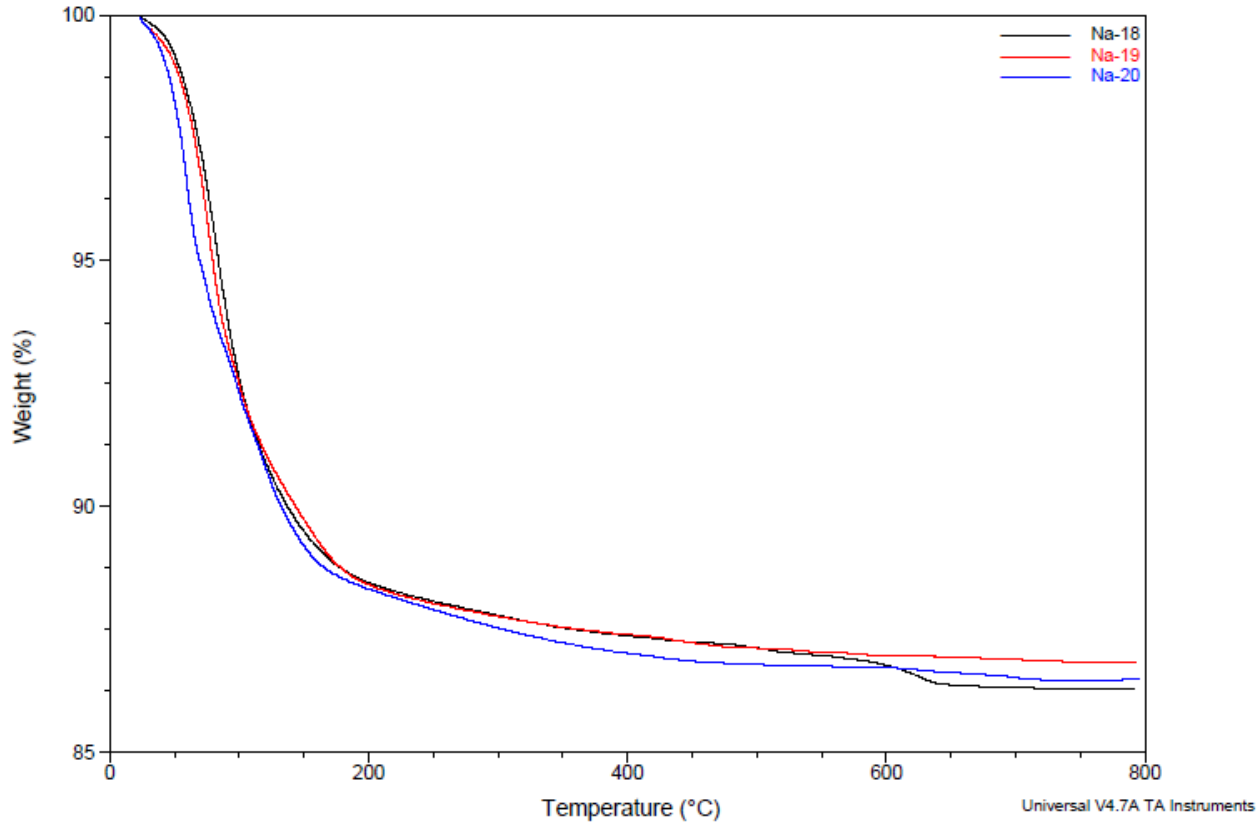

Figure 3.34. Thermograms of **Na-18** – **Na-20**.

We also decided to investigate the solution properties of the diamagnetic derivatives (Lu and Y analogues) by ^{183}W and ^{89}Y NMR spectroscopy. The experiments were carried out on **Na-16**, **Na-17**, **Na-19**, and **Na-20** redissolved in H_2O/D_2O. Many attempts were made to produce solution NMR spectra of the diamagnetic derivatives **16**, **17**, **19** and **20** (Lu and Y analogues). The major difficulty was the low solubility of the compounds, since a high concentration of the polyanion (> 0.1 M) is needed in order to get good signals in the ^{183}W NMR spectrum. Attempts to dissolve the compounds by heating eventually lead to partial decomposition of the polyanions and showed a less number (< 12) for both **16** and **17** (Figure 3.35 (a)), and a large number (> 6) peaks in the ^{183}W NMR spectra of **Na-19** (Figure 3.35 (b)), probably arising from a mixture of species in the solution. On the other hand, the ^{89}Y NMR spectrum for **17** showed a singlet at 19 ppm (Figure 3.36) which could not be assigned whether for the mono- or di-yttrium derivative of $\{Sb_2W_{22}\}$.

We also tried ion exchange using Li^+ loaded resin, which led eventually to the total dissolution of the compounds due to the replacement of the countercations with lithium. However, the ^{183}W NMR spectra for **16**, **17**, **19** and **20** were not conclusive and gave a less number (< 6) peaks. We speculate that the ion exchange method may have stripped the Lu^{3+} and Y^{3+} from the polyanion framework and thus lead to partial decomposition to various side products.

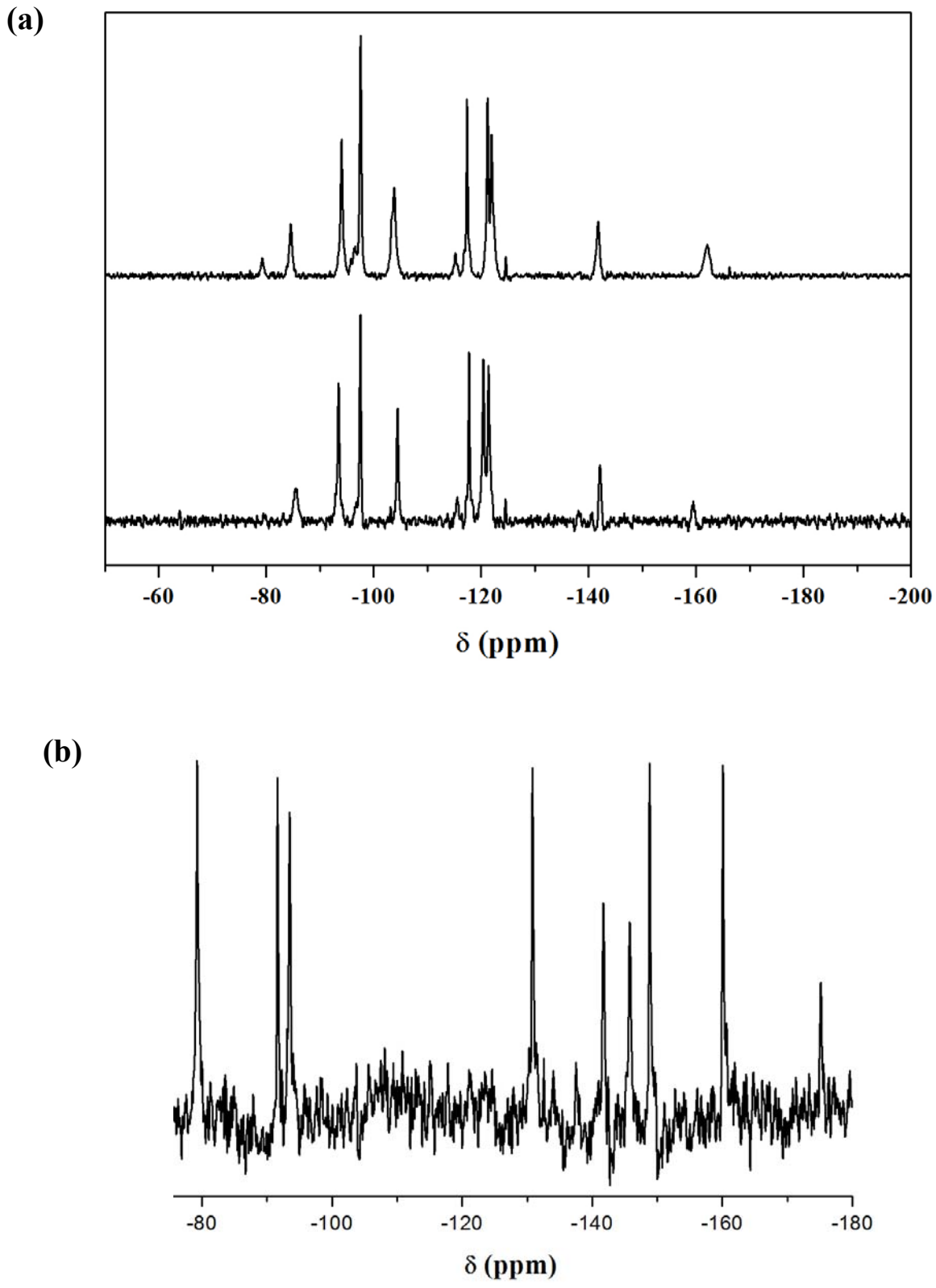

Figure 3.35. (a) Solution ^{183}W-NMR spectra of **Na-16 (**upper spectrum) and **Na-17** (lower spectrum)**,** and (b) **Na-19**, all redissolved in H_2O/D_2O. The spectra are not conclusive and may indicate decomposition of the polyanions.

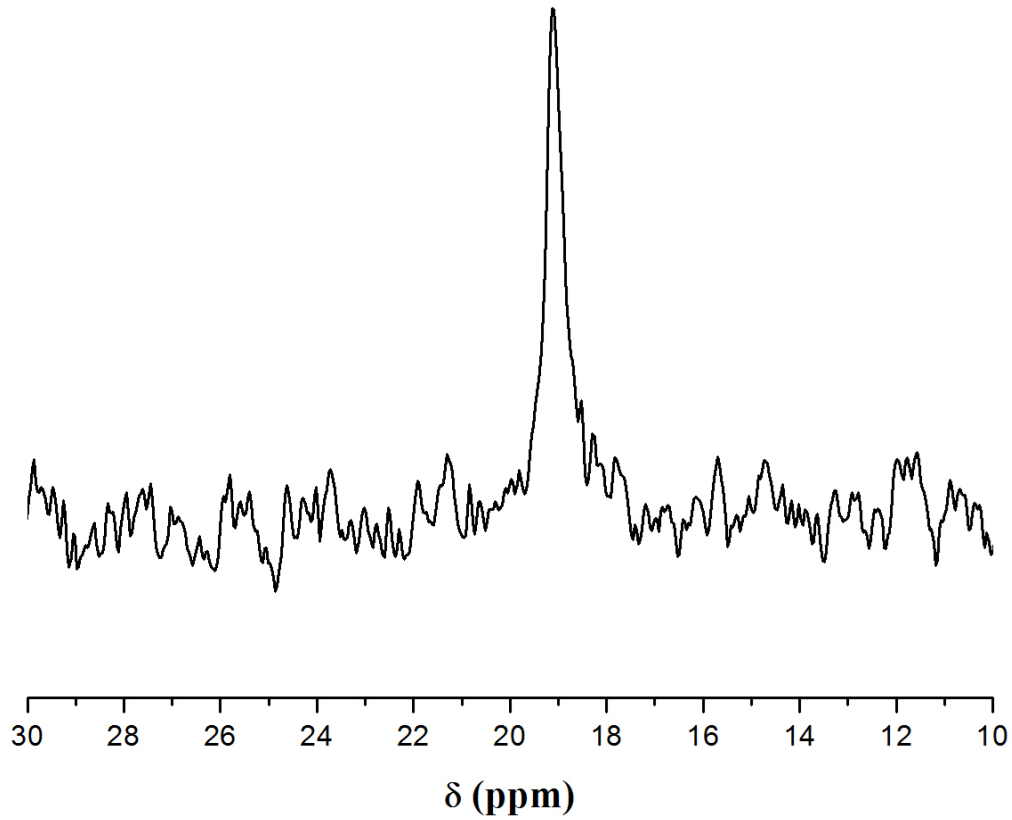

Figure 3.36. ^{89}Y-NMR of **Na-17** dissolved in H_2O/ D_2O.

3.B.2.5. Conclusions

The mono- and di-lanthanide(III) tungstoantimonates(III) $[Ln(H_2O)_3Sb_2W_{21}O_{72}(OH))]^{10-}$ (Ln = Yb (**15**), Lu(**16**), Y(**17**)) and $[Ln_2(H_2O)_6Sb_2W_{20}O_{70})]^{8-}$ (Ln = Yb (**18**), Lu(**19**), Y(**20**)) have been structurally characterized in the solid state by IR spectroscopy, single-crystal XRD, TGA and elemental analyses. Polyanions **15**–**20** were synthesized in simple, one-pot reactions of Ln^{3+} ions with the trilacunary polyanion precursor **SbW_9** or the **Sb_2W_{22}** precursor. Polyanions **15**–**20** crystallize as sodium salts in the triclinic system, space group $P\bar{1}$. The structure of **15**–**17** comprises the **Sb_2W_{20}** fragment with one incorporated Ln^{3+} ion, whereas two ions of **18**–**20**. Different synthetic strategies were needed to deliberately and selectively prepare mono- and di-lanthanide derivatives of **Sb_2W_{20}**. In this context it was the pH a crucial

parameter as well-known in the synthesis of polyoxometalates using the trilacunary polyanion precursor **SbW_9**. The terminal, labile water ligands in **15**–**20** are of interest for structural modifications and applications. We currently explore aqua ligand substitution for other mono- and polydentate exogenous ligands, including chiral ones, and we envision potential applications in Lewis acid catalysis. Efforts to isolate lipophilic salts of **15**–**20** in order to study their catalytic properties in organic media are also underway.

3.B.2.6. References

[1] a) M. T. Pope in *Heteropoly and Isopoly Oxometalates*, Springer-Verlag, Berlin, 1983; b) M. T. Pope, A. Müller, *Angew. Chem.,* **1991**, *103*, 56, *Angew. Chem., Int. Ed. Engl.* **1991**, *30*, 34; c) M. T. Pope, A. Müller in *Polyoxometalates: From Platonic Solids to Anti- Retroviral Activity* (Eds.: M. T. Pope, A. Müller), Kluwer: Dordrecht, The Netherlands, 1994; d) A. Müller, H. Reuter, S. Dillinger, *Angew. Chem.,* **1995**, *107*, 2505, *Angew. Chem., Int. Ed. Engl.* **1995**, *34*, 2328; e) C. Hill in *Polyoxometalates: Chemical Reviews*, 1998 (special thematic issue on polyoxometalates); f) M. T. Pope, A. Müller in *Polyoxometalate Chemistry: From Topology via Self-Assembly to Applications (*Eds.: M. T. Pope, A. Müller), Kluwer: Dordrecht, The Netherlands, 2001; g) T. Yamase, M. T. Pope in *Polyoxometalate Chemistry for Nano-Composite Design (*Eds.: T. Yamase, M. T. Pope), Kluwer: Dordrecht, The Netherlands, **2002**; h) D.-L. Long, E. Burkholder, L. Cronin, *Chem. Soc. Rev.* **2007**, *36*, 101; i) D.-L. Long, R. Tsunashima, L. Cronin, *Angew. Chem.* **2010**, *122*, 1780, *Angew. Chem. Int. Ed.* **2010**, *49*, 1736.

[2] a) E. V. Chubarova, M. H. Dickman, B. Keita, L. Nadjo, M. Mifsud, I. W. C. E. Arends, U. Kortz, *Angew. Chem.,* **2008**, *47*, 9542; b) N. V. Izarova, R. Ngo Biboum, B. Keita, M. Mifsud, I. W. C. E. Arends, G. B. Jameson, U. Kortz, *Dalton Trans.* **2009**, 9385; c) N. V. Izarova, M. H. Dickman, R. Ngo Biboum, B. Keita, L. Nadjo, V. Ramachandran, N. S. Dalal, U. Kortz,

Inorg. Chem. **2009**, *48*, 7504; d) N. V. Izarova, N. Vankova, T. Heine, R. Ngo Biboum, B. Keita, L. Nadjo, U. Kortz, *Angew. Chem.,* **2010**, *49*, 1886.

[3] C. Tourné, A. Revel, G. Tourné, M. Vendrell, *C. R. Acad. Sci. Ser. III* **1973**, *277*, 643.

[4] a) G. Wu, B.Y. Wang, M.Q. Cheng, P.J. Zheng, J.-P. Ding, Y.D. Gu, *Jiegon Huaxue* **1988**, *7*, 210; b) P. Mialane, J. Marrot, E. Riviere, J. Nebout, G. Herve, *Inorg. Chem.* **2001**, *40*, 44; c) U. Kortz, N.K. Al-Kassem, M.G. Savelieff, N.A. Al Kadi, M. Sadakane, *Inorg. Chem.* **2001**, *40*, 4742; d) U. Kortz, M. G. Savelieff, B. S. Bassil, B. Keita, L. Nadjo, *Inorg. Chem.* **2002**, 41, 783; e) M. Piepenbrink, D. Drewes, B. Krebs, *Private Commun.* **2002** , *2002*, 1; f) E. M. Limanski, D. Drewes, B. Krebs, *Z. Anorg. Allg. Chem.* **2004** , *630*, 523; g) L. H. Bi, M. Reicke, U. Kortz, B. Keita, L. Nadjo, R. J. Clark, *Inorg. Chem.* **2004**, *43*, 3915; h) F. Hussain, M. Reicke, V. Janowski, S. de Silva, J. Futuwi, U. Kortz, *Comptes Rendus Chim.* **2005**, *8*, 1045; i) D. Drewes, M. Piepenbrink, B. Krebs, *J. Clust. Sc.* **2006**, *17*, 361; j) A. Dolbecq, J. D. Compain, P. Mialane, J. Marrot, E. Riviere, F. Secheresse, *Inorg. Chem.* **2008**, *47*, 3371; k) L. Yinghong; M. Pengtao; W. Jingping, *J. Coord. Chem.* **2008**, *61*, 936; l) W. Jingping, M. Pengtao, L. Jie, N. Hongyu, N. Jingyang, *Chem. Asian J.* **2008**, *2008*, 822; m) S. Reinoso, M. H. Dickman, U. Kortz, *Eur. J. Inorg. Chem.* **2009**, 947.

[5] M. Boesing, I. Loose, H. Pohlmann, B. Krebs, *Chem. Eur. J.* **1997**, *3*, 1232.

[6] a) I. Loose, E. Droste, M. Bösing, H. Pohlmann, M. H. Dickman, C. Rosu, M. T. Pope, B. Krebs, *Inorg. Chem.* **1999**, *38*, 2688; b) D. Laurencin, R. Villanneau, P. Herson, R. Thouvenot, Y. Jeannin, A. Proust, *Chem. Commun.* **2005**, 5524; c) L. H. Bi, B. Li, L. X. Wu, *Inorg. Chem. Commun.* **2008**, *11*, 1184; d) L. H. Bi, B. Li, S. Bi, L. X. Wu, *J. Solid State Chem.* **2009**, *182*, 1401; e) L. H. Bi, B. Li, L. X. Wu, *J. Coord. Chem.* **2009**, *62*, 531; f) L. H. Bi, B. Li, Y. Y. Bao, L. X. Wu, *Inorg. Chim.Acta* **2009**, *362*, 1600; g) L.-H. Bi, G. Al-Kadamany, E. V. Chubarova, M. H. Dickman, L. Chen, D. S. Gopala, R. M. Richards, B. Keita, L. Nadjo, H. Jaensch, G. Mathys, U. Kortz, *Inorg. Chem.* **2009**, *48*, 10068; h) L.-H. Bi,

G.-F. Hou, S. Bi, Y.-Y. Bao, B. Li, L.-X. Wu, T. McCormac, S. S. Mal, M. H. Dickman, U. Kortz, *Eur. J. Inorg. Chem. 2009*, 5259.

[7] a) T. Yamase, H. Naruke, Y. Sasaki, *J. Chem. Dalton Trans.* **1990**, 1687; b) H. Naruke, T. Yamase, Bull. Chem. Soc. Jpn. **2002**, *75*, 1275; c) G. Xue, J. Vaissermann, P. Gouzerh, *J. Clust. Sci.* **2002**, *13*, 409.

[8] a) S. Bareyt, S. Piligkos, B. Hasenknopf, P. Gouzerh, E. Lacôte, S. Thorimbert, M. Malacria, *J. Am. Chem. Soc.* **2005**, *127*, 6788; b) C. Boglio, G. Lemiére, B. Hasenknopf, S. Thorimbert, E. Lacôte, M. Malacria, *Angew. Chem.,* **2006**, *118*, 3402, *Angew. Chem., Int. Ed. Engl.* **2006**, *45*, 3324; c) C. Boglio, G. Lenoble, C. Duhayon, B. Hasenknopf, R. Thouvenot, C. Zhang, R. C. Howell, B. P. Burton-Pye, L. C. Francesconi, E. Lacôte, S. Thorimbert, M. Malacria, C. Afonso, J.-C. Tabet, *Inorg. Chem.* **2006**, *45*, 1389; d) C. Boglio, K. Micoine, R. Rémy, B. Hasenknopf, S. Thorimbert, E. Lacôte, M. Malacria, C. Afonso, J.-C. Tabet, *Chem. Eur. J.* **2007**, *13*, 5426; e) K. Micoine, B. Hasenknopf, S. Thorimbert, E. Lacôte, M. Malacria, *Org. Lett.* **2007**, *9*, 3981; f) E. Derat, E. Lacôte, B. Hasenknopf, S. Thorimbert, M. Malacria, *J. Phys. Chem. A* **2008,** *112,* 13002; g) C. Boglio, K. Micoine, E. Derat, R. Thouvenot, B. Hasenknopf, S. Thorimbert, E. Lacôte, M. Malacria, *J. Am. Chem. Soc.* **2008**, *130*, 4553.

[9] a) U. Kortz, C. Holzapfel, M. Reicke, *J. Mol. Struct.* **2003**, *656*, 93; b) U. Kortz, *J. Clust. Sci.* **2003**, *14*, 205; c) B. S. Bassil, M. H. Dickman, B. Kammer, U. Kortz, *Inorg. Chem.* **2007**, *46*, 2452; d) B. S. Bassil, M. H. Dickman, I. Römer, B. Kammer, U. Kortz, *Angew. Chem.,* **2007**, *119*, 6305, *Angew. Chem., Int. Ed. Engl.* **2007**, *46*, 6192; e) A. H. Ismail, M. H. Dickman, U. Kortz, *Inorg. Chem.* **2009**, *48,* 1559; f) A. H. Ismail, B. S. Bassil, A. Suchopar, U. Kortz, *Eur. J. Inorg. Chem.* **2009**, 5247.

[10] A. H. Ismail, B. S. Bassil, I. Römer, N. C. Redeker, U. Kortz, *Z. Naturforsch. B*, **2010**, *65b*, 383.

[11] W. N. Lipscomb, *Inorg. Chem.* **1965**, *4*, 132.

[12] D. Altermatt, I. D. Brown, *Acta. Crystallogr.* **1985**, *B41*, 244.

3.B.3. Lanthanide Substituted Polyoxoanions Containing Bridging Acetate Ligand: $[\{Ln(\mu\text{-}CH_3COO)(H_2O)_2(GeW_{11}O_{39})\}_2]^{12-}$ (Ln = Eu, Gd, Lu)

3.B.3.1. Introduction

Polyoxometalates (POMs) represent a unique class of inorganic compounds due to the structural variety as well as interesting and often unexpected properties in fields as diverse as catalysis, medicine and magnetochemistry.[1] Although the first synthetic POM is known since 1826, the mechanism of POM formation is still not well understood and is commonly described as a self-assembly. Nevertheless the synthesis of polyoxometalates is mostly rather simple and straightforward, once the proper reaction conditions have been identified.

Lacunary polyoxometalates are usually synthesized from complete precursor ions by loss of one or more MO_6 octahedra. It has been shown that interaction of rare-earth metals with lacunary polyoxoanion precursors has been investigated predominantly by Pope and Francesconi and some structures have been identified.[2] Most lanthanide-containing polyoxoanions are composed of monolacunary Keggin and Wells–Dawson fragments (e.g., $[La(\alpha\text{-}SiW_{11}O_{39})(H_2O)_3]^{5-}$, $[\{Ce(H_2O)_4([\alpha_1\text{-}P_2W_{17}O_{61})\}_2]^{14-}$, $[\{Eu(H_2O)_3([\alpha_2\text{-}P_2W_{17}O_{61})\}_2]^{14-}$). The monolacunary Keggin and Wells–Dawson derivatives can be considered as pentadentate ligands, but close inspection of the structures of the above species indicates that the lanthanide ions are too big to enter the respective vacancies fully. They usually sit somewhat above the lacunary hole and are coordinated to the four equatorial oxo-donors of the polyoxoanion ligands. The coordination sphere is usually completed in solution by terminal water molecules, but these monomeric species have a strong tendency to dimerize upon crystallization.[2c]

Here we report the synthesis of three head-on complexes of germanotungstates [{Ln(μ-$CH_3COO)(H_2O)_2(\alpha$-$GeW_{11}O_{39})\}_2]^{12-}$ (Ln = Eu (**21**), Gd (**22**), Lu(**23**)). All polyanions **21**–**23** were structurally characterized by single-crystal X-ray diffraction, FTIR spectroscopy, thermogravimetric analysis (TGA), and multinuclear NMR spectroscopy (^{183}W, ^{13}C and ^{1}H) for the diamagnetic analogue (Lu(**23**)).

3.B.3.2. Synthesis

The precursors $K_6Na_2[\alpha$-$GeW_{11}O_{39}]\cdot 13H_2O$ and $K_8Na_2[A$-α-$GeW_9O_{34}]\cdot 25H_2O$ used for the synthesis of the reported species were synthesized according to the published procedures.[3]

$K_{12}[(Eu(GeW_{11}O_{39})(H_2O))_2(\mu$-$CH_3COO)_2]\cdot 24H_2O$ (K-21)

0.064 g of $EuCl_3\cdot 6H_2O$ was dissolved in 20 mL of 1M potassium acetate buffer at pH 4.8, followed by the addition of 0.50 g of $K_8Na_2[A$-α-$GeW_9O_{34}]\cdot 25H_2O$. Then, the solution was stirred and heated to 90 °C for 30 minutes. The solution was allowed to cool to room temperature and then filtered. Slow evaporation of the solvent at room temperature for about three days led to the formation of colorless crystals suitable for X-ray diffraction. These crystals were isolated and air-dried (yield 0.68 g, 63 %). IR data for **K-21**: 1625(m), 1530(m), 1459(m), 1397(w), 1351(sh), 950(s), 893(s), 809(s), 779(sh), 746(w), 678(s), 615(sh), 526(m), 497(sh), 466(m), 446(w) cm^{-1} (see Figure 3.37). Anal. Calcd for **K-21**: K, 6.9; Ge, 2.1; W, 59.5; Eu, 4.5; C, 0.71; H, 0.86. Found: K, 6.6; Ge, 2.1; W, 60.2; Eu, 4.5; C, 0.75; H, 0.86.

$K_{12}[(Gd(GeW_{11}O_{39})(H_2O))_2(\mu$-$CH_3COO)_2]. 24H_2O$ (K-22)

The same procedure as **K-21** was followed, except for using 0.063 g $GdCl_3\cdot 6\ H_2O$. Yield: o.671 g (62%). IR data for **K-22**: 1625(m), 1530(m), 1459(m), 1397(w), 1351(sh), 950(s), 893(s), 809(s), 779(sh), 746(w), 678(s), 615(sh), 526(m), 497(sh), 466(m), 446(w) cm^{-1} (see Figure 3.37). Anal. Calcd for **K-22**: K, 6.9; Ge, 2.1; W, 59.9; Gd, 4.6; C, 0.71; H, 0.85. Found: K, 6.8; Ge, 2.1; W, 61.2; Gd, 4.6; C, 0.76; H, 0.84.

$K_8Cs_3Na[(Lu(GeW_{11}O_{39})(H_2O))_2(\mu\text{-}CH_3COO)_2]\cdot 18H_2O$ (KCsNa-23)

The same procedure as **KCsNa-21** was followed, except for using 0.067 g $LuCl_3\cdot 6\ H_2O$ and adding of 0.5 mL of 0.5M $CsCl_{(aq)}$ to the filtrate. Yield: 0.763 g (55 %). IR data for **KCs-23**: 1625(m), 1530(m), 1459(m), 1397(w), 1351(sh), 950(s), 893(s), 809(s), 779(sh), 746(w), 678(s), 615(sh), 526(m), 497(sh), 466(m), 446(w) cm^{-1} (see Figure 3.37). Anal. Calcd for **KCsNa-23**: K, 4.5; Na, 0.33; Cs, 5.6; Ge, 2.1; W, 57.5; Lu, 5.1; C, 0.69; H, 0.72. Found: K, 4.5; Na, 0.1; Cs, 5.2; Ge, 2.1; W, 60.2; Lu, 5.1; C, 0.75; H, 0.73.

For the compounds **K-21** – **KCsNa-23**, the bands in the range from 1000 – 400 cm^{-1} represent the fingerprint region of the polyoxometalate ligand, while the region from 1351 – 1530 cm^{-1} correspond to the acetate ligands bridged to the metal centers (Figure 3.37).[1a,4]

Elemental analyses were carried out by Zentralabteilung für chemische Analysen, Forschungszentrum Jülich GmbH, Jülich, Germany.

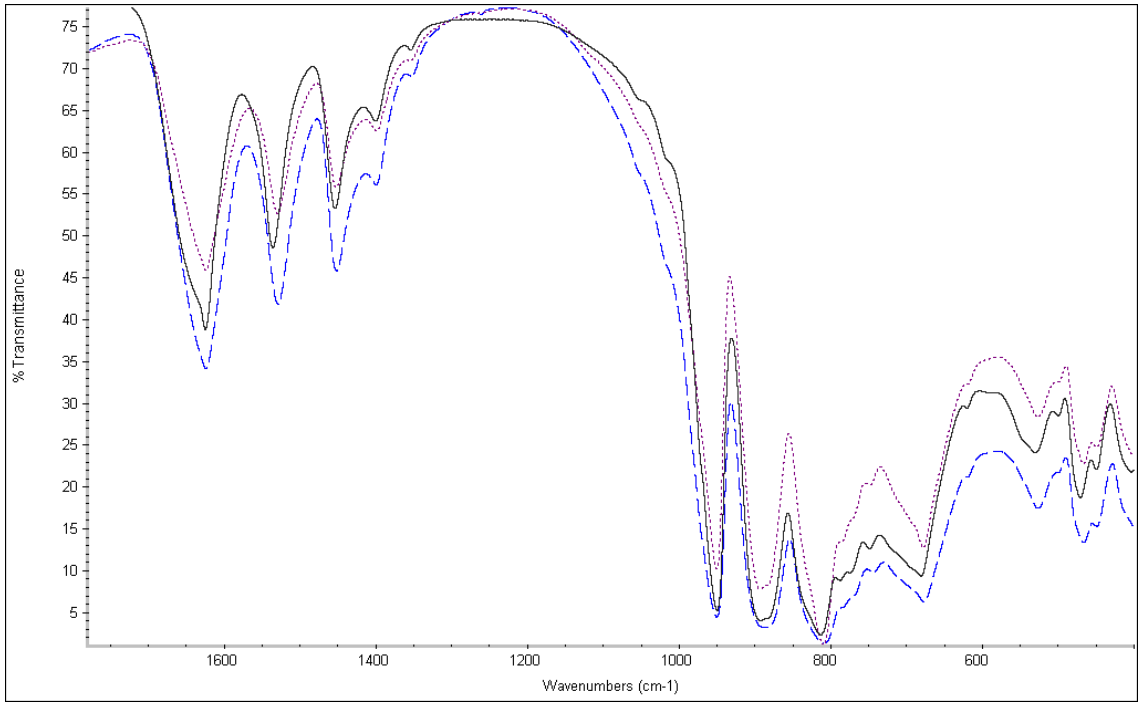

Figure 3.37. IR spectra of the **K-21** (blue line), **K-22** (balck line), and **KCsNa-23** (red line) (from bottom to top).

3.B.3.3. X-ray Crystallography

The crystallographic data are summarized in Table 3.7.

Table 3.7. Crystal Data and Structure Refinement for **K-22 – KCsNa-23**.

Code	**K-22**	**KCsNa-23**
Empirical formula	$H_{50}C_4Gd_2Ge_2O_{98}W_{22}K_{12}$	$H_{50}C_4Lu_2Ge_2O_{98}W_{22}K_{12}Cs_3Na$
MW	6561.8	8543.0
Crystal system	Monoclinic	Monoclinic
Space group (no.)	$P2_1/c$	$P2_1/c$
a/Å	19.996(5)	19.793(2)
b/Å	12.612(3)	12.5836(12)
c/Å	21.047(4)	20.952(2)
α/°	90	90
β/°	110.922(8)	111.983(5)
γ/°	90	90
V/Å^3	4957.7(19)	4839.0(9)
Z	2	2
T/ ºC	-100	-100
λ/Å	0.71073	0.71073
D/ Mg m^{-3}	4.396	5.863
μ/ mm^{-1}	27.85	30.05
R[I >2sigma(I)][a]	0.058	0.038
R_w (all data)[b]	0.142	0.121

[a] $R = \sum||F_o| - |F_c|| / \sum|F_o|$. [b] $R_w = \{\sum[w(F_o^2 - F_c^2)^2] / \sum[w(F_o^2)^2]\}^{1/2}$.

3.B.3.4. Results and Discussion

The lanthanide(III)-substituted polyoxoanions $[\{Ln(\mu\text{-}CH_3COO)(H_2O)_2(\alpha\text{-}GeW_{11}O_{39})\}_2]^{12-}$ (Ln = Eu (**21**), Gd (**22**), Lu(**23**)) consist of two $(\alpha\text{-}GeW_{11}O_{39})^{8-}$ fragments connected by a lanthanide-acetate dimer, $(Ln_2(\mu\text{-}CH_3COO)_2(H_2O)_4)^{4+}$ resulting in a head-on, trans-oid dimer with C_i symmetry (Figure 3.38). The $(\alpha\text{-}GeW_{11}O_{39})^{8-}$ entity acts as a tetradentate ligand. Each Ln^{3+} ion is eight-coordinated with a distorted square-antiprismatic geometry. Four of the eight oxo ligands are provided by the monolacunary Keggin fragment, three are from acetate groups and one is terminal water molecule. The acetate molecules are bound to the lanthanide ions in a rather peculiar fashion. Each carboxylate function contributes one oxo atom as a μ_3-bridging ligand (two Ln and one C atom) and the second oxo atom as a μ_2-bridging ligand (one Ln and one C atom). Polyanions **21**–**23** represent an example of a lanthanide substituted polyoxoanion that dimerizes via two incorporated rare earth atoms.

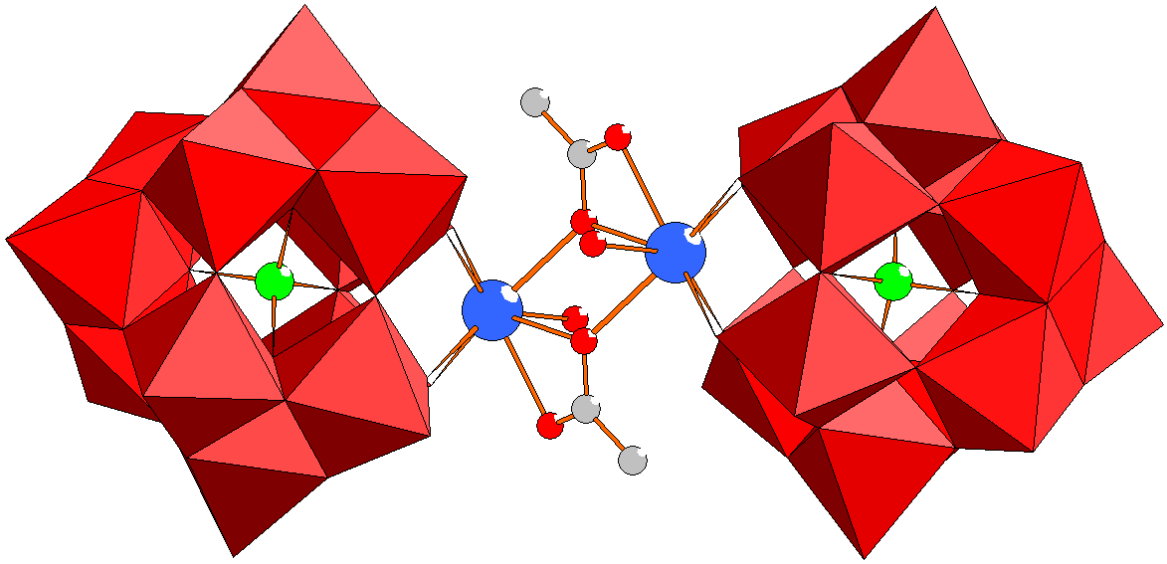

Figure 3.38. Combined polyhedral/ball-and-stick representation of $[\{Ln(\mu\text{-}CH_3COO)(H_2O)_2(\alpha\text{-}GeW_{11}O_{39})\}_2]^{12-}$ (**21**–**23**). The color code is as follows: WO_6 octahedra (red), Ge (green), Ln (blue), H_2O (pink), O (red). No hydrogen atoms shown.

This connectivity type of the acetate ligands to the lanthanide centres was first reported by our group for the lanthanum-containing Wells-Dawson dimer $[\{La(CH_3COO)(H_2O)_2(\alpha_2\text{-}P_2W_{17}O_{61})\}_2]^{16-}$ which consists of two monolacunary Wells-Dawson α_2-$\mathbf{P_2W_{17}}$ fragments connected by a lanthanum-acetate dimer, $(La_2(CH_3COO)(H_2O)_4)^{4+}$. Each La^{3+} ion is nine-coordinated in a monocapped, square-antiprismatic fashion.[5a] Later Mialane et al. synthesized the $[\{Ln(CH_3COO)(H_2O)_2(\alpha\text{-}SiW_{11}O_{39})\}_2]^{12-}$ (Ln = Gd^{3+} and Yb^{3+}) type.[5b] In analogy to **21**–**23** the Ln atoms are also eight-coordinated and have a distorted square-antiprismatic geometry. The average distance between the two lanthanide atoms in **21**–**23** is ca. 4.11 Å and the Ln–O–Ln bridging angle is 115.76°. The average bond distances around the lanthanide centers in **21**–**23** can be grouped as follows: Ln–O(W) = 2.24 – 2.31 Å, Ln–Oμ_3 (C) = 2.42 – 2.51 Å, La–Oμ_2(C) = 2.41 – 2.51 Å, and La–OH_2 = 2.33 – 2.44 Å. The average bond lengths and angles of the Keggin fragment are not unusual.

Interestingly synthesis of **21**–**23** was accomplished by reaction of Ln^{3+} ions with the tri- or monovacant Keggin precursor ($[A\text{-}\alpha\text{-}GeW_9O_{34}]^{10-}$, $[\alpha\text{-}GeW_{11}O_{39}]^{8-}$). Considering that our reaction was carried out at pH 4.8 and 90°C it is not entirely unexpected that we obtained the monolacunary Keggin fragment in our product. We were also able to synthesize other lanthanide analogues of **21**–**23**, namely $[\{Ln(\mu\text{-}CH_3COO)(H_2O)_2(\alpha\text{-}GeW_{11}O_{39})\}_2]^{12-}$ (Ln = Nd, Sm, Dy, Yb), based on the FTIR studies.

Thermogravimetric analyses (TGA) were performed on the salts of **21**–**23** to determine the respective degree of hydration and the thermal stability. The thermograms of all three compounds showed the expected weight loss domain between 25 and 400 ºC corresponding to dehydration (lattice water molecules), see Figure 3.39. The degree of hydration was calculated for all compounds and gave 24 water molecules per formula unit for **K-21** and **K-22** while 18 for **KCsNa-23**.

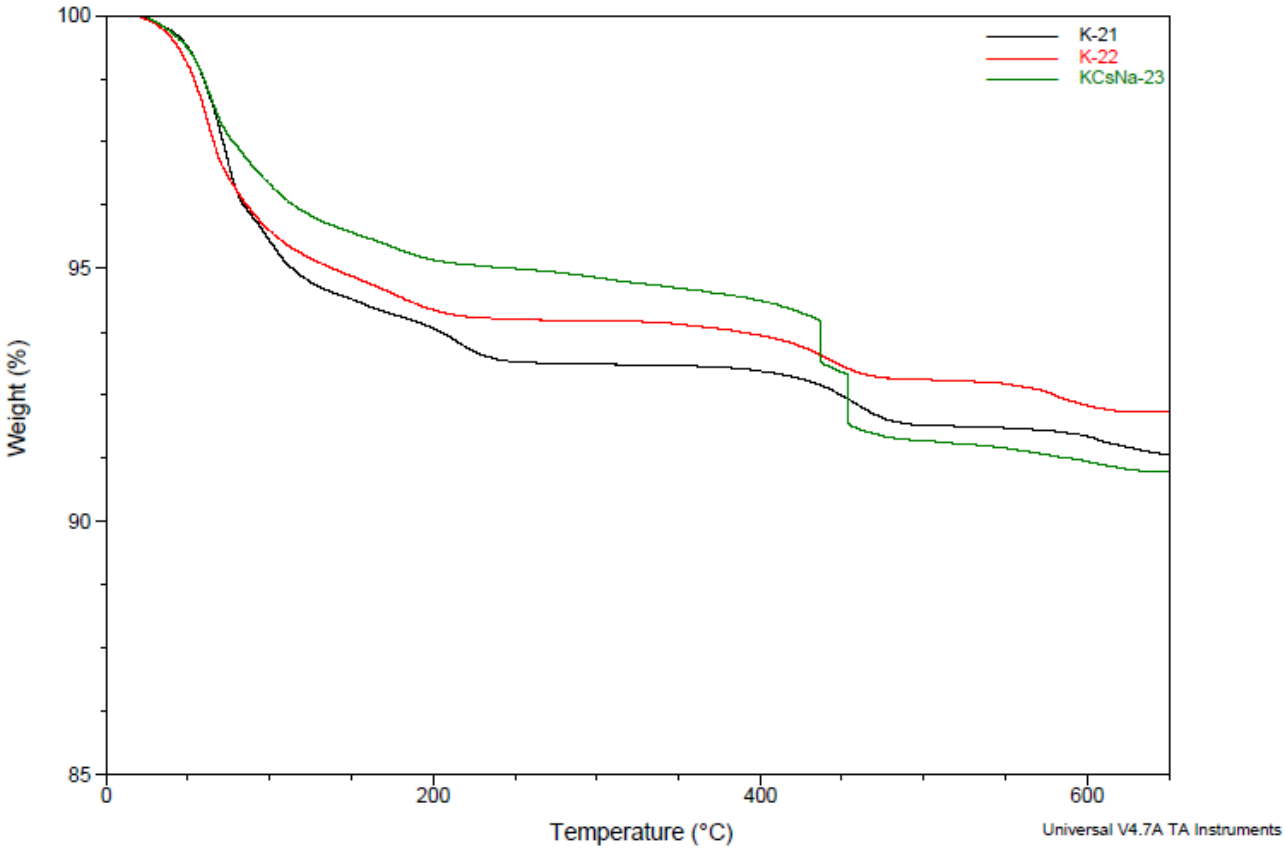

Figure 3.39. Thermograms of **K-21** – **KCsNa-23**.

The diamagnetic derivative (Lu analogue) allows us to investigate the stability of the polyanion **23** in solution by ^{183}W, ^{13}C NMR and ^{1}H NMR spectroscopy. The samples of the **KCsNa-23** were redissolved in H_2O/D_2O to perform^{183}W and ^{13}C NMR while in D_2O to perform ^{1}H NMR spectroscopy. The ^{183}W NMR spectrum shows six separated peaks in an intensity ratio of 4:4:2:4:4:4 (see Figure 3.40) at -74.9, -85.5, -100.6, -111.2, -142.5, -148.7 ppm. The ^{13}C NMR spectrum of polyanion **23** shows two signals at 23.2 and 181.3 ppm (see Figure 3.41), which is similar to the ^{13}C NMR spectrum of [{Y(R-$SbW_9O_{31}(OH)_2)(CH_3COO)(H_2O)\}_3(WO_4)]^{17-}$,[6] and the ^{1}H NMR spectrum shows a singlet at 1.7 ppm (see Figure 3.42). Addition of free acetate to the polyanion solution did not result in additional ^{13}C or ^{1}H NMR signals, indicating that the acetate linkers in the polyanion appear to be labile. As a result the dimeric structure of **23** is expected to break down and the observed NMR spectra may indeed correspond to the monomeric decomposition product. Other

techniques (e.g. mass spectrometry) are needed to confirm this point. The situation is probably analogous for the structural analogue $[\{Y(\mu\text{-}CH_3COO)(H_2O)_2(\alpha\text{-}GeW_{11}O_{39})\}_2]^{12-}$.[7]

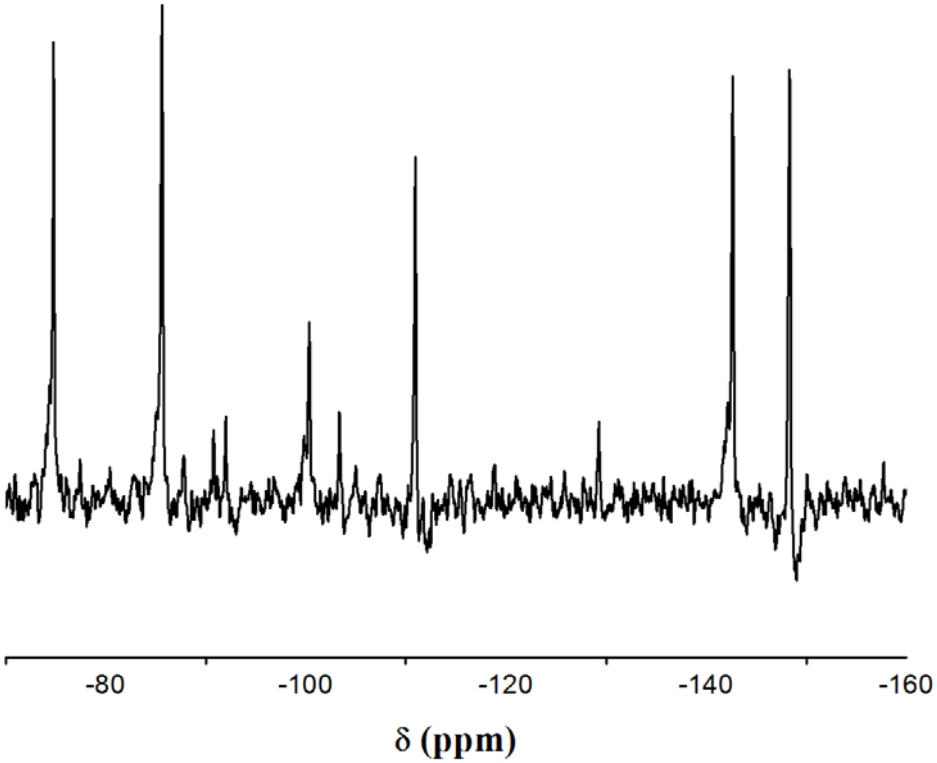

Figure 3.40. ^{183}W-NMR spectrum of **KCsNa-23** dissolved in H_2O/D_2O.

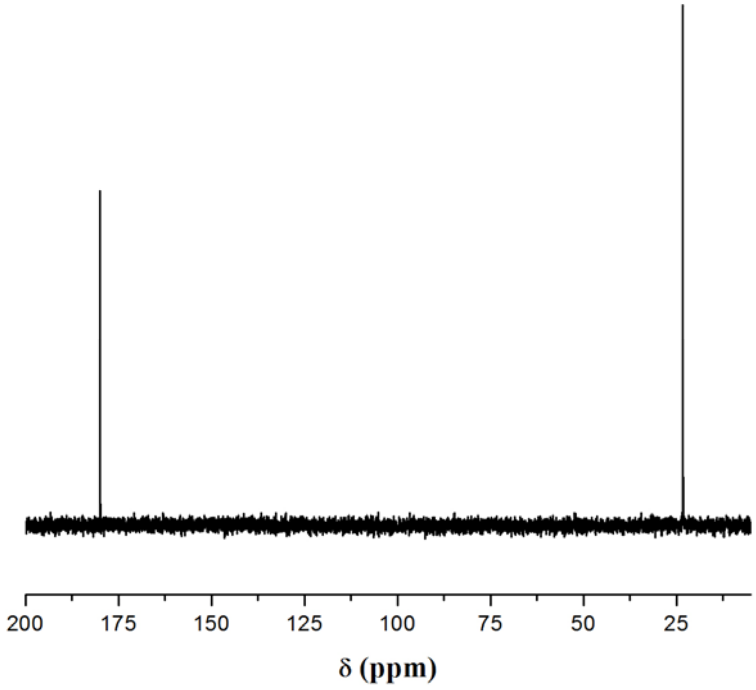

Figure 3.41. ^{13}C-NMR spectrum of **KCsNa-23** dissolved in H_2O/D_2O.

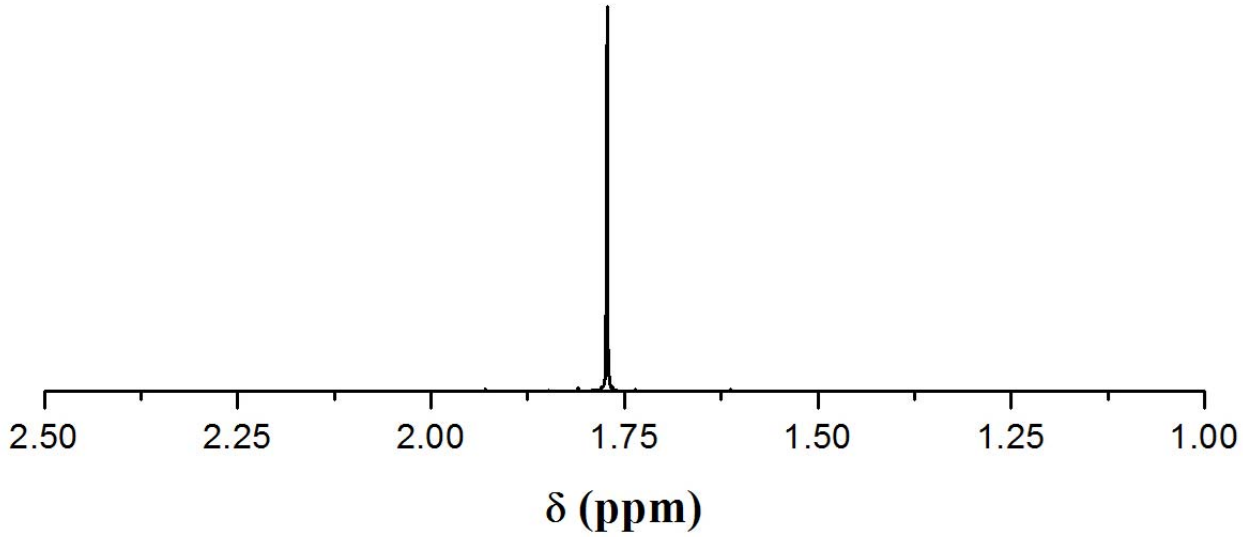

Figure 3.42. ^{1}H-NMR spectrum of **KCsNa-23** dissolved in D_2O.

3.B.3.5. Conclusions

The lanthanide-substituted polyoxometalates $[\{Ln(\mu\text{-}CH_3COO)(H_2O)_2(\alpha\text{-}GeW_{11}O_{39})\}_2]^{12-}$ (Ln = Eu (**21**), Gd (**22**), Lu(**23**)) have been synthesized and characterized by IR spectroscopy and elemental analysis. Single-crystal X-ray analyses were carried out on the potassium salts of **21** and **22** while on the mixed-potassium cesium of **23**. The head-on dimer **21**–**23** consist of two $(\alpha\text{-}GeW_{11}O_{39})^{8-}$ fragments connected by a lanthanide-acetate dimer, $(Ln_2(\mu\text{-}CH_3COO)_2(H_2O)_4)^{4+}$. Each Ln^{3+} ion is eight-coordinated in a distorted square-antiprismatic fashion. The solution properties of the diamagnetic derivatives (Lu analogue) by ^{183}W, ^{13}C NMR and ^{1}H NMR spectroscopy were also investigated.

3.B.3.6. References

[1] a) M. T. Pope in *Heteropoly and Isopoly Oxometalates*, Springer-Verlag, Berlin, 1983; b) M. T. Pope, A. Müller, *Angew. Chem.,* **1991**, *103*, 56, *Angew. Chem., Int. Ed. Engl.* **1991**, *30*, 34; c) M. T. Pope, A. Müller in *Polyoxometalates: From Platonic Solids to Anti- Retroviral Activity* (Eds.: M. T. Pope, A. Müller), Kluwer: Dordrecht, The Netherlands, 1994; d) A. Müller, H. Reuter, S. Dillinger, *Angew. Chem.,* **1995**, *107*, 2505, *Angew. Chem., Int. Ed. Engl.* **1995**, *34*, 2328; e) C. Hill in *Polyoxometalates: Chemical Reviews*, 1998 (special thematic issue on polyoxometalates); f) M. T. Pope, A. Müller in *Polyoxometalate Chemistry: From Topology via Self-Assembly to Applications (*Eds.: M. T. Pope, A. Müller), Kluwer: Dordrecht, The Netherlands, 2001; g) T. Yamase, M. T. Pope in *Polyoxometalate Chemistry for Nano-Composite Design (*Eds.: T. Yamase, M. T. Pope), Kluwer: Dordrecht, The Netherlands, **2002**; h) D.-L. Long, E. Burkholder, L. Cronin, *Chem. Soc. Rev.* **2007**, *36*, 101; i) D.-L. Long, R. Tsunashima, L. Cronin, *Angew. Chem.* **2010**, *122*, 1780, *Angew. Chem. Int. Ed.* **2010**, *49*, 1736.

[2] a) K. Wassermann, M. H. Dickman, M. T. Pope, *Angew. Chem., Int. Ed. Engl.* **1997**, *36*, 1445; b) M. Sadakane, M. H. Dickman, M. T. Pope, *Angew. Chem., Int. Ed. Engl.* **2000**, *39*, 2914; c) M. Sadakane, M. H. Dickman, M. T. Pope, *Inorg. Chem.* **2001**, *40*, 2715; d) Q. H. Luo, R. C. Howell, M. Dankova, J. Bartis, C. W. Williams, W. D. Horrocks, V. G. Young, A. L. Rheingold, L. C. Francesconi, *Inorg. Chem.* **2001**, *40*, 1894 ; e) G. L. Xue, J. Vaissermann, P. Gouzerh, *J. Clust. Sci.* **2002**, *13*, 409 ; f) Q. H. Luo, R. C. Howell, J. Bartis, M. Dankova, W. D. Horrocks, A. L. Rheingold, L. C. Francesconi, *Inorg. Chem.* **2002**, *41*, 6112; g) M. Sadakane, M. H. Dickman, M. T. Pope, *Angew. Chem.* **2000**, *112*, 3036; *Angew. Chem. Int. Ed.* **2000**, *39*, 2914; h) P. Mialane, L. Lisnard, A. Mallard, J. Marrot, E. Antic-Fidancev, P. Aschehoug, D. Vivien, F. Sécheresse, *Inorg. Chem.* **2003**, *42*, 2102.

[3] a) N. Haraguchi, Y. Okaue, T. Isobe, Y. Matsuda, *Inorg. Chem.* **1994,** *33*, 1015; b) L.-H. Bi, U. Kortz, S. Nellutla, A. C. Stowe, J. van Tol, N. S. Dalal, B. Keita, L. Nadjo, Inorg. Chem. 2005, 44, 1015.

[4] C. Rocchiccioli-Deltcheff, M. Fournier, R. Franck, R. Thouvenot, *Inorg. Chem.* **1893**, *22*, 207.

[5] a) U. Kortz, *J. Clust. Sci.* **2003**, *14*, 205; b) P. Mialane, A. Dolbecq, E. Riviere, J. Marrot, F. Sécheresse, *Eur. J. Inorg. Chem.* ***2004,*** 33.

[6] M. Ibrahim, S. S. Mal, B. S. Bassil, A. Banerjee, U. Kortz, *Inorg. Chem.* **2011**, *50*, 956.

[7] F. Hussain, A. Degonda, S. Sandriesser, T. Fox, S. S. Mal, U. Kortz, G. R. Patzke, *Inorg. Chim. Acta,* **2010**, *363*, 4325.

Chapter IV

Mixed Lanthanide/d-Transition Metal Containing POMs

Ring opening in the cyclic Phosphotungstate $[Fe_{16}O_2(OH)_{23}(H_2O)_9(P_8W_{49}O_{189})Ln_4(H_2O)_{20}]^{11-}$

4.1. Introduction

Polyoxometalates (POMs) represent a class of discrete structurally and chemically diverse nanosized metal-oxygen molecular anions (hence the 'oxometalate' terminology).[1a] Due to this diversity, POMs have acquired interesting chemical and physical properties useful for applications in fields such as photochemistry, clinical chemistry, magnetism, catalysis and materials science.[1-2]

Phosphotungstates are part of a subclass of POMs known as heteropolytungstates where the metal is tungsten (VI) and the 'heterogroup' is phosphate. The majority of known phophotungstate structures are based on the classical Keggin $[PW_{12}O_{40}]^{3-}$ and Wells-Dawson $[P_2W_{18}O_{62}]^{6-}$ types; the Keggin type having one heterogroup and the Wells-Dawson type having two. The Wells-Dawson type phosphotungstates are known to have distinct chemical behaviour compared to the Keggin type ones, although some common properties arise for both.[1a]

Mono-, tri-, and hexa-vacant species of the Wells-Dawson molecule $[P_2W_{18}O_{62}]^{6-}$ (**P_2W_{18}**) can be formed and isolated in aqueous solution depending on the pH and counter-cations present during their synthesis. The monovacant anion $[P_2W_{17}O_{61}]^{10-}$ (**P_2W_{17}**) is isolated as a potassium salt by hydrolysis of **P_2W_{18}** at pH 6-7 using $KHCO_3$. The trivacant anion $[P_2W_{15}O_{56}]^{12-}$ (**P_2W_{15}**) is however formed by hydrolysis of **P_2W_{18}** using Na_2CO_3 without the presence of potassium at pH 9-10, and is isolated as a sodium salt. Finally, the hexavacant anion $[H_2P_2W_{12}O_{48}]^{12-}$ (**P_2W_{12}**) is formed by interaction of **P_2W_{18}** with the base (tris-hydroxymethylaminomethane) and is isolated as a potassium salt.[1f,3] Although **P_2W_{12},**

being hexavacant, is regarded as a multi-dentate ligand for interaction with electrophiles, in particular transition metal cations, very few compounds are known to form from such interaction due the metastability of $\mathbf{P_2W_{12}}$ in solution.[4]

Contant and Tézé were able to condense four $\mathbf{P_2W_{12}}$ units in lithium acetate buffer, resulting in the cyclic polyanion $[H_7P_8W_{48}O_{184}]^{33-}$ ($\mathbf{P_8W_{48}}$) which can be isolated as a mixed potassium/lithium salt.[5] The wheel-shaped phosphotungstate $\mathbf{P_8W_{48}}$ polyanion is stable at an unusually large pH range (1-8) and has D_{4h} point symmetry.

The multi-vacant $\mathbf{P_8W_{48}}$, having 16 donor oxygens and a large central cavity (diameter of around 10 Å), can be considered as 'super-lacunary', but its stability and inertness were noteworthy. Although the wheel-shaped polyanion was reported in 1985,[5] the first transition metal derivative was reported twenty years later by our group.[6] The large, wheel-shaped $[Cu_{20}Cl(OH)_{24}(H_2O)_{12}(P_8W_{48}O_{184})]^{25-}$ was synthesized by direct reaction of Cu(II) ions with the precursor $\mathbf{P_8W_{48}}$ in aqueous medium. This indicated that the terminal oxygens in the cavity of the tungstophosphate precursor $\mathbf{P_8W_{48}}$ can actually interact with transition-metal ions. This cavity is occupied by a highly symmetrical copper-hydroxo cluster ($\mathbf{Cu_{20}}$) where all 20 copper centers are bridged to adjacent copper ions by protonated μ_3-oxo ligands. The $\mathbf{Cu_{20}}$-containing polyanion exhibits a highly symmetrical D_{4h} structure. Furthermore, the copper cluster is composed of three structurally unique types of Cu^{II} ions with different coordination numbers and geometries (Jahn-Teller-distorted octahedral, square-pyramidal, and square-planar geometry). The center of the cluster cavity which has a diameter of around 7 Å is occupied by a chloride ion. The $\mathbf{Cu_{20}}$ polyanion was further studied by electrochemistry and magnetism, and proved to form nanosized 'blackberry' assemblies in water; furthermore, other halide derivatives of $\mathbf{Cu_{20}}$ were synthesized.[7] Since then, more 3d and 4d transition metal derivatives of the cyclic $\mathbf{P_8W_{48}}$ polyanion have been synthesized and reported.[8]

The cyclic **P_8W_{48}** is also known to react with lanthanide cations. Pope et al. reported the only lanthanide (Ln) derivative of **P_8W_{48}** known to date. The lanthanide series $[K\subset P_8W_{48}O_{184}(H_4W_4O_{12})_2Ln_2(H_2O)_{10}]^{25-}$ (Ln = La, Ce, Pr, Nd) was synthesized by the reaction of **P_8W_{48}** polyanion with lanthanide cations under hydrothermal and conventional conditions resulting in 3D networks; with the central cavity of the **P_8W_{48}** occupied by lanthanide cations and W_4O_{12} groups.[9]

Recently, our group reported the synthesis and structure of the 16-iron(III)-containing **P_8W_{48}** derivative, $[Fe_{16}(OH)_{28}(H_2O)_4(P_8W_{48}O_{184})]^{20-}$ (**$Fe_{16}P_8W_{48}$**), which was identified independently in Bremen and Bielefeld.[10] This polyanion contains a cationic $[Fe_{16}(OH)_{28}(H_2O)_4]^{20+}$ (**Fe_{16}**) 'guest' cluster with 16 edge and corner-sharing FeO_6 octahedra grafted to the inner surface of the **P_8W_{48}** 'host'; therefore exhibiting a highly symmetrical D_{4h} geometry (see Figure 4.1). Each of the 16 equivalent Fe^{3+} centers in the **Fe_{16}** cluster is bound to **P_8W_{48}** via a Fe-O(W) and a Fe-O(P) bond, resulting in a tight anchoring of the 16-iron-hydroxo core, meaning that the eight phosphate groups of **P_8W_{48}** are involved in the binding to the cationic **Fe_{16}** cluster guest.

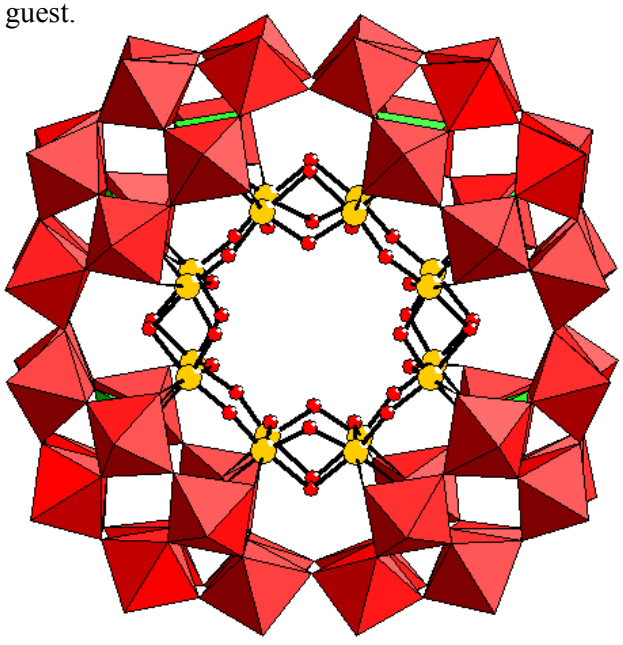

Figure 4.1. Combined polyhedral/ball-and-stick representation of the previously reported **$Fe_{16}P_8W_{48}$**. The color code is as follows: WO_6 octahedral (red); PO_4 tetrahedral (green); W (black); Fe (yellow); O (red).

Few examples in literature on mixed incorporation of lanthanides and d-transition metal ions into POMs (also known as 3d-4f heterometalic POMs) are known.[11-15] Krebs et al. successfully synthesized $[((VO)_2Dy(H_2O)_4K_2(H_2O)_2Na(H_2O)_2)(\alpha\text{-}B\text{-}AsW_9O_{33})_2]^{8-}$, which is constructed from two trilacunary Keggin anions, two VO^{2+} and one Dy^{3+} ion forming a sandwich-type structure with C_{2v} symmetry.[11] Kögerler et al. reported two compounds,[12] $[(CH_3)_2NH_2]_6H_2[\{\alpha\text{-}P_2W_{16}O_{56}(OH)_2\}\{Ce^{IV}Mn^{IV}{}_6O_9(O_2CCH_3)_8\}]\cdot 20H_2O$ and $K_{36}Na_{11}[\{\alpha\text{-}P_2W_{15}O_{56}\}_6\{Ce_3Mn_2(\mu_3\text{-}O)_4(\mu_2\text{-}OH)_2\}_3(\mu_2\text{-}OH)_2(H_2O)_2(PO_4)]\cdot 106H_2O$, which were synthesized by interaction of the high oxidation state heterometallic clusters$[CeMn_6O_9(O_2CCH_3)_9(NO_3)(H_2O)_2]$ and $[Ce_3^{IV}Mn_2^{IV}O_6(OH)_2]^{6+}$ respectively with the tri-vacant Wells-Dawson phosphotungstate $[\alpha\text{-}P_2W_{16}O_{56}]^{12-}$.[12] Mialane's group synthesized polyanions containing Cu(II) and Ln(III) cations by reaction of the $[A\text{-}\alpha\text{-}SiW_9O_{34}]^{10-}$ unit with the Cu(II) acetate and $Ln(NO_3)_3$.[13] As well, Wang et al. have been synthesizing several polyanions containing 3d-transition metal centers and having lanthanide cations as linkers between the different POM units.[14] They also reported the synthesis of a polyanion based 3d-4f heterometallic aggregate, constructed from three $\{\alpha\text{-}AsW_9O_{38}\}$ fragments bridged by three $\{Fe\text{-}(\mu_3\text{-}O)_3\text{-}Ce\}$ heterometalic clusters.[14c] Reinoso et al. reported $[\{Ce(H_2O)_2\}_2Mn_2(B\text{-}\alpha\text{-}GeW_9O_{34})_2]^{8-}$ polyanion constituting the first example of a heterometallic 3d-4f cluster related to the Weakley-type dimeric structure, and it contains $Ce^{III}{}_2Mn^{III}{}_2O_{20}$ rhomblike moiety.[15]

Therefore, the cyclic phophotungstate $\mathbf{P_8W_{48}}$ represented for us a good candidate towards synthesis of new heterometallic polyanion. As mentioned above, $\mathbf{P_8W_{48}}$ is known to interact with both 3d-transition metals and lanthanides. Furthermore, a paramagnetic 3d metal oxo-cluster interacting with paramagnetic lanthanide centers is an interesting combination for magnetic interactions. Therefore, we decided to study the formation of the known $\mathbf{Fe_{16}P_8W_{48}}$, previously reported by our group, in the presence of lanthanides. This has resulted in the synthesis and structural characterization of the europium(III) and gadolinium(III)-coupled 16-

iron(III) containing phosphotungstates $[Fe_{16}O_2(OH)_{23}(H_2O)_9P_8W_{49}O_{189}\ Ln_4(H_2O)_{19}]^{11-}$ reported herein.

4.2. Synthesis

The precursor $\mathbf{P_8W_{48}}$ used for the synthesis of the reported species was synthesized according to the published procedure by Contant and Tézé.[5]

$K_{8.5}Na_{0.5}Li_{0.5}Eu_{0.5}[P_8W_{49}O_{189}Fe_{16}O_2(OH)_{23}(H_2O)_9Eu_4(H_2O)_{20}]\cdot 70H_2O$ (KLiNa-24)

0.17 g (0.625 mmol) of $FeCl_3\cdot 6H_2O$ and 0.11 g of $EuCl_3\cdot 6H_2O$ (0.300 mmol) were dissolved in 20 mL of $LiCH_3COO/CH_3COOH$ buffer (1M, pH 4.0). Then 0.37 g of $K_{28}Li_5[H_7P_8W_{48}O_{184}]\cdot 92H2O$ (0.025 mmol) was added, followed by 25 drops of 30% H_2O_2. The mixture was heated to 80 ºC for 1 hour with vigorous stirring and filtered while hot. After cooling to room temperature, 0.5 mL $NaCl_{(aq)}$ was added to the filtrate which was kept in an open vial for crystallization. Reddish brown crystals were obtained after a month, which were filtered off and air-dried (yield 0.04 g, 10.0 %). IR data for **KLiNa-24**: (1069 (s), 1020 (w), 948(s), 914 (w), 839 (sh), 802 (w), 737 (m), 622 (w), 558 (w), 520 (w), 412 (w)) cm^{-1}. Anal. Calcd (%) **KLiNa-24**: P, 1.5; W, 54.8; Fe, 5.4; Eu, 4.2; Li, 0.1; K, 2.2. Found (%):P, 1.5; W, 54.7; Fe, 5.3; Eu, 4.3; Li, 0.2; K, 2.2, Na, <0.1.

$K_9LiNa[P_8W_{49}O_{189}Fe_{16}O_2(OH)_{23}(H_2O)_9Gd_4(H_2O)_{20}]\cdot 50H_2O$ (KLiNa-25)

The same procedure of **KLiNa-24** was followed using 0.11 g of $GdCl_3\cdot 6H_2O$ instead. Reddish brown crystals were obtained after a month, which were filtered off and air-dried (yield 0.04 g, 9.7 %). IR data for **KLiNa-25**: (1071 (s), 1024 (w), 952 (s), 917 (w), 836 (sh), 795 (w), 740 (m), 622 (w), 559 (w), 523 (w), 416 (w)) cm^{-1}. Anal. Calcd (%) **KLiNa-25**: P, 1.5; W, 56.3; Fe, 5.5; Gd, 3.9; Li, 0.1; K, 2.2. Found (%): P, 1.5; W, 56.6; Fe, 5.5; Gd, 3.9; Li, 0.3; K, 2.4, Na, <0.1.

Elemental analyses were carried out by Zentralabteilung für chemische Analysen, Forschungszentrum Jülich GmbH, 52425 Jülich, Germany.

4.3. X-ray Crystallography

The crystallographic data are summarized in Table 4.1.

Table 4.1. Crystal Data and Structure Refinement for **KLiNa-24** and **KLiNa-25**.

Code	**KLiNa-24**	**KLiNa-25**
Empirical formula	$K_{8.5}Li_{0.5}Na_{0.5}Eu_{4.5}Fe_{16}P_8W_{49}O_{313}H_{221}$	$K_9LiNaGd_4Fe_{16}P_8W_{49}O_{293}H_{181}$
MW	16411.9	16031.3
Crystal system	Triclinic	Triclinic
Space group (no.)	$P\bar{1}$ (2)	$P\bar{1}$ (2)
a/Å	26.6844(12)	26.7348(18)
b/Å	27.2118(11)	27.1921(15)
c/Å	27.4619(10)	27.4514(17)
α/°	61.803(2)	61.840(2)
β/°	77.476(2)	77.508(3)
γ/°	63.977(2)	64.028(3)
V/Å^3	15791.6(11)	15816.3(17)
Z	2	2
T/ ºC	-100	-100
λ/Å	0.71073	0.71073
D/ Mg m^{-3}	3.452	3.366
μ/ mm^{-1}	19.62	19.54
R[I >2sigma(I)][a]	0.101	0.077
R_w (all data)[b]	0.271	0.232

[a] $R = \sum|F_o| - |F_c| \; |\sum| \; |F_o|$. [b] $R_w = \{\sum[w(F_o^2 - F_c^2)^2] / \sum[w(F_o^2)^2]\}^{1/2}$.

4.4. Results and Discussion

We have synthesized and structurally characterized the open-ring 16-iron(III)-containing polyanions $[Fe_{16}O_2(OH)_{23}(H_2O)_9P_8W_{49}O_{189}Ln_4(H_2O)_{19}]^{11-}$ (Ln = Eu (**24**), and Gd (**25**)) in a one-pot reaction of Ln^{3+}, Fe^{3+} and $\mathbf{P_8W_{48}}$ in acidic aqueous medium and in the presence of hydrogen peroxide. Polyanions **42** and **25** crystallize as hydrated mixed salts (**KLi-24**) and (**KLi-25**), both in the triclinic space group $P\bar{1}$, see experimental section. These salts were characterized in the solid state by FTIR, single-crystal XRD, TGA and elemental analysis.

Polyanions **24** and **25** are isostructural. They contain the $[Fe_{16}O_2(OH)_{23}(H_2O)_9]^{21+}$ nanocluster coordinating to a novel open-ring shaped $[P_8W_{49}O_{189}]^{44-}$ ($\mathbf{P_8W_{49}}$) forming $\{Fe_{16}O_2(OH)_{23}(H_2O)_9P_8W_{49}O_{189}\}$ fragment ($\mathbf{Fe_{16}P_8W_{49}}$) which is in turn coordinated to four lanthanide(III) cations (see Figure 4.2). In other words, four lanthanide(III) cations and a $[Fe_{16}O_2(OH)_{23}(H_2O)_9]^{21+}$ cluster are being grafted to the inner surface of the unprecedented open-ring $\mathbf{P_8W_{49}}$ "host". Polyanions **24** and **25** exhibit a low symmetry C_s structure. The structures of the previously reported ($\mathbf{Fe_{16}P_8W_{48}}$)[10] and polyanions **24** and **25** are very similar but not identical. In relation with ($\mathbf{Fe_{16}P_8W_{48}}$), the structures of polyanions **24** and **25** are derived from the $\mathbf{Fe_{16}}$ cluster and the $\mathbf{P_8W_{48}}$ unit. They consist of 16 Fe^{3+} centers which are arranged as edge and corner-shared FeO_6 octahedra grafted to the inner surface of the $\mathbf{P_8W_{49}}$ "host". Each of the 16 Fe^{3+} centers is bound to $\mathbf{P_8W_{49}}$ via a Fe–O(W) and a Fe–O(P) bond (see Figure 4.2).

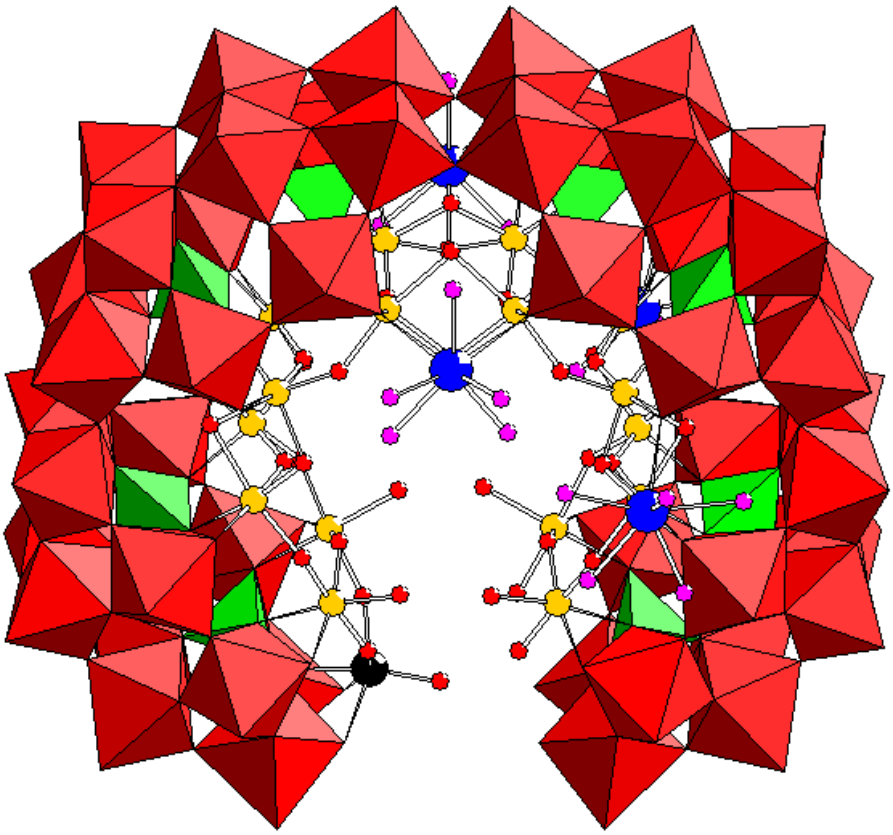

Figure 4.2. Combined polyhedral/ball-and-stick representation of open-ring-shaped polyanions **24** and **25**. The color code is as follows: WO_6 octahedral (red); PO_4 tetrahedral (green); W (black); Fe (yellow); Ln (blue); H_2O (pink); O (red).

Furthermore, The Fe_{16} nanocluster ring is cleaved between four Fe centers (Fe1–Fe2 from one side and Fe15–Fe16 from the other). Fe1 and Fe2 ions are connected with an extra tungsten atom through two μ_2-oxo bridges one each with average Fe–O bond lengths ca. 1.96 Å (see Figure 4.3). This extra tungsten atom in **24** and **25** is by its turn connected to the novel open-ring $\mathbf{P_8W_{48}}$* fragment through one μ_4-oxo bridge and two μ_2-oxo bridges.

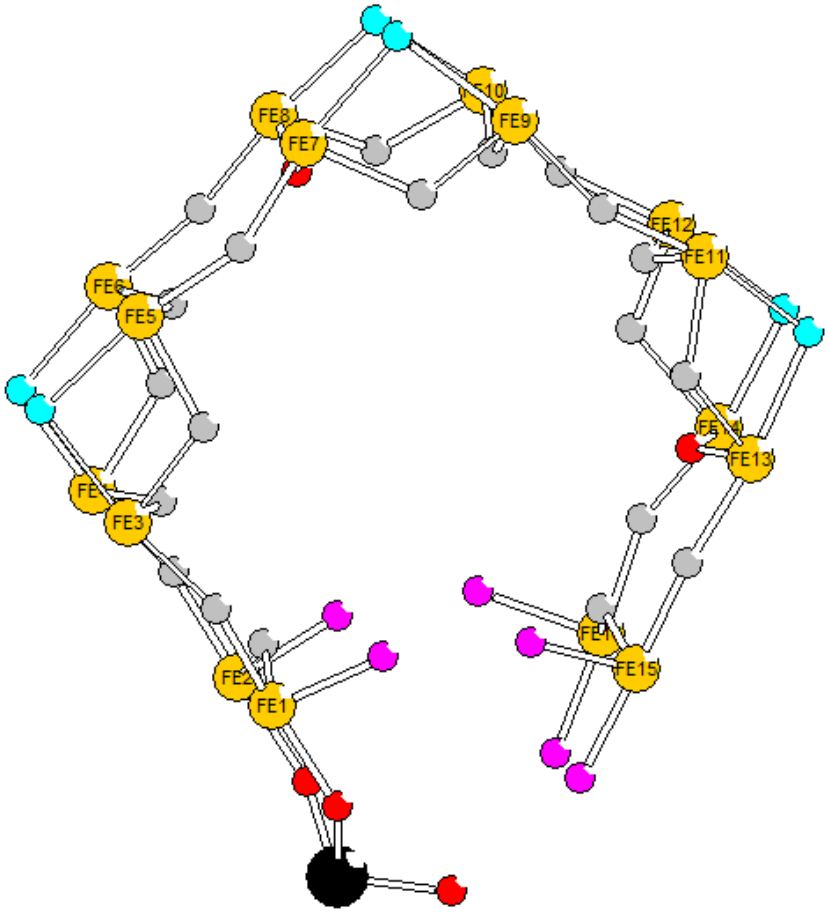

Figure 4.3. Ball-and-stick representation of $\{Fe_{16}O_2(OH)_{23}(H_2O)_9WO_3\}$ showing the protonation within the cleaved **Fe_{16}** cluster and its coordination to the extra tungsten. The color code is as follows: W (black); Fe (yellow); O (red); HO as mono-protonated μ_2-oxygen (gray); H_2O as di-protonated μ_2-oxygen (pink); disordered H_2O or HO as protonated μ_2-oxygen (turquoise).

It is noteworthy that in the solid state the extra tungsten atom is disordered over two positions with 60/40 % occupancy within the cavity which due to the C_s symmetry of the molecule. In other words, the cleavage of the original cyclic **P_8W_{48}** unit to form the open-ring **P_8W_{48}*** has led to an available vacancy with four basic oxygens. This vacancy however could only be occupied by one extra tungsten(VI) atom. Due to the equivalency of the two positions within the vacancy, the extra tungsten is disordered in the solid state over these two positions (see Figure 4.4).

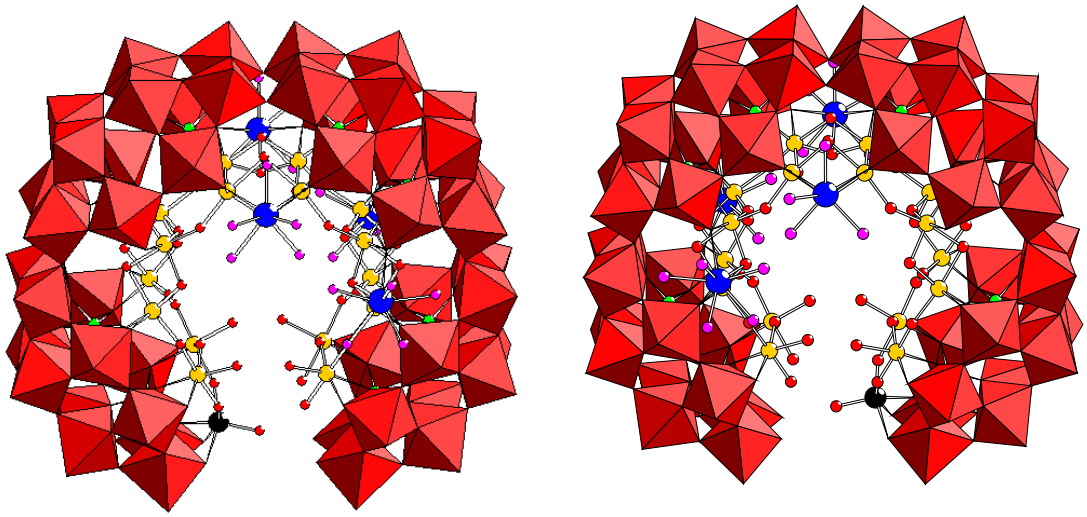

Figure 4.4. Combined polyhedral/ball-stick representation of polyanions **24** and **25** emphasizing the two equivalent positions within the vacancy which is occupied by the disordered extra tungsten atom.

In polyanions **24** and **25** each of the four lanthanide ions is bound to ($\mathbf{Fe_{16}P_8W_{49}}$) via three μ_3-oxo bridges coming from one Fe–O–Fe and two W–O–Fe bridges. In addition, the remaining coordination sphere is filled by five terminal aqua ligands, giving a total coordination number of eight for each lanthanide in a distorted square-antiprismatic geometry (see Figures 4.2 and 4.5). The Eu–O bond length ranges between 2.26(3) and 2.64(3) Å in **24**, and the Gd–O bond length ranges between 2.29(3) and 2.53(3) Å in **25**. Single-crystal XRD on the salts of polyanions **24** and **25** showed extra disordered lanthanide atoms acting as counter cations. These results were also confirmed by elemental analysis.

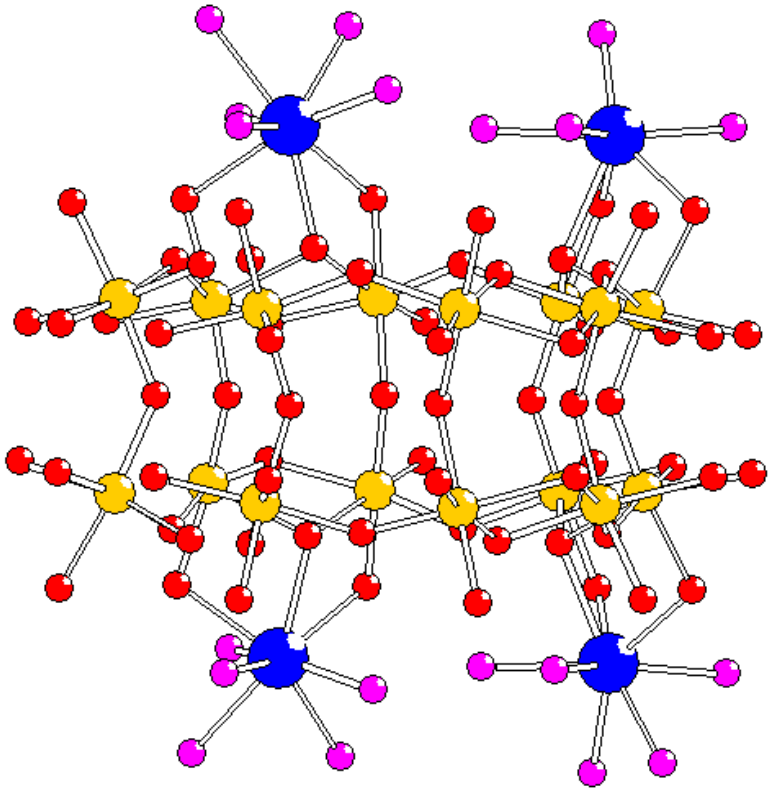

Figure 4.5. Side view of ball-and-stick representation of the **Fe_{16}** cluster emphasizing the coordination of the four lanthanide ions. The color code is as follows: Fe (yellow); Ln (blue); H_2O (pink); O (red).

Bond valence sum (BVS) calculations for **24** and **25** are consistent with all tungsten atoms being in the +6 oxidation state, and all lanthanide and iron ions being in the +3 oxidation state.[16] In addition, 23 mono- and nine di-protonated oxygen atoms were identified in **Fe_{16}** oxo cluster (see Figure 4.3). The ranges of BVS for mono- and di-protonated oxygen atoms are respectively 1.02 – 1.28 and 0.40 – 0.56. The six terminal oxygens of Fe1, Fe2, Fe15 and Fe16 are diprotonated and correspond to terminal water molecules (pink color in Figure 4.3). Furthermore, 20 of the 28 bridging Fe–O–Fe oxygens are monoprotonated (gray color in Figure 4.3). This leaves eight other bridging oxo atoms. The six bridging Fe3–Fe5, Fe4–Fe6, Fe7–Fe9, Fe8–Fe10, Fe11–Fe13 and Fe12–Fe14 (turquoise color in Figure 4.3) show a BVS range of 0.59 – 0.67, which is between mono- and diprotonation and led us to believe that we are looking at three water and three hydroxo ligand disordered over these six sites. This type

of disorder is also found in the previously reported **$Fe_{16}P_8W_{48}$**. Finally, the BVS of Fe7–O–Fe8 is ca. 1.70 and of Fe13–O–Fe14 is ca. 1.65, indicating that these oxo bridges are non protonated. These protonations lead to a total charge of –11 for polyanions **24** and **25**. In addition, terminal aqua ligand molecules coordinate to the lanthanide ions. All terminal W=O oxygen have lower BVS values than expected (~ 1.5), which is typical for a distorted W=O bond and does not indicate additional protonation.

Polyanions **24** and **25** are synthesized under mild acidic conditions by interaction of the precursor **P_8W_{48}** with Fe(III) and Ln(III) ions in aqueous lithium acetate buffer solution and in the presence of hydrogen peroxide. We followed the synthetic procedure of the previously reported **$Fe_{16}P_8W_{48}$** which has been done based on H_2O_2 (Bremen method).[10] Polyanions **24** and **25** can also be synthesized in 1 M sodium acetate buffer solution, as confirmed by FTIR. Besides **24** and **25** we were also able to synthesize the samarium analogue, as confirmed by FTIR (see Figure 4.6).

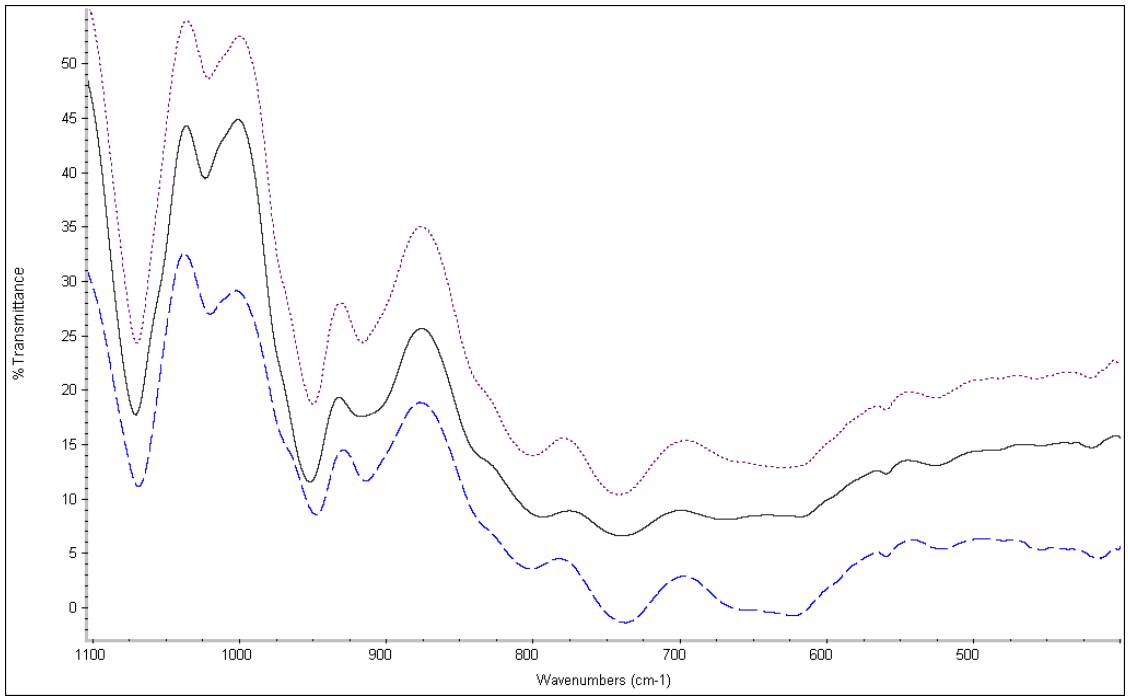

Figure 4.6. IR spectra of **KLiNaEu-24** and **KLiNaGd-25** and samarium analogue measured on KBr pellets (from bottom to top).

Thermogravimetric analyses (TGA) on the salts **KLiNa-24** and **KLiNa-25** were performed in order to determine the degree of hydration and thermal stability. The thermograms showed the expected weight loss domain between 25 and 400 ºC corresponding to dehydration. We calculated 70 and 50 water molecules per formula unit **KLiNa-24** and **KLiNa-25**. These results are also supported by elemental analysis (Figures 4.7 and 4.8).

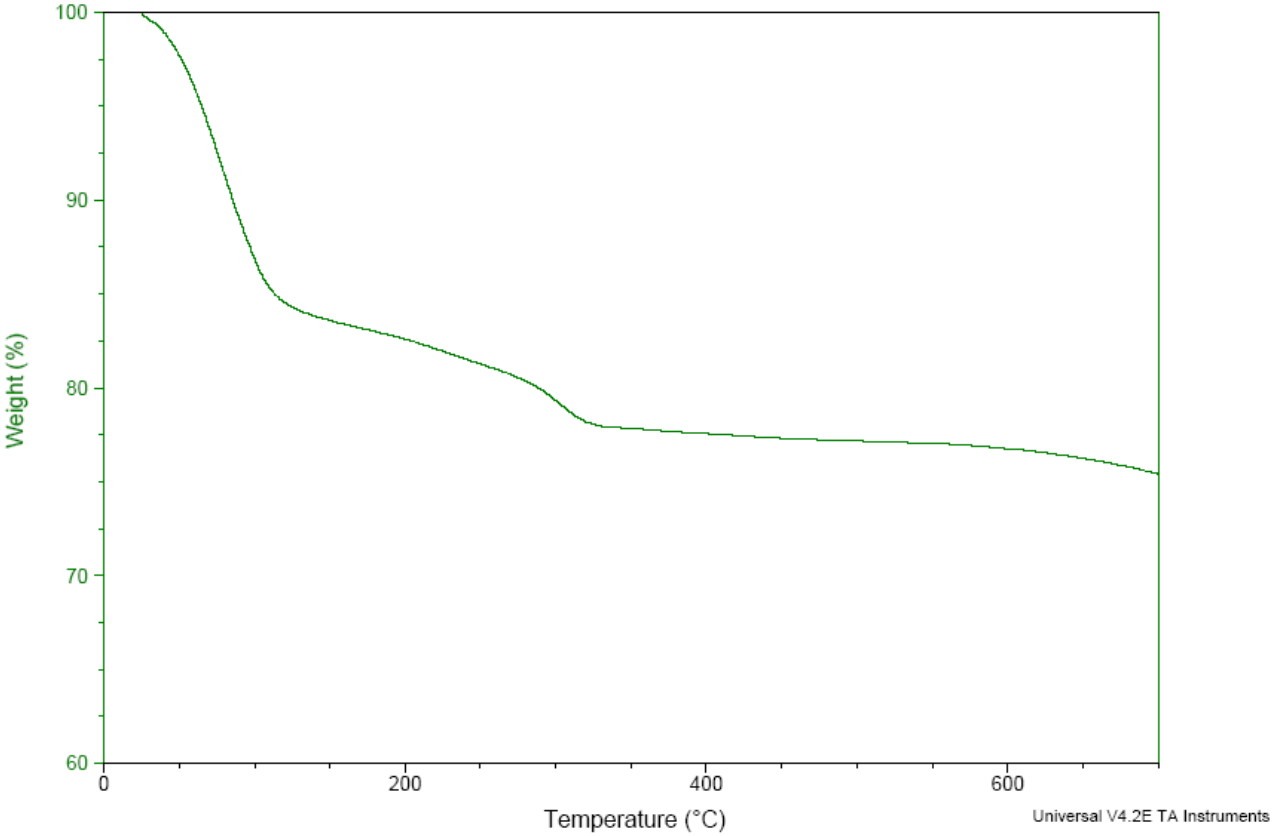

Figure 4.7. Thermogram of **KLiNaEu-24**.

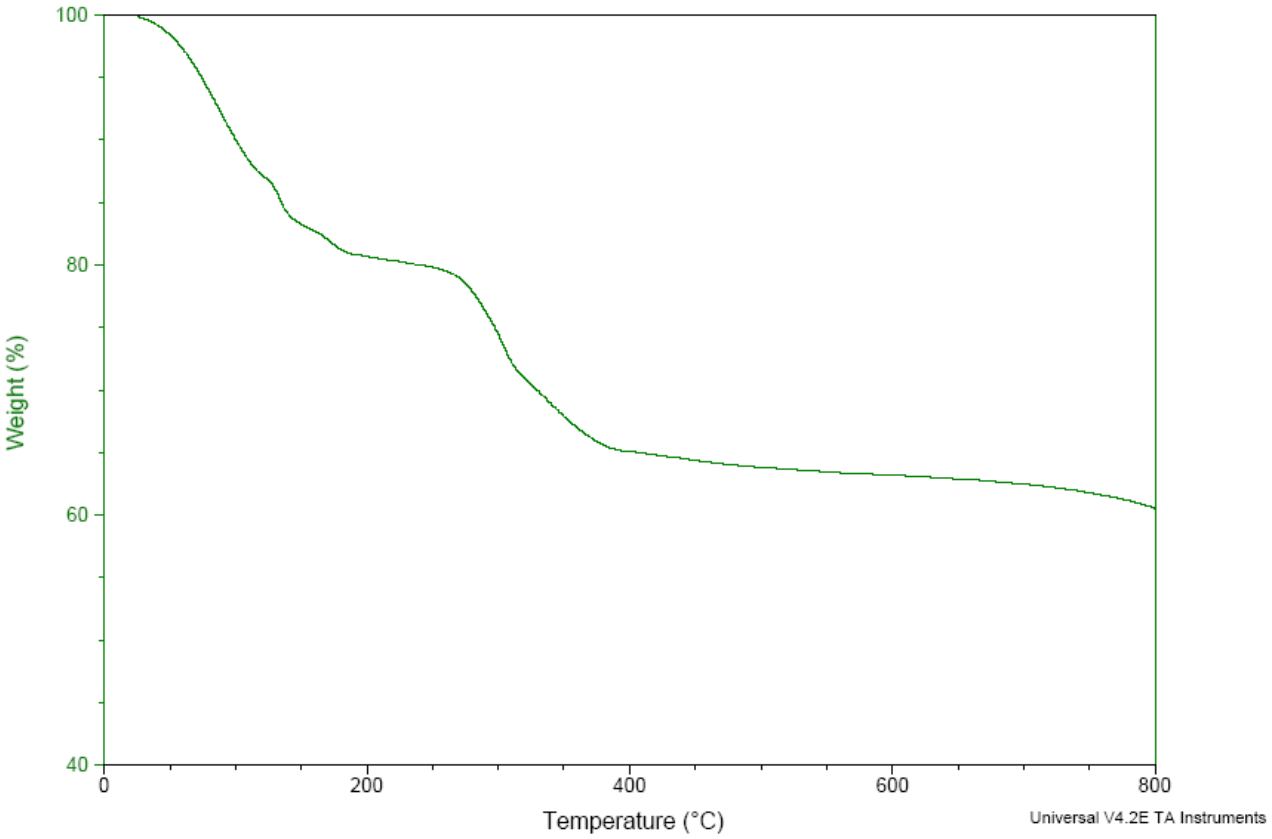

Figure 4.8. Thermogram of **KLiNaGd-25**.

The novel open ring phosphotungstate $[P_8W_{49}O_{189}]^{44-}$ **(P_8W_{49})** is unprecedented structurally and chemically. Other open and closed ring derivatives of the **P_2W_{12}** subunit are known in literature. Wang et al. have very recently reported $[K_3\subset\{GdMn(H_2O)_{10}\}\{HMnGd_2(Tart)O_2(H_2O)_{15}\}\{P_6W_{42}O_{151}(H_2O)_7\}]^{11-}$ and $[K_3\subset\{GdCo(H_2O)_{11}\}\{P_6W_{41}O_{148}(H_2O)_7\}]^{13-}$ polyanions which contain a crown-type polyanion shell $[\{WO(H_2O)\}_3\{P_2W_{12}O_{48}\}_3]^{30-}$**($P_6W_{39}$)** with the vacant site having three or two W(VI) ions in addition to the transition metal ions as "guest" ions.[14e] The three units of **P_2W_{12}** are connected by three $WO(H_2O)$ fragments via corner-sharing octahedra, leading to the closed ring derivative of **P_2W_{12}** unit. Recently, our group reported the opened ring derivative of the **P_2W_{12}** unit, uranyl-containing "U-shaped" **P_6W_{36}** polyanion $[Li(H_2O)K_4(H_2O)_3\{(UO_2)_4(O_2)_4(H_2O)_2\}_2(PO_3OH)_2P_6W_{36}O_{136}]^{25-}$.[17]

This polyanion is composed of three units of $\mathbf{P_2W_{12}}$ fused via the respective caps leading to the open trimeric $\mathbf{P_6W_{36}}$ cluster which has no extra tungsten atoms but two extra dangling phosphate groups instead. Furthermore, the parent $\mathbf{P_8W_{48}}$ is known to pick up tungsten atoms during reaction with transition metal ions.[8a,8f,9]

However, the cyclic tungsten-oxo skeleton of $\mathbf{P_8W_{48}}$ has been known to be chemically robust and to date no reaction in relatively mild acidic pH such the one used in this synthesis has led to such dramatic altering in the $\mathbf{P_8W_{48}}$ skeleton. It is still not clear whether this ring opening is a result of interaction with the lanthanide centers or hydrogen peroxide or both. Several attempts to obtain the open-ring $\mathbf{Fe_{16}P_8W_{49}}$ in the absence of lanthanide ions using different synthetic pathways are so far unsuccessful. Therefore, we believe that the presence of lanthanide cations in the solution seems to be a crucial factor in the successful synthesis and isolation of polyanions **24** and **25**. Moreover, the extra WO_6 group comes most probably from *in situ* partial or complete decomposition of some $\mathbf{P_8W_{48}}$ precursors in solution. The formation pathway of **24** and **25** from $\mathbf{Fe_{16}P_8W_{48}}$ can be postulated as follows:

- Ring opening in $[Fe_{16}(OH)_{28}(H_2O)_4(P_8W_{48}O_{184})]^{20-}$ through cleavage of four Fe–O–Fe and two W–O–W and insertion of a tungsten center to give $[Fe_{16}O_2(OH)_{23}(H_2O)_9(P_8W_{49}O_{189})]^{23-}$ ($\mathbf{Fe_{16}P_8W_{49}}$).
- Coordination of four lanthanide centers to $\mathbf{Fe_{16}P_8W_{49}}$ to give the title polyanions **24** and **25**.

Structural changes arising from the ring opening are reflected in the interatomic distance between W1 and W47 as well as W2 and W48, with an average value of ca. 8.4 Å for **24** and **25** in comparison with 3.7 Å for $\mathbf{Fe_{16}P_8W_{48}}$. In addition, the average of the W23–O–W25 and W24–O–W26 angles is around 133˚ for **24** and 136˚ for **25**, in comparison with 144˚ for $\mathbf{Fe_{16}P_8W_{48}}$.

4.5. Conclusions

We have synthesized two 16-iron(III)-containing phosphotungstates coordinated to four lanthanide centers and composed of an unprecedented open-ring $\mathbf{P_8W_{49}}$ unit, $[Fe_{16}O_2(OH)_{23}(H_2O)_9(P_8W_{49}O_{189})Ln_4(H_2O)_{20}]^{11-}$ (Ln = Eu (**24**) and Gd (**25**)). They are synthesized in simple, one-pot reactions of Ln(III) and Fe(III) salts with the large superlacunary polyanion precursor $\mathbf{P_8W_{48}}$ and isolated as hydrated mixed potassium-lithium-sodium-lanthanide salts **KLiNa-24** and **KLiNa-25**. These salts have been studied in the solid state by IR spectroscopy, single-crystal X-ray diffraction, TGA and elemental analysis. It is apparent that the presence of lanthanide ions is a crucial parameter in the synthesis of **24** and **25**. However, the mechanism cleavage of the wheel-shaped $\mathbf{P_8W_{48}}$ is still unclear. Attempts to synthesize the open-ring $\mathbf{Fe_{16}P_8W_{49}}$ in the absence of lanthanides ions are still underway using different synthetic procedures. Furthermore, isolation the novel $\mathbf{P_8W_{49}}$ or $\mathbf{P_8W_{48}}$* as new precursors, starting from either the wheel-shaped $\mathbf{P_8W_{48}}$ or other phosphotungstate precursors such as $\mathbf{P_2W_{12}}$ and $\mathbf{P_4W_{24}}$ will be the scope of further studies.

4.6. References

[1] a) M. T. Pope in *Heteropoly and Isopoly Oxometalates*, Springer-Verlag, Berlin, 1983; b) M. T. Pope, A. Müller, *Angew. Chem.* **1991**, *103*, 56, *Angew. Chem. Int. Ed. Engl.* **1991**, *30*, 34; c) M. T. Pope, A. Müller in *Polyoxometalates: From Platonic Solids to Anti- Retroviral Activity* (Eds.: M. T. Pope, A. Müller), Kluwer: Dordrecht, The Netherlands, 1994; d) A. Müller, H. Reuter, S. Dillinger, *Angew. Chem.* **1995**, *107*, 2505, *Angew. Chem. Int. Ed. Engl.* **1995**, *34*, 2328; e) C. Hill in *Polyoxometalates: Chemical Reviews*, 1998 (special thematic issue on polyoxometalates); f) J. J. Borrás-Almenar, E. Coronado, A. Müller, M. T. Pope, in *Polyoxometalate Molecular Science* (Eds.: J. J. Borrás-Almenar, E. Coronado, A. Müller, M. T. Pope), Kluwer: Dordrecht, The Netherlands, 2001; g) M. T. Pope, A. Müller in *Polyoxometalate Chemistry: From Topology via Self-Assembly to Applications (*Eds.: M. T. Pope, A. Müller), Kluwer: Dordrecht, The Netherlands, 2001; h) T. Yamase, M. T. Pope in *Polyoxometalate Chemistry for Nano-Composite Design (*Eds.: T. Yamase, M. T. Pope), Kluwer: Dordrecht, The Netherlands, 2002; i) D.-L. Long, E. Burkholder, L. Cronin, *Chem. Soc. Rev.* **2007**, *36*, 101; j) D.-L. Long, R. Tsunashima, L. Cronin, *Angew. Chem.* **2010**, *122*, 1780, *Angew. Chem. Int. Ed.* **2010**, *49*, 1736.

[2] a) A. Mylonas, A. Hiskia, E. Papaconstantinou, *J. Mol. Catalysis A: Chem.* **1996**, *114*, 191; b) A. Hiskia, A. Troupis, E. Papaconstantinou, *Int. J. Photoenergy* **2002**, *4*, 35; c) E. Gkika, P. Kormali, S. Antonaraki, D. Dimoticali, E. Papaconstantinou, A. Hiskia, Int. *J. Photoenergy* **2004**, *6*, 227; d) A. Hiskia, A. Troupis, S. Antonaraki, E. Gkika, P. Kormali, E. Papaconstantinou, *Int. J. Envir. Anal. Chem.* **2006**, 233; e) P. Kormali, A. Troupis, T. Triantis, A. Hiskia, E. Papaconstantinou, *Catalysis Today* **2007**, *124*, 149; f) G. R. J. Choppin, *Nucl. Radiochem. Sci.* **2005**, *6*, 1.

[3] R. Contant. *Inorg. Synth.* **1990**, *27*, 108.

[4] a) D. A. Judd, Q. Chen, C. F. Campana, C. L. Hill, *J. Am. Chem. Soc.* **1997**, *119*, 5461; b) R. Belghiche, R. Contant, Y. W. Lu, B. Keita, M. Abbessi, L. Nadjo, J. Mahuteau, *Eur. J. Inorg. Chem.* **2002**, 1410; c) U. Kortz, *J. Clust. Sci.* **2003**, *14*, 205 205; d) B. Godin, J. Vaissermann, P. Herson, L. Ruhlmann, M. Verdaguer, P. Gouzerh, *Chem. Commun.* **2005**, 5624; e) B. Godin, Y.-G. Chen, J. Vaissermann, L. Ruhlmann, M. Verdaguer, P. Gouzerh, *Angew. Chem.* **2005**, *117*, 3132, *Angew. Chem. Int. Ed.* **2005**, *44*, 3072; f) Z.-M. Zhang, S. Yao, Y.-G. Li, Y.-H. Wang, Y.-F. Qi, E.-B. Wang, *Chem. Commun.,* **2008**, 1650; g) A. Qstunit, M. T. Pope, *C. R. Acad. Sci. Sér. IIc*, **2000**, *3*, 199.

[5] R. Contant, A. Tézé, *Inorg. Chem.* **1985** *24,* 4610.

[6] S. S. Mal, U. Kortz, *Angew. Chem.* **2005**, *117*, 3843, *Angew. Chem. Int. Ed. Engl.* **2005**, *44*, 3777.

[7] a) D. Jabbour, B. Keita, L. Nadjo, U. Kortz, S. S. Mal, *Electrochem. Commun.* **2005**, *7*, 841; b) G. Liu, T. Liu, S. S. Mal, U. Kortz, *J. Am. Chem. Soc.* **2006**, *128*, 10103; c) L. Chen, J. Hu, S. S. Mal, U. Kortz, H. Jaensch, G. Mathys, R. M. Richards, *Chem. Eur. J.* **2009**, *15*, 7490; d) Y.-Y. Bao, L.-H. Bi, L.-X. Wu, S. S. Mal, U. Kortz, *Langmuir* **2009**, *25*, 13000; e) S. S. Mal, B. S. Bassil, M. Ibrahim, S. Nellutla, J. van Tol, N. S. Dalal, J. A. Fernández, X. López, J. M. Poblet, R. Ngo Biboum, B. Keita, U. Kortz, *Inorg. Chem.* **2009**, *48*, 11636.

[8] a) S. S. Mal, N. H. Nsouli, M. H. Dickman, U. Kortz, *Dalton Trans* **2005**, 2627; b) A. Müller, M. T. Pope, A. Todeo, H. Bögge, J. Slageren, M. Dressel, P. Gouzerh, R. Thouvenot, B. Tsukerblat and A. Bell, *Angew. Chem.* **2007**, *119*, 4561, *Angew. Chem. Int. Ed.* **2007**, *46*, 4477; c) C. Pichon, P. Mialane, A. Dolbecq, J. Marrot, E. Rivière, B Keita, L. Nadjo, F. Sécheresse, *Inorg. Chem.* **2007**, *46*, 4292; d) S. G. Mitchell, D. Gabb, C. Ritchie, N. Hazel, De-L. Longa, L. Cronin, *CrystEngComm.* **2009**, *11*, 36; e) S. G. Mitchell, C. Streb, H. N. Miras, T. Boyd, De-L. Long, L. Cronin, *Nat. Chem.* **2010**, DOI: 10.1038/NCHEM.581; f) B.

S. Bassil, M. Ibrahim, S. S. Mal, A. Suchopar, R. N. Biboum, B. Keita, L. Nadjo, S. Nellutla, J. van Tol, N. S. Dalal, U. Kortz, *Inorg. Chem.* **2010**, DOI: 10.1021/ic100050r.

[9] M. Zimmermann, N. Belai, R. J. Butcher, M. T. Pope, E. V. Chubarova, M. H. Dickman, U. Kortz, *Inorg. Chem.* **2007**, *46*, 1737.

[10] S. S. Mal, M. H. Dickman, U. Kortz, A. M. Todea, A. Merca, H. Bögge, T. Glaser, A. Müller, S. Nellutla, N. Kaur, J. Van Tol, N. S. Dalal, B. Keita, L. Nadjo, *Chem. Eur. J.* **2008**, *14*, 1186.

[11] A. Merca, A. Müller, J. van Slageren, M. Läge, B. Krebs, *J. Clust. Sci.* **2007**, *16*, 711.

[12] a) X. Fang and P. Kögerler, *Chem. Commun.* **2008**, 3396; b) X. Fang and P. Kögerler, *Angew. Chem.* **2008**, *120*, 8243, *Angew. Chem. Int. Ed.* **2008**, *47*, 8123.

[13] B. Nohra, P. Mialane, A. Dolbecq, E. Riviére, J. Marrot, F. Séecheresse, *Chem. Commun.* **2009**, 2703.

[14] a) W.-L. Chen, Y.-G. Li, Y.-H. Wang, E.-B. Wang, *Eur. J. Inorg. Chem.* **2007**, 2216; b) Z.-M. Zhang, Y.-G. Li, W.-L. Chen, E.-B. Wang, X.-L. Wang, *Inorg. Chem. Commun.* **2008**, 11, 879; c) W.-L. Chen, Y.-G. Li, Y.-H. Wang, E.-B. Wang, Z.-M. Zhang, *Dalton Trans.* **2008**, 865. d) Y-W. Li, Y-G. Li, Y-H. Wang, X-J. Feng, Y Lu, E.-B. Wang, *Inorg. Chem.* **2009,** *48*, 6452; e) S. Yao, Z. Zhang, Y. Li, Y. Lu, E.-B. Wang, Z. Su, *Cryst. Growth Des.* **2010**, *10*, 135.

[15] S. Reinoso, J. R. Galán-Mascarós, *Inorg. Chem.* **2010**, *49*, 377.

[16] D. Altermatt, I. D. Brown, *Acta. Cryst.* **1985**, *B41*, 244.

[17] S. S. Mal, M. H. Dickman, U. Kortz, *Chem. Eur. J.* **2008**, *14*, 9851.

Chapter V

Non-Lanthanide-Containing POMS

5.A. Tellurium-Containing POMs

5.A.1. Tellurium-Containing Polyoxotungstates: The 20-Tungsto-4-Tellurate(IV) $[H_2Te_4W_{20}O_{80}]^{22-}$ and the 15-Tungstotellurate(IV) $[NaTeW_{15}O_{54}]^{13-}$

A. H. Ismail, N. H. Nsouli, M. H. Dickman, U. Kortz, *J. Clust. Sc.* **2009**, *20,* 453

5.A.1.1. Introduction

Polyoxometalates (POMs) represent a large class of nanosized metal-oxygen cluster anions. POMs are remarkable not only in terms of molecular and electronic structural versatility, but also due to their applications in many fields such as catalysis, medicine, electronics, multifunctional materials, and analytical chemistry.[1] In recent years there has been developing interest in these remarkable compounds of tungsten, molybdenum, vanadium, niobium, and tantalum. POM clusters have been known for a long time (first prepared in 1826 by Berzelius) but the mechanism of their formation is still not completely understood, and is often described as "self-assembly".[1a]

POMs are formed through condensation reactions of metalate ions in acidified solutions (usually aqueous), through aggregation of octahedral $[MO_6]$ building blocks sharing corners, edges, and rarely faces. Many of the reported POMs are based on the well-known Keggin ion ($[XM_{12}O_{40}]^{n-}$), or lacunary fragments of that structure, where X is the central heteroatom and M the addenda atom. The heteroatom can be one of many elements of the periodic table, most commonly P, As, Si, Ge or B.

Also tellurium can act as a heteroatom, but the number of such POMs is rather limited. In 1948 Evans reported the first structure of a tellurium containing polyanion, $[TeMo_6O_{24}]^{6-}$.[2] Many other inorganic salts of the Anderson-Evans type molybdotellurate(VI) $[TeMo_6O_{24}]^{6-}$ have been reported meanwhile.[3] Molybdotellurates containing organic counter-cations have also been described.[4] The first examples of the Anderson-Evans type tungstotellurate $[TeW_6O_{24}]^{6-}$ were reported by Ganelina and Ripan.[5] Tungstotellurates with organic cations have also been reported.[6]

Some examples of tellurium(IV) containing POMs are also known. In 1992, Yurchenko reported on a Cu-containing tungstotellurate(IV), but no XRD crystal structure was shown.[7] Between 1998 and 2003 Krebs' group reported the transition metal containing derivatives $[Mn_3(H_2O)_{10}(\beta\text{-}TeW_9O_{33})_2]^{8-}$, $[Co_3(H_2O)_8(WO_2)(\beta\text{-}TeW_9O_{33})_2]^{8-}$, $[(V(H_2O)_3)_2(VO_2)(WO_2)(\beta\text{-}TeW_9O_{33})_2]^{6-}$, $[(Zn(H_2O)_3)_2(WO_2)_2(\beta\text{-}TeW_9O_{33})_2]^{8-}$, $[Cu_3(H_2O)(\alpha\text{-}TeW_9O_{33})_2]^{10-}$, $[Pd_3(\alpha\text{-}TeW_9O_{33})_2]^{10-}$) as well as several others.[8] In 2001 our group reported the structure of $[Cu_3(H_2O)_3(\alpha\text{-}TeW_9O_{33})_2]^{10-}$.[9] In the following year we reported on $[Fe_4(H_2O)_{10}(\beta\text{-}TeW_9O_{33})_2]^{4-}$ and isostructural derivatives of Cr^{III}, Mn^{II}, Co^{II}, Ni^{II}, Cu^{II}, Zn^{II}, Cd^{II} and Hg^{II}.[10] Finally, Pope and coworkers reported the synthesis and structural characterization of $[UO_2(H_2O)_2(TeW_9O_{33})_2]^{12-}$.[11] In the same paper the synthesis of the tungstotellurate(IV) $[TeW_9O_{33}]^{8-}$ precursor was reported. This species was characterized by infrared spectroscopy, but no single-crystal X-ray structure was presented.

The complete lack of structurally characterized tungstotellurates(IV) without any incorporated transition metals provides an impetus to prepare such species.[12] Herein we report on a novel tungstotellurate containing two pairs of face-shared WO_6 octahedra.

5.A.1.2. Synthesis

$Na_{22}[H_2Te_4W_{20}O_{80}]\cdot 64H_2O$ (Na-26)

A sample of 10.00 g of $Na_2WO_4\cdot 2H_2O$ (30.3 mmol) was dissolved in 20 mL 1M NaCl, followed by dropwise addition of a solution of 1.07 g of TeO_2 (6.7 mmol) in 2.5 mL concentrated HCl. Then the pH was adjusted to 7.5 using 4M aqueous HCl, and a white sticky precipitate was formed. The mixture was vigorously stirred at room temperature for 1 h, and then the precipitate was filtered off and discarded. The filtrate was kept in an open vial for crystallization at room temperature. After a day, colorless crystals of paradodecatungstate ($[H_2W_{12}O_{42}]^{10-}$) started to appear and were filtered off successively and discarded until needle-shaped, colorless crystals of **Na-26** were formed (after ~1 week). These crystals were in turn filtered off and air-dried. Yield: 0.77 g (7.1 %). IR for **Na-26** in cm^{-1} (only between 400-1000 cm^{-1}): 925(m), 873(m), 848(w), 801(sh), 738(s), 692(m), 619(w), 475(w), 421(w), see Figure 5.1.

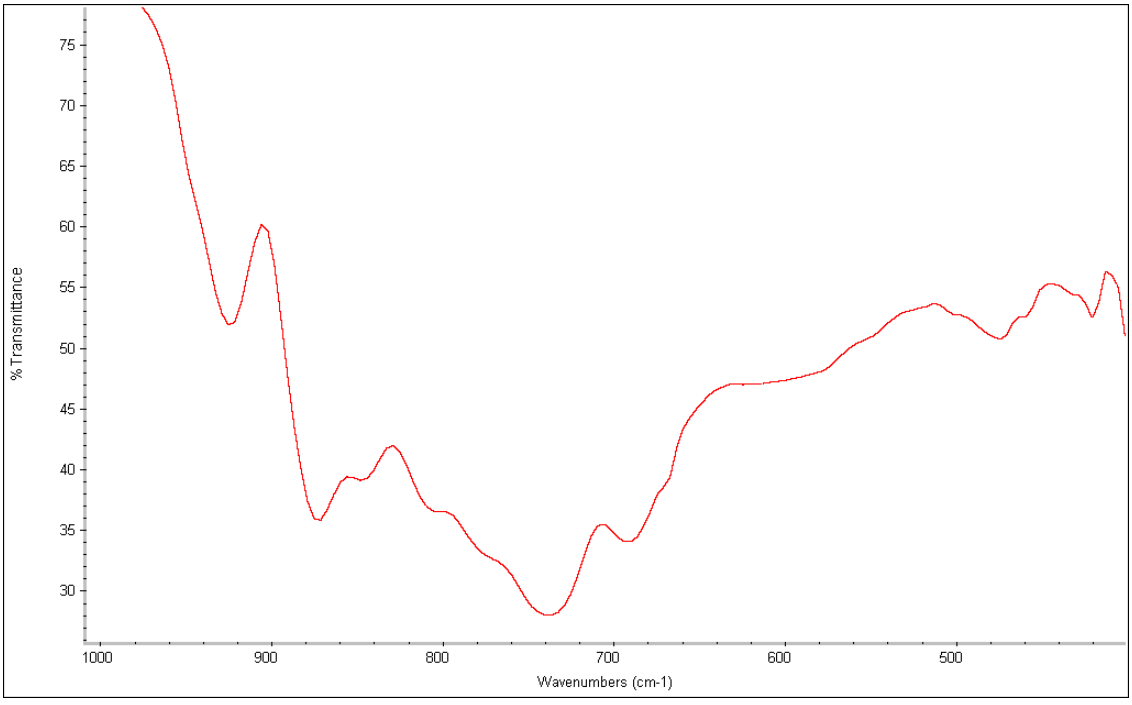

Figure 5.1. IR spectrum of $Na_{22}[H_2Te_4W_{20}O_{80}]\cdot 64H_2O$ (**Na-26**).

5.A.1.3. X-ray Crystallography

All crystals were mounted in Hampton cryoloops using light oil, for data collection at low temperature. Indexing and data collection were performed using a Bruker X8 APEX II CCD diffractometer with kappa geometry and Mo K_α radiation (λ = 0.71073 Å). Data integration and routine processing were performed using the SAINT software suite. Further data processing, including multi-scans absorption corrections, was performed using SADABS.[13] Direct methods (SHELXS97) solutions successfully located the W atoms, and successive Fourier syntheses (SHELXL97) revealed the remaining atoms.[13] Refinements were full-matrix least squares against F^2 using all data. Some cations and waters of hydration were modeled with varying degrees of occupancy, a common situation for polyoxotungstate structures. In the final refinements, all nondisordered heavy atoms (W, Te) were refined anisotropically, while the O and Na atoms were refined isotropically. No H atoms were included in the models. The crystallographic data are provided in Table 5.1. Selected bond lengths and angles are listed in Table 5.2 and Table 5.3, respectively.

Table 5.1. Crystal Data and Structure Refinement for **(Na-26)** and **(Na-27)**.

Code	**Na-26**	**Na-27**
Empirical formula	$H_{130}Na_{22}O_{144}Te_4W_{20}$	$H_{52}\ Na_{14}\ O_{80}Te\ W_{15}$
MW	7172.18	4539.42
Crystal system	Triclinic	Orthorhombic
Space group (no.)	$P\bar{1}$ (2)	Pccn
a/Å	12.741(2)	11.8841(5)
b/Å	16.842(3)	20.8934(11)
c/Å	17.197(4)	31.801(2)
α/°	93.961(10)	90
β/°	107.466(8)	90
γ/°	108.548(8)	90
V/Å^3	3281.5(11)	7896.3(7)
Z	1	4
T/ ºC	-100(2)	-100(2)
λ/Å	0.71073	0.71073
D/ Mg m^{-3}	3.629	3.753
μ/ mm^{-1}	18.53	22.29
R[I >2sigma(I)][a]	0.037	0.074
R_w (all data)[b]	0.100	0.225

[a] $R = \sum|F_o| - |F_c| \,|\sum|\, |F_o|$. [b] $R_w = \{\sum[w(F_o^2 - F_c^2)^2] / \sum[w(F_o^2)^2]\}^{1/2}$.

Table 5.2. Te–O(W) Bond Lengths (Å) for **Na-26**.

Te1	**Å**	**Te2**	**Å**
Te – O5TE	1.853(6)	Te – O10E	1.853(6)
Te – O12T	1.884(6)	Te – O6TE	1.859(6)
Te – O24T	1.986(6)	Te – O789	2.061(6)
Te – O6T	2.332(6)	Te – O5A	2.199(6)

Table 5.3. Selected Bond Angles (/°) for **Na-26**.

Te1	/°	**Te2**	/°
O5TE– Te1– O12T	97.8(3)	O10E–Te2–O6TE	99.6(3)
O5TE– Te1–O24T	94.9(3)	O10E–Te2–O789	92.2(3)
O12T–Te1–O24T	90.6(3)	O6TE–Te2–O789	88.1(3)
O5TE–Te1– O6T	82.1(2)	O10E–Te2–O5A	83.7(3)
O12T–Te1–O6T	81.2(2)	O6TE–Te2–O5A	83.8(3)
O24T–Te1–O6T	170.8(2)	O789–Te2–O5A	170.1(2)

Table 5.4. Selected W–O Bond Lenghths (Å) for **Na-26**.

W–O	**Å**	W–O	**Å**
W1–O1T	1.716(7)	W7–O7T	1.743(6)
W1– O14	1.787(6)	W7–O710	1.822(6)
W1– O110	1.867(7)	W7–O67	1.882(6)
W1– O123	1.974(6)	W7–O79	1.890(6)
W1– O12	2.111(6)	W7–O78	2.098(6)
W1– O12T	2.382(6)	W7–O789	2.338(6)
W2–O2T	1.738(7)	W8–O8T	1.752(7)
W2–O2A	1.780(7)	W8–O8A	1.759(7)
W2–O12	1.883(6)	W8–O68	1.895(6)
W2–O23	1.952(6)	W8–O89	1.967(6)
W2–O123	2.092(6)	W8–O78	2.215(6)
W2–O12T	2.385(6)	W8–O789	2.217(6)

5.A.1.4. Results and Discussion

We perfomed a systematic study on the interaction of tellurium(IV) ions with sodium tungstate in neutral, aqueous medium, and at a ratio of 1 : 5 we were able to isolate crystals of $Na_{22}[H_2Te_4W_{20}O_{80}]\cdot 64H_2O$ (**Na-26**). Four reaction parameters are crucial for the successful formation and isolation of $[H_2Te_4W_{20}O_{80}]^{22-}$ (**26**) in a pure form: reaction temperature, concentration of reagents, molar ratio of reagents, and pH of the solution. The polyanion **26** is formed at room temperature, but if the solution is heated then a mixture of products is present: **26**, the well-known paradodecatungstate ion $[H_2W_{12}O_{42}]^{10-}$, and another novel tungstotellurate(IV), $[NaTeW_{15}O_{54}]^{13-}$ (**27**). Polyanions **26** and **27** were crystallized as sodium salts and characterized by IR and single-crystal XRD.

The yield of **26** is affected by the concentration of the starting material. A tungstate concentration as high as 1.5 M and a TeO_2 and Na_2WO_4 ratio of 1: 5 are needed to isolate pure crystalline **Na-26**. Finally, the pH of the reaction solution affects the formation of **26** and yield of **Na-26**. A pH window of 7.4-7.6 resulted in a successful synthetic procedure, with pH 7.5 being optimal. A pH lower than 7.4, or higher than 7.6, resulted in paratungstate as the main product. Experimentally, the filtration of the reaction solution after one hour of stirring is important to decrease the amount of paratungstate formed. Obviously, the formation of paratungstate accounts for the low yield of **26**. Interestingly, we discovered **26** in the first place when trying to reproduce and crystallize $[TeW_9O_{33}]^{8-}$ following the synthetic procedure of Gaunt et al.[11]

The polyanion **26** crystallized as a hydrated sodium salt in the triclinic space group $P\bar{1}$. The single-crystal X-ray analysis showed that **26** consists of four tellurium atoms sandwiched between two novel decatungstate $\{W_{10}\}$ units. The structure of **26** comprises two $[HTe_2W_{10}O_{40}]^{11-}$ fragments which are connected through Te−O−W μ_2-oxo bridges. Hence polyanion **26** can be described as a dimeric molecular entity composed of two

$[HTe_2W_{10}O_{40}]^{11-}$ half units related by an inversion center. Furthermore, there are three sodium ions coordinated to the central cavity of **26** and one of them is present at the inversion center of the polyanion (see Figure 5.2). Each Te^{4+} ion is linked to one of the $\{W_{10}\}$ units through three μ-oxo bridges and another such bridge links to the other half-unit, resulting in coordination number four and a see-saw coordination geometry for the Te atom (see Figure 5.3).

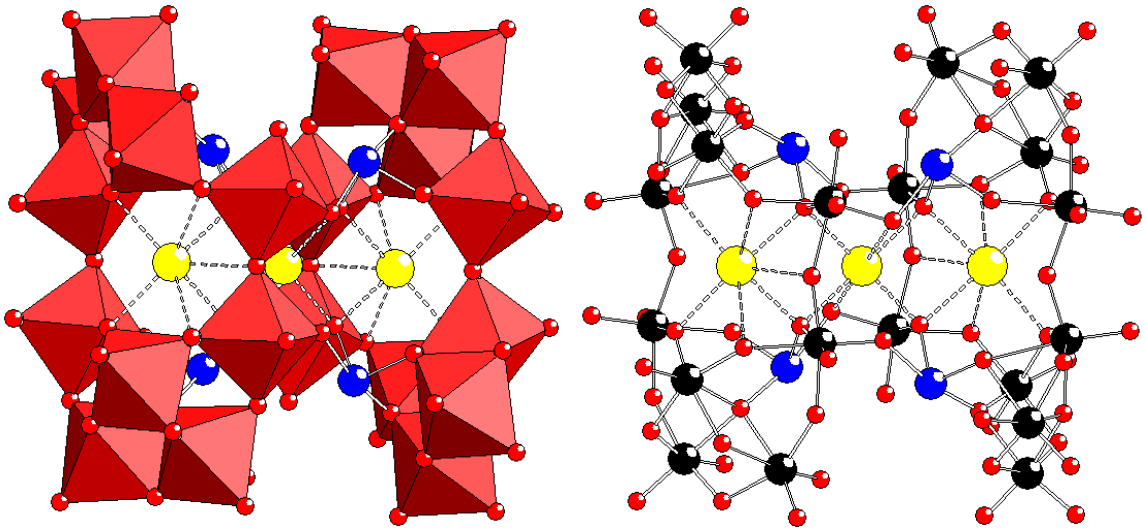

Figure 5.2. Polyhedral (left) and ball-and-stick (right) representations of $[H_2Te_4W_{20}O_{80}]^{22-}$ (**26**). The color code is as follows: WO_6 octahedra (red); Te (blue), W (black); O (red), Na (yellow).

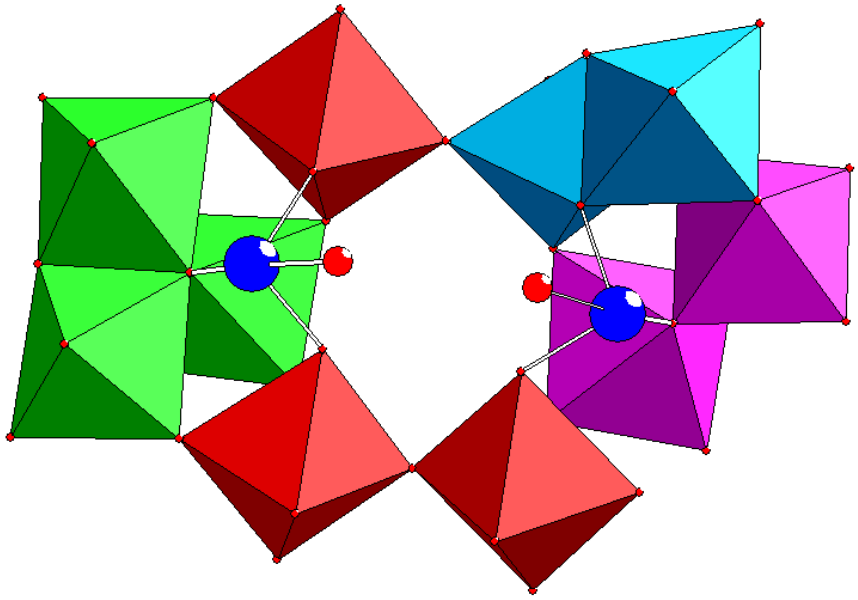

Figure 5.3. Polyhedral representation of the $[HTe_2W_{10}O_{40}]^{11-}$ half-unit of **26**. The color code is as follows: WO_6 octahedra (green, light blue, pink, red); Te (blue); O (red). The WO_6 octahedra were colored differently for clarity. See also text and Figure 5.4. The eight Te–O(W) bond distances range from 1.853(6) to 2.332(6) Å.

The decatungstate $\{W_{10}\}$ unit can be considered as an assembly of four types of 'building blocks' (see Figure 5.4):

- One tritungstate $\{W_3\}$ fragment (green in Figure 5.4) made of three edge-shared $[WO_6]$ octahedra connected via a μ_3-oxo bridge. This fragment can be viewed as a single 'triad' of the well-known Keggin and Wells-Dawson structures.[1a]
- One ditungstate $\{W_2\}$ subunit (light blue in Figure 5.4) made of two face-shared $[WO_6]$ octahedra connected via three μ_2-oxo bridges. This feature is very rare in POM chemistry.[1a] Face-shared $W^{VI}O_6$ octahedra result in large coulombic repulsion between the highly positively charged metal centers. In **26,** the separation between the face-shared tungsten atoms (W1···W2) is 3.060(7) Å, shorter than the separations in corner-shared or edge-shared octahedra (approximately 3.7 and 3.4 Å, respectively). In 1968 Dexter and Silverton presented the first example of a polyanion containing

face-shared octahedra, $[CeMo_{12}O_{42}]^{8-}$.[14] This species consists of six pairs of face-shared octahedra (Mo_2O_9 unit)

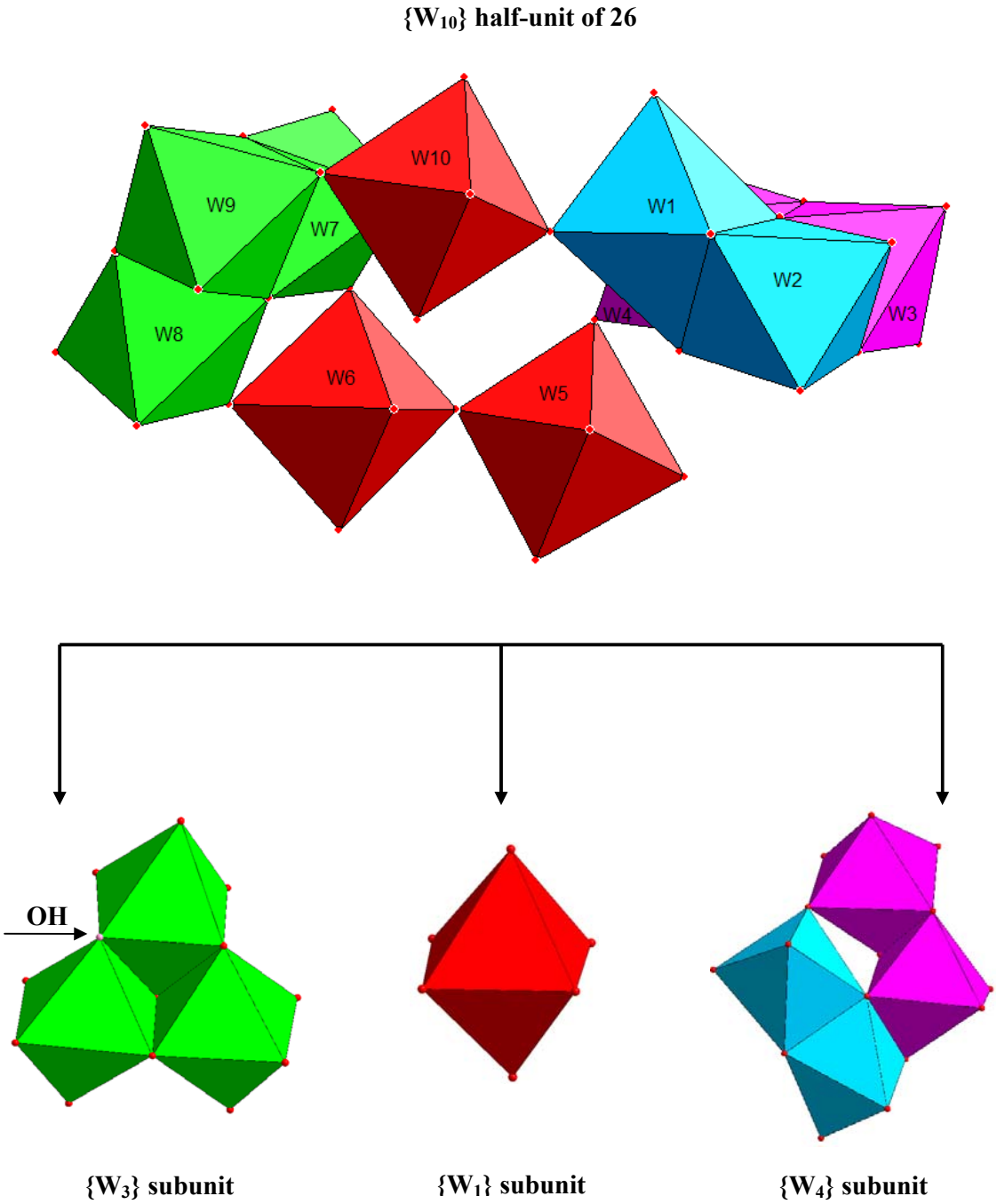

Figure 5.4. Polyhedral representation of the building blocks forming the decatungstate $\{W_{10}\}$ unit. The color code is as follow: W_3 (green), W_2; face-shared octahedra (light blue), W_2; edge-shared octahedra (pink), W_1 (red), oxygen (red), mono-protonated μ_2-oxygen (rose). The four subunits were colored differently for clarification.

resulting in icosahedral geometry. Since then some other POMs containing face-shared octahedra have been reported, but this feature still remains rare.[15]

- One ditungstate $\{W_2\}$ subunit (pink in Figure 5.4) made of two edge-shared $[WO_6]$ octahedra connected through two μ_2-oxo bridges. These two types of the ditungstate subunits (face- and edge-shared octahedra) are connected through an edge and a corner forming a tetratungstate $\{W_4\}$ fragment (see Figure 5.4).
- Three monotungstate $\{W_1\}$ fragments (red in Figure 5.4), which are connected to each other or to other fragments through corners.

The $\{W_3\}$ subunit shares two corners with each of two adjacent $\{W_1\}$ subunits, one of them shares a corner with the $\{W_4\}$ subunit and the other one with the third $\{W_1\}$ subunit to build up the decatungstate $\{W_{10}\}$ unit, of which two are present in **26** (see Figures 5.3 and 5.4).

Polyanion **26** represents the first example of a tellurium-containing polyanion exhibiting face-shared WO_6 octahedra and a coordination number of four for Te. Each tellurium(IV) ion is linked to the $\{W_{10}\}$ unit through three μ-oxo bridges and to the other $\{W_{10}\}$ unit through another μ-oxo bridge (see Figure 5.2). The eight μ-oxo bridges of the two tellurium(IV) ions can be described as follows:

- A bridge to the $\{W_3\}$ subunit.
- A bridge to the $\{W_2\}$ subunit (face-shared octahedra).
- A bridge to the $\{W_2\}$ subunit (edge-shared octahedra).
- Three bridges to the three $\{W_1\}$ subunits.
- And two bridges to two $\{W_1\}$ subunits of the other $\{W_{10}\}$ unit.

As shown in Figure 5.3, one tellurium(IV) ion is linked to two $\{W_2\}$ subunits and to one $\{W_1\}$ subunit. The other tellurium(IV) ion is linked to two other $\{W_1\}$ subunits and to the $\{W_3\}$ subunit. All these individual fragments are well-known. However, the $\{W_{10}\}$ unit in **26**, which represents an assembly of distinct 'building blocks' (see Figure 5.4), has not been reported before. Most of the known polyanions containing face-shared octahedra are

polymolybdates. Hence, **26** combines three important features previously unknown for tungstotellurate anions. First, the structure involves face-shared WO_6 octahedra; second, the $\{W_{10}\}$ unit coordinated to tellurium(IV) atoms is novel; and third, the tellurium atoms adopt a see-saw configuration.

Another novel tungstotellurate(IV), $[NaTeW_{15}O_{54}]^{13-}$ (**27**), is present in a mixture of products if the synthesis solution of **26** is heated. Single-crystal X-ray diffraction analysis revealed that $[NaTeW_{15}O_{54}]\cdot 26H_2O$ (**Na-27**) crystallizes in the orthorhombic space group Pccn. Polyanion **27** is composed of a triangular assembly of 15 edge- and corner-shared WO_6 octahedra, surrounding a trigonal-pyramidal tellurium(IV) center located in the central cavity and a capping sodium ion (Figure 5.5). The tellurium and the sodium atom, both closely associated with the polyanion, are disoredered showing 50 % occupancy for each. Polyanion **27** is composed of three identical $\{W_5\}$ building-blocks which are made up of five WO_6 octahedra.

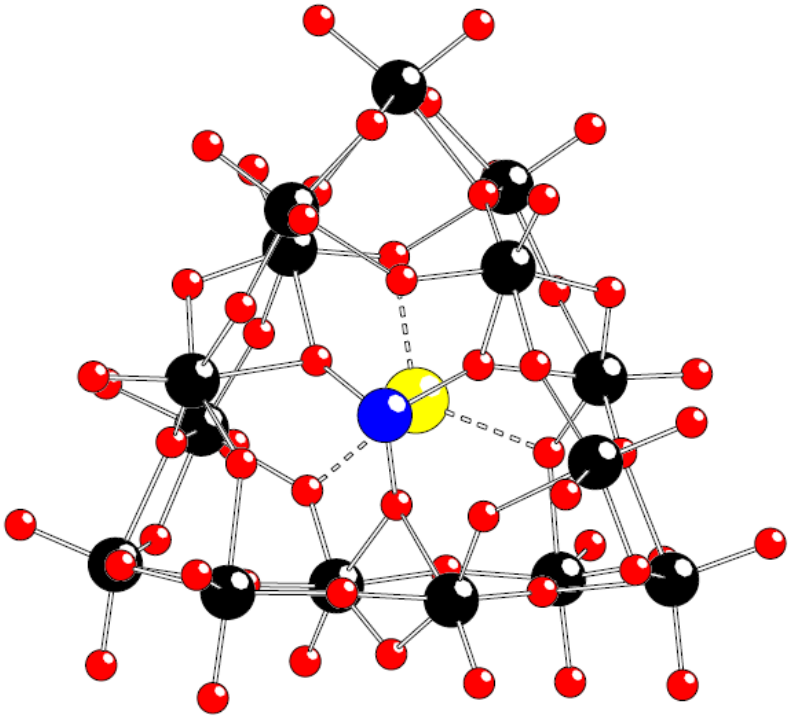

Figure 5.5. Ball-and-stick representations of $[NaTeW_{15}O_{54}]^{13-}$ (**27**). The color code is as the same as Figure 5.2.

The pentatungstate $\{W_5\}$ unit can be considered as an assembly comprising two types of building blocks (see Figure 5.6):

- One tritungstate $\{W_3\}$ fragment (green in Figure 5.6) made of three edge-shared $[WO_6]$ octahedra connected through four μ_2-oxo bridges. This $\{W_3\}$ fragment differs significantly from the $\{W_3\}$ fragment present in polyanion **26** since it lacks the μ_3-oxo bridge which is responsible for the C_3 symmetry in each of the well- known "Keggin" triads.
- One ditungstate $\{W_2\}$ subunit (red in Figure 5.6) composed of two edge-shared $[WO_6]$ octahedra linked to the $\{W_3\}$ fragment through two μ_2-oxo bridges and one μ_3-oxo bridge.

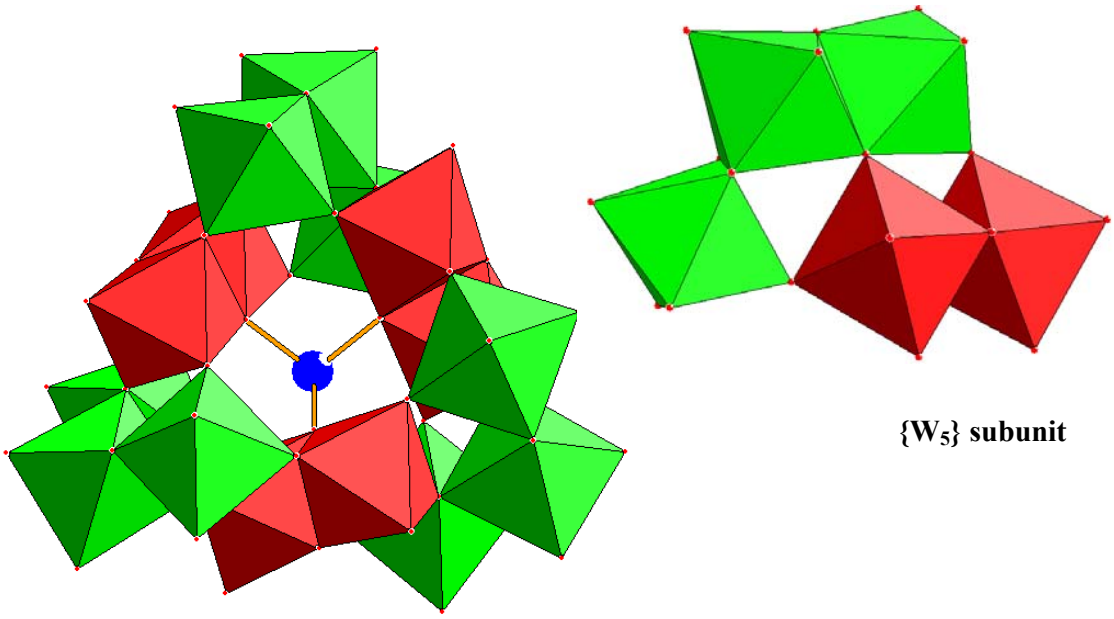

Figure 5.6. Polyhedral representations of the **{TeW$_{15}$}** and the basic building-block unit $\{W_5\}$ of (**27**). The color code is as follows: W_3 (green), W_2 (red), Te (blue). The two subunits were colored differently for clarification.

Each of the $\{W_2\}$ subunits shares three corners with $\{W_3\}$ of another pentatungstate $\{W_5\}$ unit, consequently forming the isopolytungstate unit $\{W_{15}\}$ with a D_3 point group symmetry. The cavity of the $\{W_{15}\}$ isopolytungstate unit adapts the tellurium atom which is coordinated to the three $\{W_2\}$ subunits resulting in a trigonal pyramidal geometry, and the sodium atom. The Te and Na atoms have 50 % occupancy eachin their positions. Crystallographically, the pentadecatungstate unit $\{W_{15}\}$ has an asymmetric unit consisting of eight WO_6 octahedra, $\{W_8\}$, with one of them being unique. A related pentadecatungstate $\{W_{15}\}$ unit capped by two Ce^{3+} ions has been reported recently by the Cao group.[16]

Bond valence sum (BVS) calculations for **26** and **27** are consistent with all tungsten atoms being in the +6 oxidation state, and all tellurium ions being in the +4 oxidation state.[17] In addition, in **26,** one monoprotonated oxygen was identified in the asymmetric half-unit, (BVS ~ 1.06), one of the three μ_2-oxo bridges of the $\{W_3\}$ fragment, namely the μ_2-oxo group of W7 and W8 (pink in Figure 5.4). This results in two OH groups for **26** and a total charge of -22 for the polyanion. The range of BVS for non-protonated bridging oxygens is (2.06 – 1.49). The terminal W=O oxygen BVS values are low (~ 1.5), but this is typical for the distorted W=O geometry and does not indicate additional protonation. Polyanion **27** has no apparent protonation sites.

Thermogravimetric analyses (TGA) were performed on **Na-26** to determine its degree of hydration and thermal stability. The TGA graph showed a region of weight loss due to dehydration, with a one-step weight loss in the range ~25-400 ˚C. We calculated 64 water molecules per formula unit of **Na-26** which agrees well with the results obtained by single-crystal XRD. Furthermore, the absence of any additional weight loss indicated that **Na-26**, after loss of the crystal waters, was thermally stable up to 800-900 °C (see Figure 5.7). As stated above, polyanion **27** was synthesized and co-crystallized in a mixture of products, preventing the interpretation of the thermal stability of **Na-27**. However, we were able to obtain the IR spectrum of **Na-27** (see Figure 5.8).

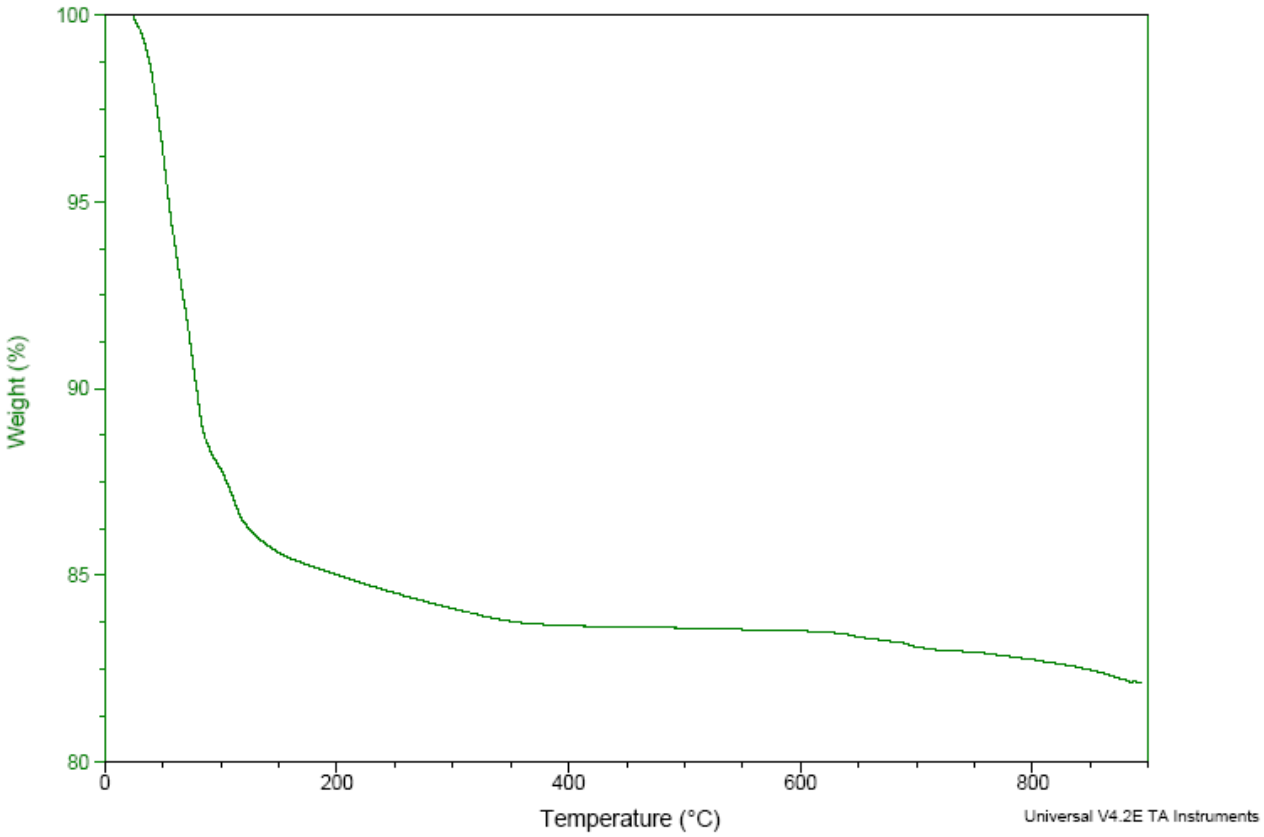

Figure 5.7. Thermogram of **Na-26**.

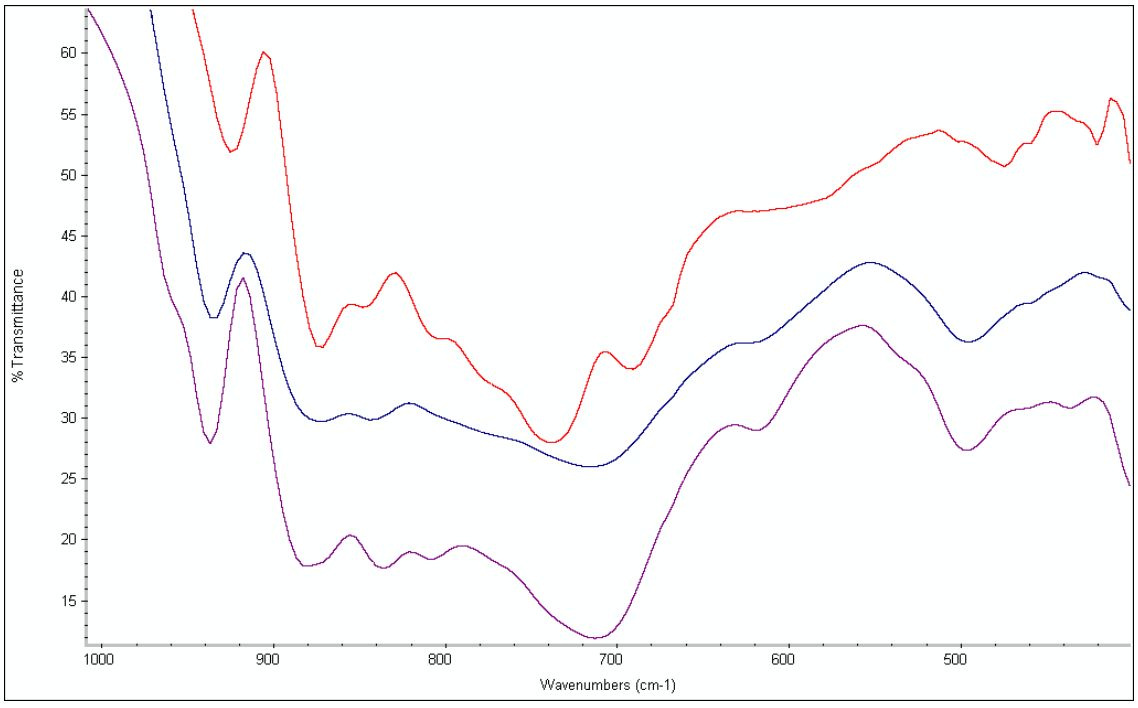

Figure 5.8. IR spectra of the sodium salts of $[H_2Te_4W_{20}O_{80}]^{22-}$ (**26**, red curve), $[NaTeW_{15}O_{54}]^{13-}$ (**27**, blue curve), and paradodecatungstate $[H_2W_{12}O_{42}]^{10-}$ (violet curve).

Although we followed exactly the synthetic procedure for $[TeW_9O_{33}]^{8-}$ published by Gaunt et al.,[11] we were unable to confirm the existence of this compound. Instead, we obtained the two novel tungstotellurate polyanions **26** and **27**. In order to test whether a mixture of the sodium salts of **26** and paradodecatungstate would react to yield POMs containing the $[TeW_9O_{33}]^{8-}$ unit, we added such a mixture of crystals (sodium salts of **26** and $[H_2W_{12}O_{42}]^{10-}$) to a solution of $CuCl_2 \cdot 2H_2O$ in sodium acetate buffer (pH 4.8). This reaction mixture was heated to 90 ˚C for 1 h and filtered after cooling, and then a few drops of 1M KCl solution were added. Slow evaporation at room temperature led to the formation of green crystals of $K_9Na[Cu_3(H_2O)_3(\alpha\text{-}TeW_9O_{33})_2]$.[9] We note, however, that the IR spectrum reported by Gaunt et al. is not identical to the one we obtained; therefore, the question of whether uncomplexed $[TeW_9O_{33}]^{8-}$ can be isolated is still an open one.

5.A.1.5. Conclusions

We have successfully synthesized and structurally characterized by IR spectroscopy, TGA and single crystal X-ray diffraction a novel tellurium containing, polytungstate, $[H_2Te_4W_{20}O_{80}]^{22-}$ (**26**). This polyanion was synthesized in aqueous sodium chloride medium by reaction of Na_2WO_4 with TeO_2 at pH 7.5. Polyanion **26** was isolated as a sodium salt and crystallized in the triclinic space group $P\bar{1}$. Single crystal X-ray structural analysis showed that **26** is composed of a 20-tungsten polyanion unit $\{W_{20}\}$ coordinated to four tellurium ions having coordination number four. The 20-tungstate unit $\{W_{20}\}$ consists of two $\{W_{10}\}$ subunits which are connected by a total of four Te-O-W bridges. The decatungstate $\{W_{10}\}$ subunit has not been reported before. Each $\{W_{10}\}$ subunit contains a pair of face-shared octahedra and two tellurium(VI) ions having a see-saw type geometry. In addition, we have synthesized and structurally characterized by IR spectroscopy and single crystal X-ray diffraction another novel tellurium-containing polytungstate $[NaTeW_{15}O_{54}]^{13-}$ (**27**). Polyanion **27** could not be obtained as a bulk pure material because it co-crystallized with two other species.

5.A.1.6. References

[1] a) *Heteropoly and Isopoly Oxometalates*; M. T. Pope, Springer-Verlag: Berlin, 1983; b) M. T. Pope, A. Müller, *Angew. Chem. Int. Ed. Engl.* **1991**, *30*, 34; c) *Polyoxometalates: From Platonic Solids to Anti- Retroviral Activity*; M. T. Pope, A. Müller, Eds.; Kluwer: Dordrecht, The Netherlands, 1994; d) A. Müller, H. Reuter, S. Dillinger, *Angew. Chem. Int. Ed. Engl.* **1995**, *34*, 2328; e) *Polyoxometalates: Chemical Reviews*, C. Hill, **1998** (special thematic issue on polyoxometalates); f) *Polyoxometalate Chemistry: From Topology via Self-Assembly to Applications,* M. T. Pope, A. Müller, Eds.; Kluwer: Dordrecht, The Netherlands, 2001; g) *Polyoxometalate Chemistry for Nano-Composite Design;* T. Yamase, M. T. Pope, Eds.; Kluwer: Dordrecht, The Netherlands, 2002; h) G. R. J. Choppin, *Nucl. Radiochem. Sci.* **2005**, *6*, 1.

[2] a) J. S. Anderson, *Nature* **1937**, *140*, 850; b) H. T. Jr. Evans, *J. Am. Chem. Soc.* **1948**, *70*, 1291. (c) H. T. Jr. Evans, *Acta. Cryst.* **1974**, *B30*, 2095.

[3] a) K. J. Schmidt, G. J. Schrobilgen, J. F. Sawyer, *Acta Crystallogr.* **1986**, *C42*, 1115; b) A. Sagasaki, Y. Sasaki, *Bull. Chem. Soc. Jpn* **1987**, *60*, 763; c) T. Ozeki, A. Yagasaki, H. Ichida, Y. Sasaki, *Polyhedron* **1988**, *7*, 1131; d) M. S. Grigorev, Yu. T. Struchkov, A. M. Feddoseev, A. B. Yusov, A. I. Yanovskii, *Z. Neorg. Khim.* **1992**, *37*, 2507; e) C. Robl, M. Frost, *Z. Anorg. Allg. Chem.* **1993**, *619*, 1834; f) C. Robl, M. Frost, *Z. Anorg. Allg. Chem*, **1993**, *619*, 1137; g) C. Robl, M. Frost, *Z. Anorg. Allg. Chem.* **1993**, *619*, 1132; h) C. Robl, M. Frost, *Z. Anorg. Allg. Chem.* **1993**, *619*, 1624; i) C. Robl, M. Frost, *Z. Naturforsch. B*, **1993**, *48*, 404; j) P. A. Lorenzo-Luis, P. Martin- P. Zarza, R. Gili, Saez-Puche, J. Jimenez-Jimenez, E. Rodriguez-Castellon, C. Ruiz-Perez, J. Gonzalez-Platas, X. Solans, *Eur. Solid State Inorg.Chem.* **1997**, *34, 1271*; j) D. Drewes, E. M. Limanski, B. Krebs, *Dalton*, **2004**, 2087; k) D. Drewes, E. M. Limanski, B. Krebs, *Eur. Inorg. Chem.* **2004**, 4849; l) D. Drewes, B. Krebs, *Z. Anorg. Allg. Chem.* **2005**, *631*, 2591; m) I. A. Charushnikova, A. B. Yusov, A. M. Feddoseev, I. N.

Polyakova, *Z. Neorg. Khim.* **2004**, *49*, 1481; n) I. A. Charushnikova, A. M. Feddoseev, A. B. Yusov, C. D. Auwer, *Crystallogr. Reports* **2005**, *50*, 191; o) G. Bo, L. Shu-Xia, X. Lin-Hua, Y. Miao, Z. Chung-Dan, S. Chung-Yan, C. Hai-Yan, *J. Solid State Chem.* **2006**, *179*, 1689.

[4] a) P. A. Lorenz-Luis, P. Martin-Zarza, A. Sanchez, M. Hernandez-Molina, X. Solans, P. Gili, *Inorg. Chim. Acta* **1998**, *277*, 139; b) P. Gili, P. A. Lorenz-Luis, P. Martin-Zarza, S. Dominguez, A. Sanchez, J. M. Arrieta, E. Rodriguez-Castellon, J. Jimenez-Jimenez, C. Ruiz-Perez, M. Hernandez-Molina, X. Solans, *Transiton Met. Chem.* **1999**, *24*, 141; c) F. Wang, S.-X. Liu, C.-L. Wang, R.-G. Cao, J.-F. Cao, *Acta Crystallogr.* **2007**, *E63*, m1708; d) Z.-H. Xu, P.-X. Xi, F.-J. Chen, Z.-Z. Zeng, *Analytical Sciences* **2007**, *23*, x235.

[5] a) E. S. Ganelina, *Russ. J. Inorg. Chem.* **1962**, *7*, 812; b) E. S. Ganelina, N. I. Nerevyatkina, *Russ. J. Inorg. Chem.* **1965**, *10*, 483; c) R. Ripan, N. Calu, *Stud.Univ. Babes-Bolyai, Chem.* **1965**, *10*, 135.

[6] P. A. Lorenz-Luis, P. Gili, *Transiton Met. Chem.* **1999**, *24*, 686.

[7] E. N. Yurchenko, *Koord. Khim.* **1992**, *18*, 944.

[8] a) M. Bösing, A. Nöh, I. Loose, B. Krebs, *J. Am. Chem. Soc.* **1998**, *120,* 7252; b) B. Krebs, M. Droste, M. Piepenbrink, pages 89-99 in ref. 1f; c) E. M. Limanski, D. Drewes, E. Droste, R. Böhner, B. Krebs, *J. Mol. Struct.* **2003**, *656*, 17.

[9] U. Kortz, N. K. Al-Kassem, M. G. Savelieff, N. A. Al Kadi, M.Sadakane, *Inorg. Chem.* **2001**, *40*, 4742.

[10] U. Kortz, M. G. Savelieff, B. S. Bassil, B. Keita, L. Nadjo, *Inorg. Chem.* **2002**, *41*, 783.

[11] A. J. Gaunt, I. May, R. Copping, A. I. Bhatt, D. Collison, O. D. Fox, K. T. Holman, M. T. Pope, *Dalton Trans.* **2003**, 3009.

[12] W. Levason, *Coord. Chem. Rev.* **1997**, *161*, 33; *Chem. Rev.* an issue devoted to polyoxometalates (guest editor C. L. Hill) **1998**, *98*.

[13] G. M. Sheldrick, *Acta. Cryst.* **2008**, *A64*, 122.

[14] D. D. Dexter, J. V. Silverton, *J. Am. Chem. Soc.* **1968**, *90*, 3589.

[15] a) W. Kwak, L. M. Rajkovic, M. T. Pope, C. O. Quicksall, K. Y. Matsumoto, Y. Sasaki, *J. Am. Chem. Soc.* **1977**, *99*, 6463; b) K. Y. Matsumoto, *Bull. Chem. Soc. Jpn.* **1978**, *51*, 492; c) S. H. Wasfi, M. L. Pope, K. M. Barkigia, R. J. Butcher, C. O. Quicksall, *J. Am. Chem. Soc.* **1978**, *100*,7786; d) L. Ben-Yao, G. Yi-Dong, W. Xin, *Chin. J. Chem.* **1990**, *8*, 37; e) E. O. Tolkacheva, V. S. Sergienko, A. B. Ilykukhin, *Russ. J. Inorg. Chem.* **1997**, *42*, 752; f) E. Dumas, S. C. Sevov, *Inorg. Chem.* **2002**, *41*, 144; g) Y-G. Chen, L-K. Yan, X-R. Hao, K. Liu, X-H. Wang, P-P. Lu, *Inorg. Chim. Acta* **2002**, *359*, 2550; h) B. J. S. Johnson, R. C. Scharoden, C. Zhu, V. G. Young, A. Stein, *Inorg. Chem.* **2002**, *41*, 2213.

[16] T. Li, F. Li, J. Lü, Z. Guo, S. Gao, R. Cao, *Inorg. Chem.* **2008**, *47*, 5612.

[17] D. Altermatt, I. D. Brown, *Acta. Cryst.* **1985**, *B41*, 244.

5.A.2. Tellurium-Containing Polyoxomolybdates: The 44-Molybdo-24-Tellurate(IV), $[H_2Te_{24}Mo_{44}O_{198}]^{34-}$

5.A.2.1. Introduction

Polyoxometalates (POMs) represent a large class of nanosized metal-oxygen cluster anions. POMs are remarkable not only in terms of molecular and electronic structural versatility, but also due to their applications in many fields such as catalysis, medicine, electronics, multifunctional materials, and analytical chemistry.[1] In recent years there has been developing interest in these remarkable compounds of tungsten, molybdenum, vanadium, niobium, and tantalum. POM clusters have been known for a long time (first prepared in 1826 by Berzelius) but the mechanism of their formation is still not completely understood, and is often described as "self-assembly".[1a]

POMs are formed through condensation reactions of metalate ions in acidified solutions (usually aqueous), via aggregation of octahedral $[MO_6]$ building blocks sharing corners, edges, and rarely faces. Many of the reported POMs are based on the well-known Keggin ion ($[XM_{12}O_{40}]^{n-}$), or lacunary fragments of that structure, where X is the central heteroatom and M the addenda atom. The heteroatom can be one of many elements of the periodic table, most commonly P, As, Si, Ge or B.

Also tellurium can act as a heteroatom, but the number of such POMs is rather limited. In 1948 Evans reported the first structure of a tellurium containing polyanion, $[TeMo_6O_{24}]^6$.[2] Many other inorganic salts of the Anderson-Evans type molybdotellurate(VI) $[TeMo_6O_{24}]^{6-}$ have been reported ever since.[3] Molybdotellurates containing organic counter-cations have also been described.[4] The first examples of the Anderson-Evans type tungstotellurate $[TeW_6O_{24}]^{6-}$ were reported by Ganelina and Ripan.[5] Some examples of tellurium(IV) containing polymolybdates are also known. The manganese derivative of the classical

Anderson-Evans type molybdotellurate(VI) has been reported by Bo et al. The same research group also reported the cerium derivative one.[6] A series of lanthanide polyoxomolybdates was synthesized before by the Krebs group by reaction of lanthanide cations with the Anderson-Evans type anion $[TeMo_6O_{24}]^{6-}$.[7]

On the other hand, we recently reported two tungstotellurate(IV) anions $[H_2Te_4W_{20}O_{80}]^{22-}$ and $[NaTeW_{15}O_{54}]^{13-}$.[8] The two polyanions were synthesized by the reaction of WO_4^{2-} and Te^{4+} in aqueous medium (pH 7.5). The polyanion $[H_2Te_4W_{20}O_{80}]^{22-}$ comprises two $\{HTe_2W_{10}O_{40}\}$ fragments, connected through Te−O−W μ_2-oxo bridges, and each containing a pair of face-shared WO_6 octahedra. The polyanion $[NaTeW_{15}O_{54}]^{13-}$ is composed of a triangular assembly of 15 edge- and corner-shared WO_6 octahedra, surrounding a trigonal-pyramidal tellurium(IV) center located in the central cavity and a capping sodium ion.

The complete lack of molybdotellurates(IV) as such $[H_2Te_4W_{20}O_{80}]^{22-}$ and $[NaTeW_{15}O_{54}]^{13-}$ analogues provides an impetus to try to prepare such species. Herein we report on a novel chiral molybdotellurate(IV) structure.

5.A.2.2. Synthesis

$Na_{34}[H_2Te_{24}Mo_{44}O_{198}]\cdot 84H_2O$ (Na-28)

A sample of 5.0 g of $Na_2MoO_4\cdot 2H_2O$ (20.7 mmol) was dissolved in 20 mL H_2O, followed by dropwise addition of a solution of 0.66 g of TeO_2 (4.1 mmol) in 2 mL concentrated HCl. Then the pH was adjusted to 6.5 using 6M aqueous NaOH. The mixture was vigorously stirred at room temperature for 1 hour, and then filtered. The filtrate was kept in an open vial for crystallization at room temperature. Colorless crystals of **Na-28** were obtained after three days which were in turn filtered off and air-dried. Yield: 1.18 g (53.6 %). IR for **Na-28** in cm^{-1} (only between 400-1000 cm^{-1}): 925(m), 867(s), 849(s), 808(m), 772(s), 705(m), 667(s),

610(m), 569(m), 503(m), 432(m), 407(m) (see Figure 5.9). Anal. Calcd (%) for **Na-28**: Na, 6.1; Mo, 33.1; Te, 24.2. Found (%): Na, 6.3; Mo, 33.2; Te, 24.3.

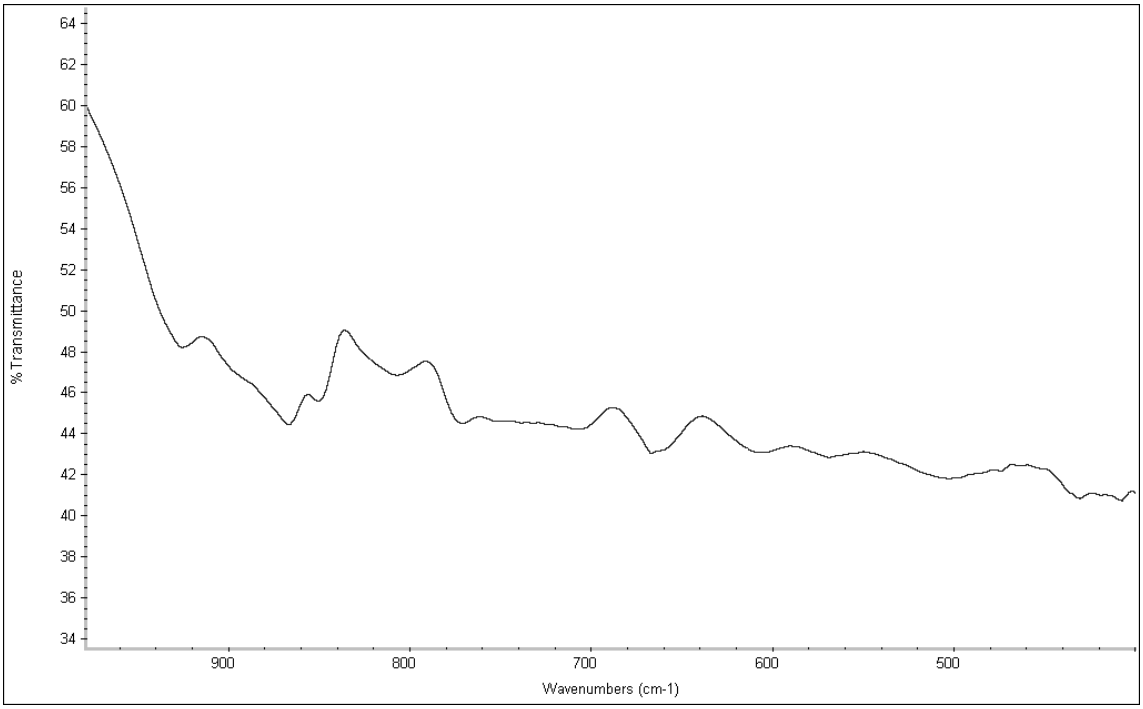

Figure 5.9. IR spectrum of the compound **Na-28**.

5.A.2.3. X-ray Crystallography

All crystals were mounted in Hampton cryoloops using light oil, for data collection at low temperature. Indexing and data collection were performed using a Bruker X8 APEX II CCD diffractometer with kappa geometry and Mo K_α radiation (λ = 0.71073 Å). Data integration and routine processing were performed using the SAINT software suite. Further data processing, including multi-scans absorption corrections, was performed using SADABS. Direct methods (SHELXS97) solutions successfully located the W atoms, and successive Fourier syntheses (SHELXL97) revealed the remaining atoms.[10] Refinements were full-matrix least squares against F^2 using all data. Some cations and waters of hydration were modeled with varying degrees of occupancy, a common situation for polyoxotungstate structures. In the final refinements, all nondisordered heavy atoms (Mo, Te) were refined

anisotropically, while the O and Na atoms were refined isotropically. No H atoms were included in the models. The crystallographic data are summarized in Table 5.5.

Table 5.5. Crystal Data and Structure Refinement for $Na_{34}[H_2Te_{24}Mo_{44}O_{198}]\cdot 84H_2O$ **(Na-28)**.

Code	**Na-28**
Empirical formula	$H_2Na_{34}O_{282}Te_{24}Mo_{44}$
MW	12748.8
Crystal system	Triclinic
Space group (no.)	$P\bar{1}$ (2)
a/Å	17.301(11)
b/Å	25.419(19)
c/Å	36.150(3)
α/°	74.402(3)
β/°	77.461(2)
γ/°	77.488(2)
V/Å^3	14733.4(18)
Z	2
T/ ºC	-100(2)
λ/Å	0.71073
D/ Mg m^{-3}	2.874
μ/ mm^{-1}	4.304
R[I >2sigma(I)][a]	0.110
R_w (all data)[b]	0.263

[a] $R = \sum|F_o| - |F_c| \,|\sum| \,|F_o|$; [b] $R_w = \{\sum[w(F_o^2 - F_c^2)^2] / \sum[w(F_o^2)^2]\}^{1/2}$.

5.A.2.4. Results and Discussion

We performed a systematic study on the interaction of tellurium(IV) ions with sodium molybdate in neutral, aqueous medium, and at a ratio of 1 : 5 we were able to isolate crystals of $Na_{34}[H_2Te_{24}Mo_{44}O_{198}]\cdot 84H_2O$ (**Na-28**). Four reaction parameters are crucial for the successful formation and isolation of $[H_2Te_{24}Mo_{44}O_{198}]^{34-}$ (**1**) in a pure form: solvent, reaction temperature, molar ratio of reagents, and pH of the solution. Polyanion **1** is formed in water but the same reaction performed in 1M NaCl or sodium acetate buffer solution resulted in a different product based on FTIR which has not been characterized yet. Polyanion **1** is formed at room temperature, but if the solution is heated then a considerable amount of unidentified white precipitate was formed during the synthetic procedure which affects the yield observed. Thus, polyanion **1** also form upon heating, but the yield is much higher at room temperature. The ratio of the reagents TeO_2 and Na_2MoO_4 should be 1: 5 to obtain a pure product and high yield. It is noteworthy that the ratio 1: 2 which is similar to that obtained in the structure (1: 1.8) gives a significant yellow precipitate during the synthetic procedure which gives a low yield at this ratio. Finally, the pH of the reaction solution affects the formation of **1** and yield of **Na-28**. A pH window of 6.1-6.9 resulted in a successful synthetic procedure, with pH 6.5 being optimal. A pH lower than 6.1 resulted undistinguished compound as the main product while at higher than 6.9 resulted $Na_2MoO_4\cdot 2H_2O$ as the main product or as co-crystalline material with **1** as based on FTIR and single-crystal XRD.

Interestingly, we discovered **1** when we were trying to crystallize the molydotellurate(IV) analogues of $[H_2Te_4W_{20}O_{80}]^{22-}$ or $[NaTeW_{15}O_{54}]^{13-}$ following the synthetic procedures that were used before.[8]

Polyanion **1** crystallized as a hydrated sodium salt in the triclinic space group $P\bar{1}$. The single-crystal X-ray analysis showed that **1** consists of 24 tellurium atoms coordinated to novel building blocks stabilizing the 44 isopolymolybdate. The structure of

$[H_2Te_{24}Mo_{44}O_{198}]^{34-}$ (**1**) comprises two $\{HTe_{12}Mo_{22}O_{98}\}$ $\{\mathbf{Te_{12}Mo_{22}}\}$ fragments which are connected via two μ_2-oxo bridges (Te−O−Te). Hence polyanion **1** can be described as a dimeric molecular entity composed of two $\{\mathbf{Te_{12}Mo_{22}}\}$ half units which lack any kind of symmetry element (see Figure 5.10 and 5.11).

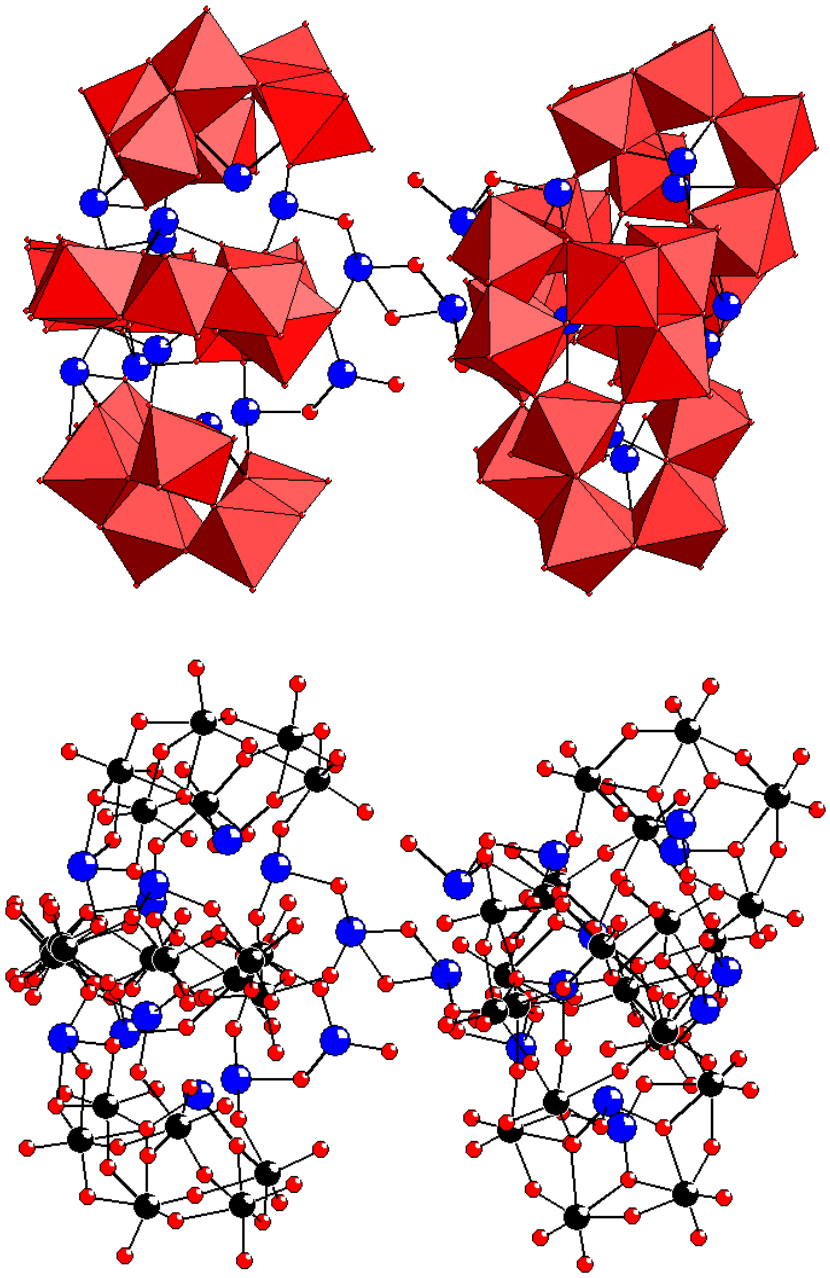

Figure 5.10. Polyhedral (upper) and ball-and-stick (lower) representations of $[H_2Te_{24}Mo_{44}O_{198}]^{34-}$. The color code is as follows: MoO_6 octahedra (red); Te (blue), Mo (black); O (red).

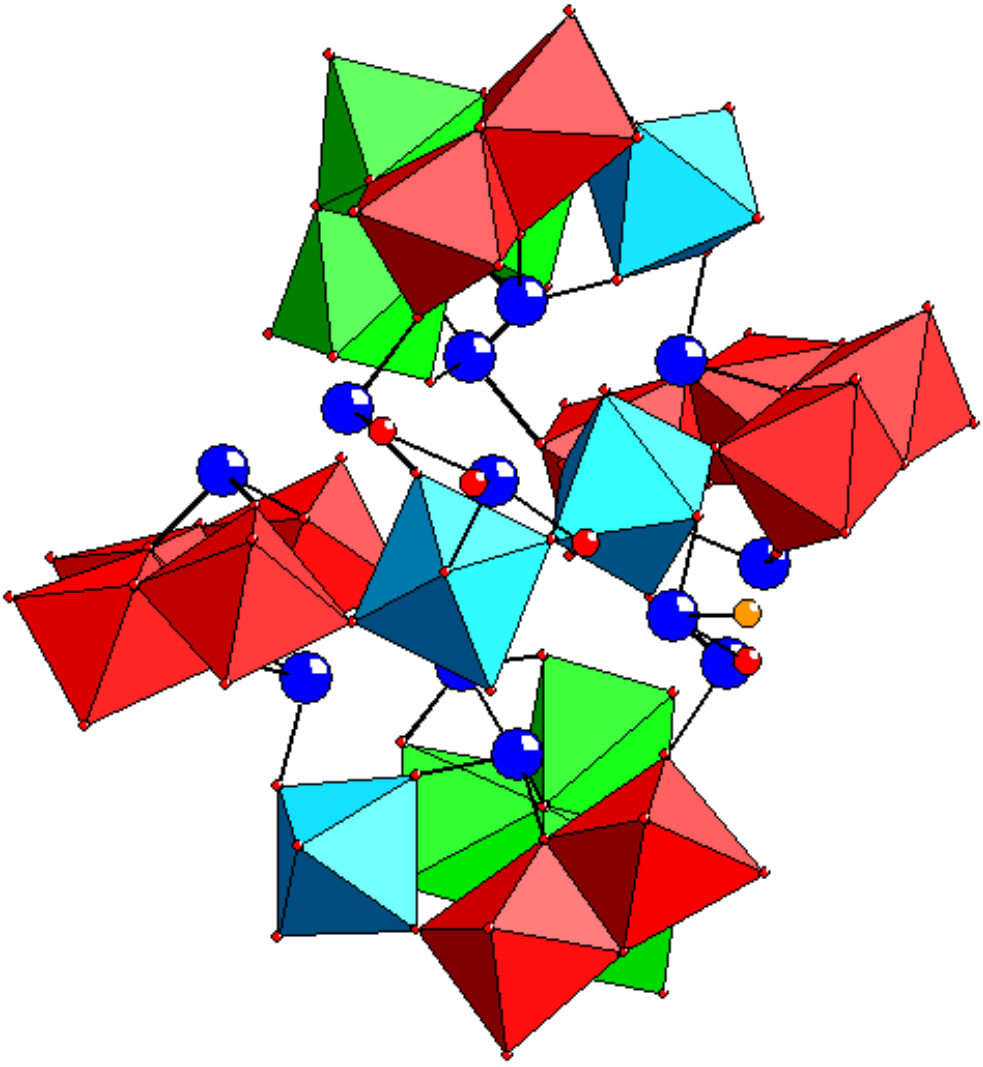

Figure 5.11. Polyhedral representation of the asymmetric $\{HTe_{12}Mo_{22}O_{98}\}$ half-unit. The color code is as follows: MoO_6 octahedra (green, red, light blue); Te (blue); O (red), mono-protonated oxygen (orange). The MoO_6 octahedra were colored differently for clarity.

Each {**$Te_{12}Mo_{22}$**} unit can be considered as an assembly of three types of 'building blocks' (see Figure 5.11 and 5.12) and this unit can be considered as two caps and a belt. Each cap (a hexamolybdate {Mo_6} subunit) consists of three building blocks:

- One trimolybdate {Mo_3} fragment (green in Figure 5.12) made of three edge-shared [MoO_6] octahedra connected via a μ_3-oxo bridge. This fragment can be viewed as a single 'triad' of the well-known Keggin and Wells-Dawson structures.[1a]
- One dimolybdate {Mo_2} subunit (red in Figure 5.12) made of two edge-shared [MoO_6] octahedra connected through two μ_2-oxo bridges.
- One monomolybdate {Mo_1} subunit (blue in Figure 5.12). These three subunits ({Mo_3}, {Mo_2}, and {Mo_1}) are connected to each other via three corners forming a hexamolybdate {Mo_6} subunit. The {Mo_3} subunit shares two corners with the adjacent {Mo_2} and a corner with the {Mo_1} subunit to build up this {Mo_6} subunit.

Belt ({Mo_{10}} subunit) consists of two building blocks:

- Two tetramolybdates {Mo_4} subunits (red in Figure 5.12) made of four edge-shared [MoO_6] octahedra connected through six μ_2-oxo bridges.
- Two monomolybdate {Mo_1} subunits (blue in Figure 5.12). These two types of the subunits ({Mo_4} and {Mo_1}) are connected to each other via corners forming a decamolybdate {Mo_{10}} subunit.

The two caps {Mo_6} and the belt {Mo_{10}} units are connected to each other via Te−O−Mo μ_2-oxo bridges, through six Te^{4+} ions each. The Te atoms have coordination number three and four leading to a trigonal-pyramidal and a see-saw coordination geometry.

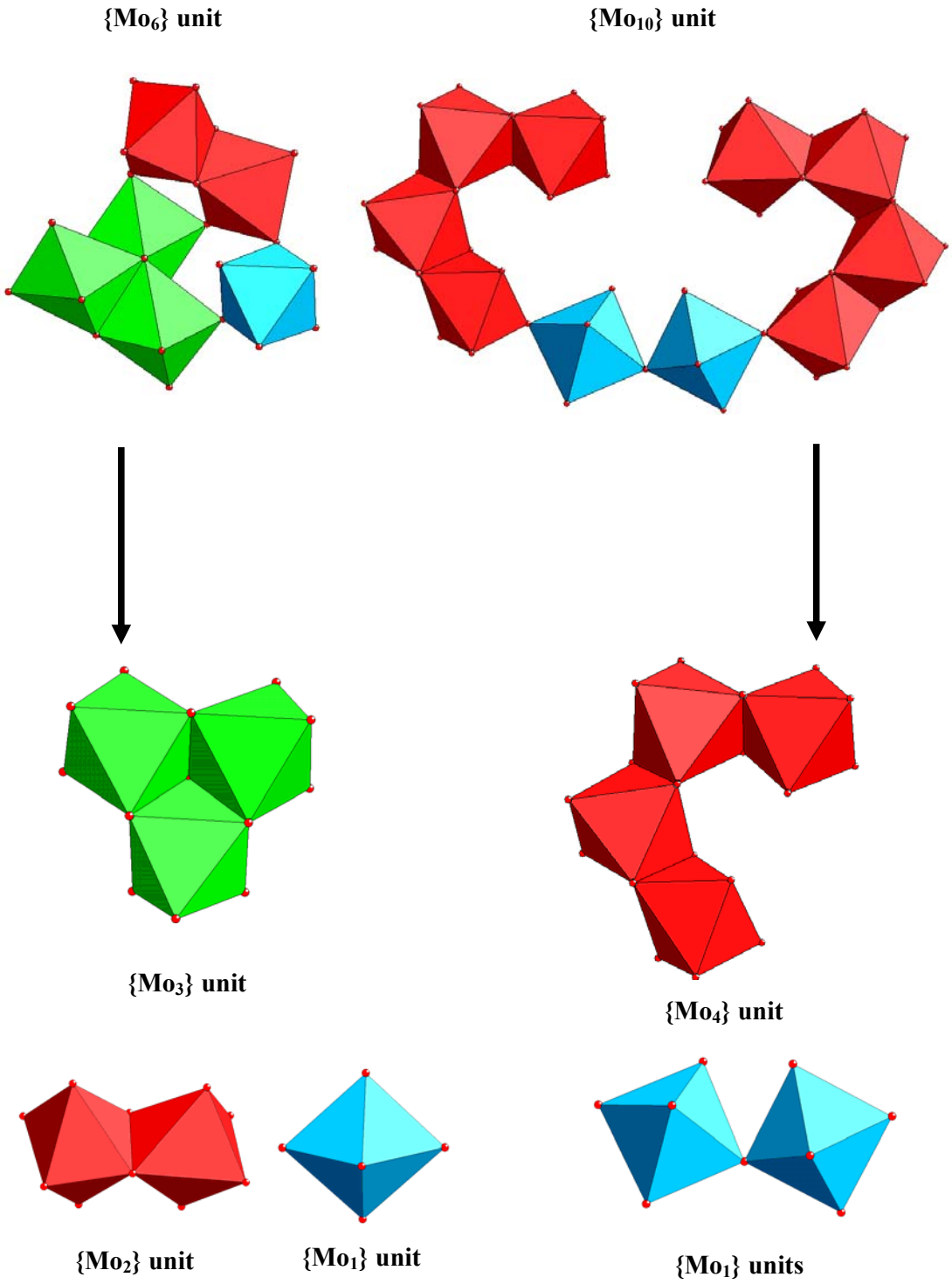

Figure 5.12. Polyhedral representation of the building blocks forming the hexa- and deca-molybdates, $\{Mo_6\}$ and $\{Mo_{10}\}$, units. The color code is as follow: Mo_3 (green), Mo_2 (red), Mo_1 (light blue), Mo_4 (red). The four subunits were colored differently for clarification.

As shown in Figure 5.11, the tellurium(IV) ions are linked to the $\{Mo_4\}$, $\{Mo_3\}$, $\{Mo_2\}$, and $\{Mo_1\}$ subunits. All these individual fragments are well-known. However, the $\{Mo_6\}$ and $\{Mo_{10}\}$ units in **1**, which represents an assembly of distinct 'building blocks' (see Figure 5.12), has not been reported previously. Hence, **1** combines three significant features not previously reported for molybdotellurate anions. Firstly, the $\{Mo_6\}$ and $\{Mo_{10}\}$ units coordinated to tellurium(IV) atoms are novel; secondly, the tellurium atoms adopt a trigonal-pyramidal and a see-saw configuration; and thirdly, the structure of **1** consists of two $\mathbf{Te_{12}Mo_{22}}$ fragments which are connected via two Te−O−Te bridges.

Bond valence sum (BVS) calculations for **1** is consistent with all molybdenum atoms being in the +6 oxidation state, and all tellurium ions being in the +4 oxidation state.[9] In addition, one monoprotonated oxygen was identified in the asymmetric half-unit, (BVS ~ 1.12), the only terminal oxo bridge of the tellurium ions (orange in Figure 5.11). This results in two OH groups for **1** and a total charge of -34 for the polyanion. The range of BVS for non-protonated bridging oxygens is (2.12 – 1.51). The terminal Mo=O oxygen BVS values are low (~ 1.5), but this is typical for the distorted Mo=O geometry and does not indicate additional protonation.

Thermogravimetric analyses (TGA) was performed on the sodium salt of polyanion **1** to determine its degree of hydration and thermal stability. The TGA graph showed a region of weight loss due to dehydration, with a one-step weight loss in the range ~25-400 ˚C. We calculated 84 water molecules per formula unit of **Na-28**. This result was also supported by elemental analysis. Furthermore, the absence of any additional weight loss indicated that **Na-28**, after loss of the crystal waters, was thermally stable up to 800-900 °C (see Figure 5.13).

Although we followed exactly the synthetic procedure for $[H_2Te_4W_{20}O_{80}]^{22-}$ published by our group,[8] we were unable to identify such this analogue in NaCl solution. Instead, we obtained the novel molybdotellurate polyanion **1** in water. In order to identify the obtained

compound in NaCl solution, we tried to re-crystallize the product but we obtained a mixture of the sodium salts of **1**, the starting material, MoO_4^{2-} and an undistinguished compound.

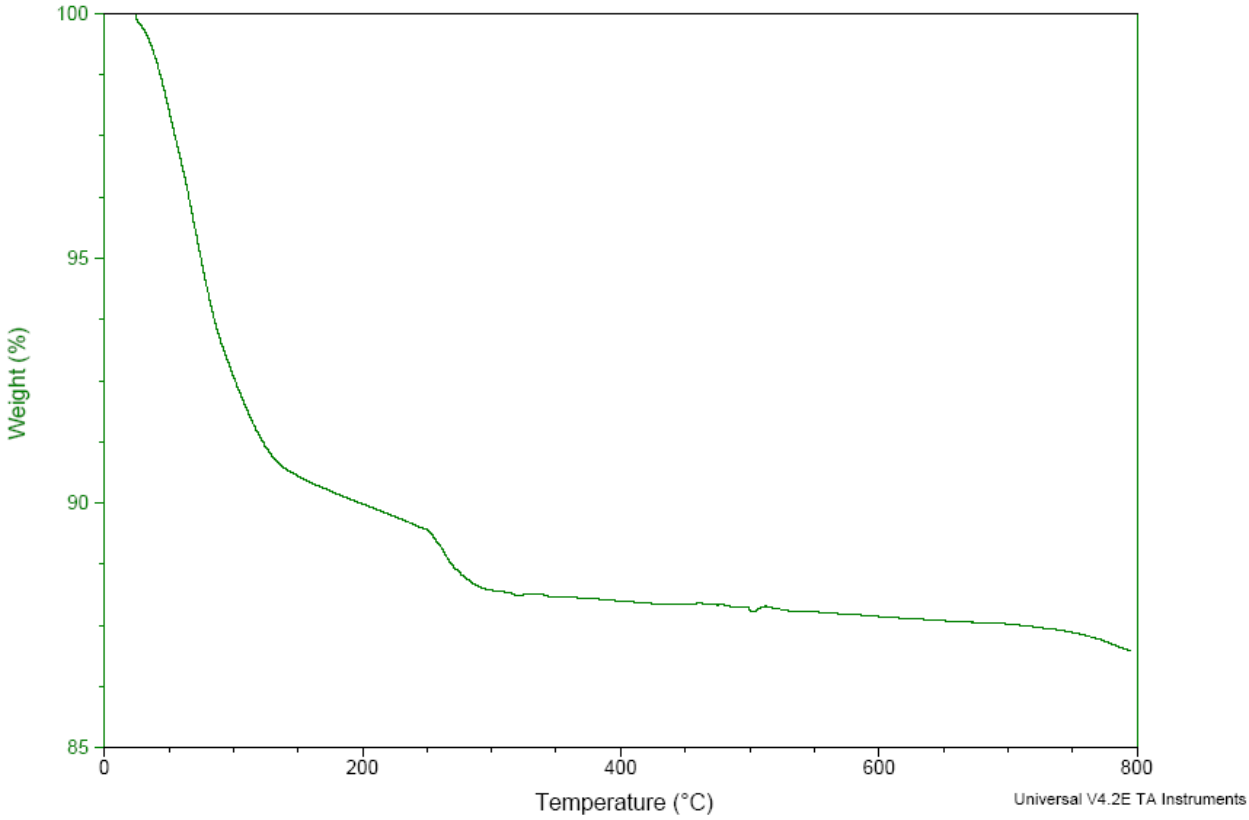

Figure 5.13. Thermogram of **Na-28**.

5.A.2.5. Conclusions

We have successfully synthesized and structurally characterized by FTIR spectroscopy, TGA and single crystal X-ray diffraction a novel tellurium containing, polymolybdate, $[H_2Te_{24}Mo_{44}O_{198}]^{34-}$ (**1**). This polyanion was synthesized in aqueous medium starting from Na_2MoO_4 and TeO_2. Polyanion **1** was isolated as a sodium salt and crystallized in the triclinic space group $P\bar{1}$. Single crystal X-ray structural analysis showed that **1** is composed of a 44-molybdenum and 24 tellurium ions having coordination number three and four, leading to a trigonal-pyramidal and a see-saw coordination geometry. Polyanion **1** comprises two $\{HTe_{12}Mo_{22}O_{98}\}$ fragments, connected via two Te−O−Te μ_2-oxo bridges. Polyanion **1** is a chiral structure having a C_2 symmetry. The 44-tmolybdate fragments are assembled from two

novel $\{Mo_6\}$ and $\{Mo_{10}\}$ subunits connected by Te−O−W bridges. These hexa- and deca-molybdates, $\{Mo_6\}$ and $\{Mo_{10}\}$, subunits have not been reported before.

The rare existence of structurally characterized of d-transition metals containing molybdotellurates(IV) provides an impetus to try to prepare new species of molybdotellurates(IV). Hence, we tried to incorporate d-transition metal ions (Mn^{2+}, Fe^{3+}, Co^{2+}, Ni^{2+}, Cu^{2+}, Zn^{2+}, and Pd^{2+}) in polyanion **1** using different synthetic pathways. So far, we could not identify the crystalline materials obtained by using single-crystal X-ray diffraction and this will be the scope of further studies.

5.A.2.6. References

[1] a) M. T. Pope in *Heteropoly and Isopoly Oxometalates*, Springer-Verlag, Berlin, 1983; b) M. T. Pope, A. Müller, *Angew. Chem.,* **1991**, *103*, 56, *Angew. Chem., Int. Ed. Engl.* **1991**, *30*, 34; c) M. T. Pope, A. Müller in *Polyoxometalates: From Platonic Solids to Anti- Retroviral Activity* (Eds.: M. T. Pope, A. Müller), Kluwer: Dordrecht, The Netherlands, 1994; d) A. Müller, H. Reuter, S. Dillinger, *Angew. Chem.,* **1995**, *107*, 2505, *Angew. Chem., Int. Ed. Engl.* **1995**, *34*, 2328; e) C. Hill in *Polyoxometalates: Chemical Reviews*, 1998 (special thematic issue on polyoxometalates); f) M. T. Pope, A. Müller in *Polyoxometalate Chemistry: From Topology via Self-Assembly to Applications (*Eds.: M. T. Pope, A. Müller), Kluwer: Dordrecht, The Netherlands, 2001; g) T. Yamase, M. T. Pope in *Polyoxometalate Chemistry for Nano-Composite Design (*Eds.: T. Yamase, M. T. Pope), Kluwer: Dordrecht, The Netherlands, 2002; h) D.-L. Long, E. Burkholder, L. Cronin, *Chem. Soc. Rev.* **2007**, *36*, 101; i) D.-L. Long, R. Tsunashima, L. Cronin, *Angew. Chem.* **2010**, *122*, 1780, *Angew. Chem. Int. Ed.* **2010**, *49*, 1736.

[2] a) J. S. Anderson, *Nature* **1937**, *140*, 850; b) H. T. Jr. Evans, *J. Am. Chem. Soc.* **1948**, *70*, 1291; c) H. T. Jr. Evans, *Acta. Cryst.* **1974**, *B30*, 2095.

[3] a) K. J. Schmidt, G. J. Schrobilgen, J. F. Sawyer, *Acta Crystallogr.* **1986**, *C42*, 1115; b) A. Sagasaki, Y. Sasaki, *Bull. Chem. Soc. Jpn* **1987**, *60*, 763; c) T. Ozeki, A. Yagasaki, H. Ichida, Y. Sasaki, *Polyhedron* **1988**, **7**, 1131; d) M. S. Grigorev, Yu. T. Struchkov, A. M. Feddoseev, A. B. Yusov, A. I. Yanovskii, *Z. Neorg. Khim.* **1992**, *37*, 2507; e) C. Robl, M. Frost, *Z. Anorg. Allg. Chem.* **1993**, *619*, 1834; f) C. Robl, M. Frost, *Z. Anorg. Allg. Chem.* **1993**, *619*, 1137; g) C. Robl, M. Frost, *Z. Anorg. Allg. Chem.* **1993**, *619*, 1132; h) C. Robl, M. Frost, *Z. Anorg. Allg. Chem.* **1993**, *619*, 1624; i) C. Robl, M. Frost, *Z. Naturforsch. B*, **1993**, *48*, 404; j) P. A. Lorenzo-Luis, P. Martin- P. Zarza, R. Gili, Saez-Puche, J. Jimenez-Jimenez, E. Rodriguez-Castellon, C. Ruiz-Perez, J. Gonzalez-Platas, X. Solans, *Eur. Solid State Inorg. Chem.* **1997**, *34, 1271*; j) D. Drewes, E. M. Limanski, B. Krebs, *Dalton*, **2004**, 2087; k) D. Drewes, E. M. Limanski, B. Krebs*Eur. Inorg. Chem.* **2004**, 4849; l) D. Drewes, B. Krebs, *Z. Anorg. Allg. Chem.* **2005**, *631*, 2591; m) I. A. Charushnikova, A. B. Yusov, A. M. Feddoseev, I. N. Polyakova, *Z. Neorg. Khim.* **2004**, *49*, 1481; n) I. A. Charushnikova, A. M. Feddoseev, A. B. Yusov, C. D. Auwer, *Crystallogr. Reports* **2005**, *50,* 191; o) G. Bo, L. Shu-Xia, X. Lin-Hua, Y. Miao, Z. Chung-Dan, S. Chung-Yan, C. Hai-Yan, *J. Solid State Chem.* **2006**, *179*, 1689.

[4] a) P. A. Lorenz-Luis, P. Martin-Zarza, A. Sanchez, M. Hernandez-Molina, X. Solans, P. Gili, *Inorg. Chim. Acta* **1998**, *277*, 139; b) P. Gili, P. A. Lorenz-Luis, P. Martin-Zarza, S. Dominguez, A. Sanchez, J. M. Arrieta, E. Rodriguez-Castellon, J. Jimenez-Jimenez, C. Ruiz-Perez, M. Hernandez-Molina, X. Solans, *Transiton Met. Chem.* **1999**, *24,* 141; c) V. Balraj, K. Vidyasagar, *Inorg. Chem.* **1999**, *38,* 1394; d) F. Wang, S.-X. Liu, C.-L. Wang, R.-G. Cao, J.-F. Cao, *Acta Crystallogr.* **2007**, *E63*, m1708; e) Z.-H. Xu, P.-X. Xi, F.-J. Chen, Z.-Z. Zeng, *Analytical Sciences* **2007**, *23,* x235.

[5] a) E. S. Ganelina, *Russ. J. Inorg. Chem.* **1962**, *7,* 812; b) E. S. Ganelina, N. I. Nerevyatkina, *Russ. J. Inorg. Chem.* **1965**, *10,* 483; c) R. Ripan, N. Calu, *Stud.Univ. Babes-Bolyai, Chem.* **1965**, *10,* 135.

[6] G. Bo, L. Shuxia, X. Linhua, Y. Miao, Z. Chundan, S. Chunyan, C. Haiyan, *J. Solid State Chem.* **2006**, *179,* 1681.

[7] D. Drewes, E. M. Limanski, B. Krebs, *Dalton Trans.* **2004**, 2087.

[8] A. H. Ismail, N. H. Nsouli, M. H. Dickman, U. Kortz, *J. Clust. Sc.* **2009**, *20,* 453.

[9] D. Altermatt, I. D. Brown, *Acta. Crystallogr.* **1985**, *B41*, 244.

[10] G. M. Sheldrick, *Acta. Crystallogr.* **2008**, *A64*, 112.

5.B. Transition Metal-Containing Heteropolytungstates:

Copper-, Cobalt-, and Manganese-Containing 17-Tungsto-2-Germanates

N. H. Nsouli, A. H. Ismail, I. S. Helgadottir, M. H. Dickman, J. M Clemente-Juan, U. Kortz, *Inorg. Chem.* 2009, *48*, 5884

5.B.1. Introduction

Polyoxometalates (POMs) are metal-oxide clusters formed of early d-block elements in high oxidation states (e.g., W^{6+}, V^{5+}), and they constitute a unique class of inorganic compounds. POMs were discovered in 1826 by Berzelius when he noted the formation of a yellow precipitate after the reaction of ammonium molybdate with phosphoric acid.[1] The chemistry of POMs is a rapidly growing field because they exhibit a combination of tunable properties, including composition, size, shape, charge density, redox potentials, and solubility.[2] As a result, POMs have potential applications in many fields such as catalysis, medicine, photochemistry, electrochemistry, and magnetism.[3] The mechanism of formation of polyanions is not well understood and is usually described as self-assembly. One important goal in POM synthesis is the incorporation of transition metals, lanthanides, organometallic entities, or any other functional unit(s) into lacunary (i.e., vacant) polyanion precursors, leading to a tremendous diversity of structures. In particular, polytungstates are of importance in this respect, as a large number of stable lacunary precursors are known (as opposed to polymolybdates or polyvanadates).

From a magnetic point of view, POMs containing more than one paramagnetic transition metal ion in close proximity may exhibit exchange-coupled spins. Polyanions with high-spin ground states and magnetic anisotropy are of technical interest in areas such as data storage and magnetic switches and so on.[4] In the past decades, much attention has been devoted to the synthesis of transition-metal substituted POMs with multiple, spin-coupled magnetic centers in the area known as molecular magnetism.[5]

Transition-metal-containing POMs are usually prepared in a one-pot reaction of transition metal ions (e.g., Cu^{2+}, Fe^{3+}) with lacunary polytungstate precursors. In particular, the class of copper-containing POMs is very rich with respect to the number of Cu^{2+} ions and the shape of the magnetic cluster, for example, $[Cu_3(H_2O)_3(\alpha\text{-}XW_9O_{33})_2]^{n-}$ (n = 12, X = As^{III}, Sb^{III}; n = 10, X = Se^{IV}, Te^{IV}),[6] $[Cu_4(H_2O)_2(B\text{-}\alpha\text{-}XW_9O_{34})_2]^{n-}$ (X = P^V, As^V, *n* = 10; X = Si^{IV}, *n* = 12),[7] $[Cu_4K_2(H_2O)_8(\alpha\text{-}AsW_9O_{33})_2]^{n-}$,[8] $[Cu_5(OH)_4(H_2O)_2(A\text{-}\alpha\text{-}SiW_9O_{33})_2]^{10-}$,[9] $[\{(SiW_9O_{34})(SiW_9O_{33}(OH))(Cu(OH))_6Cu\}_2X]^{23-}$ (X = Cl, Br),[10] and $[Cu_{20}Cl(OH)_{24}(H_2O)_{12}(P_8W_{48}O_{184})]^{25-}$.[11]

However, the number of transition-metal-containing tungstogermanates is still limited. The subclass of organic-inorganic hybrid tungstogermanates includes a handful of structures. The group of Yang prepared $[Ni_4(Hdap)_2(B\text{-}\alpha\text{-}HGeW_9O_{34})_2]^{8-}$ (dap = 1,2-diaminopropane),[12] $[Cu_5(2,2'\text{-bpy})_6\text{-}(H_2O)][B\text{-}\beta\text{-}GeW_8O_{31}]$ and $\{[Cu_5(2,2'\text{-bpy})_5(H_2O)][B\text{-}\alpha\text{-}GeW_9O_{34}]\}_2$ (2,2′-bpy = 2,2′-bipyridine).[13] On the other hand, Niu et al. reported the copper-containing species $[Cu(DMF)_4(\alpha\text{-}GeW_{12}O_{40})_2]^{6-}$ (DMF = N,N-dimethylformamide),[14] $\{[Cu(phen)(\mu_2\text{-}CH_3COO)_2Cu(phen)(H_2O)]_2[Ge_2W_{23}CuO_{80}]\}^{8-}$ (phen = phenanthroline),[15] and $[Cu(en)_2(H_2O)]_2\{[Cu_4(GeW_9O_{34})_2][Cu(en)_2]\}^{3-}$.[16]

Our group has contributed several tungstogermanates with different incorporated or grafted transition metals: $[(RuC_6H_6)_2GeW_9O_{34}]^{6-}$,[17] $[Ru(dmso)_3(H_2O)GeW_{11}O_{39}]^{6-}$,[18] $[\{Ru(C_6H_6)(H_2O)\}\{Ru(C_6H_6)\}(\gamma\text{-}GeW_{10}O_{36})]^{4-}$,[19] $[Fe_6(OH)_3(A\text{-}\alpha\text{-}GeW_9O_{34}(OH)_3)_2]^{11-}$,[20] $K(H_2O)(\beta\text{-}Fe_2GeW_{10}O_{37}(OH))(\gamma\text{-}GeW_{10}O_{36})]^{12-}$ and $[\{\beta\text{-}Fe_2GeW_{10}O_{37}(OH)_2\}_2]^{12-}$,[21] and the Weakley-type dimers $[M_4(H_2O)_2(B\text{-}\alpha\text{-}GeW_9O_{34})_2]^{12-}$ (M = Mn^{2+}, Cu^{2+}, Zn^{2+}, Cd^{2+}).[22]

Other transition-metal-containing tungstogermanates include $[Cu_{10}(H_2O)_2(N_3)_4(GeW_9O_{34})_2(GeW_8O_{31})_2]^{24-}$,[23] $[Y(GeW_{11}O_{39})(H_2O)_2]^{5-}$,[24] $[Ti_6(OH)_3(GeW_9O_{37})_2]^{11-}$,[25] and the open Wells-Dawson structure $[\{Co(H_2O)\}(\mu\text{-}$

$H_2O)_2K(Ge_2W_{18}O_{66})]^{13-}$.[26] Recently Wang's group reported $[Mn_2(H_2O)_8Mn_4(H_2O)_2(B\text{-}\alpha\text{-}GeW_9O_{34})_2]^{8-}$ which is composed of Weakley-type $[Mn_4(H_2O)_2(B\text{-}\alpha\text{-}GeW_9O_{34})_2]^{12-}$ units connected via two Mn^{2+} ions forming a 1D chain.[27a] Yamase et al. reported the synthesis of $[Cu_4(GeW_9O_{34})_2]^{12-}$ showing a Cu_4^{8+} tetragon α-conjugated to two $[B\text{-}\alpha\text{-}GeW_9O_{34}]^{10-}$ Keggin moieties.[27b]

A few years ago, we reported the synthesis and structural characterization of the dilacunary decatungstogermanate $[\gamma\text{-}GeW_{10}O_{36}]^{8-}$.[28] Since then, we have been exploring its reactivity with various transition metal and rare earths ions, organometallic groups, and other electrophiles. Some of these results have already been published.[19,21] Here, we report on the synthesis and structural characterization of dimeric copper-, cobalt-, and manganese-containing tungstogermanates.

5.B.2. Synthesis

The dilacunary precursor $K_8[\gamma\text{-}GeW_{10}O_{36}]$ was synthesized according to the published procedure and its purity was confirmed by infrared spectroscopy.[28]

$K_{12}[Cu_3(H_2O)(B\text{-}\beta\text{-}GeW_9O_{33}(OH))(B\text{-}\beta\text{-}GeW_8O_{30}(OH))]\cdot 31H_2O$ (K-29)

A 0.05 g (0.28 mmol) sample of $CuCl_2\cdot 2H_2O$ was dissolved in 20 mL of 1M potassium acetate buffer at pH 4.8, followed by the addition of 0.50 g (0.17 mmol) of $K_8[\gamma\text{-}GeW_{10}O_{36}]\cdot 6H_2O$. Then, the solution was stirred and heated to 50 °C for 30 minutes. The solution was allowed to cool to room temperature and then filtered. Slow evaporation of the solvent at room temperature for about one day led to the formation of light-green crystals suitable for X-ray diffraction. These crystals were isolated and air-dried (yield 0.08 g, 14 %). IR for **K-29**: 940 (m), 900 (m), 872 (m), 815 (sh), 790 (sh), 766 (s), 713 (s), 503 (w), 449 (w), 430 (sh) cm^{-1} (see Figure 5.14). Anal. Calcd (%) for **K-29**: K, 8.5; W, 56.3; Cu, 3.4; Ge, 2.6. Found (%): K, 8.7; W, 55.2; Cu, 3.5; Ge, 2.7.

$K_{22}[Co(H_2O)_2\{Co_3(B\text{-}\beta\text{-}GeW_9O_{33}(OH))(B\text{-}\beta\text{-}GeW_8O_{30}(OH))\}_2]\cdot 52H_2O$ (K-30)

The synthetic procedure was identical to that of **K-29**, but 0.07 g of $CoCl_2\cdot 6H_2O$ (0.28 mmol) was used instead of $CuCl_2\cdot 2H_2O$. Slow evaporation of the solvent at room temperature for two weeks resulted in dark-purple crystals. These crystals were isolated and air dried (yield 0.07 g, 13 %). IR for **K-30**: 941 (m), 889 (m), 867 (m), 841 (m), 812 (sh), 789 (s), 764 (s), 696 (s), 506 (w), 449 (w) cm^{-1} (see Figure 5.14). Anal. Calcd (%) for **K-30**: K, 7.9; W, 57.5; Co, 3.8; Ge, 2.7. Found (%): K, 7.0; W, 56.9; Co, 3.5; Ge, 2.5.

$K_{22}[Mn(H_2O)_2\{Mn_3(H_2O)(B\text{-}\beta\text{-}GeW_9O_{33}(OH))(B\text{-}\beta\text{-}GeW_8O_{30}(OH))\}_2]\cdot 45H_2O$ (K-31)

The synthetic procedure was identical to **K-29**, but 0.06 g of $MnCl_2\cdot 4H_2O$ (0.28 mmol) was used instead of $CuCl_2\cdot 2H_2O$. Slow evaporation of the solvent at room temperature for one day resulted in yellow crystals. These crystals were isolated and air dried (yield 0.08 g, 19 %). IR for **K-31**: 940 (m), 870 (m), 852 (m), 805 (sh), 789 (s), 764 (s), 706 (m), 520 (w), 494 (w), 449 (w) cm^{-1} (see Figure 5.14) Anal. Calcd for **K-31**: K, 8.0; W, 58.1; Mn, 3.6; Ge, 2.7. Found (%): K, 7.1; W, 57.3; Mn, 3.8; Ge, 2.4.

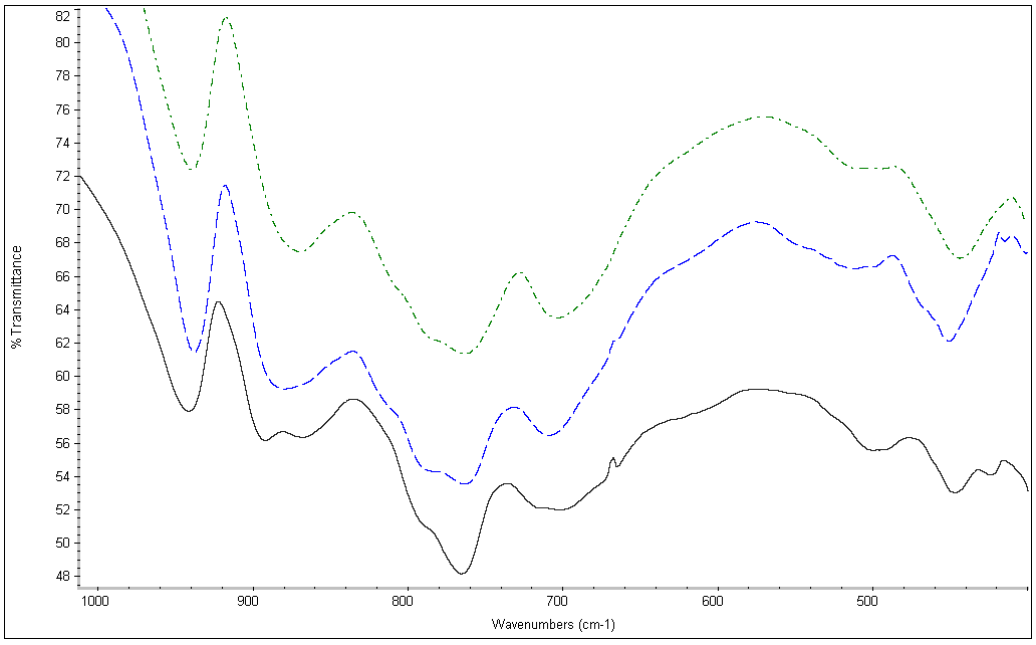

Figure 5.14. IR spectra of **K-29** (black curve), **K-30** (blue curve) and **K-31** (green curve) measured on KBr pellets.

5.B.3. X-ray Crystallography

Crystals were mounted on a Hampton cryoloop in light oil for data collection at -100 °C. Indexing and data collection were performed on a Bruker D8 SMART APEX II CCD diffractometer with kappa geometry and Mo Kα radiation (graphite monochromator, λ = 0.71073 Å). Data integration was performed using *SAINT*.[29] Routine Lorentz and polarization corrections were applied. Multiscan absorption corrections were performed using *SADABS*.[30] Direct methods (*SHELXS97*) successfully located the tungsten atoms, and successive Fourier syntheses (*SHELXL97*) revealed the remaining atoms.[30] Refinements were full-matrix least-squares against F^2 using all data. In the final refinement, all non-disordered heavy atoms were refined anisotropically; oxygen atoms and disordered cations were refined isotropically. No hydrogen atoms were included in the models. Crystallographic data are summarized in Table 5.6.

Table 5.6. Crystal Data and Structure for **K-29**, **K-30** and **K-31**.

	K-29	**K-30**	**K-31**
empirical formula	$H_{66}Cu_3Ge_2K_{12}O_{97}W_{17}$	$H_{112}Co_7Ge_4K_{22}O_{184}W_{34}$	$H_{102}Ge_4K_{22}Mn_7O_{179}W_{34}$
fw	5549.0	10870.9	10752.9
T (K)	173(2)	173(2)	296(2)
wavelength (Å^3)	0.71073	0.71073	0.71073
crystal system	triclinic	monoclinic	triclinic
space group	$P\bar{1}$	$P2_1/n$	$P\bar{1}$
a (Å)	12.6684(3)	19.593(7)	12.2372(16)
b (Å)	20.7927(5)	24.700(13)	17.9117(18)
c (Å)	33.4049(8)	34.010(13)	18.963(3)
α (deg)	83.4747(12)	90	91.154(4)
β (deg)	80.1672(14)	101.626(13)	96.737(5)
γ (deg)	73.8061(12)	90	101.122(4)
V (Å^3)	8305.7(3)	16121(12)	4046.4(9)
Z	4	4	1
d_{calcd} (Mg/m^3)	4.438	4.479	4.413
abs coeff (mm^{-1})	25.64	26.28	26.00
goodness-of-fit on F^2	1.01	1.07	1.07
$R[I > 2\sigma(I)]^a$	0.050	0.070	0.079
R_w (all data)^b	0.148	0.205	0.230

$^a R = \sum ||F_o| - |F_c|| / \sum |F_o|$. $^b R_w = [\sum w(F_o^2 - F_c^2)^2 / \sum w(F_o^2)^2]^{1/2}$.

5.B.4. Results and Discussion

Reaction of $CuCl_2 \cdot 2H_2O$, $CoCl_2 \cdot 6H_2O$, or $MnCl_2 \cdot 4H_2O$ with $K_8[\gamma\text{-}GeW_{10}O_{36}] \cdot 6H_2O$ in a ratio of 1.5:1 in a potassium acetate buffer (pH 4.8) at 50 °C resulted in the sandwich-type tungstogermanates $[Cu_3(H_2O)(B\text{-}\beta\text{-}GeW_9O_{33}(OH))(B\text{-}\beta\text{-}GeW_8O_{30}(OH))]^{12-}$ (**29**), $[Co(H_2O)_2\{Co_3(B\text{-}\beta\text{-}GeW_9O_{33}(OH))(B\text{-}\beta\text{-}GeW_8O_{30}(OH))\}_2]^{22-}$ (**30**), and $[Mn(H_2O)_2\{Mn_3(H_2O)(B\text{-}\beta\text{-}GeW_9O_{33}(OH))(B\text{-}\beta\text{-}GeW_8O_{30}(OH))\}_2]^{22-}$ (**31**), respectively.

Polyanion **29** is composed of two non-equivalent Keggin units, ($B\text{-}\beta\text{-}GeW_8O_{31}$) and ($B\text{-}\beta\text{-}GeW_9O_{34}$). These two units are held together by three copper(II) ions in such a way that there is a plane of symmetry passing through both Ge atoms and the unique Cu atom resulting in a sandwich-type structure with C_s symmetry (Figure 5.15).

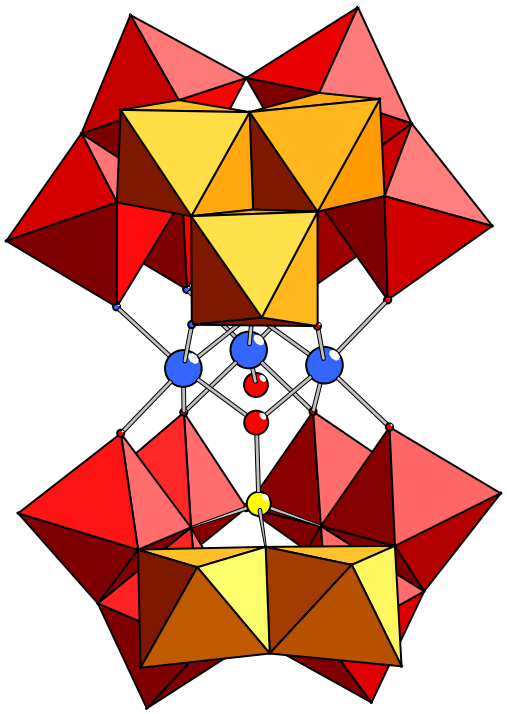

Figure 5.15. Combined ball-and-stick/polyhedral representation of $[Cu_3(H_2O)(B\text{-}\beta\text{-}GeW_9O_{33}(OH))(B\text{-}\beta\text{-}GeW_8O_{30}(OH))]^{12-}$ (**29**). Polyhedra represent WO_6 (red or orange) and the balls represent germanium (yellow), copper (blue) and oxygen (red). The rotated WO_6 octahedra are shown in orange for clarity.

Each Keggin fragment in **29** is linked to three Jahn-Teller distorted octahedral Cu^{2+} ions. The Cu atoms are linked to each of the lacunary units via two Cu-O-W bonds. The two structurally equivalent Cu atoms are also linked to an oxygen atom of each GeO_4 hetero group. The unique Cu completes its octahedral coordination sphere by an oxygen atom of the GeO_4 hetero group of the (*B*-*β*-GeW_9O_{34}) fragment and a terminal water ligand.

We also performed bond valence sum (BVS) calculations for **29**, and the values for O2C (1.26), O117 (1.12) and O1Cu (0.09) indicate mono-protonation of the first two and di-protonation of the latter.[31] The presence of two hydroxo and one aqua ligand in **29** results in a total polyanion charge of -12.

We believe that both tungstogermanate fragments in **29** are formed by the decomposition of [*γ*-$GeW_{10}O_{36}$]$^{8-}$. Figure 5.16 indicates a possible two-step transformation pathway of [*γ*-$GeW_{10}O_{36}$]$^{8-}$ resulting first in (*B*-*β*-GeW_8O_{31}) via a loss of two edge-shared, rotated WO_6 octahedra, and then in (*B*-*β*-GeW_9O_{34}) via a gain of a WO_6 unit forming a complete, rotated triad. Such a transformation has a precedent in tungstosilicate chemistry, namely for [*γ*-$SiW_{10}O_{36}$]$^{8-}$ which is the well-known silicon analogue of [*γ*-$GeW_{10}O_{36}$]$^{8-}$.[32]

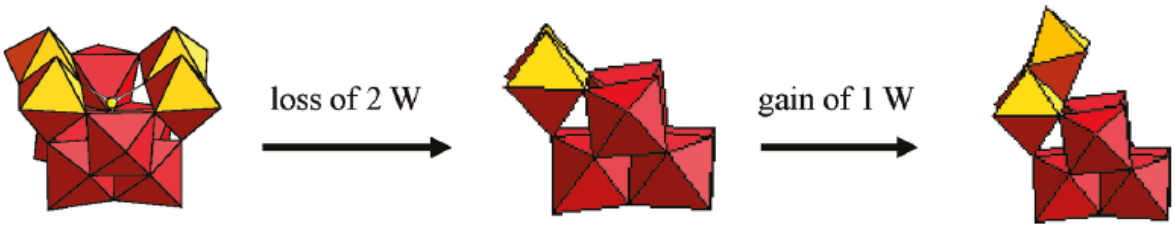

Figure 5.16. Possible Two-Step Transformation Pathway of [*γ*-$GeW_{10}O_{36}$]$^{8-}$ Resulting First in (*B*-*β*-GeW_8O_{31}) via a Loss of Two Edge-Shared, Rotated WO_6 Octahedra, and Then in (*B*-*β*-GeW_9O_{34}) via a Gain of a WO_6 Unit Forming a Complete Rotated Triad. The color code is the same as in Figure 5.15.

Our group observed both the (*B*-*β*-SiW_9O_{34}) and (*B*-*β*-SiW_8O_{31}) fragments in the 3-cobalt(II)-containing $[Co_3(H_2O)(B\text{-}\beta\text{-}SiW_9O_{33}(OH))(B\text{-}\beta\text{-}SiW_8O_{29}(OH)_2)]^{11-}$,[32a] and only the (*B*-*β*-SiW_8O_{31}) fragment in the 15-Co(II)-containing $[Co_6(H_2O)_{30}\{Co_9Cl_2(OH)_3(H_2O)_9(B\text{-}\beta\text{-}SiW_8O_{31})_3\}]^{5-}$.[32c] The germanium analogue of the tetralacunary fragment (*β*-GeW_8O_{31}) was first observed by Wang et al. in the copper-containing $[Cu_5(2,2'\text{-bpy})_6(H_2O)][GeW_8O_{31}]\cdot 9H_2O$.[13] Polyanion **29** is similar in structure to our cobalt(II) containing tungstosilicate $[Co_3(H_2O)(B\text{-}\beta\text{-}SiW_9O_{33}(OH))(B\text{-}\beta\text{-}SiW_8O_{29}(OH)_2)]^{11-}$, which forms a dimer in the solid state.[32a] The Cu_3-containing **29** has C_s symmetry with the plane of symmetry passing through the rotated W_3O_{13} triad of the (*B*-*β*-GeW_9O_{34}) fragment. This is not the case for the asymmetrical Co_3-containing tungstosilicate which possesses C_1 symmetry because the rotated W_3O_{13} triad is located "on the side". Cronin et al. have recently shown that $[Co_3(H_2O)(B\text{-}\beta\text{-}SiW_9O_{34})(B\text{-}\beta\text{-}SiW_8O_{29}(OH)_2)]^{12-}$ can be synthesized at pH 8.0 and when the pH was increased to 8.8, $[Co_3(H_2O)(B\text{-}\alpha\text{-}SiW_9O_{34})(B\text{-}\beta\text{-}SiW_8O_{31})]^{14-}$ was formed.[32e] The structure of the former is identical to our $[Co_3(H_2O)(B\text{-}\beta\text{-}SiW_9O_{33}(OH))(B\text{-}\beta\text{-}SiW_8O_{29}(OH)_2)]^{11-}$ (vide supra), but it did not dimerize in the solid state. On the other hand, the latter contains a (*B*-*α*-SiW_9O_{34}) Keggin unit rather than a (*B*-*β*-SiW_9O_{34}) fragment. Our $[Co_3(H_2O)(B\text{-}\beta\text{-}SiW_9O_{33}(OH))(B\text{-}\beta\text{-}SiW_8O_{29}(OH)_2)]^{11-}$, which represents the Si analogue of polyanion **30**, was formed as a mixed potassium/sodium salt in a 0.5 M sodium acetate buffer (pH 4.8) using a $CoCl_2\cdot 6H_2O$ to $K_8[\gamma\text{-}SiW_{10}O_{36}]\cdot 6H_2O$ ratio of 2:1.[32a] On the other hand, the sodium salt of the satellite-shaped Co-15 silicotungstate $[Co_6(H_2O)_{30}\{Co_9Cl_2(OH)_3(H_2O)_9(B\text{-}\beta\text{-}SiW_8O_{31})_3\}]^{5-}$ was prepared in a 13:1 ratio of the above reagents in a 1 M NaCl medium and the pH was adjusted to 5.5 by the addition of 0.1 M NaOH.[32c]

It is also of interest to compare **29** to Wang and coworkers' copper-containing tungstogermanate $[Cu_{10}(H_2O)_2(N_3)_4(B\text{-}\alpha\text{-}GeW_9O_{34})_2(B\text{-}\beta\text{-}GeW_8O_{31})_2]^{24-}$.[23] The latter consists of a $\{Cu_{10}(N_3)_4\}$cluster, two (*B*-*β*-GeW_8O_{31}) units and two (*B*-*α*-GeW_9O_{34}) units forming two equivalent sandwich fragments. Each fragment is composed of a (*B*-*β*-GeW_8O_{31}) and a (*B*-*α*-

GeW_9O_{34}) unit linked by four Cu^{2+} ions. One of the Cu^{2+} ions is linked to three nitrogens of three azide groups and to three oxygens of the neighboring Cu atoms. Two of the azide ligands form a linkage with the two equivalent sandwich fragments. The fifth Cu^{2+} ion is coordinated to four oxygen atoms and to two azide ligands, one of which holds the two fragments together.

The cobalt-containing polyanion $[Co(H_2O)_2\{Co_3(B\text{-}\beta\text{-}GeW_9O_{33}(OH))(B\text{-}\beta\text{-}GeW_8O_{30}(OH))\}_2]^{22-}$ (**30**) contains two equivalent sandwich-type fragments $[Co_3(B\text{-}\beta\text{-}GeW_9O_{33}(OH))(B\text{-}\beta\text{-}GeW_8O_{29}(OH)_2)]^{11-}$ (**30a**) arranged almost orthogonally to each other and linked via two equivalent Co-O-W bonds. Each fragment **30a** comprises a ($B\text{-}\beta\text{-}GeW_8O_{31}$) and a ($B\text{-}\beta\text{-}GeW_9O_{34}$) capping a triangular cobalt(II) cluster. These structural aspects resemble our previously reported tungstosilicate $[Co_3(H_2O)(B\text{-}\beta\text{-}SiW_9O_{33}(OH))(B\text{-}\beta\text{-}SiW_8O_{29}(OH)_2)]^{11-}$.[32a] In **30** the presence of an extra cobalt(II) ion (with two trans-aqua ligands) ensures the formation of a 1-D network via coordination to the pairs of rotated WO_6 groups within each ($B\text{-}\beta\text{-}GeW_8O_{31}$) unit (Figure 5.17).

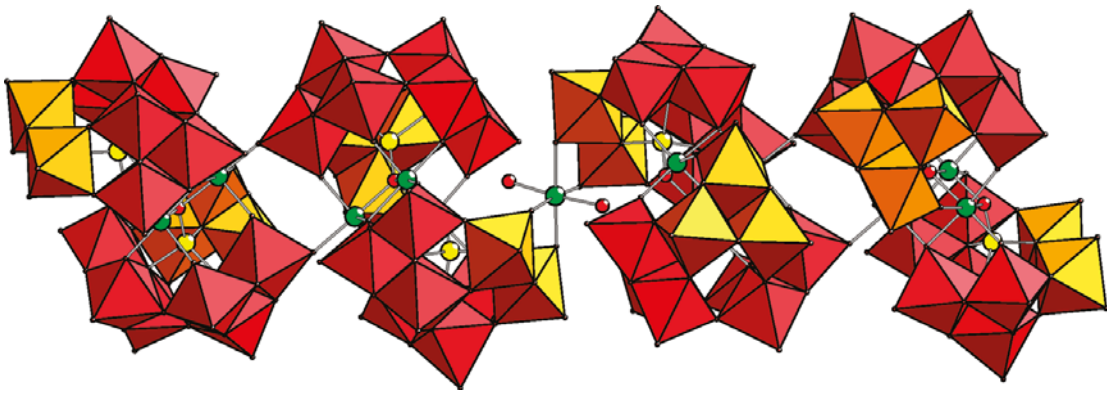

Figure 5.17. Combined ball-and-stick/polyhedral presentation of the solid-state arrangement of **30**. The polyhedra represent WO_6 (red or orange) and the balls represent germanium (yellow), cobalt (green) and oxygen (red).

Both polyanions **29** and **30a** are composed of the same Keggin fragments, but there is still a major difference between them. Polyanion **29** has a plane of symmetry which passes through the rotated triad of the (*B*-*β*-GeW_9O_{34}) unit (Figure 5.18a), while **30a** lacks a plane of symmetry due to the positioning of the rotated triad "on the side" of the polyanion (Figure 5.18b).

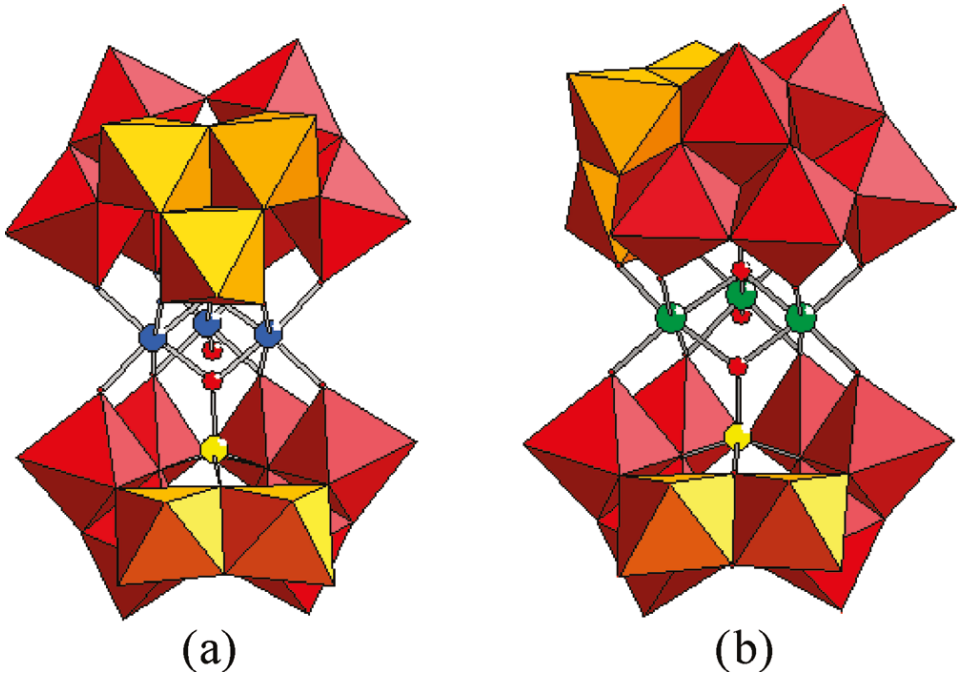

Figure 5.18. Polyhedral representation of the copper(II) containing **29** (left, a) and the cobalt(II) containing fragment **30a** (right, b). Notice the different orientation of the rotated triad in the respective "upper" (*B*-*β*-GeW_9O_{34}) units.

We believe that the different electron configurations and hence coordination geometries of Cu^{2+} (d^9) and Co^{2+} (high-spin d^7) are most likely the origin of the structural differences for **29** and **30a**. Copper(II) ions exhibit the well-known Jahn-Teller distortion, resulting in axially elongated octahedral coordination. It appears that such a distorted trinuclear copper(II) cluster (Figure 5.19) can be accommodated better in the cisoid conformation of **29**, whereas the trinuclear cobalt(II) cluster can be accommodated better in the transoid conformation of **30a**. Taking a closer look at the Cu-O bond lengths in **29** indicates that the equatorial bonds are in the normal range (Cu1-O_{eq} 1.95(3) Å, Cu2-O_{eq} 1.96(2) Å, Cu3-O_{eq} 1.98(1) Å). As expected,

the axial Cu-O bonds are longer and actually fall in the two categories long and very long (Cu1-O_{ax} 2.35(1), 2.55(1) Å; Cu2-O_{ax} 2.30(1), 2.54(1) Å; Cu3-O_{ax} 2.31(1), 2.52(1) Å), (Table 5.7).

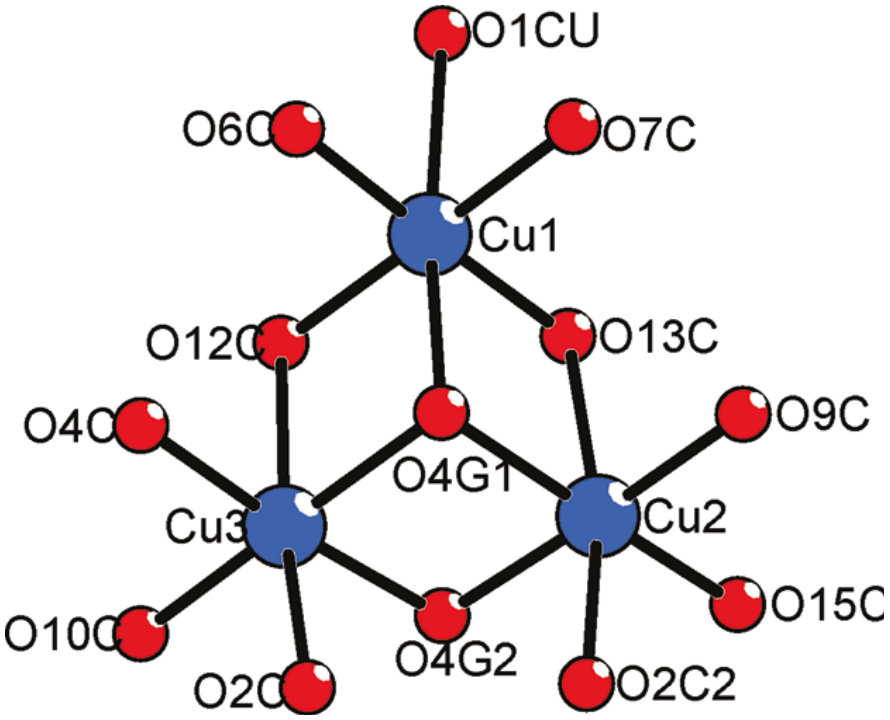

Figure 5.19. Ball-and-stick representation of the Cu_3-core of **29** and the labeling scheme.

We also performed BVS calculations for **30**. The values for two of the oxygens, O2C7 (0.23) and O3C7 (0.29), connected to the Co linker in **30** show that they are diprotonated. In addition, we discovered monoprotonation in each of the (*B*-*β*-GeW_9O_{34}) units, one of them being O26A (1.10) in the first sandwich-type fragment and the second being O3C3 (1.09) in the other fragment. Moreover, a proton is disordered over two positions in each (*B*-*β*-GeW_8O_{31}) unit. The first proton is shared by oxygens O137 (1.27) and O146 (1.40) in the first fragment and the other by O272 (1.53) and O283 (1.43).

Table 5.7. Selected Cu–O and Co–O bond lengths [Å] for **29** and **30**, respectively[a]

Code	**1**		**2**
$Cu(1)\text{-}O(6C)_{eq}$	1.91(1)	Co(1)-O	1.97(3), 2.00(2),
$Cu(1)\text{-}O(13C)_{eq}$	1.94(1)		2.02(2), 2.03(3),
$Cu(1)\text{-}O(7C)_{eq}$	1.95(1)		2.04(2), 2.21(2)
$Cu(1)\text{-}O(12C)_{eq}$	1.99(1)	Co(2)-O	2.02(2), 2.06(2),
Avg. $Cu(1)\text{-}O_{eq}$	**1.95(3)**		2.06(2), 2.12(2),
			2.15(2), 2.25(2)
$Cu(2)\text{-}O(15C)_{eq}$	1.93(1)	Co(3)-O	2.06(2), 2.08(2),
$Cu(2)\text{-}O(4G2)_{eq}$	1.96(1)		2.08(3), 2.09(2),
$Cu(2)\text{-}O(4G1)_{eq}$	1.97(1)		2.09(2), 2.12(2)
$Cu(2)\text{-}O(9C)_{eq}$	1.98(1)	Co(4)-O	2.04(3), 2.07(2),
Avg. $Cu(2)\text{-}O_{eq}$	**1.96(2)**		2.08(2), 2.09(2),
			2.12(3), 2.18(2)
$Cu(3)\text{-}O(4G2)_{eq}$	1.97(1)	Co(5)-O	2.03(2), 2.03(2),
$Cu(3)\text{-}O(4C)_{eq}$	1.98(1)		2.04(3), 2.05(2),
$Cu(3)\text{-}O(10C)_{eq}$	1.98(1)		2.08(2), 2.19(2)
$Cu(3)\text{-}O(4G1)_{eq}$	2.00(1)	Co(6)-O	2.04(2), 2.05(2),
Avg. $Cu(3)\text{-}O_{eq}$	**1.98(1)**		2.06(2), 2.07(2),
			2.11(2), 2.17(2)
$Cu(1)\text{-}O(4G1)_{ax1}$	2.35(1)		
$Cu(2)\text{-}O(2C2)_{ax1}$	2.30(1)		
$Cu(3)\text{-}O(2C)_{ax1}$	2.31(1)		
Avg. $Cu\text{-}O_{ax1}$	**2.32(3)**		
$Cu(1)\text{-}O(1CU)_{ax2}$	2.55(2)		
$Cu(2)\text{-}O(13C)_{ax2}$	2.54(1)		
$Cu(3)\text{-}O(12C)_{ax2}$	2.52(1)		
Avg. $Cu\text{-}O_{ax2}$	**2.54(2)**		

[a]Mean values are indicated in bold.

The manganese(II) containing polyanion **31** is composed of two fragments of $[Mn_3(H_2O)(B\text{-}\beta\text{-}GeW_9O_{33}(OH))(B\text{-}\beta\text{-}GeW_8O_{30}(OH))]^{12-}$ linked through an octahedrally coordinated Mn^{2+} ion. In close analogy to **30**, this extra metal ion links the two sandwich fragments by coordinating to the pair of rotated tungsten centers in each ($B\text{-}\beta\text{-}GeW_8O_{31}$) unit and it also has two trans-related terminal water ligands (Figure 5.20).

Polyanion **31** exhibits a small degree (~15%) of crystallographic alpha/beta disorder of two W_3O_{13} triads in the ($B\text{-}\beta\text{-}GeW_9O_{34}$) unit. We were able to resolve this issue by assigning partial occupancies to the involved W atoms.

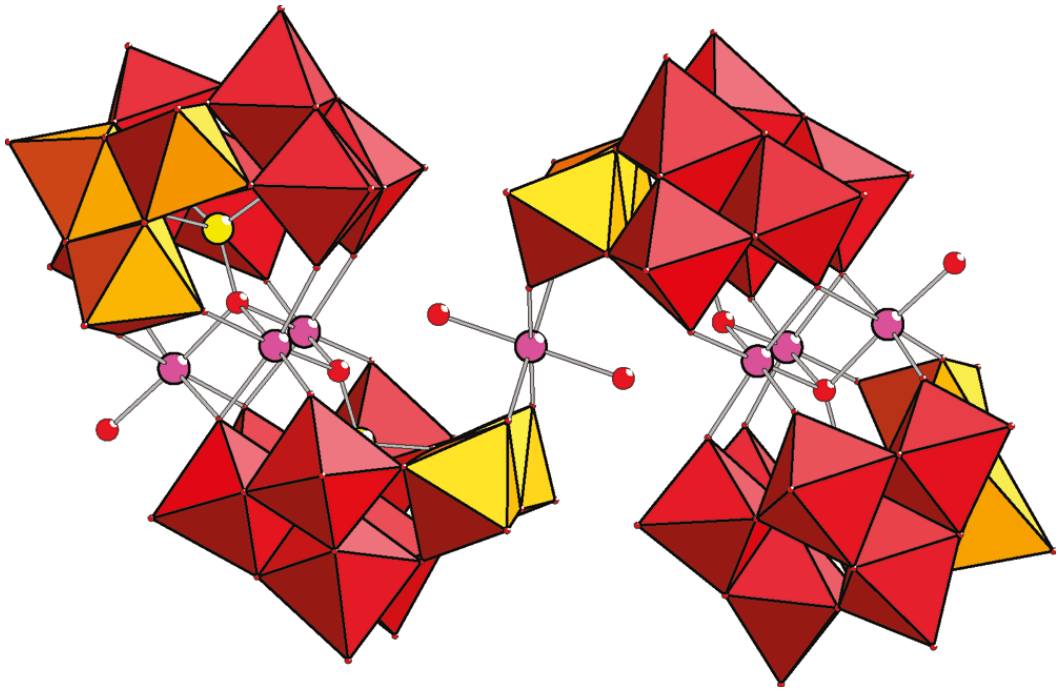

Figure 5.20. Combined polyhedral/ball-and-stick representation of **31**. The pink spheres represent Mn^{2+} (**31**). Otherwise, the color code is the same as in Figures 5.15 – 5.19.

5.B.5. Conclusions

We have prepared the three dimeric, sandwich-type tungstogermanates $[Cu_3(H_2O)(B\text{-}\beta\text{-}GeW_9O_{33}(OH))(B\text{-}\beta\text{-}GeW_8O_{30}(OH))]^{12-}$ (**29**), $[Co(H_2O)_2\{Co_3(B\text{-}\beta\text{-}GeW_9O_{33}(OH))(B\text{-}\beta\text{-}GeW_8O_{29}(OH)_2)\}_2]^{20-}$ (**30**) and $[Mn(H_2O)_2\{Mn_3(H_2O)(B\text{-}\beta\text{-}GeW_9O_{33}(OH))(B\text{-}\beta\text{-}GeW_8O_{30}(OH))\}_2]^{22-}$ (**31**) in simple, one-pot reactions using aqueous, buffered pH 4.8 medium. All three polyanions **29-31** have been fully characterized by single-crystal X-ray diffraction, FTIR, elemental analysis, and thermogravimetric analysis. The magnetic properties of **K-29, K-30** and **K-31** have been also studied. We used Cu^{2+}, Co^{2+} or Mn^{2+} to $[\gamma\text{-}GeW_{10}O_{36}]^{8-}$ ratios of 1.5:1 for the synthesis of **29-31.** Our results demonstrate that the reactivity of $[\gamma\text{-}GeW_{10}O_{36}]^{8-}$ with 3d metal ions in an aqueous acidic medium is similar to that of its silicon analogue $[\gamma\text{-}SiW_{10}O_{36}]^{8-}$. Both species can easily rearrange to different isomers of trilacunary "XW_9" and tetralacunary "XW_8" fragments which coordinate to the d-block metal ions, resulting in sandwich-type assemblies. We have shown that $[\gamma\text{-}GeW_{10}O_{36}]^{8-}$ is a highly flexible lacunary POM precursor which can adjust to the specific coordination requirements of the respective type of transition metal ion (e.g. Cu^{2+} vs Co^{2+}). We believe that **29-31** could also be interesting for homogeneous or heterogeneous oxidation catalysis applications. Currently, we are exploring the reactivity of $[\gamma\text{-}GeW_{10}O_{36}]^{8-}$ with other d- and f-block metal ions.

5.B.6. References

[1] J. J. Berzelius, *Pogg. Ann.* **1826**, *6*, 369.

[2] a) M. T. Pope, *Heteropoly and Isopoly Oxometalates*; Springer: Berlin, 1983; b) M. T. Pope, A. Müller, *Angew. Chem., Int. Ed. Engl.* **1991**, *30*, 34; c) M. T. Pope, In *Comprehensive Coordination Chemistry II*; J. A. McCleverty, T. J. Meyer, Eds.; Elsevier Ltd.: Oxford, U.K., 2004; d) C. L. Hill, In *Comprehensive Coordination Chemistry II*; A. G. Wedd, Ed.; Elsevier Ltd.: Oxford, U.K., 2004.

[3] a) *Polyoxometalates: From Platonic Solids to Anti Retroviral Activity*; M. T. Pope, A. Müller, Eds.; Kluwer: Dordrecht, 1994; b) *Chem. Rev.* **1998**, *98*, 1-389 (Special Thematic Issue on Polyoxometalates); c) *Polyoxometalate Chemistry: From Topology Via Self-Assembly to Applications*; M. T. Pope, A. Müller Eds.; Kluwer: Dordrecht, 2001; d) *Polyoxometalate Chemistry for Nano-Composite Design*; T. Yamase, M. T. Pope, Eds.; Kluwer: Dordrecht, 2002; e) *Polyoxometalate Molecular Science*; J. J. Borrás-Almenar, E. Coronado, A. Müller, M. T. Pope, Eds.; Kluwer: Dordrecht, The Netherlands, 2003; f) M. Vazylyev, D. Sloboda-Rozner, A. Haimov, G. Maayan, R. Neumann, *Top. Catal.* **2005**, *34*, 93.

[4] a) R. Sessoli, D. Gatteschi, A. Caneschi, M. A. Novak, *Nature*, **1993**, *365*, 141; b) P. Gambardella, S. Rusponi, M. Veronese, S. S. Dhesi, C. Grazioli, A. Dallmeyer, I. Cabria, R. Zeller, P. H. Dederichs, K. Kern, C. Carbone, H. Brune, *Science*, **2003**, *300*, 1130; c) J. R. Long, in *Chemistry of Nanostructured Materials*, P. Yang, Ed. World Scientific Publishing, Hong Kong, **2003**, pages 241; d) M. Bode, O. Pietzsch, A. Kubetzka, R. Wiesendanger, *Phys. Rev. Lett.*, **2004**, *92*, 067201; e) D. Gatteschi, R. Sessoli, J. Villain, *Molecular Nanomagnets*, Oxford Univ. Press, Oxford, **2006**.

[5] a) T. Yamase, B. Botar, E. Ishikawa, K. Fukaya, *Chem. Lett.* **2001**, 56; b) N. Laronze, J. Marrot, G. Hervé, *Inorg. Chem.* **2003**, *42*, 5857; c) T. M. Anderson, W. A. Neiwert, K. I. Hardcastle, C. L. Hill, *Inorg. Chem.* **2004**, *43*, 7353; d) S. Nellutla, J. van Tol, N. S. Dalal, L.

H. Bi, U. Kortz, B. Keita, L. Nadjo, G. A. Khitrov, A. G. Marshall, *Inorg. Chem.* **2005**, *44*, 9795; e) B. Godin, Y. G. Chen, J. Vaissermann, L. Ruhlmann, M. Verdaguer, P. Gouzerh, *Angew. Chem., Int. Ed.* **2005**, *44*, 3072; f) B. Godin, J. Vaissermann, P. Herson, L. Ruhlmann, M. Verdaguer, P. Gouzerh, *Chem. Commun.* **2005**, 5624; g) C. Pichon, P. Mialane, A. Dolbecq, J. Marrot, E. Rivière, B. Keita, L. Nadjo, F. Sécheresse, *Inorg. Chem.* **2007**, *46*, 5292; h) U. Kortz, A. Müller, J. van Slageren, J. Schnack, N. S. Dalal, M. Dressel, *Coord. Chem. Rev.* **2009**, *253*, in press.

[6] U. Kortz, N. K. Al-Kassem, M. G. Savelieff, N. A. Al Kadi, M. Sadakane, *Inorg. Chem.* **2001**, *40*, 4742.

[7] a) T. J. R. Weakley, R. G. Finke, *Inorg. Chem.* **1990**, *29*, 1235; b) U. Kortz, S. Isber, M. H. Dickman, D. Ravot, *Inorg. Chem.* **2000**, *39*, 2915; c) L.-H. Bi, R.-D. Huang, J. Peng, E.-B. Wang, Y. H. Wang, C.-W. Hu, *J. Chem. Soc., Dalton Trans.* **2001**, 121.

[8] U. Kortz, S. Nellutla, A. C. Stowe, N. S. Dalal, J. van Tol, B. S. Bassil, *Inorg. Chem.* **2004**, *43*, 144.

[9] L.-H. Bi, U. Kortz, *Inorg. Chem.*, **2004,** 7961.

[10] P. Mialane, A. Dolbecq, J. Marrot, E. Rivière, F. Sécheresse, *Angew. Chem., Int. Ed.* **2003**, *42*, 3523.

[11] S. S. Mal, U. Kortz, *Angew. Chem. Int. Ed.* **2005**, *44*, 3777.

[12] J.–W. Zhao, B. Li, S.–T. Zheng, G.–Y. Yang, *Cryst. Growth Des.,* **2007***, 7,* 2658.

[13] C.–M. Wang, S.–T. Zheng, G.–Y. Yang, *Inorg. Chem.*, **2007**, *46*, 616.

[14] J.–Y. Niu, Q.–X. Han, Wang, J.–P. *J. Coord. Chem.*, **2003**, *56*, 523.

[15] J.–P. Wang, Q. Ren, J.–W. Zhao, J.–Y. Niu, *Inorg. Chem. Commun.*, **2006**, *9*, 1281.

[16] J.–P. Wang, X.–D. Du, J.–Y. Niu, *Chem.Lett.*, **2006**, *35*, 1408.

[17] L.-H. Bi, U. Kortz, M. H. Dickman, B. Keita, L. Nadjo, *Inorg. Chem.* **2005,** *44,* 7485.

[18] L.-H. Bi, U. Kortz, B. Keita, L. Nadjo, *Dalton Trans.* **2004**, 3184.

[19] L.-H. Bi, E. V. Chubarova, N.H. Nsouli, M. H. Dickman, U. Kortz, B. Keita, L. Nadjo, *Inorg. Chem.,* **2006**, *45*, 8575.

[20] L.-H. Bi, U. Kortz, S. Nellutla, A. C. Stowe, N. S. Dalal, B. Keita, L. Nadjo, *Inorg. Chem.,* **2005**, *44*, 896.

[21] N. H. Nsouli, S. S. Mal, M. H. Dickman, U. Kortz, B. Keita, L. Nadjo, J. M. Clemente-Juan, *Inorg. Chem.*, **2007**, 46, 8763.

[22] U. Kortz, S. Nellutla, A. C. Stowe, N. S. Dalal, U. Rauwald, W. Danquah, D. Ravot, *Inorg. Chem.* **2004,** *43*, 2308.

[23] Z. Zhang, Y. Qi, C. Qin, Y. Li, E. Wang, X. Wang, Z. Su, L. Xu, *Inorg. Chem.* **2007**, *46*, 8162.

[24] J.–P. Wang, X.-Y. Duan, X.–D. Du, J. –Y. Niu, *Cryst. Growth Des.* **2006***, 6,* 2266.

[25] T. Yamase, T. Ozeki, H. Sakamoto, S. Nishiya, A. Yamamoto, *Bull. Chem. Soc. Jap.* **1993**, *66*, 103.

[26] C.-Y. Sun, S.-X. Liu, C.-L. Wang, L.-H. Xie, C.-D. Zhang, G. Bo, Z.-M. Su, H.-Q. Jia, *J. Mol. Struct.* **2006**, *785*, 170.

[27] a) X. Gan, Z. Zhang, S. Yao, W. Chen, E. Wang, H. Zhang, *J. Clust. Sci.*, **2008**, *19,* 401; b) T. Yamase, H. Abe, E. Ishikawa, H. Nojiri, Y. Ohshima, *Inorg. Chem.*, **2009**, *48*, 138.

[28] N. H. Nsouli, B. S. Bassil, M. H. Dickman, U. Kortz; B. Keita, L. Nadjo, *Inorg. Chem.* **2006**, *45*, 3858.

[29] *SAINT*, Bruker AXS Inc., Madison, Wisconsin, USA, **2007**.

[30] G. M. Sheldrick, *Acta Crystallogr.* **2007**, *A64*, 112.

[31] I. D. Brown, D. Altermatt, *Acta Crystallogr.* **1985**, *B41*, 244.

[32] a) B. S. Bassil, U. Kortz, A. S. Tigan, J. M. Clemente-Juan, B. Keita, P. de Oliveira, L. Nadjo, *Inorg. Chem.*, **2005**, *44*, 9360; b) P. Mialane, A. Dolbecq, J. Marrot, E. Rivière, F. Sécheresse, *Chem.–Eur. J.* **2005**, *11*, 1771; c) B. S. Bassil, S. Nellutla, U. Kortz, A. C. Stowe, J. van Tol, N. S. Dalal, B. Keita, L. Nadjo, *Inorg. Chem.* **2005**, *44*, 2659; d) L.; Lisnard, P.

Mialane, A. Dolbecq, J. Marrot, J. M. Clemente-Juan, E. Coronado, B. Keita, P. D. Oliveira, L. Nadjo, F. Sécheresse, *Chem.–Eur. J.* **2007**, *13*, 3525; e) S. G. Mitchell, C. Ritchie, D. L. Long, L. Cronin, *Dalton Trans.* **2008**, 1415.

[33] C. J. Gómez-García, E. Coronado, J. J. Borrás-Almenar, *Inorg Chem.* **1992**, *31*, 1667.

[34] J. Tercero, E. Ruiz, S. Alvarez, A. Rodríguez-Fortea, P. Alemany, *J. Mater. Chem.* **2006**, *16*, 2729.

[35] a) H. Andres, J. M. Clemente-Juan, M. Aebersold, H. U. Güdel, E. Coronado, H. Büttner, G. Kearly, J. Melero, R. Burriel, *J. Am. Chem. Soc.* **1999**, *121*, 10028; b) J. M. Clemente-Juan, E. Coronado, A. Gaita-Ariño, C. Giménez-Saiz, G. Chaboussant, H. U. Güdel, R. Burriel, H. Mutka, *Chem. Eur. J.* **2002**, *8*, 5701; c) J. M. Clemente-Juan, E. Coronado, A. Gaita-Ariño, C. Giménez-Saiz, H. U. Güdel, R. Sieber, B. Bircher, H. Mutka, *Inorg. Chem.* **2005**, *44*, 3389.

[36] C. J. Gómez-García, E. Coronado, P. Gómez-Romero, N. Casañ-Pastor, *Inorg. Chem.* **1992**, *32*, 3378.

Appendix

A. Curriculum Vitae

B. Published Articles